

Université de Montréal

**Arginine methylation by PRMT1 and PRMT5
regulates B cell activation, germinal center
expansion and differentiation into plasma cells**

par Ludivine Litzler

Département de Biochimie
Faculté de médecine

Thèse présentée
en vue de l'obtention du grade de doctorat
en biochimie

Mai, 2018

© Ludivine Litzler, 2018

Résumé

L'immunité adaptative se repose sur la capacité des cellules B à générer des anticorps spécifiques contre des antigènes étrangers. Les cellules B se développent dans la moelle osseuse, menant à l'expression d'un anticorps fonctionnel à leur surface. Les cellules B ensuite migrent vers les organes lymphoïdes secondaires, où elles seront exposées à des peptides étrangers. Suite à la rencontre avec un antigène spécifique, les cellules B prolifèrent rapidement et migrent à la frontière du follicule B où elles entreront en contact avec les lymphocytes T, avant de retourner au sein du follicule pour former des centres germinatifs. Dans les centres germinatifs, les cellules B vont effectuer deux étapes de maturation leur permettant de diversifier la fonction des anticorps et d'augmenter leur affinité avec les antigènes : le changement de classe des anticorps et la maturation d'affinité des immunoglobulines. Après ces deux étapes, les cellules B quittent les centres germinatifs en se différenciant soit en (i) cellules B mémoires qui peuvent être rapidement réactivées suite à une deuxième rencontre avec le pathogène soit (ii) en cellules plasma qui sécrètent des anticorps en circulation pour neutraliser et éradiquer le pathogène. Les modifications post-traductionnelles régulent différents aspects de la biologie des cellules B, comme leur développement, leur activation et leur différenciation. Ma thèse investigate le rôle de la méthylation des arginines dans les cellules B au cours de réponses immunitaires dépendantes des lymphocytes T, et en particulier le rôle de deux enzymes : « protein arginine methyltransferase 1 et 5 » (PRMT1 et PRMT5), en utilisant des modèles de souris. Nous avons découvert que Prmt5 était nécessaire pendant le développement des cellules B. Plus précisément, Prmt5 est requis au stade « pro-B » à travers un mécanisme dépendant de p53, puis au stade « pre-B » d'une manière indépendante de p53. De plus, Prmt5 permet l'expansion du centre germinatif en promouvant la prolifération des cellules B et en limitant la différenciation en cellules plasma. Pour expliquer ces fonctions, avons montré que Prmt5 était nécessaire pour l'épissage d'ARN messagers et régulait l'expression de certains gènes dans ces cellules. Nous avons aussi découvert que Prmt1 était un important régulateur négatif de la

différenciation, particulièrement suite à une stimulation du récepteur CD40. De plus, nous avons démontré que Prmt1 et Prmt5 agissaient de façon synergique en régulant négativement la différenciation en cellules plasma. En effet, la méthylation des arginines par Prmt1 et Prmt5, à travers différents mécanismes, influencent le destin des cellules B en réprimant leur différenciation en cellules plasma, ce qui les maintient dans le centre germinatif. De cette façon, Prmt1 et Prmt5 promeuvent la réponse humorale et renforcent la maturation d'affinité.

Mots-clés : Immunité humorale, destin des cellules B, centre germinatif, méthylation des arginines, PRMT1, PRMT5.

Abstract

Adaptive immunity relies in part on the ability of B cells to generate specific antibodies against foreign antigens. B cells develop in the bone marrow, and once they express a functional antibody at their surface, they reach secondary lymphoid organs where they will be exposed to foreign poly-peptides. Upon encounter with a cognate antigen, B cells proliferate rapidly, migrate to the border of the B cell follicle to receive T cell help and move back within the B cell follicle to form structures called germinal centers (GC). In GCs, B cells undergo affinity maturation, which increase the affinity of the antibodies, and antibody class switching to diversify their function. B cells exit GCs by differentiating into (i) memory B cells that can rapidly be activated following a second encounter with the pathogen or (ii) plasma cells that secrete antibodies in circulation to neutralize and clear pathogens. Post-translational modifications regulate several aspects of B cell biology such as B cell development, activation and differentiation. My thesis investigates the role of arginine methylation in B cells during T-dependant immune responses, focusing on two enzymes: the protein arginine methyltransferases 1 and 5 (PRMT1 and PRMT5), using mice as models. We have uncovered that Prmt5 is necessary during B cell development. In particular, Prmt5 is required at the pro-B cell stage in a p53-dependant manner and at the pre-B cell stage in a p53-independent fashion. Prmt5 is necessary for the expansion of the GC by promoting B cell proliferation and limiting plasma cell differentiation. These functions could originate, among other mechanisms, from the Prmt5 role in enforcing splicing fidelity and regulating gene expression. We have also discovered that Prmt1 is a major negative regulator of plasma cell differentiation, particularly following CD40 stimulation. Furthermore, we obtained evidence that Prmt1 and Prmt5 function synergistically to negatively regulate plasma cell differentiation. Overall arginine methylation by Prmt1 and Prmt5, via different mechanisms, influences GC B cell fate; by promoting B cells to remain in the GC reaction, at least in part by repressing plasma cell differentiation, thereby supporting antibody responses and enhancing affinity maturation.

Keywords : humoral immunity, B cell fate, germinal center, arginine methylation, PRMT1, PRMT5.

Préface

I have chosen to present the results of my research in a manuscript format. The results are described in Chapters II and III and will soon be submitted:

1. **Litzler LC**, Zahn A, Meli A, Hébert S, Patenaude AM, Methot SP, Sprumont A, Bois T, Kitamura D, Costantino S, King I, Kleinman CL, Richard S, Di Noia JM. *PRMT5 is essential for antibody responses by promoting mature B cell survival and germinal center expansion by p53-independent mechanisms*. Manuscript in preparation.

2. **Litzler LC**, Sprumont A, Zahn A, Methot SP, Patenaude AM, Jung S, Richard S, Di Noia JM. *Prmt1 supports antibody affinity maturation and represses plasma cell differentiation*. Manuscript in preparation.

During my doctoral studies I have also contributed to the following publications:

- Methot SP*, **Litzler LC***, Subramani GP, Eranki A, Fifield H, Patenaude AM, Gilmore JC, Santiago GE, Bagci H, Côté J-F, Larijani M, Verdun RE, Di Noia JM. *A licensing step links AID to transcription elongation for B cell mutagenesis*. *Nature Communications*, 2018, 9(1):1248. doi: 10.1038/s41467-018-03387-6.
- **Litzler LC**, Methot SP, Patenaude AM, Zahn A, Di Noia JM. *Cell-based Assays to Monitor AID Activity*. *Bio-protocol* 2016; 6(3): e1724. <http://www.bio-protocol.org/e1724.551>.

- Montamat-Sicotte D, **Litzler LC**, Abreu C, Safavi S, Zahn A, Orthwein A, Muschen M, Opezzo P, Muñoz DP, Di Noia JM. *HSP90 inhibitors decrease AID levels and activity in mice and in human cells. Eur. J. Immunol.* 2015, 48:2365-2376.
- Methot SP, **Litzler LC**, Trajtenberg F, Zahn A, Robert F, Pelletier J, Buschiazzi A, Magor BG, Di Noia JM. *Consecutive interactions with HSP90 and eEF1A underlie a functional maturation and storage pathway of AID in the cytoplasm. J. Exp. Med.* 2015, 212:581-596.

Table des matières

Résumé	1
Abstract	3
Préface	5
Liste des tableaux.....	11
Liste des figures	1
Liste des abréviations.....	2
Remerciements	3
1 Chapter I: INTRODUCTION.....	6
1.1 B cells.....	6
1.1.1 Humoral Response	6
1.1.1.1 Antibodies.....	7
1.1.1.2 The B-cell receptor	8
1.1.1.3 Secreted antibodies: the humoral response.....	11
1.1.2 B-cell development	11
1.1.2.1 VDJ recombination	12
1.1.2.2 B cell stages in the bone marrow	12
1.1.2.3 Controlling the B cell repertoire through apoptosis	15
1.1.3 B-cell mediated immune response.....	15
1.1.3.1 T-independent antibody responses	17
1.1.3.2 T-dependent antibody responses.....	18
1.1.4 Germinal Center formation.....	18
1.1.4.1 GC kinetics	19
1.1.4.2 GC Dynamics	21
1.1.4.3 Antibody gene diversification in the GC	25
1.1.4.4 Surviving the GC reaction	26
1.1.4.5 The GC B cell transcriptional program	28
1.1.5 B cell differentiation	30
1.1.5.1 Memory B cells	30
1.1.5.2 Antibody secreting cells.....	31
1.1.5.3 The ASC transcriptional program	32

1.1.6	B cells and cancer development	33
1.1.7	Post-translational modifications in B cell biology	34
1.2	Arginine Methylation	37
1.2.1	Arginine methyltransferases	37
1.2.2	Arginine methylation, readers and erasers.....	41
1.2.3	PRMT5	42
1.2.3.1	Structure	42
1.2.3.2	Expression	42
1.2.3.3	Cellular processes regulated by PRMT5.....	43
1.2.3.4	Functional regulation of PRMT5.....	50
1.2.3.5	Cellular impact of PRMT5 activity	52
1.2.4	PRMT1	54
1.2.4.1	Expression.....	54
1.2.4.2	Processes regulated by PRMT1.....	54
1.2.4.3	Functional regulation	56
1.2.4.4	Cellular impact of PRMT1 activity	57
1.2.5	Arginine methylation in lymphocytes.....	58
1.2.5.1	T cells	58
1.2.5.2	B cells	59
2	Chapter II:	64
	PRMT5 is essential for antibody responses by promoting mature B cell survival and germinal center expansion by p53-independent mechanisms.....	64
2.1	Abstract.....	65
2.2	Introduction	66
2.3	Results	68
2.3.1	Distinct regulation of Prmt5 in proliferating B cells	68
2.3.2	Prmt5 promotes survival of activated B cells <i>in vivo</i>	71
2.3.3	Prmt5 prevents B cell apoptosis at the time of activation	74
2.3.4	Prmt5 promotes activated B cell proliferation independently of apoptosis	78
2.3.5	Prmt5 is essential for antibody responses.....	78
2.3.6	Prmt5 is required for GC expansion and dynamics	81
2.3.7	Prmt5 regulates transcription and affects splicing fidelity in B cells	85
2.3.8	Prmt5 prevents spontaneous DNA damage in GC B cells.....	89

2.3.9	A p53 response eliminates Prmt5-deficient pro-B cells	90
2.3.10	Prmt5 prevents p53-independent apoptosis during B cell activation	92
2.3.11	Prmt5 promotes B cell proliferation independently of p53	94
2.3.12	Prmt5 functions in light zone B cells.....	95
2.3.13	Prmt5 prevents premature B cell differentiation in the GC.....	98
2.4	Discussion	101
2.5	Material and Methods.....	105
2.6	Acknowledgments.....	114
2.7	Supplemental material	114
3	Chapter III.....	128
	Prmt1 supports antibody affinity maturation and represses plasma cell differentiation	128
3.1	Abstract.....	129
3.2	Introduction	129
3.3	Results	132
3.3.1	Prmt1 is upregulated in activated and GC B cells	132
3.3.2	Prmt1 is required for GC formation	134
3.3.3	Prmt1 in GC B cells is required for the antibody response to complex antigen.	136
3.3.4	Prmt1 is required for GC expansion and LZ homeostasis	140
3.3.5	Prmt1 promotes B cell proliferation but is dispensable for isotype switching	143
3.3.6	Prmt1 represses plasma cell differentiation.....	146
3.3.7	Synergistic effect of Prmt1 and Prmt5 on plasma cell differentiation	150
3.3.8	Prmt1 prevents premature plasma cell differentiation <i>in vivo</i>	152
3.4	Discussion	154
3.5	Material and Methods.....	158
3.6	Acknowledgments.....	166
3.7	Supplemental material	166
4	Chapter IV: DISCUSSION	172
4.1	Expression of Prmts and their substrates.....	172
4.2	Roles of Prmt1 and Prmt5 along B cell lifespan.....	174
4.2.1	BM development.....	174
4.2.2	Mature B cells homeostasis	177

4.2.3	B cell activation.....	178
4.2.3.1	Arginine dimethylation and B cell proliferation	178
4.2.3.2	Arginine dimethylation and B cell survival	183
4.2.3.3	Arginine dimethylation and B cell differentiation	185
4.2.4	Arginine methylation influences GC dynamics and GC output	188
5	Conclusion	192
	Bibliographie.....	i

Liste des tableaux

Supplementary Table 2.5 - Antibodies.....	125
Supplementary Table 2.6 - Primers.....	127
Supplementary Table 3.1 - Antibodies.....	170
Supplementary Table 3.2 - Primers.....	171

Liste des figures

Chapter I

Figure 1.1 - Antibody structure	8
Figure 1.2 - B cell receptor signalling and antigen uptake	9
Figure 1.3 - B cell development.....	13
Figure 1.4 - Secondary lymphoid organs.....	16
Figure 1.5 - FO B cell activation	20
Figure 1.6 - GC B cell dynamics: balance between affinity maturation and differentiation.....	23
Figure 1.7 - Arginine methylation.....	39
Figure 1.8 - Inhibitors of arginine methylation.....	40
Figure 1.9 – PRMT5 and PRMT1 play multiple roles in the cell	49
Figure 1.10 - Cre-driver mice used or discussed in the thesis.....	60
Figure 1.11 - Role of Prmt1 in BM B cell development.....	63

Chapter II

Figure 2.1 – Regulated Prmt5 expression in B cells	70
Figure 2.2 - Prmt5 is required for the survival of activated B cells in vivo.....	73
Figure 2.3 – Prmt5 protects B cells from apoptosis and promotes proliferation.....	76
Figure 2.4 – Antibody response and GC defects caused by Prmt5 deficiency	80
Figure 2.5 – Prmt5 is necessary for GC expansion	83
Figure 2.6 – Prmt5 regulates gene expression and maintains splicing fidelity in B cells	87
Figure 2.7 – Prmt5 is required for B cell development.....	91
Figure 2.8 – Prmt5 loss induces p53-independant apoptosis.....	93
Figure 2.9 – Prmt5 acts in the light zone to prevent B cell differentiation	96

Supplementary Figure 2.1 – Normal B cell development in Prmt5 ^{F/F} CD19-cre mice	115
Supplementary Figure 2.2 – Efficiency of Prmt5 depletion over time in Prmt5 ^{F/F} CD19-cre and Prmt5 ^{F/F} Cγ1-cre iGBs	117
Supplementary Figure 2.3 – T cell populations in mice infected with <i>H. polygyrus</i> .	119
Supplementary Figure 2.4 – RNA-seq and p53 response additional analyses.....	121
Supplementary Figure 2.5 – Expression of Prmt5 in GC light zone B cells	123

Chapter III

Figure 3.1 – Prmt1 expression in B cells	133
Figure 3.2 – Prmt1 is required for GC formation.....	135
Figure 3.3 – Prmt1 is necessary for humoral response against complex antigen....	138
Figure 3.4 – Prmt1 is necessary for GC expansion and dynamics	141
Figure 3.5 – Prmt1 is necessary for GC homeostasis	145
Figure 3.6 – Prmt1 limits B cell differentiation per division	148
Figure 3.7 – Prmt1 cooperates with Prmt5 to restrict plasma cell differentiation	151
Figure 3.8 – Prmt1 limits B cell differentiation in vivo	153
Supplementary Figure 3.1 – Prmt1 depletion in CH12F3 B cells.....	167
Supplementary Figure 3.2 – Plasma cell differentiation ex vivo	169

Chapter IV

Figure 4.1 - Prmts expression in GC B cell subsets	173
Figure 4.2 - Il7r expression level	176
Figure 4.3 - Stages regulated by Prmt1 and Prmt5 during B cell development.....	176
Figure 4.4 - Gene expression upon Prmt5-depletion	182
Figure 4.5 - Pro-GC genes are induced in high affinity centrocytes	189
Figure 4.6 - Prmt1 and Prmt5 influence GC B cell fate.....	191

Liste des abréviations

aDMA: asymmetric dimethylarginine

AID: activation induced deaminase

ASC: antibody-secreting cells

ASC: antibody-secreting cells

B-NHL: non-Hodgkin lymphoma

BAF: Brg1 associated factors

BCL-6: B-cell lymphoma 6 protein

BCR: B cell receptor

BM: Bone Marrow

Brd7: bromodomain containing 7

CD40L: CD40 ligand

CLP: common lymphoid progenitor

CRC: CXCL12-expressing reticular cells

CSR: Class Switch Recombination

CXCL: CXC-chemokine ligand

CXCR: CXC-chemokine receptor

DC: dendritic cell

DLBCL: diffuse large B cell lymphoma

DZ: dark zone

EBV: Epstein-Barr virus

ER: endoplasmic reticulum

ERK1/2: extracellular signal-related kinase

EZH2: Enhancer of zeste homologue 2

Fab: Fragment antigen-binding

Fc: Fragment crystallisable

FDC: follicular dendritic cell

FO: follicular

FRC: fibroblastic reticular cell

GANP: GC-associated nuclear protein

GC: germinal center

GTI: GC-T cell zone interface

HDAC: histone deacetylases

ICOS: inducible co-stimulatory molecule

Ig: Immunoglobulin

IgH: Immunoglobulin heavy chain

IgL: Immunoglobulin light chain

IKK: I κ B kinase

IL-7 : interleukin-7

ITAM : immunoreceptor tyrosine activating motif

KLF4: Krüppel-like factor 4

LPS: lipopolysaccharide

LZ: light zone

MEK1/2: Mitogen-activated ERK
kinases

MHC : major histocompatibility
complex

MHCII: class II major histocompatibility
complex

MZ: marginal zone

NF- κ B: nuclear factor- κ B

NK: natural killer

NuDR: nucleosome remodelling
deacetylase

PBs: plasmablast

PC: plasma cell

Plk2: Polo-like kinase 2

PRC2: polycomb repressive complex-2

PRMT: Protein arginine methyl-
transferase

PRMT: protein arginine
methyltransferase

PTM: post translational modification

RAF: Rapidly accelerated fibrosarcoma

RAS : rat sarcoma virus

RSS: recombination signal sequence

SAM, AdoMet: S-adenosylmethionine

sDMA: symmetric dimethylarginine

T-dependant: TD

T-independent: TI

TCR : T cell receptor

Tfh: T follicular helper cell

TLR : toll-like receptor

TNFR: tumour necrosis factor receptor

TRAF: TNFR-associated factor

UPR: unfolded-protein response

Wt: Wild type

XBP1: X-box binding protein

“On peut passer sa vie à ânonner que le but est secondaire et que seul compte le chemin mais si l'on en fait pas l'expérience pour de bon en se vautrant dans l'ornière, ça ne reste qu'une image”

Stéphanie Bodet.

Remerciements

Je tiens à remercier mon superviseur, Javier, qui m'a beaucoup soutenue tout au long de mon doctorat et qui a toujours gardé sa porte ouverte pour m'aider dans mes projets. Javier m'a également accordée énormément de confiance, ce qui m'a poussée au travail et a été déterminant pour garder ma motivation.

Merci aux membres du jury pour l'évaluation de ma thèse : Dr Jacques Drouin, Dr Jennifer Gommerman, Dr Woong Kyung Suh and Dr Eric Milot.

Je remercie les autres membres du laboratoire, passés et présents: Alexandre, Damien, Anil, Debashree, Shiva, Ganesh, Thérance, Adrien. Merci particulièrement à Anne-Marie, qui avait toujours de bons conseils et gardait un sourire rassurant dans toutes les situations; à Astrid que j'ai appris à connaître grâce au temps partagé à la paillasse et au Fortessa, à discuter d'LKB1/PRMTs mais pas seulement ... ,-) et à Steve qui m'aura soutenue, au lab et en dehors, dans mes projets grâce à nos discussions scientifiques mais aussi dans tous les aspects de ma vie au long de ces six dernières années. Steve m'a aussi énormément aidée pour la rédaction de mon mémoire de thèse en anglais, merci pour ta patience et les heures de relecture.

Je remercie les membres de mon comité de thèse, qui s'est réuni tous les ans pour suivre l'évolution de mes projets: Jean François Côté, Eric Lécuyer et Benoît Coulombe.

Je remercie également tous nos collaborateurs qui nous ont aidés à mener ces projets à bien grâce à leur aide technique et à nos discussions: Dr Stéphane Richard, Sara Calabretta, Claudia Kleinman, Steven Hébert, Irah King, Alexandre Meli, Santiago Costantino et Seolkyoung Jung.

Je souhaite aussi remercier particulièrement le laboratoire voisin, le « labo Mörröy » qui m'aura soutenue techniquement et aidé dans mes réflexions. Je pense en particulier à Jennifer, Hugues, Charles, Julie, Damien, Anne, Riyan, Mathieu, Peiman et Marissa. Merci à tous, sans oublier Marion, de partager avec moi les restes du

petit-déjeuner le jeudi matin, les chocolats de Pâques, les gâteaux en toutes occasions et les sorties !

Pour terminer avec l'aide technique, je tiens à remercier Eric Massicotte, à qui je dois mes beaux graphiques de FACS, et qui m'aura aussi procuré un soutien moral infailible à chaque visite au 1^{er} =).

Merci à Damien, pour cette époque où nous étions à quatre inséparables et constamment au lab ... pour créer des déguisements, manger du Bocadillo, regarder des films et vider des citrouilles.

Merci à Eszter, un rayon de soleil qui m'a toujours encouragée dans les moments chouettes, et les moins chouettes aussi. Tu m'as beaucoup aidé à voir la vie sous un autre angle et à apprécier chaque instant.

Merci à April, ma première amie au Canada, ma prof d'anglais et mon sensei culinaire. Tu es l'une des raisons pour lesquelles je suis revenue à Montréal. Merci pour ta joie de vivre et ton « BC humour » insupportable.

Merci aux copines de pauses de thés, sorties au Spa, calmars et n'importe quoi : Marine, Carine, Noumeira et Jen =). Merci à Yves, Adeline, Julien, Jen, Elliott, Iannis, Fanny, Max, Fabien, Anaïs, Justine pour les beaux moments entre ami(e)s.

Merci aussi à Alexandra, amie et initiatrice à la vie de hipster dans le MileEnd. Tu m'as initié à des choses auxquelles je n'aurais même pas pensé ... comme l'ultimate et le hors-piste (ce qui n'est toujours pas gagné) ! Merci pour ton soutien au cours des années, ta confiance et ta joie de vivre. Merci aussi aux PRIMERS pour le BEAU TRAVAIL d'équipe: Julien Jen, Aurèle, Steve, Max, Thomas, Jin, Sarah, Noumeira, Alex, Steve et Vas.

Merci à mon amie, colocataire, compagne d'aventures, partenaire d'escalade Jennifer qui a toujours su me récupérer, à la petite cuillère ou au bout d'une corde (grâce à son superbe dynamisme =)). Tu m'auras aidé et éclairé de ta bonne humeur tout au long de mon doctorat.

Je remercie aussi ma famille Canadienne du Québec : Evangéline, René, Michelle, Richard et Marie-Claire et de Colombie Britannique : Chryso, Julien et Paulo, pour leur présence et leur soutien.

Merci à mes amis de l'autre côté de l'Atlantique, avec qui rien ne change malgré le temps et les minces nouvelles : Léa, Sébastien, Antoine et Jérôme.

Finalement merci à ma famille en Europe, Hyacinthe, Clémence et la nouvelle venue Margot, qui me soutiennent à coups de joyeux Skypes cacophoniques ! Merci à Papa et Maman, qui ont ravalés leur salive à mon départ, et qui malgré tout m'encouragent en permanence. Merci aussi à mes grands-parents et à mamie qui est partie trop vite.

Et finalement merci encore à Steve, pour sa patience au pays de la raclette =).

1 Chapter I: INTRODUCTION

Upon an infection, the body's initial defense is mediated by the innate immune system. This involves different cell types (macrophages, granulocytes, mast cells), which attempt to destroy the pathogens. These cells originate from hematopoietic stem cells (HSC) in the bone marrow (BM). Innate immunity is rapid and can fight a wide range of invaders, however it lacks pathogen-specificity and does not generate immunological memory (Parkin and Cohen, 2001).

Vertebrates have developed an additional immune response based on the recognition of pathogens by cells called lymphocytes, which also originate from HSCs. This response is called adaptive immunity (Boehm and Swann, 2014). There are two types of lymphocytes: T-lymphocytes and B-lymphocytes. Both can generate specificity to a particular pathogen and can remain in circulation after the infection is cleared in order to produce a robust response upon further exposure to the same pathogen. My thesis will focus on B-lymphocytes, also called B cells. B cells are responsible for the production of antibodies, which are blood-circulating molecules that specifically bind pathogens, and promote their clearance.

1.1 B cells

1.1.1 Humoral Response

In order to clear invading pathogens, B cells underpin antibody-mediated immunity, also called the humoral response. In most vertebrate species, B cells develop in the bone marrow (BM), qualified as a primary lymphoid organ in the adult. Once mature, B cells leave the BM via the blood stream in order to reach the secondary lymphoid organs such as the lymph nodes, the spleen and the Peyer's patches. These organs are connected to a network of lymphatics that drain extracellular fluids containing pathogen fragments, or antigens, from peripheral tissues. Common antigens include proteins from invading pathogens like viruses or polysaccharides from bacterial membranes. Every B cell expresses a unique antibody, with unique antigen

specificity. B cells constantly circulate between the blood and secondary lymphoid organs in a quiescent state, until they encounter their cognate antigen and are stimulated to initiate a humoral response.

1.1.1.1 Antibodies

The function of antibodies is to bind antigens, and the segment of antigen that is recognized by a particular antibody is called an epitope. As an antigen generally contains multiple epitopes, multiple antibodies can simultaneously bind the same antigen as long as they recognize distinct epitopes.

Antibodies are encoded by the immunoglobulin (*Ig*) genes, and can be expressed as transmembrane proteins at the B-cell surface and/or as secreted proteins, depending on the B-cell stage. Antibodies are composed of two heavy (IgH) and two light (IgL) chains joined by disulphide bonds (Harris et al., 1992) as shown in (**Fig. 1.1**). The association of light chains with the N-terminal domains of the heavy chain form the so-called fragment antigen-binding (Fab) domain of the antibody, which contains the variable region that binds antigen (**Fig. 1.1**). The dimeric structure determined by the C-terminal domains of each IgH is referred to as the fragment crystallisable (Fc) region, which provides functional specialization to the antibody depending on its IgH class (Amzel and Poljak, 1979; Davies and Metzger, 1983). The different classes of IgH, also called isotypes: IgM, IgD, IgG, IgA and IgE, determine whether the antibody can be transported to specific sites in the body and/or promote distinct sets of effector mechanisms (Ward and Ghetie, 1995). Indeed, in the blood, most antibodies are IgG and IgE, whereas IgA is secreted into the intestinal and respiratory tracts (Brandtzaeg, 2009). IgE can also bind to mast cells, which harbour IgE-specific receptors. Upon antigen binding to IgE, mast cells release mediators and cytokines that can help clear an infection (Stone et al., 2010).

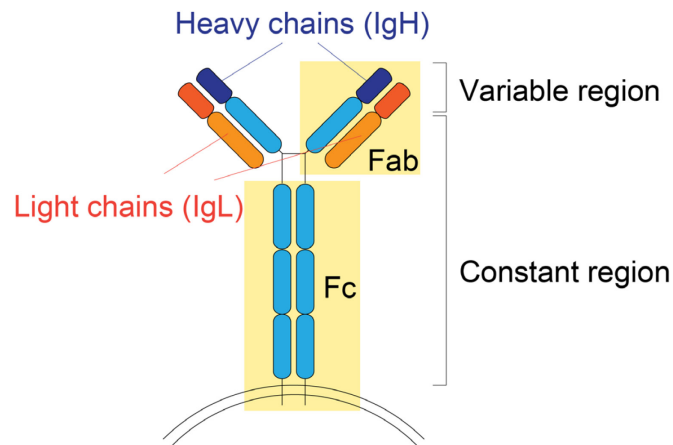


Figure 1.1 - Antibody structure

Schematic of an antibody expressed at the B cell surface. Fab: Fragment antigen-binding, Fc: Fragment crystallisable.

Recently-generated mature B cells that exit the BM only express IgM but subsequently express IgM and IgD simultaneously in the secondary lymphoid organs. Upon activation in the periphery, B cells can switch their IgM for another isotype. The B cell environment, dictated by cellular interactions and cytokines released by other immune cells will directly influence the isotype choice, promoting a context-specific antibody response (Lutzker et al., 1988).

For the humoral immune response to be efficient, antibodies must (i) be highly diversified in order to recognize a vast spectrum of antigens, (ii) acquire high affinity for the antigen it recognizes, and (iii) elicit the appropriate immune response in order to efficiently clear the infection. This diversity is generated along the B cell life, from their development until their mature activated stage.

1.1.1.2 The B-cell receptor

Antibody molecules expressed at the B cell surface are the major subunits of the B cell receptor (BCR). The antibody is non-covalently associated with the signalling molecules $Ig\alpha$ (CD79 α) and $Ig\beta$ (CD79 β), which both have cytoplasmic tails containing immunoreceptor tyrosine activating motifs (ITAMs) (**Fig. 1.2A**). Binding of an antigen to the BCR induces signalling cascades initiated with phosphorylation of

the ITAMs (Monroe, 2006) (**Fig. 1.2A**). Depending on the B cell stage and environment these cascades result in different outputs, such as differentiation, survival and/or clonal expansion (Niiro and Clark, 2002).

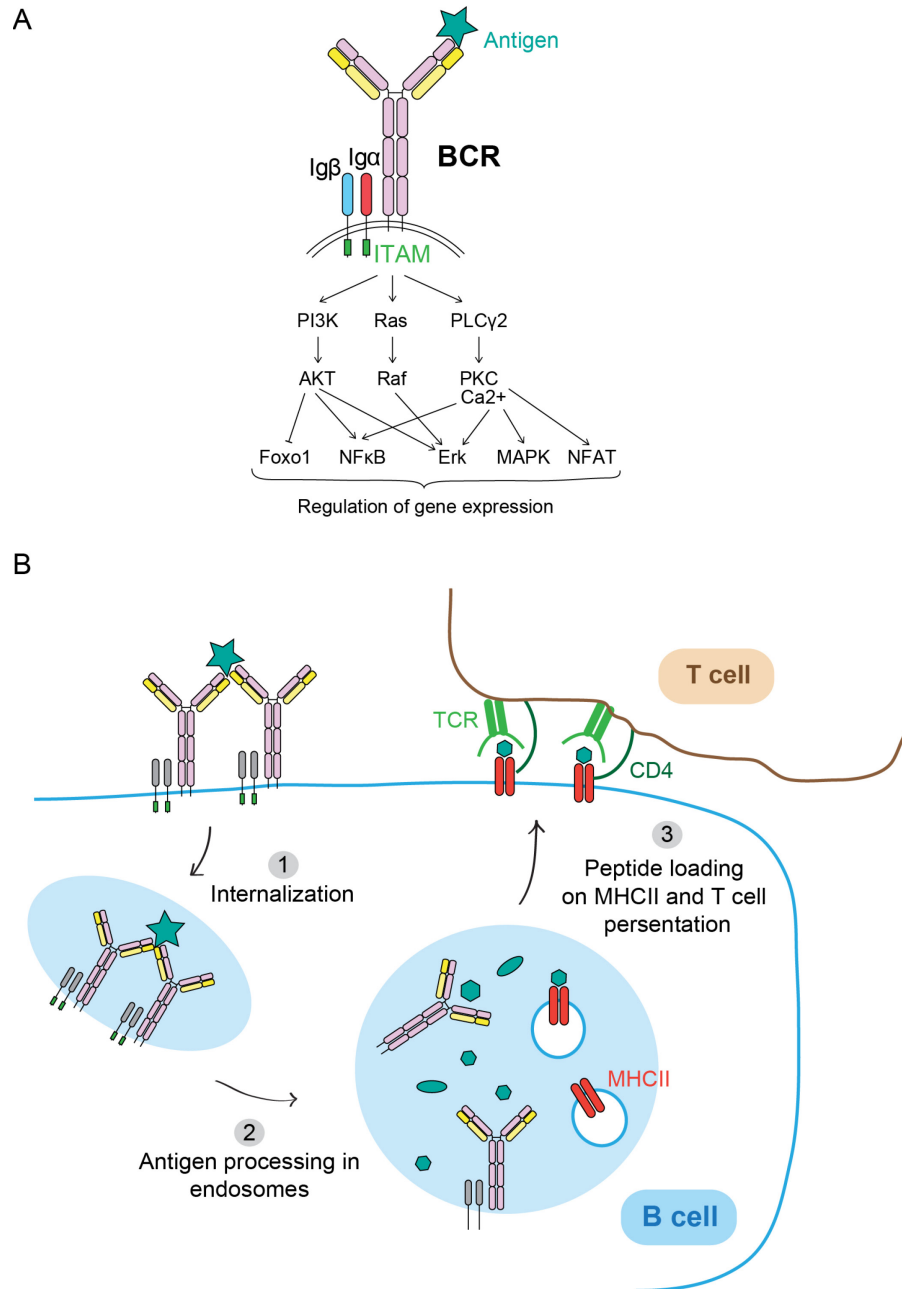


Figure 1.2 - B cell receptor signalling and antigen uptake

A) Schematic of the BCR, with downstream signalling pathways induced upon BCR stimulation (adapted from (Niiro and Clark, 2002) and (Kurosaki et al., 2010)).

B) Schematic of BCR internalization and antigen presentation to helper T cells. 1) Upon BCR crosslinking with a cognate antigen, the BCR is internalized with the antigen. 2) The antigen-BCR complex is targeted to MHC class II-containing endosomes, where the antigen is processed into short peptides that are loaded on MHCII receptors. 3) MHCII-peptide complexes are exported to the B cell surface, where CD4+ T cells can recognize the peptide in the context of MHCII (adapted from (Kurosaki et al., 2010)).

Developing B cells

During B cell development (explained in more detail below), cross-linking of the pre-BCR (containing only IgH and a surrogate light chain) or the BCR ensures the production of one functional antibody per B cell. Firstly, this signaling prevents further *Ig* rearrangements. Secondly, only B cells that properly rearranged their *Ig* will properly signal via their BCR and survive. This mode of B cell selection is called the BCR checkpoint.

Mature B cells

The BCR on mature B cells plays a dual role, as:

1. A signalling receptor

BCR cross-linking on mature B cells induces a signalling cascade through phosphorylation events and Ca²⁺ release from the endoplasmic reticulum, this in turn modifies the B cell transcriptional program, promoting B cell activation and subsequently antibody diversification and production (Avalos and Ploegh, 2014).

2. An endocytic receptor

In the periphery, BCR association with cognate antigen triggers internalization of the antibody-antigen complex, cleavage of the antigen and loading of epitopes onto class II major histocompatibility complex (MHCII) at the B cell surface (Lanzavecchia, 1985). The display of processed antigen at the membrane is necessary for B cells to interact with and receive activation and survival signals by T lymphocytes (Lanzavecchia, 1985) (**Fig. 1.2B**).

1.1.1.3 Secreted antibodies: the humoral response

There are four main mechanisms by which antibodies can block and/or clear pathogens (Murphy et al., 2012).

First, binding of antibodies to pathogens such as viruses can prevent their access and potential infection of host cells. This mode of action is called neutralization, and eventually results in the phagocytosis of the pathogen by macrophages.

Second, antibodies can coat the antigen, forming immune complexes. This mechanism is named opsonisation. Macrophages and dendritic cells (DCs) express Fc receptors at their membrane, which bind to immune complexes. Depending on the Fc receptor type, it will either be internalized, leading to phagocytosis and destruction of the pathogen, or stay on the membrane, remaining accessible for B cells to interact with the native antigens via their BCR.

Third, antibodies can induce the recruitment of the complement system through their Fc fragment. Complement is composed of a variety of different proteins, such as proteases, that can associate to a pathogen and together promote its destruction and/or the recruitment of immune cells such as macrophages.

Finally, antibodies developed against malignant cells can recruit and activate cytotoxic lymphocytes such as natural killer (NK) cells, leading to the targeted cells death. This process is called antibody-dependent cellular cytotoxicity (Wang et al., 2015).

1.1.2 B-cell development

B cells develop in the BM from hematopoietic precursors called common lymphoid progenitors (CLP). Each step of B cell development is characterized and defined by the rearrangement of gene segments within the *Ig* variable region, resulting in the assembly of functional Ig genes and production of one random antibody specificity.

1.1.2.1 VDJ recombination

The *IgH* variable region is encoded by three gene segments called V (for variable), D (for diversity), and J (for joining). The variable region of *IgL* is encoded by a V and a J segment. In germline configuration, the *IgH* and *IgL* loci are not functional, because the V, D and J segments are separated. A functional Ig gene results from stepwise gene segment recombination, a process termed V(D)J recombination that is initiated by a heterodimeric recombinase composed of the Rag-1 and Rag-2 subunits. Rag-1 and Rag-2 are expressed specifically in developing B cells (as well as developing T cells). The Rag enzyme recognizes recombination signal sequences (RSS) that are located at each gene segment extremity. Rag, aided by additional factors, can align the two RSS sequences and perform a cleavage at the RSS that will be then resolved by the DNA repair machinery of the non-homologous end-joining pathway, in order to join the two segments (Roth, 2014). The diversity of antibody specificities in the B cell repertoire generated by the process of V(D)J recombination arises from three components: (i) There are multiple copies of each gene segment, leading to combinatorial V-D-J and V-J diversity. (ii) The recombination process promotes the addition or removal of nucleotides at the junction between two segments, leading to junctional diversity. (iii) The antigen binding site of the antibody is formed by variable regions of both the *IgH* and *IgL* chains, so different combinations are possible.

1.1.2.2 B cell stages in the bone marrow

There are four main stages of B cell development in the BM, characterized by the expression of different cell surface markers originally described by Dr. Richard Hardy (Hardy's fractions) (Hardy and Hayakawa, 2001), as shown in **Fig. 1.3**. Depending on their developmental stage, B cells dramatically alter their proliferation state, ranging from rapid expansion to resting status.

Pre-pro B cells

Pre-pro B cells (fraction A) have not started V(D)J recombination. They arise from CLPs, which themselves arise from HSCs.

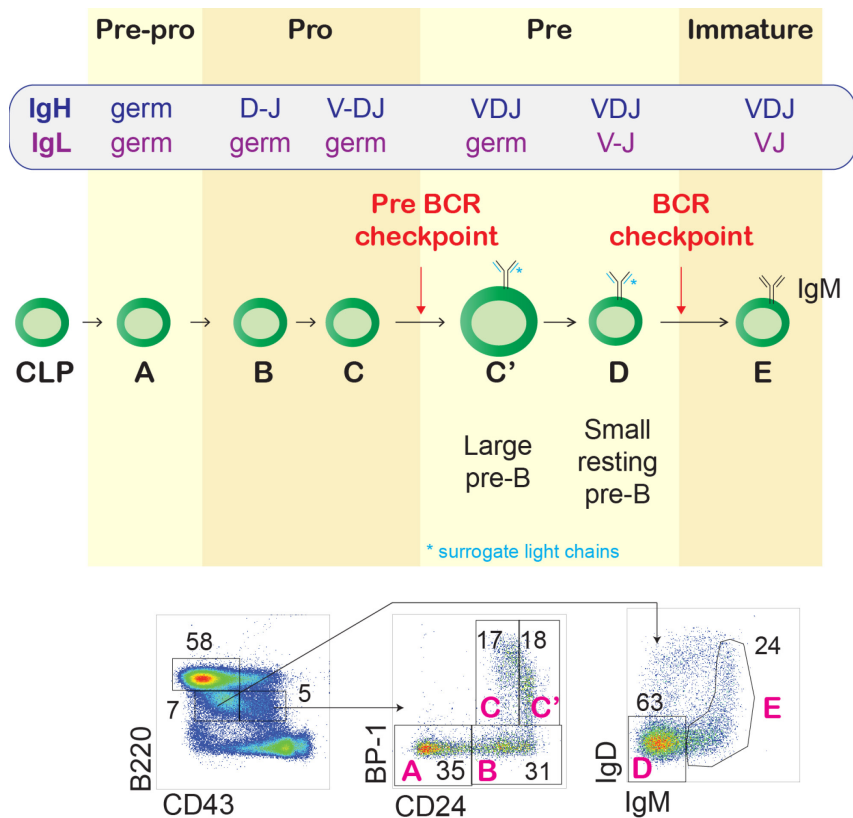


Figure 1.3 - B cell development

Schematic of bone marrow B cell development. The Ig rearrangement stages and BCR checkpoints are indicated, as well as representative flow cytometry plots depicting the gating strategy to distinguish Hardy's fractions: A, B, C, C', D and E from a wild type mouse at the bottom. CLP: common lymphoid progenitor.

Pro-B cells

This stage corresponds to the onset of the *IgH* rearrangement. Pro-B cells express the *Rag* genes and recombine *IgH* D-J fragments (fraction B). Pro-B cells will then recombine a V fragment to the previously recombined D-J segment (fraction C). Murine pro-B cells require interleukin-7 (IL-7), produced by BM stromal cells, for their survival and proliferation (Clark et al., 2014). Although in human, the IL-7 receptor is dispensable for BM B cell development (Prieyl and LeBien, 1996).

Pre-B cells

Upon productive *IgH* rearrangement, pro-B cells will express the recombined IgH, which by default is IgM (Ig μ), assembled with a surrogate invariable light chain and the signalling subunits Ig α and Ig β at the B cell surface. The surrogate light chain is a substitute for *IgL*, which is not yet rearranged. This structure is called the pre-BCR and is capable of transducing signal into the cells. The pre-BCR checkpoint stops V-D-J rearrangement, reduces *Rag* genes expression and induces allelic exclusion in order for B cells to only express a single *IgH* variant. Pre-BCR signalling also promotes B cell proliferation and initiation of *IgL* rearrangement. Only one quarter of pro-B cells will advance past the pre-BCR checkpoint (Osmond, 1991).

B cells that successfully undergo the pre-BCR checkpoint are called large pre-B cells and correspond to fraction C'. They are still dependent on IL-7 signalling, which stimulates the PI3K-AKT pathway, supporting their rapid proliferation (Clark et al., 2014). Clonal expansion of large pre-B cells promotes the expansion of a B cell repertoire expressing productive *IgH*, thus counteracting the dramatic cell loss following the pre-BCR-checkpoint. Pre-BCR signalling antagonizes IL-7R signalling and promotes cell cycle arrest and transition to the next stage: small resting pre-B cells (fraction D). Small pre-B cells re-express the *Rag* genes to undergo rearrangement of the V-J fragments of the *IgL*. There are two IgL loci, containing the genes for the κ chain and the λ chain. In addition to allelic exclusion, *IgL* also undergoes isotypic exclusion. In this case, *Igk* is rearranged first, and if this is productive, *Ig λ* will be silenced. On the other hand, if *Igk* rearrangement is unsuccessful, *Ig λ* can be rearranged. Again, these mechanisms allow B cells to express a unique BCR.

Immature B cells

Immature B cells have successfully rearranged their *IgL*, express antibody molecules on their membrane and have been selected by the BCR checkpoint, meaning that BCR signalling is functional upon cross-linking. All immature B cells express a functional IgM antibody, however a final checkpoint must be cleared before the B cells can access the periphery. B cells that recognize self-antigen must be eliminated

from the B cell repertoire because they could lead to the development of autoimmune diseases (Murphy et al., 2012). Self-reactive B cells can either (i) undergo apoptosis, (ii) become anergic, or (iii) undergo new rounds of *IgL* rearrangement, a process called receptor editing. Only 10% of BM-produced immature B cells will access the periphery (Rolink et al., 2001).

1.1.2.3 Controlling the B cell repertoire through apoptosis

Elimination of dysfunctional BM B cells begins at the pro-BCR checkpoint (Lu and Osmond, 2000). Indeed, pro-B cells that generate non-productive or aberrant Igu undergo apoptosis. One of the most important regulators of the pro-BCR checkpoint, is p53, a transcription and DNA damage response factor encoded by the *Trp53* (*Trp53* in mice) gene. P53, which promotes the expression of anti-proliferative and pro-apoptotic genes (Kruse and Gu, 2009), is activated in pro-B cells that are unable to repair Rag-induced lesions during *IgL* V-J recombination. Indeed, *Trp53*^{-/-} mice show increased pro-B cell survival compared to wild type (wt) mice (10% apoptosis in *Trp53*^{-/-} versus 70% in wt) (Lu et al., 1999). On the other hand, pre-B cells are unaffected in *Trp53*^{-/-}, highlighting a specific role for p53 at the pro-B cell stage (Lu et al., 1999). Moreover, pro-B cells from *scid* mice, which are lost due to DNA repair defects during VDJ recombination, can be restored by crossing with *Trp53*^{-/-} mice (Guidos et al., 1996). As a result of the increased survival of genetically unstable cells, *Trp53*^{-/-} *scid* mice develop pro-B cell lymphomas. Altogether, p53-dependant apoptosis promotes clearance of pro-B cells that have undergone faulty VDJ rearrangement at the *IgH*.

1.1.3 B-cell mediated immune response

Once they exit the BM, immature IgM⁺ B cells migrate via the blood vessels to secondary lymphoid organs where they complete their development to become mature B cells (Rolink et al., 1999). Lymph nodes have an organized structure, with Follicular (FO) B cells at the periphery, forming B cell follicles, and T-lymphocytes at the center, forming T cell zones (**Fig. 1.4A**). Naïve FO B cells, free antigen and DCs enter the lymph node via the bloodstream, and migrate through the T cell zones

(Batista and Harwood, 2009). FO B cells are characterized by high expression of CD23 and CD21, and are continuously circulating between the different secondary lymphoid organs (Hoek et al., 2010).

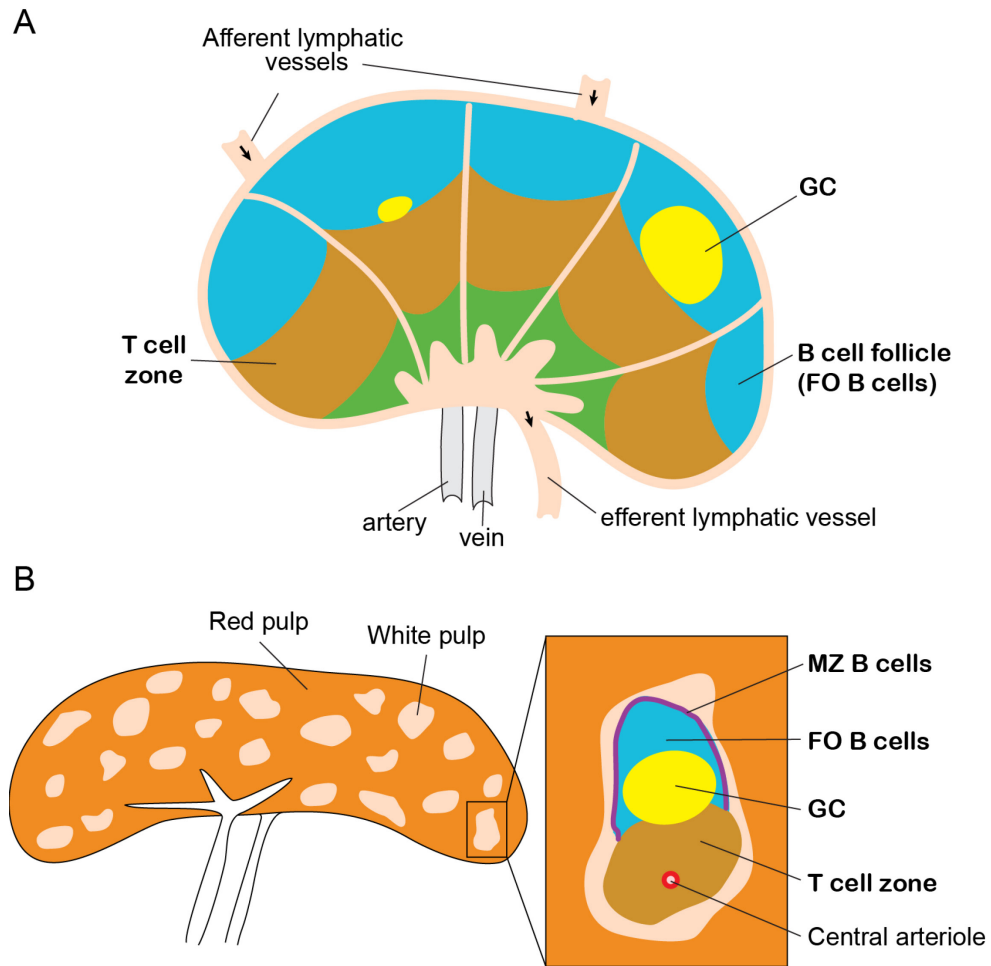


Figure 1.4 - Secondary lymphoid organs

A) Schematic of a lymph node. Extracellular fluids from body tissues containing pathogens are drained by lymphatic vessels, which converge to lymph nodes by the afferent lymphatic vessels and exit the lymph node by the efferent lymphatic vessels. Lymphocytes enter the lymph node from the bloodstream and exit via the efferent lymphatic vessels. Germinal centers (GCs) develop in the B cell follicle, in proximity to the T cell zone.

B) Schematic of a spleen. The spleen collects antigen from the blood. The red pulp is the zone of red blood cell destruction. Lymphocytes enter the spleen via central arterioles, where they accumulate to

form the white pulp. The B cell follicle is composed of follicular (FO) B cells, surrounded by marginal zone (MZ) B cells.

In the spleen, there is an additional kind of mature B cell: Marginal zone (MZ) B cells, which are spleen-specific non-circulating cells, characterized by low expression of CD23 and high expression of CD21 at the membrane. The spleen is composed of many arterioles, around which lymphocytes accumulate to form the white pulp. The white pulp contains B cell follicles, composed of FO B cells that are sequestered by a network of stromal cells, called follicular dendritic cells (FDCs) (Cyster et al., 2000). FDCs express the chemokine CXC-chemokine ligand 13 (CXCL13) that binds the receptor CXC-chemokine receptor 5 (CXCR5) on B cells. MZ B cells form a ring surrounding the B cell follicles. T cells are located in zones that are adjacent to the B cell follicles and surround the arteriole (**Fig. 1.4B**).

1.1.3.1 T-independent antibody responses

MZ B cells can mount an immune response on their own, without any T cell help, which is referred to as a T cell-independent (TI) response. TI responses occur following encounter with two major types of blood-borne, usually non-protein antigens: T-independent (TI)-1 and TI-2 antigens. TI antigens can be polysaccharides or glycolipids from encapsulated bacteria. TI-1 antigens, such as lipopolysaccharides (LPS), preferentially provide mitogenic stimuli to MZ B cells compared to FO B cells, resulting in polyclonal activation (Genestier et al., 2007). This stimulation proceeds via the toll-like receptors (TLRs), and therefore remains independent of BCR specificity (Bekeredjian-Ding and Jegou, 2009). TI-2 antigens, such as Ficoll, present a repetitive epitope that can simultaneously engage multiple BCRs, thereby inducing a clonal B cell activation and antigen-specific B cell responses (Vos et al., 2000). TI immune responses lead to a rapid B cell activation and differentiation into antibody secreting cells (ASCs) that produce low-affinity IgM antibodies.

For most humoral immune responses, FO B cells require interactions with T cells to initiate antibody responses.

1.1.3.2 T-dependent antibody responses

T cell progenitors arise from CLPs in the BM (Lai and Kondo, 2008), but migrate to the thymus, where T cell development takes place. Like B cells, T cells recombine their T cell receptor (TCR) genes by the mechanism of V(D)J recombination (Murphy et al., 2012). In the end, each T cell expresses a unique TCR on its surface, which is able to bind antigenic peptides loaded on MHC molecules. The TCR recognizes antigen together with a co-receptor, either CD4 in the context of MHCII or CD8 in the context of MHCI. The T cells that interact with B cells are typically CD4⁺. Several types of CD4⁺ T cells exist, each specialized for a certain type of immune response (Zhu et al., 2010), but those most relevant for this thesis are those that can provide activating stimuli to B cells, generally called “helper” T cells. DCs and B cells are able to present peptides to CD4⁺ T cells via their MHCII (**Fig 1.2B**). When CD4⁺ T cells bind antigen from DCs via their TCR, they are activated and seek B cells that can present the same antigen on their MHCII. In the ensuing interaction, T cells provide activating and survival signals to the B cells.

In contrast to TI responses, T-dependent (TD) immune responses result in the production of high-affinity and class-switched antibodies. In search of cognate antigens, resting FO B cells are constantly circulating between secondary lymphoid organs (Cyster, 2010). Upon BCR cross-linking, antigen will be internalized, processed and presented at the B cell surface as peptides on MHCII. T helper cells that were primed by DCs presenting the same cognate antigen on their MHCII, can then recognize the MHCII-bound antigen presented by the B cells. The T cells will deliver cytokines and co-stimulatory signals to the cognate B cell, leading to B cell activation and the formation of structures called germinal centers (GCs).

1.1.4 Germinal Center formation

GCs are transient anatomical structures that form in the B cell follicle in response to antigenic challenge. GCs are composed of B cells, T cells, FDCs and macrophages and the interactions between these cell types are important for generating a high-quality antibody response. In the GC, B cells will mutate their *Ig*, in order to generate

antibody variants of higher affinity for the antigen. This process, which requires a selection step for advantageous mutations, is called affinity maturation. In addition, another mechanism of recombination at the *IgH*, distinct from VDJ recombination, will lead to antibody isotype switching from IgM to another class, diversifying the antibody function.

1.1.4.1 GC kinetics

The kinetics of a GC reaction will vary depending on the type of infection or immunization as well as the secondary lymphoid organ implicated; however, all GCs proceed via the same steps. Broadly, after an initiation phase, a GC will rapidly expand to create a mature GC, where B cells undergo affinity maturation and isotype switching. Once these processes are complete, the GC will produce high affinity B cells that have differentiated into memory B cells or antibody secreting cells, before finally contracting and dissipating (De Silva and Klein, 2015).

B cell activation

In the follicle, most mature B cells are quiescent, which means they are not in the cell cycle. B cells will enter the cell cycle only after engaging cognate antibody-antigen interactions and receiving T cell help. B cells rapidly undergo major transcriptional changes following mitogenic stimulation. As an example, within 2 days of incubation with the mitogen LPS and the cytokine IL-4, *ex vivo* B cells will expand dramatically in size, increase RNA levels by 10-fold, increase total histone acetylation by 3- to 7-fold and undergo differentiation to ASCs (Kouzine et al., 2013).

FO B cells seek either free soluble antigen that arrives via the circulation, or antigens exposed on the surface of FDCs, macrophages and DCs. FDCs (Qin et al., 2000), macrophages (Phan et al., 2007) and DCs (Bergtold et al., 2005) can trap unprocessed antigens by binding immune complexes via their Fc receptors. If a B cell binds to its cognate antigen through the BCR, the antigen is captured (i.e. engulfed together with the BCR), processed, and loaded on its surface in association with MHCII (**Fig. 1.5**).

Early GC initiation

The primed B cell then migrates to the T-B border of the follicle, where it searches for associated T helper cells that have been activated by the same antigen. Long-lived T-B cells interactions, which can last up to one hour (Okada et al., 2005), provide co-stimulatory signals and secreted cytokines from the T cells. This promotes rapid B cell proliferation at the T-B border (Coffey et al., 2009), which typically happens at day 1-2 for model antigens like NP (Kerfoot et al., 2011) (**Fig. 1.5**).

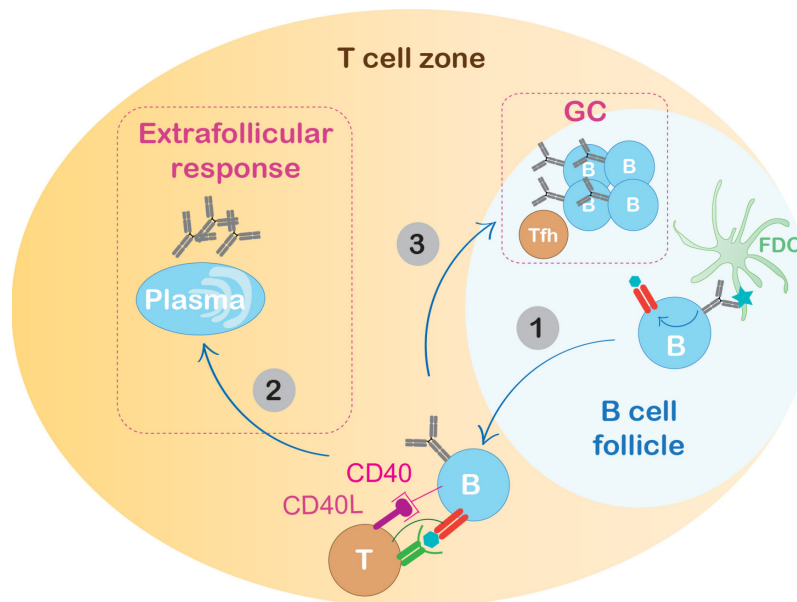


Figure 1.5 - FO B cell activation

Schematic of events following an encounter with TD antigens. 1) B cells that bind to cognate antigens get activated, present antigen peptides on their MHCII (as shown on Figure 1.2B) and migrate to the T-B border where CD4⁺ helper T cells provide additional stimulation upon peptide-MHCII recognition. 2) If the B cell affinity for antigen is high, they differentiate into short-lived ASC, generating the extrafollicular response. 3) If the B cell expresses a BCR of lower affinity, it will migrate back to the follicle, and form a GC. Activated CD4⁺ helper T cells differentiate into Tfh and migrate to the B cell follicle where they participate in the GC reaction.

Late GC initiation or extrafollicular response

B cells then migrate back to the follicle, attracted by FDCs that secrete CXCL13, and it is here that the B cells will initiate an early GC. Prolonged T-B interaction also induces the cognate helper T cells to proliferate and differentiate into T follicular

helper cells (Tfh). Tfh cells also express the CXCL13 receptor CXCR5, which will promote their migration into the follicle in order to join the GC (Vinuesa et al., 2016).

Alternatively, activated B cells at the T-B border can differentiate into short-lived ASC that will quickly secrete low-affinity antibodies. This is explained in detail further in **section 1.1.5.2 (Fig. 1.5)**.

Expansion

GC B cells undergo rapid proliferation, up to one division every 6 hours; this promotes swift GC expansion (Zhang et al., 1988). Mature GCs become polarized into two compartments, known as the dark zone (DZ) and the light zone (LZ), which are visible by day 7 for a typical immunization with NP (Victora et al., 2010). The DZ is a region densely populated by highly proliferative B cells called centroblasts. Within the DZ compartment, B cells mutate their *Ig* variable regions by the mechanism of somatic hypermutation (see **section 1.1.4.3**). B cells are called centrocytes in the LZ, where they are more spread out and interact with FDCs, Tfh cells and macrophages. In this compartment, a careful dynamic permits the selection of centrocytes harbouring a BCR with higher affinity for the antigen displayed by FDCs (see GC dynamics, **section 1.1.4.2 (Fig. 1.6)**).

Contraction

The timing of GC termination depends on the type of immune stimulus. Prolonged GC reactions are necessary for antibodies to reach sufficient affinity in order to effectively fight an infection (Pappas et al., 2014). On the other hand, long-lived GCs can be detrimental, as they can give rise to self-reactive antibodies due to extensive *Ig* mutations (Vinuesa et al., 2005), or they can promote the development of GC-derived lymphomas due to the accumulation of genomic instability intrinsic to *Ig* diversification (Robbiani et al., 2015).

1.1.4.2 GC Dynamics

Stromal cells in lymphoid organs form a matrix of non-hematopoietic origin that contributes to lymphoid cell homeostasis (Aguzzi et al., 2014). For instance,

fibroblastic reticular cells (FRCs) support the structure and function of the T cell zone (Link et al., 2007). However FDCs promote B cell follicle formation (Cyster et al., 2000). In the GC, B cells can migrate between the LZ and DZ, which is mediated by the release of chemokines from stromal cells in either compartment and the differential expression of receptors in B cells. B cells in the LZ express CXCR5, the receptor for the chemokine CXCL13 that is secreted by FDCs (Cyster et al., 2000), while DZ B cells express CXCR4 that binds the chemokine CXCL12, released by CXCL12-expressing reticular cells (CRC) residing in the DZ (Allen et al., 2004; Rodda et al., 2015).

The GC B cell traffic is bidirectional, but many more cells migrate from DZ to LZ than vice versa (Victoria et al., 2010). In the LZ, centrocytes use their BCR to acquire antigen from the surface of FDCs. B cells can retrieve antigen by BCR internalization, and high affinity BCRs are better at capturing antigen compared to lower affinity BCRs (Batista and Neuberger, 2000; Victoria et al., 2010). The centrocytes can then present antigen on their MHCII to Tfh cells, with B cells that have higher affinity BCR presenting more peptide-MHC (Victoria et al., 2010). In the DZ, the class II MHC complexes are down-regulated, allowing B cells to reset their antigen content and prepare for a new round of antigen uptake and selection in the LZ (Bannard et al., 2016).

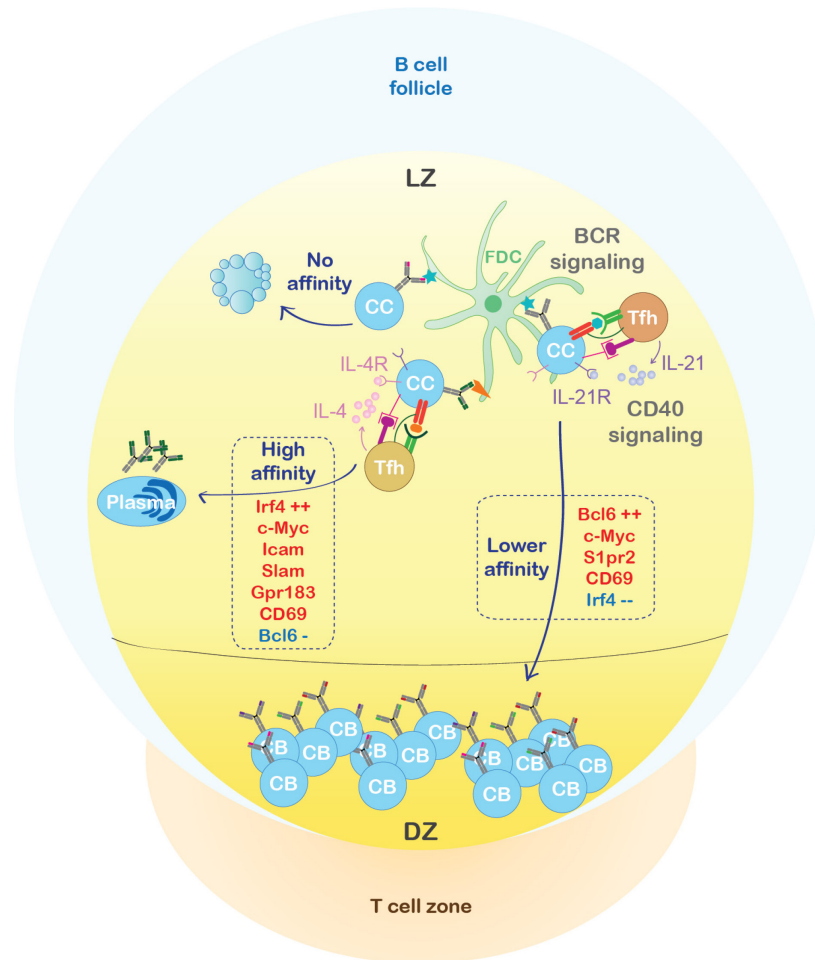


Figure 1.6 - GC B cell dynamics: balance between affinity maturation and differentiation

GCs are separated into two compartments: the light zone (LZ) composed of centrocytes and the dark zone (DZ) composed of centroblasts. B cells proliferate and undergo SHM in the DZ, then they migrate to the LZ where they receive (i) signals from cognate antigens via their BCR and (ii) T cell help through CD40 and cytokine receptors. GC B cell fate is influenced by the strength of these signals, which are proportional to the antibody affinity and induce the expression of different markers (Krautler et al., 2017) (Ise et al., 2018). Centrocytes that cannot bind antigen or compete for T cell help undergo apoptosis. Centrocytes that do bind antigen and receive T cell help can be separated into two populations that correspond to high and low affinity BCRs. Both populations are selected and induce expression of CD69 and c-Myc (Dominguez-Sola et al., 2012) (Luo et al., 2018) (Ise et al., 2018). B cells bearing lower affinity BCRs repress *Irf4*, express the pro-GC marker *Bcl6* and are believed to go back to the DZ for further rounds of affinity maturation (Ise et al., 2018). The high affinity B cells express high levels of *Irf4*, reduce *Bcl6* levels and experience strong T-B interactions due to the up-

regulation of adhesion molecules such as Icam and Slam. These cells induce the plasma cell transcriptional program and are believed to differentiate and exit the GC (Ise et al., 2018). The type of cytokines received from Tfh also influence GC B cell fate. Tfh first express IL-21, found to support GC maintenance, but later switch to IL-4, which promotes GC maintenance as well as B cell differentiation (Weinstein et al., 2016).

Tfh cells provide the critical signals to centrocytes for selection (Victora et al., 2010), resulting in either DZ re-entry or differentiation, with only 10-30% of B cells returning to the DZ (Meyer-Hermann et al., 2012). This process promotes selection of the B cells that express high-affinity antibodies. The extent of Tfh cell help provided to B cells is proportional to the T-B interaction strength and determines the number of cellular divisions that B cells can undergo in the DZ (Gitlin et al., 2014) (Bannard et al., 2013). However, while these mechanisms would promote the expansion and dominance of high affinity clones, studies have shown that GCs contain high intra- and inter- clonal diversity (Tas et al., 2016) (Kuraoka et al., 2016). Indeed, when mice are exposed to complex antigens, upon a viral infection for instance, despite overall antibody affinity improving with time, low affinity GC B cells as well as GC clonal diversity are still retained (Kuraoka et al., 2016). Centrocyte selection in the LZ is still an important field of research (Bannard and Cyster, 2017).

At the molecular level, productive T-B interactions are enforced by a positive feed-forward loop, mediated by inducible co-stimulatory molecule (ICOS) expressed on T cells that binds its ligand (ICOSL), at the B cell surface. ICOS-ICOSL interactions up-regulate the co-stimulatory molecule CD40 ligand (CD40L) at the T cell surface. CD40L binds to CD40 on B cells, and in turn promotes ICOSL expression by B cells (Liu et al., 2015a). Selection of high affinity B cells by Tfh cells is also enforced by secretion of cytokines IL-4 or IL-21 that support GC development (Shulman et al., 2014; Weinstein et al., 2016). Indeed, mice depleted for either *Il21* or *Il4Ra* show altered GC formation and antibody responses (Linterman et al., 2010) (King and Mohrs, 2009). *Il21*^{-/-} mice also show defective plasma cell production (Zotos et al., 2010). Interestingly, early Tfh cells express IL-21 and then switch to IL-4 expression as they differentiate (Weinstein et al., 2016). While both cytokines sustain the GC

reaction, IL-4 preferentially promotes plasma cell differentiation (Weinstein et al., 2016). Furthermore, Tfh cells express the pro-survival factor BAFF (Goenka et al., 2014), which supports the observation that low affinity B cells are more likely to undergo apoptosis, compared to high affinity ones (Anderson et al., 2009) (**Fig. 1.6**).

1.1.4.3 Antibody gene diversification in the GC

Ig mutations by AID

At the molecular level, affinity maturation depends on the process of somatic hypermutation (SHM). This entails the introduction of single point mutations at the variable exons of both the *IgH* and *IgL*, which randomly alter the affinity of antibodies for their cognate antigen. The mechanism is initiated by the enzyme activation induced deaminase (AID), encoded by the *Aicda* gene that is expressed almost exclusively in activated and GC B cells (Orthwein and Di Noia, 2012). AID induces point mutations by deaminating cytosine bases in single stranded DNA.

AID is expressed predominantly in centroblasts (Cattoretti et al., 2006), thus helping to separate mutagenesis from affinity selection, which occurs in the LZ. Thus, B cells that are positively selected in the LZ and re-enter the DZ will undergo additional rounds of SHM and acquire more mutations (Di Noia and Neuberger, 2007), which can increase their chance to acquire affinity-enhancing mutations (Rajewsky, 1996). B cells can also acquire mutations that perturb the expression of their BCR, leading to apoptosis (discussed later in **section 1.1.4.4**) (Mayer et al., 2017).

AID also deaminates specialized DNA regions, called switch regions, which are located up-stream of the *IgH* exons encoding each of the constant region classes. Processing of deamination within these regions can result in double stranded DNA breaks, triggering recombination between two switch regions. This results in a new constant region becoming associated to the variable region. This process allows antibodies to diversify their function and is called class switch recombination (CSR). Environmental stimuli, such as cytokine production, influence AID targeting to

different switch regions (Matthews et al., 2014), and thereby influence the isotype choice for CSR.

Thus, GC B cells, in particular centroblasts, undergo constant programmed DNA damage initiated by AID, which poses an additional challenge for their survival (discussed later in **section 1.1.4.4**).

P53 levels and DNA damage tolerance

For efficient SHM and CSR during the GC reaction, B cells must down-regulate the mechanisms that monitor for DNA-damage. Indeed, it has been shown in GC B cell lines that p53 transcription is repressed due to the binding of the transcription factor Bcl6 to its promoter region (Phan and Dalla-Favera, 2004). This observation is controversial though, as another study using primary B cells, demonstrated that reduced Bcl6 levels did not impact p53 protein but did reduce expression of Atr, a DNA damage sensor (Ranuncolo et al., 2007). On the other hand, p53 protein expression may still be regulated during the GC reaction, as activated B cells seem to store p53 mRNA in translationally silent stress granules (Diaz-Munoz et al., 2017). Stress granules are short-term repositories for mRNAs, preventing their degradation while limiting translation (Kedersha and Anderson, 2002), and they are induced upon B cell activation *in vitro* (Diaz-Munoz et al., 2017). Though the exact nature of p53 regulation in GC B cells remains unclear, p53 is critical for surveying genomic integrity in mature B cells; as in mice overexpressing AID, p53 depletion leads to the development of GC-derived mature B cell lymphomas (Robbiani et al., 2009). However, in a context of normal AID expression, p53 depletion in mature B cells leads to the development of lymphoma arising from non-GC cells: naïve mature B cells (Gostissa et al., 2013).

1.1.4.4 Surviving the GC reaction

Even though GC B cells undergo massive proliferation, the GC size can remain constant for several weeks (Robbiani et al., 2015), as GC homeostasis is maintained via programmed cell death of undesirable B cells. In the DZ, around half of the centroblasts express non-functional BCRs, resulting from AID-induced SHM, and

undergo apoptosis (Mayer et al., 2017). In the LZ, centrocytes undergo apoptosis by default, unless they are positively selected by Tfh_s (Mayer et al., 2017).

Apoptosis, can be triggered in the cell by two main pathways: the extrinsic pathway and the intrinsic pathway (Elmore, 2007). The extrinsic pathway is mediated by transmembrane receptors that can transmit death signals from the cell surface. These include receptors Dr5 and Fas/CD95, which are both expressed at the GC B cell surface (Crowder et al., 2011) (Hennino et al., 2001). Extrinsic pathway receptor engagement leads to activation of caspase 8, triggering the downstream caspase cascade that results in cell death (Elmore, 2007). In fact, ablating *Casp8* in mice promotes the formation of enlarged GCs and compromises antibody affinity maturation (Boulianne et al., 2013). The intrinsic pathway is dependent on the sensing of mitochondrial integrity and is triggered by non-receptor stimuli. The mitochondria outer membrane contains Bcl2-family members that are either anti-apoptotic (Bcl-2, Bcl-XL, myeloid leukemia 1 (Mcl-1), A1) or pro-apoptotic (Bax, Bak, Puma, Noxa, Bcl-2 antagonist of cell death (Bad)) (Brenner and Mak, 2009). Pro- and anti- apoptotic proteins can associate, maintaining an inactive equilibrium. Induction of pro-apoptotic genes, or down-regulation of anti-apoptotic genes disturbs this equilibrium, leading to permeabilization of the mitochondrial outer membrane and release of cytochrome-c, which activates caspases. Both the extrinsic and intrinsic pathways ultimately lead to caspase-3 activation, which triggers cell death.

In GCs, specific receptors can positively or negatively modulate B cell survival, such as Fas/CD95, CD40 and the BAFF receptor (BAFFR). CD95 is highly expressed at the GC B cell surface, and as part of the extrinsic pathway, it can induce apoptosis of B cells that have lost antigen reactivity and prevent expansion of autoreactive B cells (Butt et al., 2015). CD40 and BAFFR are both members of the tumor necrosis factor (TNF) receptor family and signal through the NF- κ B pathway to induce expression of genes that promote B cell survival and proliferation. NF- κ B signaling involves hetero- or homo-dimers, composed of the 5 NF- κ B subunits c-Rel, Rela (p65), Relb, p52 and p50. Dimers are normally inactive in the cytoplasm but upon activation they translocate to the nucleus where they induce gene transcription. The canonical NF- κ B

pathway involves the c-Rel/p50 and RelA/p50 dimers and these respond to CD40 activation. The non-canonical NF- κ B pathway involves the RelB/p52 dimer and responds to CD40 and to BAFFR as well. BAFF ligand induces B cell survival through the up regulation of Bcl-2 and Bcl-XL and down regulation of Bak (Do et al., 2000). During the GC reaction Mcl1, and not Bcl-XL, is essential (Vikstrom et al., 2010); however, Bcl-2, Mcl-1 and A1 contribute to the survival of activated B cell in vitro (Carrington et al., 2017).

1.1.4.5 The GC B cell transcriptional program

In order to perform their specific functions, centrocytes and centroblasts have slightly distinct transcriptomes (Victora et al., 2012). Centrocytes are enriched for CD40 and BCR gene expression signatures, while DZ B cells induce proliferation genes (Victora et al., 2010) (Victora et al., 2012). Transcriptional changes derive from the differential expression and/or action of key transcription factors that are specific for either centrocytes or centroblasts.

The Centrocyte program

The transcription factor c-Myc helps initiate GC formation (Calado et al., 2012), and promotes GC maintenance by stimulating cyclic DZ re-entry (Calado et al., 2012; Dominguez-Sola et al., 2012). c-Myc is only detected in a small subset of centrocytes in the LZ (Calado et al., 2012; Dominguez-Sola et al., 2012) that have received synergistic CD40 and BCR signaling (Luo et al., 2018). Mechanistically, CD40 signals through NF- κ B, inducing *c-Myc* transcription, while BCR activation promotes the degradation of Forkhead box O 1 (Foxo1, discussed later) that represses *c-Myc* transcription (Luo et al., 2018). The transcriptome of c-Myc⁺ cells displays an activated phenotype, suggesting that these cells are cycling. These c-Myc⁺ cells are also enriched for high-affinity *Ig* variants compared to the c-Myc⁻ GC B cell counterparts (Calado et al., 2012; Dominguez-Sola et al., 2012) and show a low rate of apoptosis (Mayer et al., 2017). In the DZ, *c-Myc* is repressed by Bcl6 (Dominguez-Sola et al., 2012).

NF- κ B transcription factors are found to translocate to the nucleus in a small subset of LZ B cells (Basso et al., 2004), corresponding to the B cells that received CD40 co-stimulatory signal (Luo et al., 2018). Deleting c-Rel reveals a role in maintaining the GC reaction by promoting B cell proliferation. RelA on the other hand is dispensable for the GC reaction but required for plasma cell differentiation by inducing the expression of the pro-differentiation transcriptional repressor *Prdm1* (that encodes for Blimp-1) (Heise et al., 2014).

The Centroblast program

B-cell lymphoma 6 protein (Bcl6), is a transcriptional repressor that is critical for GC formation and maintenance. Thus, Bcl6 is a master regulator of the GC program, and is not only necessary for proper GC function but also for GC B cell trafficking and survival. Indeed, Bcl6 promotes *Aicda* expression by limiting expression of AID targeting micro-RNAs (Basso et al., 2012), and prevents premature B cell exit from the GC by repressing *Prdm1* (Tunyaplin et al., 2004). Bcl6 also inhibits cell cycle arrest, by repressing *Cdkn1a*, which encodes p21 (Phan et al., 2005), and modulates B cell apoptosis by repressing the anti-apoptotic gene *Bcl-2* (Saito et al., 2009). Finally, *Bcl6*^{-/-} GC precursors are unable to migrate to the B cell follicle in mice (Kitano et al., 2011).

Foxo1 is a transcription factor that promotes the transcription of numerous genes involved in cell growth, differentiation and apoptosis (Greer and Brunet, 2005). Downstream from the PI3K-AKT pathway, Foxo1 is phosphorylated by Akt promoting its cytoplasmic localization and subsequent polyubiquitination and proteasomal degradation (Greer and Brunet, 2005). The PI3K-AKT pathway is induced downstream of BCR signalling (Luo et al., 2018), and is restricted to the LZ, thereby promoting Foxo1 degradation specifically in the LZ, while permitting nuclear Foxo1 in DZ B cells (Sander et al., 2015) (Dominguez-Sola et al., 2015). Deletion of *Foxo1* results in loss of the DZ in GCs, and a de-repression of the LZ program, suggesting that Foxo1 maintains the DZ phenotype (Sander et al., 2015) (Dominguez-Sola et al.,

2015). In contrast, abrogating BCR signalling using *Syk*^{-/-} mice enhances nuclear Foxo1 stability and DZ expansion to the cost of LZ (Luo et al., 2018).

Interferon-regulatory factor 4 (*Irf4*) is a transcription factor that plays a dose-dependent role in regulating both the LZ and the DZ GC program. Low levels of *Irf4* are required for initiation of the GC, promoting *Aicda* and *Bcl-6* expression in the DZ (Ochiai et al., 2013); however, high levels of *Irf4* repress *Bcl-6*, thereby promoting GC termination (Sciammas et al., 2006). GC termination is induced by CD40 stimulation in the LZ that boosts *Irf4* expression via NF- κ B (Saito et al., 2007).

It is becoming clear that GC B cell fate is influenced by the strength of BCR signaling (Krautler et al., 2017) and CD40 signaling (Ise et al., 2018) in the LZ, which are determined by the B cell antibody affinity for the antigen. As a result, high and lower affinity centrocytes express different markers, thereby leading to plasma cell differentiation or DZ re-entry (Ise et al., 2018) (**Fig. 1.6**).

1.1.5 B cell differentiation

Following antigen encounter and cognate T cell interaction, B cells can follow three different paths: form a GC, differentiate into memory B cells, or differentiate into short-lived ASCs. This choice is largely influenced by the B cell antibody affinity (Schwickert et al., 2011). Some activated B cells will give rise to GCs, but a portion of lower affinity cells will differentiate into memory B cells (Kurosaki et al., 2015), while a proportion of B cells with higher affinity antibodies will give rise to an extra-follicular response generating ASCs (Paus et al., 2006). During the GC reaction, LZ B cells face a similar situation: choosing to either migrate back to the DZ, differentiate into memory B cells or differentiate into long-lived ASCs.

1.1.5.1 Memory B cells

Despite the fact that some memory B cells arise independently of the GC, the vast majority are GC-derived (Shinnakasu et al., 2016). These are the first cells to exit the GC response, and are consequently of lower affinity (Weisel et al., 2016). Memory B cell differentiation is dependent on the expression of the transcriptional repressor

Bach2. Bach2 enforces low affinity memory responses, as its expression is reduced following strong T-B interactions (Shinnakasu et al., 2016). The advantage of generating low-affinity memory B cells is to promote poly-reactivity and retain the ability to adapt to changing pathogens. Upon a second antigen encounter, memory B cells can rapidly seed new GCs, or differentiate into ASCs (Smith et al., 1996).

1.1.5.2 Antibody secreting cells

ASCs provide humoral immunity by constantly secreting antibodies. As a result, ASCs undergo major cellular changes, such as increased transcription of *Ig* loci, and a shift from expression of membrane-bound to secreted antibodies, for which they expand the secretory pathway. These changes occur via Blimp-1 dependent mechanisms (Minnich et al., 2016; Shi et al., 2015). Due to a massive increase in protein synthesis, to produce secreted antibodies, ASCs induce a stress response called the unfolded-protein response (UPR). The UPR causes morphological changes to the B cell, in particular enlarging the endoplasmic reticulum (ER), which is the site of antibody biosynthesis. In order to cope with antibody production, ER chaperones and folding enzymes are up-regulated (Gass et al., 2004). Interestingly, the UPR is closely linked to ASC differentiation, as the transcription factor X-box binding protein 1 (Xbp1), which sustains the UPR, also promotes plasma cell differentiation (Reimold et al., 2001). As mentioned above, the transcription factors Irf4 (Mittrucker et al., 1997) and Blimp-1 (Shapiro-Shelef et al., 2003) are two critical transcription factors required for ASC differentiation.

The extrafollicular response

B cells that differentiate into ASCs after interacting with T cells at the T-B border are called plasmablasts (PBs), these cells are short-lived and proliferate (Nutt et al., 2015). In mice immunized with NP, PBs first appear 3 days after immunization and peak at day 7, but are gone by 2 weeks (Smith et al., 1996). PBs have the ability to undergo CSR (Meli et al., 2017); however, SHM is restricted to the GC, so PBs generally secrete lower affinity antibodies compared to GC-derived ASCs (Jacob et al., 1993). As PBs express the highest affinity antibodies among the pre-GC B cell

pool (Paus et al., 2006), the extrafollicular response provides a rapid protective response while more efficient antibodies are being produced in the GC (**Fig. 1.5, 1.6**).

Long lived ASCs

Long-lived ASCs, or plasma cells (PCs), differentiate from the GC LZ centrocytes after positive selection (Weisel et al., 2016). As a result, PCs express high affinity antibodies that have undergone SHM. A recent study showed that early-differentiated GC-derived plasmablasts exit the GC via the DZ, at the interface with the T cell zone, called the GC-T cell zone interface (GTI) (Zhang et al., 2018). Following lymphoid organ egress, PCs enter the circulation and follow a CXCL12 gradient towards the BM, due to CXCR4 expression on their surface (Tokoyoda et al., 2004). A characteristic of PCs is their quiescent state, in part due to transcriptional repression of *c-Myc* by Blimp-1 (Lin et al., 2000; Lin et al., 1997). PCs will settle in BM niches, where they can associate with stromal cells and stay in close proximity to haematopoietic cells that secrete pro-survival factors (Tangye, 2011). For instance, eosinophils express April, a factor that can bind the receptor B cell maturation antigen (Bcma), and induce the expression of Mcl-1 (Peperzak et al., 2013). PCs can persist for over one year in the BM (Slifka et al., 1998), providing long-lasting antibody production. At the molecular level, PCs express higher levels of Blimp-1 compared to PBs (Kallies et al., 2004). Upon GC exit, PCs may go through an intermediate PB-like stage, as ASCs found in the blood following immunization (most likely migrating to the BM), express intermediate levels of Blimp-1 (Blink et al., 2005) and express the proliferation marker Ki67 (Odendahl et al., 2005), both features of PBs.

1.1.5.3 The ASC transcriptional program

Differentiation of GC B cells into ASCs requires termination of the GC program, which is mediated in part by transcription factors such as Irf4. Irf4 is not only involved in GC termination by down-regulating *Bcl6* (Saito et al., 2007), but it also promotes ASC differentiation by activating *Prdm1* (Kwon et al., 2009). By repressing pro-GC genes, Blimp-1 is responsible for 40% of the gene expression changes that are observed upon B-cell differentiation (Minnich et al., 2016). Blimp-1 also induces pro-

differentiation genes such as *Xbp1* and *Irf4* (Minnich et al., 2016). Despite PCs and PBs sharing a common transcriptional signature, including genes mediating transcription, protein transport, and the UPR (Shi et al., 2015), PBs selectively induce genes that promote proliferation (Shi et al., 2015). Nonetheless, B cell differentiation to both PBs and PCs is linked to proliferation, as B cells can only acquire ASC features (i.e. defining gene expression signatures) over the course of multiple cell divisions (Hasbold et al., 2004) (Shi et al., 2015).

1.1.6 B cells and cancer development

B cells are subjected to endogenous DNA damage during development by the RAG recombinases, and in mature B cells by AID expression. Such lesions are beneficial because they promote antibody diversification and affinity maturation; however, they can also lead to B cell transformation when affecting genes outside the *Ig* loci.

Most B cell non-Hodgkin lymphomas (B-NHL) (lymphomas that do not present Reed-Sternberg cells) are derived from GC B cells (Kuppers et al., 1999). Chromosomal translocations that can fuse the *Ig* loci promoters or enhancers to proto-oncogenes result in dysregulated oncogene expression; these are common abnormalities in mature B cell lymphomas (Robbiani and Nussenzweig, 2013). Such lesions often arise from DNA double stranded breaks induced by AID simultaneously at the *Ig* locus and another off-target locus (Kuppers and Dalla-Favera, 2001). A well-studied example is the *IgH-Myc* translocation that gives rise to Burkitt's lymphoma. This translocation alleviates Bcl6 repression of *c-Myc*, leading to elevated c-Myc levels that drive lymphomagenesis (Dalla-Favera, 2015). Interestingly Burkitt's lymphoma cells resemble centroblasts, despite the fact that c-Myc is normally excluded from the DZ (Victoria et al., 2012).

Mature B cells undergo major changes during the transitions from activation and initiation of a GC, to their differentiation, and these changes involve regulatory networks. Altering these pathways can also result in lymphomagenesis (Dalla-Favera, 2015). The most common type of B-NHL is called diffuse large B cell lymphoma

(DLBCL), which can either be derived from LZ B cells (referred to as GCB-DLBCL) or cells that are committed to plasma differentiation (referred to as activated B cell type, or ABC-DLBCL). Most of DLBCL cases are linked with epigenetic perturbation due to inactivation of chromatin modifiers such as the acetyltransferase EP300 and the methyltransferase MLL2. These epigenetic changes promote B cell reprogramming and predispose to tumorigenesis (Morin et al., 2011). Other common changes involve gain of function mutations of the lysine methyltransferase Enhancer of zeste homologue 2 (Ezh2, discussed below), found in 20% of GCB-DLBCL cases (Morin et al., 2010). Mouse models carrying such mutations accumulate extensive H3K27me3 marks throughout their genome. This locks the B cells in the GC program and eventually drives development of lymphoma (Beguelin et al., 2013). Mutations deregulating BCL6 are also found in DLBCL patients, as these will also drive lymphomagenesis by maintaining B cells in a pro-proliferative state and preventing their terminal differentiation (Dalla-Favera, 2015).

1.1.7 Post-translational modifications in B cell biology

Post-translational modifications (PTM) are covalent enzymatic modifications to proteins catalyzed by specific enzymes. These include phosphorylation, methylation, acetylation and ubiquitination of different protein residues. These modifications have a major role in regulating dynamic processes such as signalling and epigenetics. The addition and removal of PTMs that mediate signaling pathways and change chromatin function are critical for B cells to respond rapidly to environmental cues, or to choose between distinct differentiation fates. While the vast majority of the work in B cells has been focused on dynamic changes in phosphorylation, the importance of unconventional posttranslational modifications, such as o-glucnacylation or methylation, is becoming increasingly clear (Mowen and David, 2014; Wu et al., 2017).

Signaling

Signaling via various membrane receptors allows B cells to sense environmental stimuli and induce major phenotype changes, altering transcription, metabolism, and

proliferation rates. Signals emanating from two receptors are particularly important for B cells:

BCR cross-linking activates protein tyrosine kinases, such as Lyn, Syk and Btk that induce a cascade of phosphorylation events, starting with the BCR components Ig α and Ig β . This cascade will lead to (i) calcium release and the activation of mitogen activated protein kinases (MAPK) resulting in apoptosis, or (ii) activation of the transcription factor NF- κ B, promoting survival and proliferation (Niuro and Clark, 2002). Ig α is methylated by the arginine methyl transferase Prmt1 at arginine 198, which is close to its last ITAM at tyrosine 193 (Infantino et al., 2010). This modification limits PI3K-AKT signaling downstream of the BCR, possibly by preventing Syk binding to Ig α . In GC B cells, as mentioned above, BCR signalling activates the Syk-PI3K-AKT pathway, resulting in Foxo1 phosphorylation and its sequestration in the cytoplasm (Luo et al., 2018).

CD40 signalling plays critical roles in B cells during activation at the T-B border, as well as in the LZ. The interaction between CD40 in B cells and CD40L on T cells promotes the recruitment of TNFR-associated factors (TRAFs) to the cytoplasmic domain of CD40, these adapter proteins will promote the activation of the NF- κ B pathway. The inhibitor proteins I κ Bs maintain NF- κ B subunits p50/Rela and p50/c-Rel in the cytoplasm. Upon CD40 cross-linking, I κ Bs are phosphorylated by I κ Bs kinase (IKK) complexes. I κ B phosphorylation leads to their ubiquitination and proteasomal degradation, allowing the active NF- κ B heterodimer to access the nucleus and activate target genes (Bonizzi and Karin, 2004; Klein and Heise, 2015; Luo et al., 2018).

c-Myc is exclusively induced in GC B cells that are simultaneously stimulated in the LZ by both the BCR and CD40 (Luo et al., 2018). In contrast, stimulating either signaling pathway alone can increase c-Myc in naïve B cells *in vitro*, showing that, similar to the gene expression program, the signalling program of GC B cells is rewired compared to resting B cells (Luo et al., 2018).

Epigenetics

B cells undergo major transcriptional changes as they transition from mature FO to GC activated cells and from GC cells to differentiated ASCs (Shi et al., 2015). Histone modifications underlie these changes by enhancing or preventing recruitment of effector proteins to the chromatin (Heinz et al., 2010). Indeed, naïve resting and GC B cells have very distinct distributions of chromatin mark (Zhang et al., 2014). Histone modifications are PTMs added by a variety of enzymes that can fall into the categories of histone acetyltransferases, which add acetyl groups to lysines, and histone methyltransferases that add methyl groups to either lysine or arginine residues. They modify the N-terminal tail of histones, thereby modulating chromatin accessibility and gene expression.

Monocytic leukemia zinc finger protein (Moz) is an histone acetyltransferase that has been shown to be important for the GC reaction, as its depletion results in a reduced number of GC B cells, due to a reduction of centroblasts (Good-Jacobson et al., 2014).

Ezh2 is a histone methyltransferase that is part of the polycomb repressive complex-2 (PRC2), which catalyzes the methylation of lysine 27 on histone 3 (H3K27me3), a repressive mark. Ezh2 is up regulated in GC B cells, particularly in centroblasts (van Galen et al., 2004) and maintains the GC program (Velichutina et al., 2010). This is in part due to its repression of the proliferation checkpoint factor *Cdkn1a* (Beguelin et al., 2013). Indeed, *Ezh2*^{-/-} B cells fail to form GCs, which are rescued when mice are crossed with *Cdkn1a*^{-/-} mice (Beguelin et al., 2017). P21, encoded by *Cdkn1a*, inhibits activity of CDK4/6 and CDK2, responsible for retinoblastoma (Rb) phosphorylation (Lundberg and Weinberg, 1998). Rb phosphorylation leads to its dissociation from the transcription factor E2f1, subsequent transcription of E2f1 targets genes and cell cycle progression into S-phase (Chen et al., 2009; Lundberg and Weinberg, 1998). E2f1 is up-regulated in GCs and promotes GC B cell proliferation in a positive feedback loop: E2f1 induces *Ezh2* transcription, which represses *Cdkn1a*, leading to increased levels of Rb phosphorylation, resulting in increased E2f1-dependent transcription (Beguelin et al., 2017). Conversely, mice expressing an Ezh2 gain of function mutant show GC hyperplasia upon immunization

(Beguelin et al., 2013). Ezh2 is also responsible for forming most bivalent genes in GC B cells (Beguelin et al., 2013). Bivalent genes are poised genes, characterized by co-localization of both the activating H3K4me3, and repressive H3K27me3 marks (Bernstein et al., 2006). Establishment of this antagonizing mark at the genes of key lineage transcription factors limits their expression until a final differentiation choice is made. Indeed, the key pro-differentiation transcription factors *Irf4* and *Prdm1* are among GC-specific bivalent genes (Beguelin et al., 2013). Therefore, like *Bcl6*, Ezh2 is a master regulator of the GC B cell phenotype, by promoting the GC program and limiting B cell differentiation.

Protein arginine methyltransferase 7 (Prmt7) is part of the PRMT enzyme family that is extensively discussed in the next section. Prmt7 is responsible for histone arginine mono-methylation, particularly at arginine 3 of the histone H4 (H4R3me1) (Ying et al., 2015). Over expression of Prmt7 in B cell lines causes the accumulation of H3R4me1 at the *Bcl6* gene and down-regulation of *Bcl6* expression (Ying et al., 2015). Conversely, Prmt7 depletion in B cells leads to increased *Bcl6* transcripts in GCs, resulting in increased GC B cell numbers (Ying et al., 2015). Thus, histone arginine methylation by Prmt7 limits GC B cell formation via *Bcl6* repression.

1.2 Arginine Methylation

1.2.1 Arginine methyltransferases

In mammals, it is estimated that around 0.5% of arginine residues throughout the proteome are methylated (Matsuoka, 1972). Arginine methylation can modify protein structures and/or their ability to interact with DNA, RNA or other proteins (Bedford and Richard, 2005); therefore, it can regulate protein function and cellular biology (Bedford and Clarke, 2009; Bedford and Richard, 2005). Arginine methylation is a post-translational modification carried out by members of the protein arginine methyltransferase (PRMT) family, and is found in all eukaryotes (Bachand, 2007). The PRMT family consists of nine members, which can catalyze the transfer of a

methyl-group from S-adenosylmethionine (AdoMet, or SAM, see **Fig. 1.8A**) to one of the two terminal guanidino nitrogen atoms in arginine (Gary and Clarke, 1998). This enzymatic reaction produces a monomethylarginine (MMA) on the target protein and S-adenosylmonocysteine as a by-product. Interestingly, only PRMT7 monomethylates arginines (Blanc and Richard, 2017), with all other PRMTs transferring an additional methyl group to the arginine. PRMTs that dimethylate arginines via the transfer of a second methyl-group to the same guanidino nitrogen atom, producing asymmetric dimethylarginine (aDMA), are classified as Type I PRMTs (PRMT1, PRMT2, PRMT3, PRMT4, PRMT6 and PRMT8). PRMTs that dimethylate arginine through the transfer of a second methyl-group to the other guanidino nitrogen atom, producing symmetric dimethylarginine (sDMA), are classified as Type II PRMTs (PRMT5 and PRMT9) (**Fig. 1.7**). In this thesis I have analyzed the function and relevance of PRMT1 and PRMT5 in B cell biology.

PRMT1 and PRMT5 are the major Type I and Type II PRMTs

PRMT1 and PRMT5 are responsible for the majority of aDMA and sDMA, respectively (Blanc and Richard, 2017; Tang et al., 2000). This also seems to be the case in activated mature B cells, as they are the two most abundant PRMT transcripts measured by RNAseq (**Fig 3.1B**). Complete knock-out of either *Prmt1* or *Prmt5* are embryonically lethal, suggesting that there is little functional redundancy between these enzymes and their type I or II counterparts, respectively (Pawlak et al., 2000) (Tee et al., 2010). However, downregulation of PRMT1 can increase arginine methylation mediated by other PRMTs, a phenomenon called substrate scavenging, suggesting that different PRMTs can compete for the same substrates (Dhar et al., 2013).

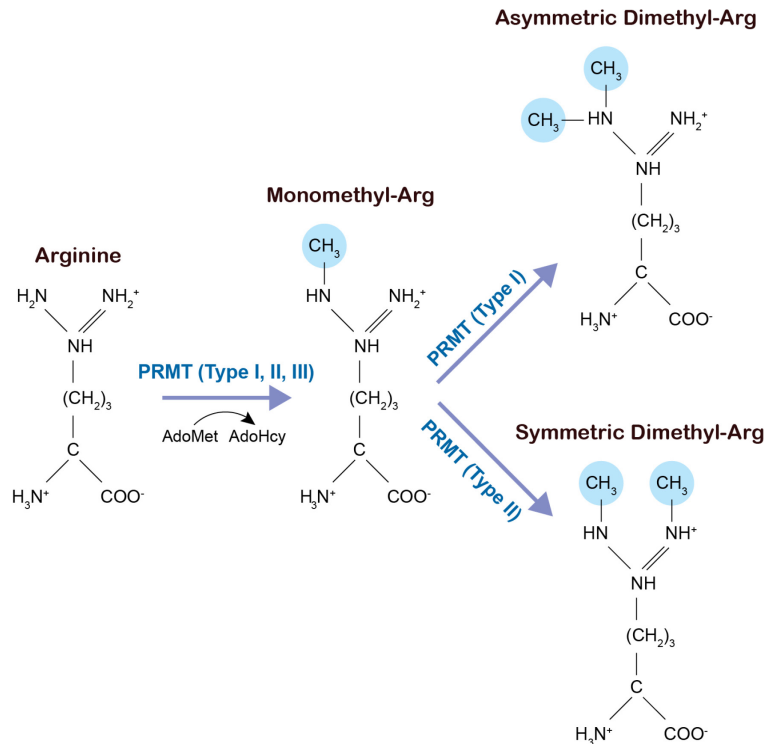


Figure 1.7 - Arginine methylation

The PRMT family of enzymes can be divided into three types. Type III PRMTs, like PRMT7, monomethylates arginines. Type I PRMTs, like PRMT1, PRMT2, PRMT3, PRMT4, PRMT6 and PRMT8 perform asymmetric dimethylation. Type II PRMTs, like PRMT5 and PRMT6, deposit symmetric dimethylation at arginines.

PRMT1 and PRMT5 are often upregulated in cancers, which has prompted the development of PRMT inhibitors (Kaniskan et al., 2018). Recent developments include a type I specific PRMT inhibitor, MS023 (Eram et al., 2016), along with a PRMT5-specific inhibitor, EPZ015666, which is in clinical trial for treatment of mantle cell lymphoma (Chan-Penebre et al., 2015) (**Fig. 1.8**). Neither EPZ015666 nor MS023 compete with SAM, nonetheless they compete with the peptide substrate (Hu et al., 2016; Kaniskan et al., 2018).

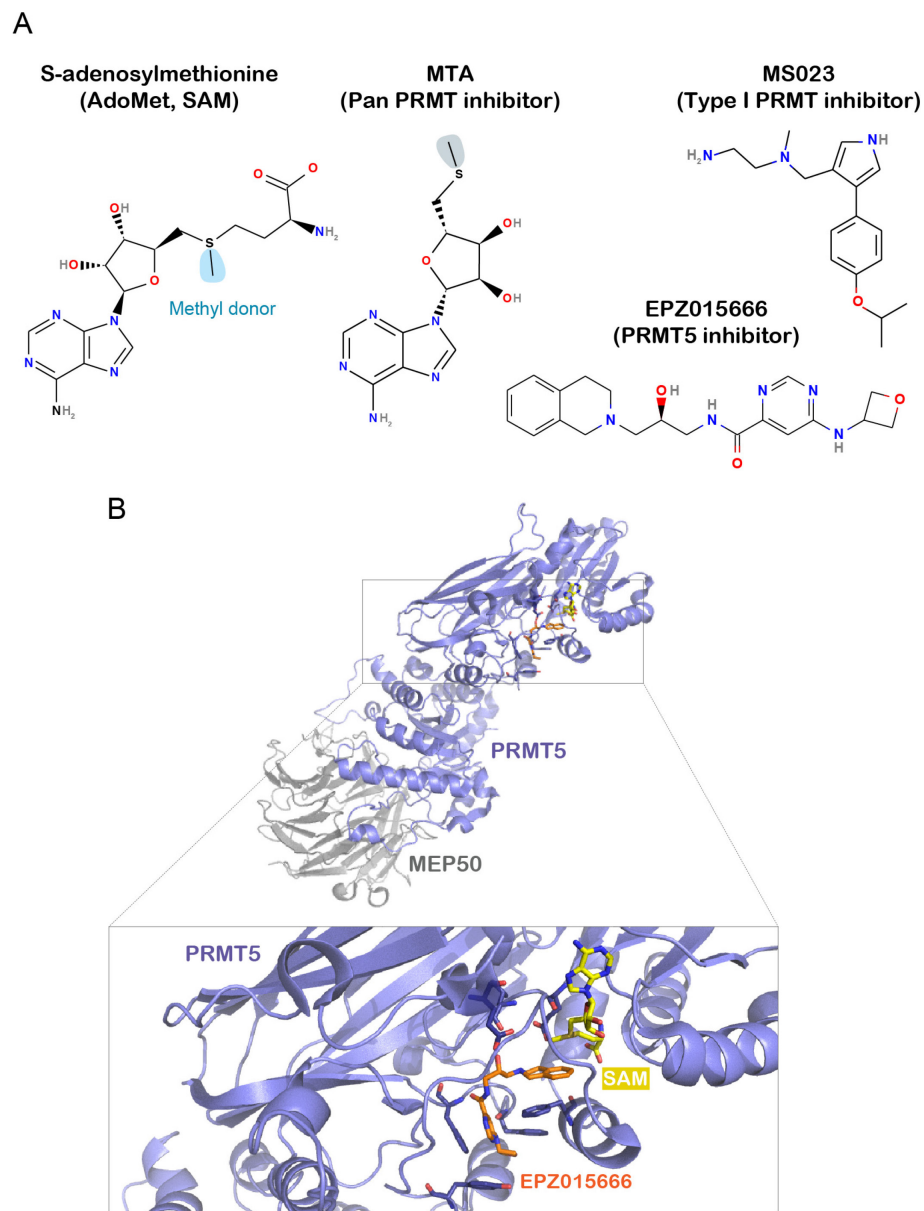


Figure 1.8 - Inhibitors of arginine methylation

A) Chemical structures of S-adenosylmethionine (SAM) and inhibitors of type I PRMTs and PRMT5, MSO23 and EPZ015666 respectively. The methyl donor of SAM transferred by PRMTs to arginines is highlighted in blue. Methylthioadenosine (MTA) is an endogenous SAM analogue, acting as a pan PRMT inhibitor.

B) Crystal structure of PRMT5 (purple) in complex with MEP50 (grey), bound to EPZ015666 (orange) and SAM (yellow) (PDB accession number: 4X61). Side chains of PRMT5 residues that are in contact with SAM and EPZ015666 are depicted.

1.2.2 Arginine methylation, readers and erasers

Target specificity

PRMTs preferentially methylate arginines within arginine- and glycine- rich motifs called RGG/RG motifs (Palaniraja Thandapani, 2013). In addition, PRMT5 methylates substrates that harbour arginines within proline- ,glycine- and methionine- rich regions, called PGM motifs (Cheng et al., 2007).

Tudor-domain proteins

Methylarginine can be recognized by specific domains. The principle type is the Tudor domain, which defines the Tudor family of proteins (Chen et al., 2011). As readers of arginine methylation, tudor domain proteins are involved in different downstream activities. For example, proper splicing (explained below) depends on binding of the tudor domain protein survival of motor neuron (SMN) to methylated Sm proteins (Friesen et al., 2001). Tudor domain proteins are also involved in regulating gene expression, by associating with methylated histones (Gayatri and Bedford, 2014). Indeed, PRMTs have been shown to methylate histone tails at H4R3, H3R8, H2AR2 positions, which can influence transcription (Di Lorenzo and Bedford, 2011). However, most arginine-methylated proteins are not histones (Bremang et al., 2013).

Arginine demethylation

Arginine methylation is involved in dynamic processes such as signalling. For instance in B cells, the BCR is methylated by PRMT1 but is quickly demethylated, within 2-5 minutes, upon BCR stimulation (Infantino et al., 2010). This suggests the existence of a demethylation mechanism; however, no specific arginine demethylases have been discovered. A recent study has demonstrated that certain lysine demethylases (KDM3A, KDM4E, KDM5C) can have arginine demethylase activity *in vitro*, but such activity has not been confirmed *in vivo* (Walport et al., 2016).

1.2.3 PRMT5

1.2.3.1 Structure

The first crystal structure of PRMT5 was from *Caenorhabditis elegans*, and was resolved in complex with S-adenosylmonocysteine (Sun et al., 2011). Soon thereafter, the structure of human PRMT5 was determined in complex with the methylome protein 50 (MEP50, also named WDR77), bound to SAM (Antonysamy et al., 2012). PRMT5 and MEP50 have been shown to form a stable and active hetero-octameric structure *in vitro* (PRMT5₄:MEP50₄) (Antonysamy et al., 2012). PRMT5 association with MEP50 is clearly important, as it is quite general (Friesen et al., 2002; Guderian et al., 2011; Tee et al., 2010), enhances PRMT5 methyltransferase activity (Antonysamy et al., 2012) and is critical for PRMT5 substrate recognition *in vitro* (Wang et al., 2014).

1.2.3.2 Expression

PRMT5 is highly expressed in several cancers, correlating with poor prognosis in B cell lymphomas (Koh et al., 2015b), glioblastomas (Yan et al., 2014), lung cancer (Gu et al., 2012a) and colorectal cancer (Zhang et al., 2015a). Some mechanisms underlying PRMT5 over-expression in different tumour cells have been identified. In the *Eμ-Myc* mouse model of pre-B cell lymphoma, c-Myc binds to the *Prmt5* promoter and stimulates *Prmt5* transcription (Koh et al., 2015b). PRMT5 expression can also be regulated post-transcriptionally by miRNAs, as seen in mantle cell lymphoma, GC-derived B cell lymphomas and Epstein-Barr virus (EBV)-transformed B cells (Alinari et al., 2015a; Pal et al., 2007; Wang et al., 2008), where down-regulation of PRMT5-specific micro-RNAs promotes PRMT5 expression.

The regulation of PRMT5 expression in normal cells has not been extensively studied. In normal B cells, information is scarce, but it has been suggested that *Prmt5* expression in mouse BM B cells is regulated post-transcriptionally, because BM B cells have comparable *Prmt5* mRNA levels with HSCs, yet protein levels are four times higher in HSCs (Liu et al., 2015b). This could be due to miRNAs, as the *Prmt5*

mRNA contains miRNA target sequences (Alinari et al., 2015b; Pal et al., 2004; Wang et al., 2008); however, the expression of Prmt5 throughout B cell development has not been studied. In mature B cells, Prmt5 transcription increases upon stimulation *in vitro*, along with increased protein and sDMA levels (Igarashi et al., 2009). Prmt5 transcripts, protein and activity have also been reported to be upregulated in GCs *in vivo* (Igarashi et al., 2009). Of note, PRMT5 is stabilized by the chaperone Hsp90 (Maloney et al., 2007), suggesting post-translational regulation as well.

1.2.3.3 Cellular processes regulated by PRMT5

Transcription

PRMT5 activity can regulate transcription in three distinct ways (**Fig 1.9**).

1. Histone methylation

PRMT5 methylation of histone H3 (H3R8me2s) and/or histone H4 (H4R3me2s) are commonly associated with repression of target genes. Known target genes include the transcription factors *St7* and *Rbl2* (Pal et al., 2007; Wang et al., 2008), the E3-ubiquitin ligase *Cula4* (Aggarwal et al., 2010), the micro-RNAs *miR-96* and *miR29-b* (Alinari et al., 2015b; Tarighat et al., 2016) and the cyclin-dependant kinase inhibitor *Cdkn1a* (Kaushik et al., 2017; Zhang et al., 2015b). PRMT5 and its target histone marks have been found to co-exist at *St7* and *Rbl2* along with the PRC2 heterochromatin complex, likely to facilitate gene silencing. This association requires recruitment by bromodomain containing 7 (BRD7) (Tae et al., 2011).

Chromatin remodelling complexes are made of different proteins that displace nucleosomes in an ATP-dependant manner, promoting transcriptional activation or repression by modifying DNA accessibility. PRMT5 associates with the chromatin remodelling complexes Brg1 associated factors (BAF) (Pal et al., 2004) and NuRD (Le Guezennec et al., 2006). Such associations between histone modifying enzymes and chromatin remodelling complexes can facilitate the conversion of chromatin from an active to a repressed state and vice versa (Pal and Sif, 2007).

Finally, the PRMT5 mark H4R3me2s recruits the DNA methyltransferase DNMT3A, which further enforces gene silencing (Zhao et al., 2009).

2. RNA polymerase II elongation

SPT5, a critical elongation factor that associates with RNA polymerase II (RNAPII), can be methylated by PRMT1 and PRMT5 (Kwak et al., 2003). SPT5 methylation by either PRMT reduces its association with RNAPII, modulating transcription elongation (Kwak et al., 2003). Moreover, RNAPII can be directly methylated by PRMT5 at its carboxy-terminal domain, which allows the recruitment of the tudor domain protein SMN to promote the resolution of RNA/DNA hybrids called R-loops (Zhao et al., 2016). This modification and function are critical for transcription termination (Zhao et al., 2016).

3. Methylation of transcription factors

PRMT5 can methylate several transcription factors: p53 (Jansson et al., 2008; Li et al., 2015b), the NF- κ B subunit RelA (Harris et al., 2014; Wei et al., 2013), Krüppel-like factor 4 (Klf4) (Hu et al., 2015) and E2f1 (Cho et al., 2012; Zheng et al., 2013). As discussed in the previous section, they play important roles in B cells.

PRMT5 can methylate p53 (Jansson et al., 2008; Li et al., 2015b), which subsequently influences p53 targeting, such as inducing *CDKN1A* transcription in a human cell line (Jansson et al., 2008). Conversely, p53 methylation has been reported to inactivate its activity in leukemic cells, making them resistant to cell death and cell cycle arrest (Li et al., 2015b). The consequence of p53 methylation by Prmt5 is therefore context dependant.

Klf4 is also methylated by PRMT5, this prevents Klf4 poly-ubiquitination and increases its stability (Hu et al., 2015). In B cells, *Klf4* expression is detectable during B cell development in the BM, increases in mature resting B cells but is repressed upon activation (Klaewsongkram et al., 2007). Klf4-depleted B cells show cell cycle defects, associated with reduced expression of cyclinD2 protein (Klaewsongkram et al., 2007). In humans, KLF4 is expressed in BM plasma cells and its expression

correlates with enhanced differentiation by upregulating plasma cell programs (Schoenhals et al., 2016). As a transcription factor, Klf4 can activate or inhibit genes involved in different processes such as cell-cycle, apoptosis, adhesion and metabolism, acting as both a tumour suppressor and as an oncogene, depending on the cellular context (Rowland and Peeper, 2006). Notably, methylation of KLF4 by PRMT5 may contribute to breast cancer development as mice implanted with human tumour cells expressing a methylation-resistant KLF4 mutant showed reduced tumour sizes (Hu et al., 2015).

PRMT5 methylation of E2F1 reduces its half-life, but enhances E2F1 binding capacity to some target genes, repressing their expression (Zheng et al., 2013) (Cho et al., 2012). E2F1 is critical for the GC reaction, as mice with E2F1-depleted B cells cannot form GCs (Beguelin et al., 2017). Indeed, E2F1 induces *Ezh2* expression in GCs (discussed in **section 1.1.7**), sustaining GC-B cell proliferation (Beguelin et al., 2017).

Finally, PRMT5 methylation of the NF- κ B subunit RelA promotes NF- κ B association to target genes and thereby enhances transcription activation (Wei et al., 2013). NF- κ B signalling is critical downstream of CD40 stimulation in the LZ to sustain GC-B cell proliferation (Luo et al., 2018) as well as for inducing plasma cell differentiation (Heise et al., 2014) (discussed in **section 1.1.4.4**). In particular, RelA was shown to be critical for B cell differentiation, as depleting RelA prevented plasma cell production *in vivo* (Wei et al., 2013).

RNA-metabolism

PRMT5 is critical for messenger RNA (mRNA) biology, as it is involved in pre-mRNA splicing in the nucleus and the formation of cytoplasmic stress granules (**Fig 1.9**).

PRMT5 is required for assembly of the spliceosome, a large complex composed of 5 small nuclear ribonucleoproteins (snRNPs) that are assembled in the cytoplasm from RNA and protein components: the small nuclear RNA (snRNA) and Sm proteins (Matera and Wang, 2014). PRMT5 methylates Sm proteins within a complex called the methylosome (Friesen et al., 2001). Sm methylation recruits the tudor protein SMN, which assembles snRNA with Sm proteins, producing snRNP subunits in the

cytoplasm. snRNP maturation requires the chaperone pICln that also associates with PRMT5 (Meister et al., 2001). The SMN complex then recruits an RNA methyltransferase that modifies the snRNAs 5', functioning as a nuclear-localization signal (Fischer and Luhrmann, 1990). Deleting Prmt5 leads to splicing defects in several systems. In plants, Prmt5 is required for alternative splicing of mRNAs coding for circadian clock-associated genes (Sanchez et al., 2010). Prmt5-depletion in mammalian cells was shown to alter constitutive pre-mRNA splicing (Bezzi et al., 2013) (Koh et al., 2015b). Prmt5^{-/-} neural stem cells showed reduced levels of snRNP maturation, resulting in increased levels of aberrant splicing events, particularly exon skipping and intron retention (Bezzi et al., 2013). The same pattern has been observed in c-Myc-driven pre-B cell tumours (Koh et al., 2015b). Prmt5 depletion results in the accumulation of abnormal splicing events, mainly retained introns and skipped exons with usage of weak 5' donor sites (Koh et al., 2015b). Interestingly, the induction of aberrant splicing at targets identified in Prmt5-depleted cells using antisense oligonucleotides could recapitulate cell growth and viability defects observed in Prmt5^{-/-} cells (Koh et al., 2015b), suggesting that the main role of Prmt5, in Eμ-Myc tumors, is to sustain splicing demand.

Knocking-down either PRMT1 or PRMT5, as well as inhibiting their activity, promotes stress granule formation (Tsai et al., 2016). Since PRMT1 and PRMT5 can methylate Ras-GAP SH3-binding protein 1 (G3BP1) (Tsai et al., 2016), an RNA-binding protein important for stress granule assembly (Tourriere et al., 2003), it is believed that G3BP1 methylation inhibits stress granule assembly.

Translation

PRMT5 can also regulate mRNA translation via different mechanisms (**Fig 1.9**). First, PRMT5 is involved in ribosomal assembly by methylating ribosomal protein s10 (RPS10), which is necessary to promote proper protein synthesis (Ren et al., 2010). Mutating the arginines that are methylated by PRMT5 destabilize RPS10 association to ribosomes, resulting in RPS10 degradation (Ren et al., 2010).

PRMT5 also facilitates translation of mRNA containing internal ribosome entry sites (IRES), which can have implications for GCs. In mouse embryonic fibroblasts, Prmt5 methylates the heterogeneous nuclear ribonucleoprotein A1 (hnRNPA1), and facilitates the interaction of hnRNPA1 with mRNAs containing an internal ribosome entry site (IRES) (Gao et al., 2017). This interaction triggers IRES-dependant translation, promoting cyclin D1 (Ccd1) and c-Myc translation, sustaining cell proliferation (Gao et al., 2017). As explained above, c-Myc is tightly regulated in GCs, which is critical for the GC reaction (**section 1.1.4.5**) (Luo et al., 2018). It remains to be explored whether Prmt5 affects c-Myc translation in GCs.

Signalling

PRMT5 can influence signal transduction by modifying receptors, co-receptors or intracellular components of several signalling pathways. For instance, PRMT5 can methylate epidermal growth factor receptor (EGFR), which enhances its auto-phosphorylation, but also forms a docking site for the phosphatase SHP1, thereby limiting overall EGFR signalling (Hsu et al., 2011). By other modes of action, PRMT5 can affect signaling pathways that regulate cellular processes that are relevant for B cell biology.

PRMT5 associates with two receptors of the Tumour necrosis factor -related apoptosis-inducing ligand (TRAIL) pathway: death receptor 4 (DR4) and DR5 (Tanaka et al., 2009). Engagement of DR4 or DR5 upon TRAIL binding triggers apoptosis by the extrinsic pathway, with caspase-8 activation (Kischkel et al., 2000). Removing PRMT5 in some cancer cells incubated with TRAIL increases apoptosis along with reducing I κ B α phosphorylation by IKK, which is characteristic of reduced canonical NF- κ B pathway activity (see **section 1.1.7**) (Rickert et al., 2011). As apoptosis in PRMT5^{-/-} cells can be rescued upon IKK overexpression, it seems that in certain cancer cells PRMT5 can prevent TRAIL induced apoptosis by inducing NF- κ B signalling (Tanaka et al., 2009). Interestingly, although TRAIL and DR5 mRNAs are expressed in resting and activated B cells, TRAIL-induced apoptosis was solely seen in plasma cells and not in activated B cells (Ursini-Siegel et al., 2002).

Moreover, incubation of *in-vivo* generated plasma cells with a blocking antibody against DR5 shows increased plasma cell viability, suggesting that plasma cells undergo apoptosis upon endogenous and exogenous TRAIL binding to DR5 (Ursini-Siegel et al., 2002). Plasma cells also have reduced levels of CD40, suggesting that plasma cell sensitivity to TRAIL may originate from the loss of pro-survival signals from CD40 signaling via NF- κ B (Ursini-Siegel et al., 2002). Interestingly, cells undergoing persistent ER stress, which occurs in plasma cells (see **section 1.1.5.2**), accumulate intracellular DR5 and induce apoptosis through caspase-8 in a ligand-independent manner (Lu et al., 2014). The possibility that Prmt5 promotes plasma cells survival via NF- κ B activation remains to be investigated.

PRMT5 can also negatively regulate MAPK signalling pathway, also called the RAS-RAF-MEK-ERK pathway (Andreu-Perez et al., 2011). The MAPK pathways can influence cell survival, proliferation and differentiation (Chung and Kondo, 2011). MAPK signalling is initiated by cytokines or growth factors binding to receptor tyrosine kinases that induce the activation of different sets of proteins via phosphorylation events (Chung and Kondo, 2011). Following receptor stimulation, the small G-proteins rat sarcoma virus (RAS) are activated, recruited to the plasma membrane and activate kinases called rapidly accelerated fibrosarcoma (RAF). RAF proteins then phosphorylate mitogen-activated ERK kinases (MEK1/2), which themselves phosphorylate extracellular signal-related kinases (ERK1/2), leading to ERK1/2 translocation to the nucleus and phosphorylation of transcription factors that regulate gene transcription. In purified naïve B cells, this pathway can be activated downstream of both BCR and CD40 signaling (Jacob et al., 2002) (Mizuno and Rothstein, 2005), promoting B cell survival (Adem et al., 2015). However, *ex vivo* activated GC B cells have recently been shown to activate the MAPK pathway mostly upon BCR stimulation (Luo et al., 2018). PRMT5 methylates at least one member of the RAF protein family, called CRAF (Andreu-Perez et al., 2011). This modification induces CRAF degradation, limiting ERK1/2 phosphorylation and resulting in enhanced proliferation. As a result, in a neuroblastoma cell line, depleting PRMT5 enhanced ERK1/2 phosphorylation and promoted differentiation (Andreu-Perez et al.,

2011). In contrast, removing Prmt5 in HSCs reduces ERK1/2 phosphorylation (Liu et al., 2015b), suggesting a context dependant role for Prmt5 in signal transduction.

PRMT5 was first been discovered as a JAK-binding protein (Pollack et al., 1999). In B cells, the JAK-STAT signaling pathway is induced following stimulation of cytokine receptors such as IL-4R and IL-21R, modulating cell growth, survival and differentiation (Jiang et al., 2000) (Avery et al., 2010). GC-associated nuclear protein (GANP) is induced in GC B cells (Kuwahara et al., 2000) and negatively regulates JAK-STAT signaling upon IL-4 stimulation, as phospho-STAT6 levels are increased in stimulated GANP^{-/-} B cells (Igarashi et al., 2009). The authors proposed that STAT6 was methylated by PRMT5, promoting JAK-STAT signaling and showed that GANP acted as a repressor of PRMT5-dependant JAK-STAT signalling (Igarashi et al., 2009).

This section highlights the pleiotropic functions of PRMT5, which can regulate gene expression and signaling at multiple levels depending on the methylated substrate. This complexity illustrates the difficulties associated with analyzing the biological roles of PRMT5 in any system, but also the fundamental importance of this enzyme.





	Cellular processes	Affected mechanism	Proteins methylated by PRMT5	Proteins methylated by PRMT1
	Transcription	Chromatin remodelling	H3R8, H4R3	H4R3
		RNApolII elongation	Spt5, RNApolII	
		Transcription initiation	p53, Rela, Klf4, E2f1	Runx1, Foxo1
	RNA metabolism	Splicing	Sm proteins	
		Stress granule assembly	G3bp1	
	Translation	Translation initiation	hnRNPA1	Aven
		Ribosomal assembly	Rps10	
	Signaling	NFκB	Rela	
		MAPK	Craf	
		BCR signaling		Igα

Figure 1.9 – PRMT5 and PRMT1 play multiple roles in the cell

Non-exhaustive list of cellular processes affected by PRMT5 and PRMT1 methylation, with the corresponding mechanisms and protein targets involved.

1.2.3.4 Functional regulation of PRMT5

Recruitment factors and PTM

PRMT5 is part of various different complexes that regulate diverse cellular mechanisms. These complexes contain co-factors that can determine PRMT5 substrate specificity by acting as recruiting factors.

For instance, PRMT5 associates with co-operator of PRMT5 (COPR5) in the nucleus, which directs methylation towards histone H4 (H4R3me2) over histone H3 (H3R8me2) (Lacroix et al., 2008). It is suggested that PRMT5, in association with COPR5, modulates transcription levels of c-Myc targets (Mongiardi et al., 2015). Interestingly, overexpressing c-Myc in epithelial cells increases H4R3me2s (Mongiardi et al., 2015), which suggests a positive feedback loop.

The role of MEP50 in PRMT5 association to the spliceosome has been described above. MEP50 phosphorylation by CyclinD1/CDK4 enhances PRMT5 methyltransferase activity (Aggarwal et al., 2010). PRMT5 itself can also be post-translationally modified. PRMT5 phosphorylation has been shown to reduce its interaction with MEP50 and attenuate its methyltransferase activity (Liu et al., 2011). As also mentioned, PRMT5 associates with pICln (Meister et al., 2001) to mediate formation of snRNPs. Interestingly, this association can be antagonized by RIOK1, which recruits PRMT5 to nucleolin, a methylation target (Guderian et al., 2011). Nucleolin is important for ribosome maturation, and arginine methylation promotes its interaction to RNA (Raman et al., 2001).

Subcellular localization

Generally, PRMT5 is localized in the cytoplasm, which is enforced by three nuclear export signals (Gu et al., 2012b). Nonetheless, depending on the cellular context PRMT5 can be found in both the cytoplasm and the nucleus (Koh et al., 2015a), this

is an important mechanism to limit PRMT5 activity to specific subcellular compartments when required.

For instance, in primordial germline cells at the embryonic stage E8.5, Blimp-1 interacts with PRMT5, leading to histone symmetric dimethylation at target genes in the nucleus. However at E11.5, the PRMT5-BLIMP-1 complex translocates to the cytoplasm, resulting in loss of histone arginine methylation and epigenetic reprogramming (Ancelin et al., 2006). As mentioned above, Blimp-1 is required for plasma cell differentiation (see **section 1.1.5.2**). In plasma cells, Blimp-1 associates with active promoters that harbour histone lysine methylation but also acetylation: H3K4me2, H3K4me3, H3K9ac, although it can also associate with the repressive mark H3K27me3 at certain target genes (Minnich et al., 2016). Blimp-1 associates with chromatin modifiers, such as the PRC2 complex via Ezh2 binding, or the nucleosome remodelling deacetylase (NuRD) complex (Lai and Wade, 2011), which removes acetyl-groups from histones (Minnich et al., 2016). Blimp-1 also associates with the chromatin remodelling BAF complex (Tang et al., 2010). As PRMT5 associates with the NuRD and BAF complexes as well (see **section 1.2.3.3**), it is possible that the Prmt5-Blimp-1 interaction occurs in B cells at the chromatin.

Inhibition by an endogenous metabolite

PRMT5 activity can be inhibited in the cell by methylthioadenosine (MTA), an endogenous analog of SAM (Bedford and Richard, 2005) (**Fig. 1.8A**). MTA inhibits PRMT5 activity by competing with SAM (Hu et al., 2016). MTA is cleaved by 5-methylthioadenosine phosphatase (MTAP) for methionine synthesis. Interestingly, the gene encoding MTAP is often deleted in human cancers, due to its close proximity with the tumour suppressor *CDKN2A*. These cells accumulate MTA and are sensitive to PRMT5 depletion (Mavrakis et al., 2016) (Kryukov et al., 2016). This discovery potentially opens the door for use of PRMT5 inhibitors in the treatment of cancers where *MTAP* is lost.

1.2.3.5 Cellular impact of PRMT5 activity

As highlighted above, PRMT5 activity regulates many molecular processes that can influence the state of a cell, including proliferation, survival and differentiation. PRMT5 has been studied in many different systems: muscles (Zhang et al., 2015b), nervous system (Bezzi et al., 2013; Huang et al., 2011), germline development (Kim et al., 2014; Li et al., 2015c), cellular reprogramming (Chu et al., 2015) (Nagamatsu et al., 2011) and hematopoiesis (Koh et al., 2015b; Liu et al., 2015a). From these studies, it has become clear that the role of PRMT5 is not predictable, and results cannot be directly extrapolated from one system to another. Depending on the cellular context, PRMT5 can either negatively or positively regulate the same process.

Proliferation

In general, PRMT5 is a positive regulator of cell proliferation. Genetic ablation or reduced expression of *Prmt5* leads to reduced cell growth in adult mouse skeletal muscle cells (Zhang et al., 2015b), in human embryonic stem cells (Gkountela et al., 2014), during germline development of primordial germline cells (Kim et al., 2014; Li et al., 2015c), in neural stem cells (Bezzi et al., 2013) and in HSCs (Liu et al., 2015b). As an example, *Prmt5* promotes proliferation of adult muscle cells by repressing *Cdkn1a* through H3R8me2s mark (Zhang et al., 2015b). *Prmt5*^{-/-} cells therefore have reduced proliferation, but this could be partially rescued by crossing with *Cdkn1a*^{-/-} mice (Zhang et al., 2015b). PRMT5 also drives proliferation of cancer cells, for instance of mantle cell lymphoma (Pal et al 2007), BM B cell lymphoma (Koh et al., 2015b) and glioblastoma (Yan et al., 2014).

However, in specific contexts PRMT5 can limit proliferation. Surprisingly, deleting *Prmt5* in HSCs increased short-term proliferation of the multipotent precursors (LSK population), while the progenitors of myeloid cells (LK cells), a more differentiated cell subset, showed reduced proliferation (Liu et al., 2015b). Similarly, reducing PRMT5 levels in human primary HSCs promotes proliferation (Liu et al., 2011).

Survival

In most cellular systems, PRMT5 promotes survival. *Prmt5* depletion in muscle cells (Zhang et al., 2015b), primordial germ cells (Kim et al., 2014) and neural stem cells (Bezzi et al., 2013) results in cell death.

In neural stem cells, *Prmt5* depletion increases apoptosis and causes early post-natal lethality through a p53-dependant mechanism (Bezzi et al., 2013). More precisely, *Prmt5* depletion affects the splicing machinery, resulting in aberrant Mdm4 splicing. Mdm4 can directly interact with p53, forming a complex on target gene promoters but preventing p53 access to the transcription machinery (Kruse and Gu, 2009). The mis-spliced variant of Mdm4 no longer inhibits p53 targeting, leading to up-regulation of pro-apoptotic and anti-proliferative genes. Importantly, depleting *Trp53* along with *Prmt5*, partially rescues apoptosis observed in tissues and delays post-natal lethality (Bezzi et al., 2013).

Many cancer cells also depend on PRMT5 for their survival. For instance, glioblastomas are heterogeneous tumours composed of undifferentiated and differentiated cells, and these distinct cells have different requirements for PRMT5. Indeed, *Prmt5* loss induces senescence, along with increased p53 and p21 levels in immature glioblastoma cells, while it induces apoptosis in mature cells (Banasavadi-Siddegowda et al., 2017). Interestingly, loss of PRMT5 in glioblastoma cell lines leads to p53-independent apoptosis (Yan et al., 2014). Finally, as described above (**section 1.2.3.3**), in cancer cells PRMT5 antagonizes the extrinsic apoptotic pathway by inhibiting TRAIL-dependant apoptosis via activation of NF- κ B signalling (Tanaka et al., 2009).

Differentiation

PRMT5 mostly opposes cell differentiation, but again the role of PRMT5 is context dependent. In primary HSCs, PRMT5 negatively regulates differentiation to erythroid cells (Liu et al., 2011). In the same way, depleting *Prmt5* in HSC-derived MLL-leukemia promotes myeloid differentiation, in a p21-dependant manner (Kaushik et al., 2017). Likewise, *Prmt5* prevents differentiation of embryonic stem cells during mouse development, and promotes pluripotency (Tee et al., 2010). In fact, when co-

expressed with critical pluripotency genes, PRMT5 can drive cell reprogramming and enhance production of induced pluripotent stem cells (iPSCs) (Nagamatsu et al., 2011).

In other systems, PRMT5 promotes differentiation. For instance, in muscle cells and oligodendrocytes, removing *Prmt5* prevents differentiation (Zhang et al., 2015b) (Huang et al., 2011). In particular, in oligodendrocytes loss of *Prmt5* causes the de-repression of anti-differentiation genes and therefore abrogates differentiation (Huang et al., 2011).

1.2.4 PRMT1

1.2.4.1 Expression

PRMT1 is responsible for around 85% of arginine methylation in mammalian cells and therefore is one of the best-studied PRMTs (Tang et al., 2000). The *Prmt1* gene can actually produce up to seven isoforms (Goulet et al., 2007), with splice variants varying in their N-terminal sequences. This N-terminal region of PRMT1 can influence its catalytic activity as well as substrate specificity (Goulet et al., 2007).

PRMT1 expression, like PRMT5, is increased in a variety of different cancers: including colorectal cancer (Papadokostopoulou et al., 2009), lung cancer (Elakoum et al., 2014) and leukemia (Zou et al., 2012). Increased PRMT1 mRNA levels are also observed in hepatocellular carcinomas, and negatively correlate with miR-503 expression (Li et al., 2015a). This seems to have functional consequences, as re-expression of mir-503 in PRMT1-overexpressing cells, caused a reduction in cell invasion and migration (Li et al., 2015a).

1.2.4.2 Processes regulated by PRMT1

PRMT1 is involved in many different processes that can be relevant for B cell biology. The following section presents a glimpse into the roles of PRMT1, as described in the literature (**Fig 1.9**).

Transcription

1. Histone methylation

PRMT1, unlike PRMT5, functions as a transcription co-activator by depositing aDMA on H4R3 (H4R3me2a). This mark has been found to recruit the tudor domain protein Tdrd3 to the transcription start site of multiple genes (Yang et al., 2010), acting as a transcriptional co-activator. Indeed, at the *c-Myc* locus, Tdrd3 recognizes H4R3me2a and can recruit topoisomerase IIIB, which helps resolve R-loops, thereby increasing *c-Myc* transcription (Yang et al., 2014). Therefore, PRMT1 histone methylation can trigger the recruitment of factors that facilitate transcription.

2. Methylation of transcription factors

PRMT1 can methylate RUNX1, a transcription factor involved in hematopoiesis (Zhao et al., 2008). RUNX1 methylation by PRMT1 triggers its dissociation from the repressor SIN3a, thus enhancing RUNX1 activity (Zhao et al., 2008). RUNX1 is necessary for B cell development, as mice depleted for *Runx1* during BM development show a pre-B cell loss (Seo et al., 2012).

PRMT1 can also methylate Foxo1, preventing its phosphorylation by AKT and thereby promoting its nuclear localization and activity (Yamagata et al., 2008). Foxo1 plays a critical role in GCs (described above in **section 1.1.4.5**), as it sustains the centroblast program (Luo et al., 2018; Sander et al., 2015).

Translation

PRMT1 has been found to modulate mRNA translation. For instance, PRMT1 methylation of the RNA-binding protein AVEN promotes translation of the protein mixed lineage leukemia (MLL) by increasing recruitment of ribosomes (Thandapani et al., 2015).

DNA repair

Double strand breaks are repaired by homologous recombination in S-phase after replication, as this mechanism uses the sister chromatid of the corresponding broken region as a template. End-resection of DNA on opposite strands of the DNA break is

a necessary step for repair and is mediated by the Mre11/Rad50/NBS1 (MRN) complex. MRE11 is methylated by PRMT1, which seems to be important for its exonuclease activity, as well as its recruitment to sites of lesions (Boisvert et al., 2005b).

Signaling

PRMT1 has been found to directly methylate some receptors, which results in modulating their downstream signaling.

As mentioned above (**section 1.1.7**), Prmt1 is involved in repressing BCR signaling through direct methylation of Ig α within the BCR, thereby promoting B cell development in the BM (Infantino et al., 2010). PRMT1 has also been found to methylate EGFR on its extracellular domain in colorectal cancer cells (Liao et al., 2015). This modification enhances ligand binding, and thereby promotes downstream EGFR signaling (Liao et al., 2015).

1.2.4.3 Functional regulation

Co-factors

PRMT1 was first discovered in a yeast two-hybrid screen for interactors of B cell translocation gene 1 (BTG1) and BTG2 (Lin et al., 1996). Interactions with PRMT1 occur via a BoxC motif in BTG1/2 (Berthet et al., 2002), enhancing PRMT1 activity (Lin et al., 1996). Further studies have found that BTG1/2 association with PRMT1 is critical in different biological processes such as B cell development in the BM (Dolezal et al., 2017). Indeed, the BTG2-PRMT1 complex is responsible for cyclin-dependent kinase 4 (Cdk4) methylation, which dissociates Cdk4 from cyclin D3 (Ccd3), preventing Cdk4 phosphorylation of Rb, leading to the retention of E2F transcription factor in the cytoplasm and finally promoting cell cycle arrest and pre-B cell differentiation (Dolezal et al., 2017). PRMT1 also associates with an interactor of BTG1, chromatin assembly factor 1 (CAF1), modulating PRMT1 activity in different cell lines (Robin-Lespinasse et al., 2007).

Post-translational modification

Phosphorylation of PRMT1 at tyrosine 291 has been observed, and this was suggested to alter PRMT1 association to and methylation of the RNA binding proteins hnRNPA1 and hnRNPH3 (Rust et al., 2014). PRMT1 can also auto-methylate itself, but the relevance of this modification remains unknown (Sayegh et al., 2007).

PRMT1 activity can also be reversibly inhibited by oxydation, as treatment with hydrogen peroxide reduced methyltransferase activity of recombinant PRMT1 in a dose-dependant manner (Morales et al., 2015). This effect could be reversed by the reducing agent DTT, and suggests that PRMT1 may modulate oxidative stress responses, but more studies need to be done.

1.2.4.4 Cellular impact of PRMT1 activity

Proliferation

PRMT1 enforces growth of different cancers, such as leukemia (Cheung et al., 2016), colorectal cancer (Liao et al., 2015) and lung cancer (Elakoum et al., 2014). PRMT1 is also necessary for breast cancer proliferation by promoting ZEB1 transcription via the H4R3me2a mark (Gao et al., 2016). In mouse embryonic fibroblasts, *Prmt1* depletion results in increased genomic instability and prevents cell growth (Yu et al., 2009). Finally, *Prmt1* is required for mature B cell growth upon activation, as *Prmt1* loss does not affect the resting B cell pool but compromises B cell proliferation after stimulation *ex vivo* (Infantino et al., 2017). Interestingly, removal of PRMT1 in muscle stem cells promotes their proliferation but this limits differentiation (Blanc et al., 2017).

Survival

PRMT1 seems to play an important role in regulating the intrinsic cell death pathway, as methylation of the pro-apoptotic molecule Bad prevents its phosphorylation by Akt, similarly to Foxo1 (Sakamaki et al., 2011). Bad methylation promotes its mitochondrial localization and association with Bcl-XL, an anti-apoptotic protein. Therefore, Bad methylation could potentially promote cell death. This is confirmed in

human cell lines, where increased survival is observed after reducing levels of PRMT1 (Sakamaki et al., 2011).

On the other hand, PRMT1 has been shown to promote survival in other systems, such as leukemic cell lines (Cheung et al., 2016), breast cancer cells (Baldwin et al., 2012) and B cells (Infantino et al., 2017). Following BCR stimulation *Prmt1*^{-/-} mature B cells are gradually lost, this is accompanied with decreased expression of the pro-survival proteins Mcl-1, Bcl-2, A1 and Bcl-XL (Infantino et al., 2017). Since *Prmt1*^{-/-} B cells can be rescued by treatment with a caspase inhibitor, it would seem that Prmt1 promotes mature B cell survival downstream of BCR signaling (Infantino et al., 2017).

Differentiation

In many systems, PRMT1 positively enforces differentiation. Indeed, PRMT1 is necessary for central nervous system development and is required for oligodendrocyte differentiation (Hashimoto et al., 2016). Another example is the requirement of PRMT1 for B cell differentiation into ASC, as stimulating *Prmt1*^{-/-} B cells *in vitro* prevents B cell differentiation (Infantino et al., 2017). Yet, in other contexts, such as in leukemic cells (Cheung et al., 2016), epidermal progenitor cell (Bao et al., 2017) and megakaryocytes (Jin et al., 2018), PRMT1 loss induces differentiation.

1.2.5 Arginine methylation in lymphocytes

1.2.5.1 T cells

Mass spectrometry analysis has revealed that arginine methylation is modulated during human T cell activation and differentiation, suggesting that PRMTs have a role in T cell biology (Geoghegan et al., 2015). PRMT1 is found to be highly expressed in helper T helper cells (Mowen et al., 2004), and PRMT5 activity is required for helper T cell expansion (Webb et al., 2017). Furthermore, engagement of the co-stimulatory receptor CD28 induces arginine methylation in T cells (Blanchet et al., 2005), and treatment with the global methyltransferase inhibitor, adenosine-2', 3'-dialdehyde (AdOx) reduces IL-2 production in T cells.

1.2.5.2 B cells

The role of arginine methylation in B cells was first studied using AdOx *in vitro* (Hata and Mizuguchi, 2013). This revealed that global PRMT inhibition affects B cell growth and CSR per division, without affecting *Aicda* transcription (Hata and Mizuguchi, 2013). Later use of mice carrying a floxed exon in different *Prmt* loci and crossed with B cell specific Cre-recombinase mice has allowed dissection of the role of individual PRMTs in B cells at specific stages *in vivo* (**Fig. 1.10**).

Monomethylation by PRMT7

Prmt7 has been found to be required for maintaining normal mature B cell populations in the spleen, as *Prmt7^{F/F}* CD19-cre mice have reduced MZ B cell numbers (Ying et al., 2015). Moreover, Prmt7 monomethylation is required to limit GC expansion, as *Prmt7^{F/F}* CD19-cre mice showed increased GC B cell numbers upon immunization due to de-repression of *Bcl6*, generating a defective antibody response (Ying et al., 2015).

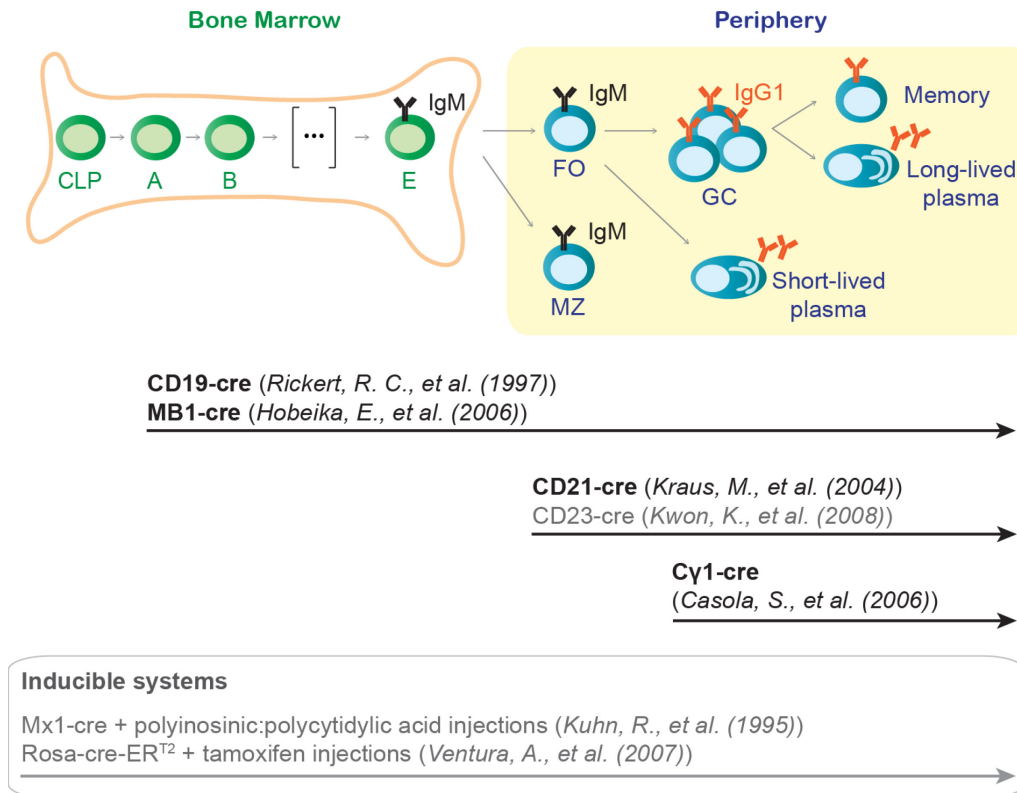


Figure 1.10 - Cre-driver mice used or discussed in the thesis

Scheme of B cell development in the BM and secondary lymphoid organs. Onset of expression for every Cre-driver mouse used in my work (in black) and discussed in the thesis (in grey) are indicated with an arrow. (Casola et al., 2006; Hobeika et al., 2006; Kraus et al., 2004; Kuhn et al., 1995; Kwon et al., 2008; Rickert et al., 1997; Ventura et al., 2007).

Symetric dimethylation by PRMT5

The role of Prmt5 has mostly been investigated in B cell progenitors and developing B cells in the BM. *Prmt5* depletion in BM cells has been performed by two different groups using different Cre-mice drivers. One study, which used the inducible Mx1-cre mouse (**Fig. 1.10**), depleted *Prmt5* in HSCs upon polyinosinic:polycytidylic acid injections. This showed that *Prmt5* deficiency leads to the loss of hematopoietic progenitors due to reduced proliferation without inducing apoptosis (Liu et al., 2015b). The second group reconstituted the BM of lethally irradiated mice with BM from *Prmt5*^{F/F} mice crossed with a tamoxifen-inducible Cre-mouse (Rosa-cre-ER^{T2}) (Koh et al., 2015b) (**Fig. 1.10**). Recipient mice treated with tamoxifen showed BM cells loss

(Koh et al., 2015b), similarly to the previous study. However, they also performed *Prmt5* depletion *in utero*, which lead to a reduction in fetal liver cellularity concomitant with an upregulation of apoptotic and p53-signalling pathways (Koh et al., 2015b). Remaining *Prmt5*^{-/-} fetal liver cells were unable to form colonies *in vitro* (Koh et al., 2015b). Altogether, both studies show that Prmt5 is required for BM cell proliferation, while its role for BM cell survival still needs further investigation.

In mature B cells, Prmt5 was shown to be induced upon activation *in vivo* and *in vitro* (Igarashi et al., 2009), but its role in normal B cells has not been investigated. However, pro-survival and pro-proliferation roles of PRMT5 have been demonstrated in B cell lymphomas (Chung et al., 2013) (Alinari et al., 2015a) (Koh et al., 2015b) and leukemias (Li et al., 2015b) (Kaushik et al., 2017) (Jin et al., 2016). The pro-apoptotic and anti-proliferation effects of deleting PRMT5 in B cell lymphoma may be due to more than one pathway. For instance, in B cell lymphoma driven by c-Myc, Prmt5 was shown to promote B cell lymphoma growth and survival by maintaining normal mRNA splicing (see **section 1.2.3.3**) (Koh et al., 2015b). Furthermore, in a model of oncogene driven leukemia, Prmt5 was shown to directly methylate p53, preventing the up-regulation of pro-apoptotic genes, thus promoting tumour survival (Li et al., 2015b). Finally, in non-Hodgkin lymphomas PRMT5 depletion indirectly led to inactivation of PRC2 and thereby de-repression of pro-apoptotic genes (Chung et al., 2013).

Although Prmt5 has been well studied in B cell lymphoma, a characterization of PRMT5's role in normal B cells is missing, as there are indications that PRMT5 plays different roles in normal and malignant B cells. Indeed, comparing the effects of Prmt5-depletion in normal and tumoral pre-B cells, by comparing *Prmt5*^{F/F} RosaERT2-cre with *Prmt5*^{F/F} RosaERT2-cre E μ -Myc pre-B cells, showed that Prmt5 was required for pre-B cell growth and survival only in a lymphoma context (Koh et al., 2015b).

Asymmetric dimethylation by PRMT1: the most studied PRMT in B cells

PRMT1 is important for B cell development, as *Prmt1^{F/F}* CD19-cre mice show a B cell development block at the pre-B cell stage (Dolezal et al., 2017) (Hata et al., 2016) (**Fig. 1.11**). This block was confirmed by the limited ability of *Prmt1^{-/-}* pre-B cells to differentiate and express a BCR *ex vivo* (Dolezal et al., 2017). Mice with *Prmt1* deletion in BM B cells have reduced numbers of pre-B cells, due to a critical role of Prmt1 in regulating pre-B cell proliferation (Dolezal et al., 2017). Prmt1, in complex with Btg2, methylates Cdk4, leading to Cdk4 dissociation from cyclin D3 and cell cycle arrest in G1 (Dolezal et al., 2017). Large pre-B cells are cycling and degrade Rag2 in order to prevent gene rearrangement. Indeed, Rag2 is phosphorylated in S-phase, which leads to its degradation (Lee and Desiderio, 1999; Lin and Desiderio, 1994). By inducing cell cycle arrest, the Prmt1-Btg2 complex promotes large pre-B cell differentiation into small resting pre-B cells potentially through Rag2 stabilization in G1 (Dolezal et al., 2017). Moreover, Prmt1 methylation of Igα has also been found to repress PI3K signalling downstream of BCR signalling, positively regulating pre-B cell differentiation into immature B cells *in vitro* (Infantino et al., 2010) (see **section 1.1.7** and **Fig. 1.11**).

Although *Prmt1^{F/F}* CD19-cre mice showed a B cell development block in the BM, mature *Prmt1^{-/-}* B cells can populate the periphery (Hata et al., 2016). This is explained by the weak excision efficiency of CD19-cre in the BM compared to the periphery (Hobeika et al., 2006). *Prmt1^{F/F}* CD19-cre mice have almost normal FO B cell numbers but a significant decrease in MZ B cells, suggesting that Prmt1 is dispensable for FO B cell homeostasis but required for MZ B cells (Hata et al., 2016). This contrasts with another study that achieved *Prmt1* depletion by breeding *Prmt1^{F/F}* mice with CD23-cre mice, which excise *Prmt1* in mature MZ and FO B cells (Infantino et al., 2017) (Kwon et al., 2008) (**Fig. 1.10**). Indeed, *Prmt1^{F/F}* CD23-cre mice showed normal FO and MZ B cell populations (Infantino et al., 2017). Both studies showed compromised antibody response against TI-antigens, while only *Prmt1^{F/F}* CD23-cre mice showed a defective antibody response against TD-antigens (Hata et al., 2016; Infantino et al., 2017). Another contrasting result is the differentiation potential of Prmt1-depleted B cells using the CD19-cre or CD23-cre mice: while, *Prmt1^{F/F}* CD19-

cre B cells showed increased proliferation and antibody production *in vitro*, *Prmt1^{F/F}* CD23-cre B cells neither proliferated nor produced plasma cells *in vivo* and *in vitro* (Hata et al., 2016; Infantino et al., 2017). The differences between the two studies must originate from differences in Cre-excision efficiency and timing, illustrating the multiple roles played by PRMT1 at different B cell stages. Nevertheless, further investigations are necessary to better understand the importance of PRMT1 in mature activated B cells. Moreover, additional systems that bypass the function of PRMT1 in early B cell activation are required to study the role of PRMT1 in GC B cells.

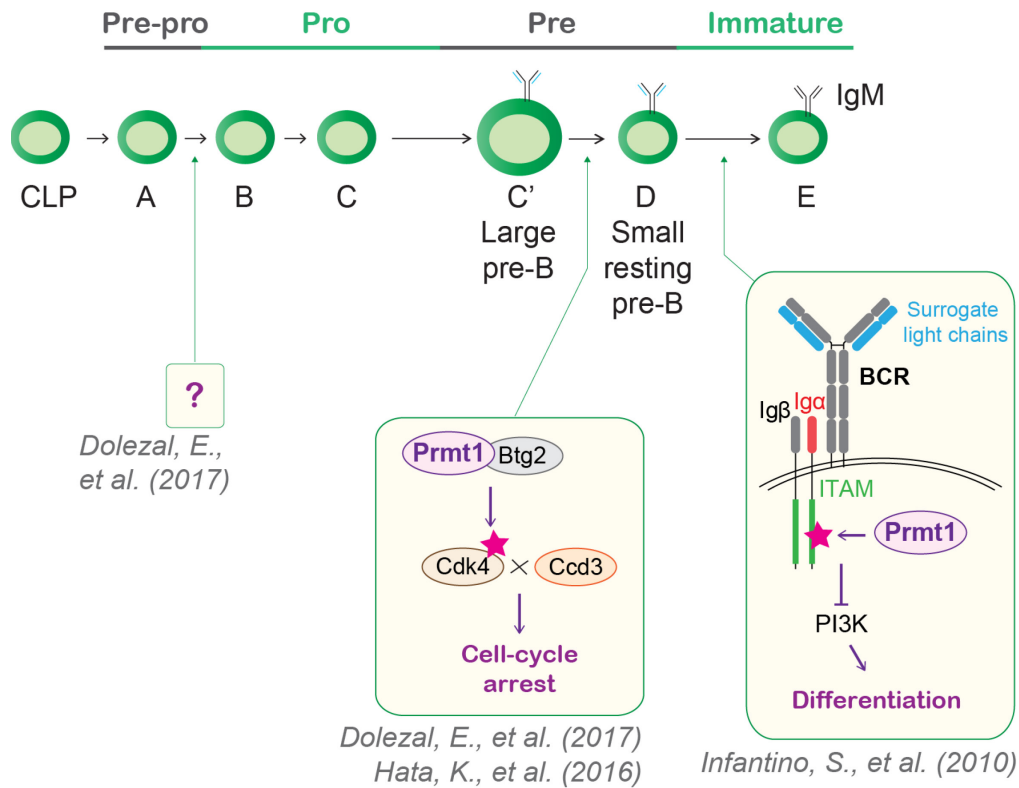


Figure 1.11 - Role of *Prmt1* in BM B cell development

Prmt1 has been found to be important at 3 stages of BM B cell development: (i) for pro-B cell development via an unknown mechanism, (ii) in pre-B cell to promote cell cycle arrest of large pre-B cells and (iii) for immature B cell development by repressing BCR signaling.

2 Chapter II:

PRMT5 is essential for antibody responses by promoting mature B cell survival and germinal center expansion by p53-independent mechanisms

Ludivine C. Litzler ^{1,2}, Astrid Zahn ¹, Alexandre Meli ³, Steven Hébert ⁴, Anne-Marie Patenaude ^{1,++}, Stephen P Methot ^{1,+}, Adrien Sprumont ¹, Thérance Bois ¹, Daisuke Kitamura ⁵, Santiago Costantino ^{6,7}, Irah King ³, Claudia L Kleinman ^{4,8}, Stéphane Richard ^{4,9}, Javier M Di Noia ^{1,2,10,11}

¹ Institut de Recherches Cliniques de Montréal, 110 av. des Pins Ouest, Montréal, QC, Canada H2W 1R7.

² Department of Biochemistry and molecular medicine, 2900 boul. Édouard-Montpetit, bureau D-360, Montréal, QC, Canada, H3T 1J4.

³ Meakins-Christie Laboratories, Department of Microbiology and Immunology, McGill University Health Centre, 1001 boul. Décarie, Block E (EM2.2232), Montreal, QC, Canada, H4A 3J1.

⁴ Segal Cancer Center, Lady Davis Institute for Medical Research, Montréal, Québec, Canada H3T 1E2.

⁵ Research Institute for Biomedical Sciences, Tokyo University of Science, Noda, Japan.

⁶ Research center of the hospital Maisonneuve-Rosemont.

⁷ Department of Ophthalmology, Université de Montréal, C.P. 6128, succ. Centre-ville, Montréal, QC, Canada, H3C 3J7.

⁸ Department of Human Genetics, Faculty of Medicine, McGill University

⁹ Departments of Oncology and Medicine, McGill University, 5100 Maisonneuve Blvd West, Suite 720; Montreal, QC, Canada H4A3T2.

¹⁰ Department of Medicine, Division of Experimental Medicine, McGill University, 1001 boul Decarie, Montreal, QC, Canada H4A 3J1.

¹¹ Department of Medicine, Université de Montréal, C.P. 6128, succ. Centre-ville, Montréal, QC, Canada, H3C 3J7.

* *Present address: Friedrich Miescher Institute for Biomedical Research, Maulbeerstrasse 66, R-1066.2.58. P.O. Box 3775. 4002 Basel, Switzerland.*

** *Present address: Genos, BioCentar Borongajska cesta 83H, 10000 Zagreb, Croatia.*

2.1 Abstract

Mechanisms regulating survival and proliferation during B cell development, activation and education in the germinal center (GC) are critical for the humoral immune response. Protein arginine methyltransferase 5 (Prmt5), which catalyzes the majority of the symmetric dimethyl arginine (sDMA) protein modification, is overexpressed in B cell lymphomas but its role in normal B cells is not well known. Here, we show that Prmt5 is essential for B cell development, by preventing a p53 response in pro-B cells, and again, but independently of p53, in pre-B cells. While Prmt5 dampens a transcriptional p53 response also in mature B cells, Prmt5 is in fact necessary for antibody responses because of multiple p53-independent functions. Thus, Prmt5 protects from apoptosis during B cell activation, promotes GC expansion and negatively regulates plasma cell differentiation. Phenotypic and RNA-seq data indicate that Prmt5 determines GC light zone B cell fate by regulating the transcriptional program directly as well as by ensuring splicing fidelity of transcriptional regulators and DNA repair factors. Thus, Prmt5 and sDMA are essential for B cell development, B cell activation and GC dynamics by distinct mechanisms.

2.2 Introduction

B lymphocytes transit through multiple cellular stages on their way to acquiring functional proficiency and producing high affinity antibodies. B cell development in the bone marrow (BM) alternates between quiescent and replicative stages, with checkpoints for the successful rearrangement of the immunoglobulin genes (*Ig*) (Clark et al., 2014; Melchers, 2015). Mature B cells in the periphery go through another series of functional transformations after cognate antigen engagement: activation, proliferation, programmed *Ig* mutation coupled to antibody affinity-based selection in the germinal center (GC), and differentiation into memory or plasma cells (De Silva and Klein, 2015). Factors regulating B lymphocyte stage transitions are critical for the immune response.

The transition of quiescent mature B cells to the activated stage after antigen exposure and T cell stimulation entails morphological and functional changes enabled by rapid transcriptional changes (Kouzine et al., 2013). Subsequent migration of activated B cells to the B cell follicles and proliferation determine the formation of GCs. This transient structure undergoes formation, expansion and attrition stages over ~2-3 weeks after antigenic challenge (De Silva and Klein, 2015). The GC is organized into two separate regions, the dark (DZ) and light (LZ) zones, which contain functionally distinct B cell stages (De Silva and Klein, 2015). The centroblast stage in the DZ is highly proliferative and undergoes *Ig* somatic hypermutation initiated by Activation induced deaminase (AID). Centrocytes in the LZ proliferate less and compete for antigen and T cell help, which select those expressing high affinity antibodies (Victoria et al., 2012). (Kouzine et al., 2013) Transcriptional changes dominated by master transcription factors like *Bcl6* and *Pax5* define a GC B cell fate, while the induction of *Irf4* and *Prdm1* define plasma cell differentiation (Nutt et al., 2015). Transcriptional differences between centrocytes and centroblasts are subtle (Victoria et al., 2010); nonetheless, additional transcriptionally defined GC B cell subsets are emerging (Dominguez-Sola et al., 2012; Ise et al., 2018). For instance, these new populations can distinguish high affinity from low affinity GC B cells (Ise et al., 2018), revealing a greater level of complexity within the GC compartment.

Post-translational modifications (PTM) can directly or indirectly regulate gene expression. While phosphorylation has received the most attention, other abundant PTM are less studied. Arginine methylation, catalyzed by a family of Protein arginine methyltransferases (PRMTs), can regulate gene expression, RNA processing and signaling (Bedford and Clarke, 2009; Blanc and Richard, 2017). The relevance of arginine methylation in B cells has been suggested by a pan-PRMT inhibitor, which reduces B cell proliferation *ex vivo* (Hata and Mizuguchi, 2013). However, each PRMT has specific functions by modifying a non-overlapping set of proteins, as shown by the unique phenotype of mice lacking each enzyme (Blanc and Richard, 2017), calling for enzyme-specific analyses. PRMTs can be mono- or dimethyltransferases. The latter are divided into type I, which transfer two methyl groups to the same nitrogen of the arginine guanidino group to produce asymmetric dimethyl-arginine, or type II, which produce symmetric DMA (sDMA) by modifying two different nitrogen atoms. Recent work on two PRMTs indicate that each has unique functions in B cells. PRMT7, a monomethyltransferase, limits GC formation (Ying et al., 2015). On the other hand, PRMT1 promotes pre-B cell differentiation and is necessary for GC formation and antibody responses (Dolezal et al., 2017; Hata et al., 2016; Infantino et al., 2010; Infantino et al., 2017). The type II enzymes, PRMT5 and PRMT9, have been barely studied in normal B cells. The observation that Prmt5 protein and sDMA levels are increased in activated mouse B cells (Igarashi et al., 2009) suggests at least a physiological function at this stage, which has not been investigated.

PRMT5 is responsible for most cellular sDMA and is not redundant with other PRMTs (Blanc and Richard, 2017). Yet, the multiplicity of potential substrates allows PRMT5 to regulate major aspects of cell physiology (Karkhanis et al., 2011). PRMT5 regulates transcription, acting mainly as a transcriptional corepressor by methylating histones but can also modulate the function of transcription factors (Karkhanis et al., 2011; Koh et al., 2015a). PRMT5 methylates Sm and other splicing factors, whereby it can regulate alternative splicing and/or splicing fidelity (Bezzi et al., 2013; Koh et al., 2015b; Sanchez et al., 2010). Interestingly, very little is known about the relevance of

splicing fidelity in normal B cells. Methylation of cytoplasmic proteins also allows PRMT5 to regulate signaling (Andreu-Perez et al., 2011). Additionally, PRMT5 can regulate DNA repair by homologous recombination (Clarke et al., 2017), a pathway of major importance to B cells expressing AID (Hasham et al., 2010).

In contrast to normal B cells, PRMT5 has been well studied in the context of B cell neoplasms because it is overexpressed in GC-experienced and mantle cell human lymphomas, correlating with poor prognosis (Koh et al., 2015b; Pal et al., 2007). Accordingly, PRMT5 promotes disease progression in mouse models of oncogene-driven leukemia (Li et al., 2015b) and its depletion reduces proliferation of B cell lymphoma (BCL) cells (Koh et al., 2015b; Pal et al., 2007; Wang et al., 2008). PRMT5 inhibition is emerging as a potential therapy against BCL (Chan-Penebre et al., 2015; Kryukov et al., 2016) but enacting any therapy would require understanding the relevance and functions of this enzyme in normal B cells.

Here, we show that Prmt5 is critical for all major proliferative B cell stages during development in bone marrow as well as in secondary lymphoid organs, being essential for antibody responses. Prmt5 regulates transcription and splicing fidelity in B cells, whereby it prevents an apoptotic p53 response that otherwise hampers the development of pro-B cells and mature B cell activation. We also uncover p53-independent roles of Prmt5 in the differentiation of pre-B cells and in promoting GC expansion, which is at least in part due to a role in negatively regulating plasma cell differentiation.

2.3 Results

2.3.1 Distinct regulation of Prmt5 in proliferating B cells

To infer the B cell stages in which Prmt5 function was more relevant, we analyzed Prmt5 gene expression. Prmt5 mRNA peaked during B cell development at the proliferative pro-B and early pre-B cell stages (**Fig. 2.1A**). Most subsequent B cell stages, including all mature B cell populations, expressed similar levels of Prmt5

mRNA, which was only highly upregulated in B cells activated *ex vivo* (**Fig. 2.1A**). Accordingly, Prmt5 protein reached maximum levels 48 h after stimulating purified resting splenic B cells with LPS and IL-4, correlating with increased sDMA detected in multiple proteins (**Fig. 2.1B**). Consistent with the gene expression profile, conditional ablation of Prmt5 using the Mb1-cre mice completely blocks B cell development at the pro-B stage, which is described below. However, using CD19-cre, which is less efficient than Mb1-cre in the BM (Hobeika et al., 2006), permitted normal B cell development (**Supplementary Fig. 2.1A**). *Prmt5^{F/F}* CD19-cre mice had normal numbers of resting B cell subsets in the spleen (**Fig. 2.1C**, **Supplementary Fig. 2.1B**) despite efficient Prmt5 depletion, as shown by WB (**Fig. 2.1D**). Prmt5 protein and sDMA levels were also reduced in *Prmt5^{F/F}* CD19-cre splenic B cells stimulated *ex vivo* with LPS and IL-4 (**Fig 2.1E**). Despite interindividual variability, Prmt5 mRNA and protein levels correlated well in activated B cells (**Fig 2.1F**). In contrast to activated B cells, GC B cells expressed Prmt5 mRNA at levels similar to resting follicular B cells (**Fig. 2.1A**). Yet, immunohistochemistry (IHC) in spleen sections from immunized mice with anti-Prmt5 revealed distinct groups of strongly reactive cells within GC, as shown by parallel PNA staining (**Fig. 2.1G**). Publicly available IHC performed on human tissues also showed higher Prmt5 expression in GC versus follicular B cells (**Supplementary Fig. 2.1C**). We conclude that Prmt5 is dispensable for the homeostasis of follicular and marginal zone B cells in the spleen and is upregulated in proliferating B cell stages. The distinct regulation of *Prmt5* in activated B cells, where it is transcriptionally induced, and GC B cells, where it is post-transcriptionally upregulated, may reflect different functions of Prmt5 in each of these stages.

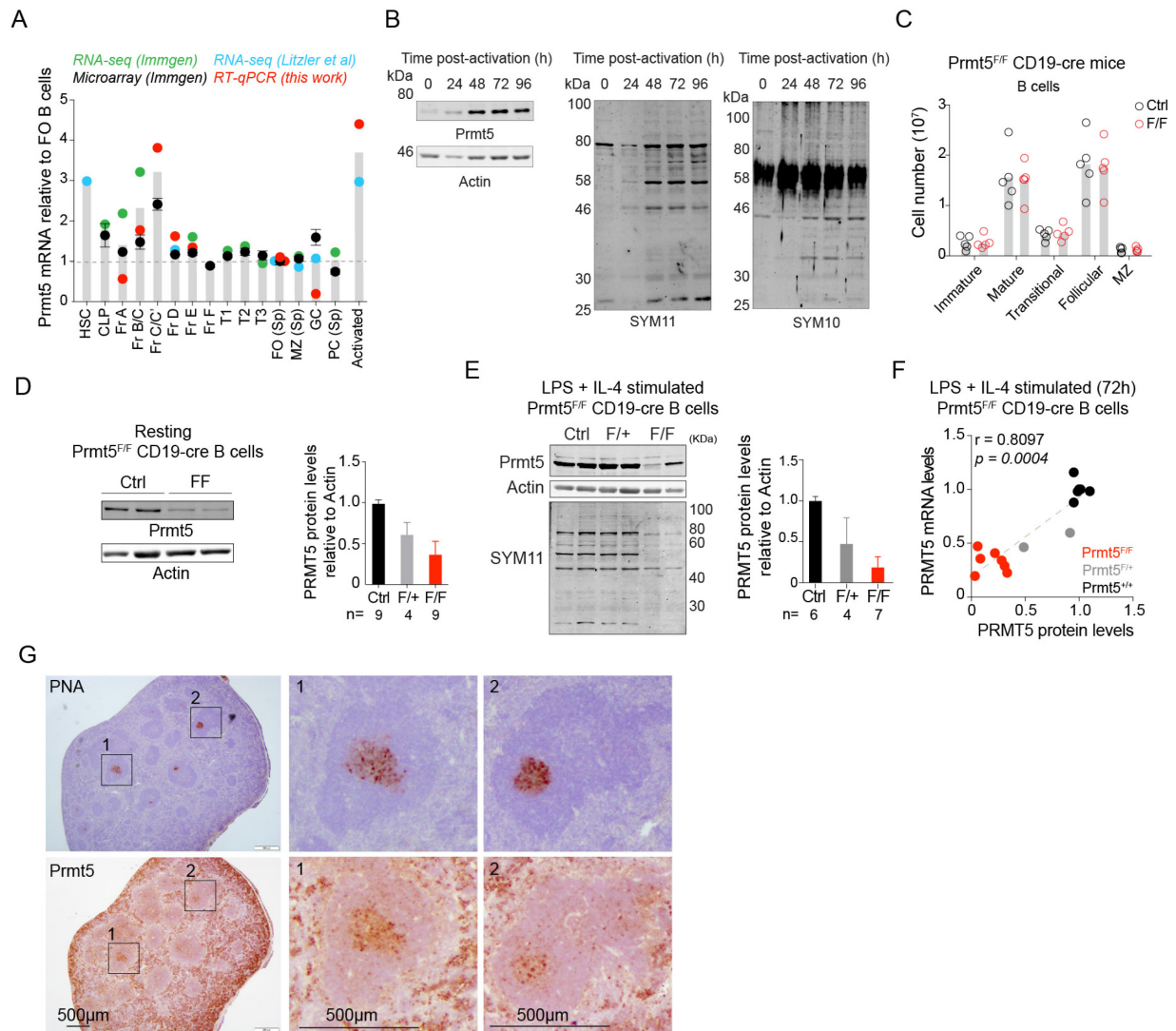


Figure 2.1 – Regulated Prmt5 expression in B cells

A) Prmt5 transcript levels in B cell stages. For comparison, each dataset was normalized to the levels in mature follicular (Fo) B cells. RT-qPCR data was normalized to Actin mRNA and obtained from a pool of two mice sorted for Hardy's BM fractions (Fr) A to E, from B220⁺ GL7⁺ CD95⁺ cells sorted from pooled splenocytes from 4 immunized mice for germinal center (GC) B cells, and from splenocytes purified from 2 mice and stimulated ex vivo with LPS and IL-4 for 48h for activated B cells. HSC, hematopoietic stem cells; CLP, common lymphoid progenitor; T1-T3, transitional B cells; MZ, marginal zone B cells; PC, plasma cells; Sp, spleen.

B) Kinetics of *Prmt5* expression and sDMA-modified proteins by WB probed with anti-PRMT5, anti-Actin (as loading control) and two anti-sDMA antibodies (SYM11 and SYM10) in extracts of splenic B cells from WT mice, stimulated *ex vivo* with LPS (5 µg/mL) and IL-4 (5 ng/mL).

C) Absolute number of B cell subpopulations in the spleen of CD19-cre (Ctrl) and *Prmt5^{F/F}* CD19-cre (F/F) mice. Values for individual mice (dots) and means (bars) are plotted.

D) Representative WB of resting splenic B cell extracts from CD19-cre (Ctrl) and *Prmt5^{F/F}* CD19-cre (F/F) mice, probed for *Prmt5* and Actin. Means + s.d. *Prmt5* levels normalized to Actin quantified from WB from *n* mice are shown, including *Prmt5^{F/+}* CD19-cre (F/+) mice.

E) Representative WB of *Prmt5*, Actin and sDMA (SYM11) in extracts of splenic B cells from mice of the same genotypes as in D) but activated with LPS (5 µg/mL) and IL-4 (5 ng/mL) for 72 h. Means + s.d. *Prmt5* levels are plotted as in D).

F) *Prmt5* mRNA level (measured by RT-qPCR) as a function of *Prmt5* protein level (measured by WB) at 72 h post-stimulation, for experiments done as in E). Spearman's test correlation coefficient (*r*) and *p*-value (*p*) are indicated.

G) Representative immunohistochemical staining for *Prmt5* and PNA (GC marker) on consecutive spleen sections from one mouse at day 14 post-immunization with NP-CGG.

2.3.2 *Prmt5* promotes survival of activated B cells *in vivo*

To assess the relevance of *Prmt5* in stimulated B cells *in vivo*, we immunized *Prmt5^{F/F}* CD19-cre mice with NP-CGG in alum and examined GC B cells 14 days later. GC B cell numbers were reduced by ~3-fold in *Prmt5^{F/F}* CD19-cre compared to control mice (**Fig. 2.2A**). Despite *Prmt5* being hardly detectable in follicular B cells in *Prmt5^{F/F}* CD19-cre mice, the GC B cells we found after immunization were consistently *Prmt5⁺* (**Fig. 2.2B**). This suggested that the few B cells that had failed to excise *Prmt5* were strongly selected to form GCs in these mice.

We were intrigued by the observation that the total lymphocyte count was reduced because of B cell loss in immunized *Prmt5^{F/F}* CD19-cre mice, which was not observed in non-immunized mice (**Fig. 2.2C**). Alum causes some polyclonal B cell activation (Marichal et al., 2011), as could be verified in our mice by the upregulation of the GL7 activation marker after injecting Alum alone (**Fig. 2.2D**). We hypothesized that *Prmt5*

might be important upon B cell activation. To test this possibility *in vivo*, we infected mice with *Heligmosomoides polygyrus*, a parasitic enteric nematode that induces polyclonal B cell activation (McCoy et al., 2008). At day 14 post-infection total B cell numbers in mesenteric lymph node (MLN) and spleen were significantly reduced in *Prmt5^{F/F}* CD19-cre but not in control mice, whilst T cells were not affected (**Fig. 2.2E**). This reduction correlated with a significant increase in apoptosis in non-GC B cells in *Prmt5^{F/F}* CD19-cre mice (**Fig. 2.2F**). In contrast, neither T cells nor GC B cells, which in these mice were mostly *Prmt5⁺* (see **Fig. 2.2B**), showed any increase in apoptosis (**Fig. 2.2F**). Interestingly, most apoptosis was found in GL7-negative splenic B cells in *Prmt5^{F/F}* CD19-cre mice (**Fig. 2.2G**), suggesting that apoptosis occurred soon after activation and *Prmt5*-deficient B cells did not survive to become GL7⁺. We conclude that *Prmt5* protects early activated B cells from cell death.

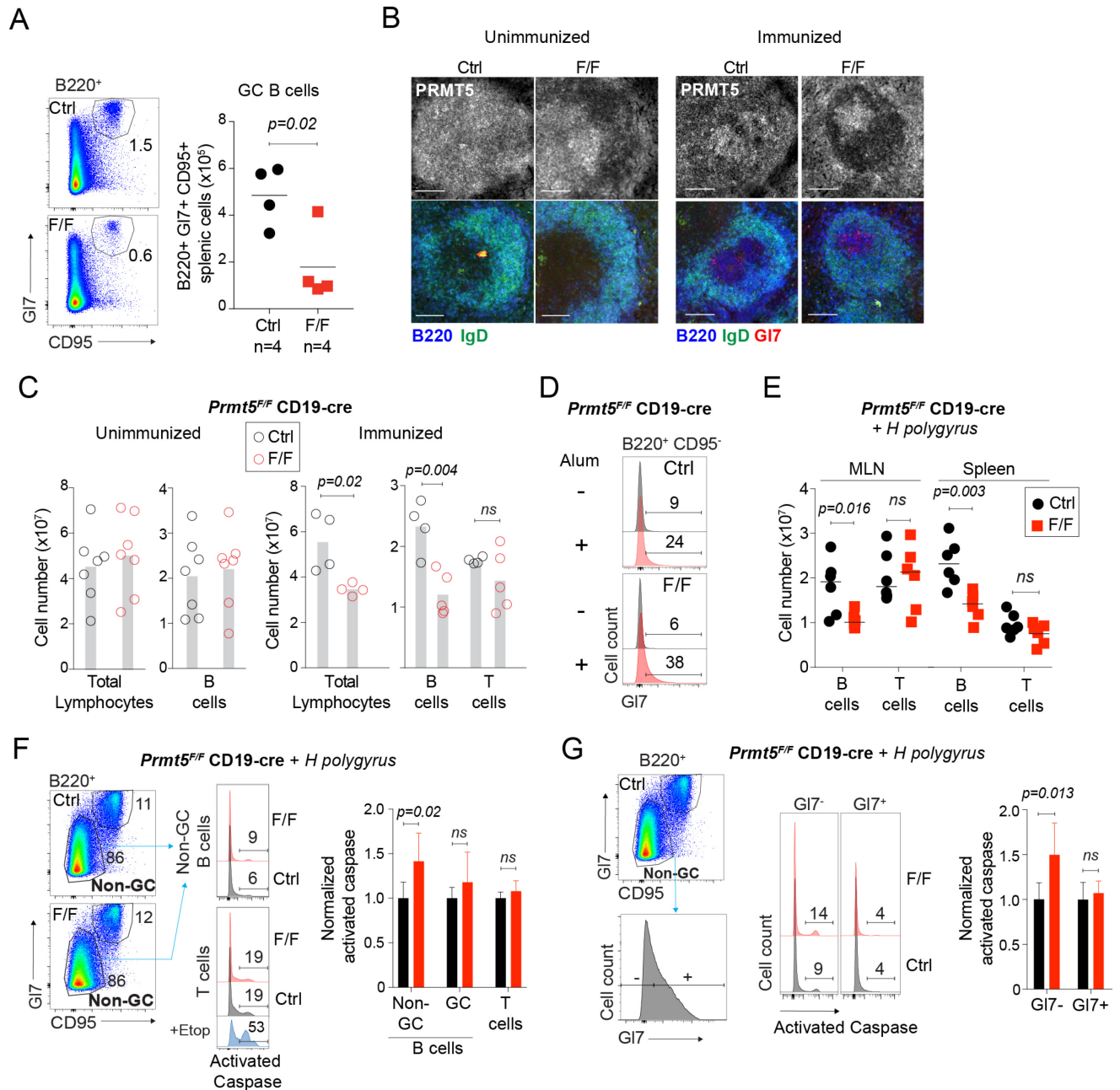


Figure 2.2 - *Prmt5* is required for the survival of activated B cells in vivo

In all panels *Prmt5*^{F/F} CD19-cre (F/F) and CD19-cre (Ctrl) mice were compared.

A) Representative flow cytometry plots showing the frequency of GC B cells (B220⁺, GL7^{high}, CD95⁺) in the spleen 14 days after immunization with NP-CGG. Total number of splenic GC B cells for individual mice (symbols) and means (bars) from 2 experiments are plotted.

B) Representative confocal microscopy of IF in spleen sections of mice pre- and 14 days post-NP-CGG immunization with anti-*Prmt5*, -B220, -GL7 and/or -IgD. One experiment, 2 mice per genotype. Scale bar, 100 μ m.

C) Absolute number of lymphocytes in spleens of individual mice (symbols) and means (bars) at 14 days post-immunization are plotted from 2 experiments.

D) Representative histograms of the distribution of GL7 expression in non-GC B cells (gated on B220⁺ CD95⁻) from mice injected or not with Alum from one experiment with 2 mice per genotype per treatment.

E) Absolute number of B cells (B220⁺) and T cells (CD3⁺) in mesenteric lymph node (MLN) and spleen of individual mice (symbols) infected with *H. polygyrus* for 14 days, from 2 experiments, with means (bars) indicated.

F) Representative flow cytometry plots showing the frequency of pan-caspase⁺ cells from non-GC B cells (B220⁺ CD95⁻) and T cells (B220⁻ CD3⁺) from the MLN of mice analyzed in E). Gates were set using cells treated with etoposide (3 μ M) to induce apoptosis. Means + s.d. proportion of pan-caspase⁺ cells from 6 mice from 2 experiments are plotted, normalized to the control average.

G) Flow cytometry gating used to define GL7⁺ and GL7⁻ fractions in non-GC splenic B cells and frequency of activated pan caspase⁺ cells in each fraction. Mean + s.d. proportion of activated pan-caspase⁺ cells in each non-GC B cell fraction for 6 mice from 2 experiments are plotted normalized to the Ctrl.

P-values throughout are indicated for significant differences by unpaired, two tailed Student-*t* tests.

2.3.3 Prmt5 prevents B cell apoptosis at the time of activation

To confirm the activation defect of Prmt5-deficient B cells, we stimulated resting splenic B cells from *Prmt5^{F/F}* CD19-cre mice *ex vivo* with LPS and IL-4. Cell enumeration and cell division tracking dye showed reduced expansion and proliferation of Prmt5-deficient B cells (**Fig. 2.3A**). Prmt5-deficient B cells presented normal cell cycle profile (**Fig. 2.3B**) but significantly increased cell death, which was inversely correlated to Prmt5 levels (**Fig. 2.3C, 2.3D**). To test whether B cell survival depended on the catalytic activity of Prmt5, we treated wt B cells with the Prmt5-specific inhibitor EPZ015666 (EPZ) (Chan-Penebre et al., 2015), which reduced sDMA in cell extracts (**Fig. 2.3E**). Inhibition of Prmt5 24 h prior to activation resulted in an EPZ dose-dependent increase in cell death and reduced cell numbers after activation (**Fig. 2.3F**). In contrast, adding EPZ simultaneously with LPS and IL-4 did not increase apoptosis compared to control, although it still reduced proliferation (**Fig.**

2.3G). This difference suggested that the anti-apoptotic function of Prmt5 was mediated by factors that were pre-methylated in resting B cells. To confirm this, we produced *Prmt5^{F/F}* Cγ1-cre mice, which express the Cre-recombinase only after B cell activation (Casola et al., 2006). We reasoned that the presence of the sDMA at the time of activation would prevent the apoptosis observed in the sDMA-depleted *Prmt5^{F/F}* CD19-cre B cells. Indeed, *Prmt5^{F/F}* Cγ1-cre B cells stimulated with LPS and IL-4 showed efficient Prmt5 depletion without any increase in apoptosis (**Fig. 2.3H**). We conclude that Prmt5 activity has an intrinsic function protecting from apoptosis at the time of B cell activation.

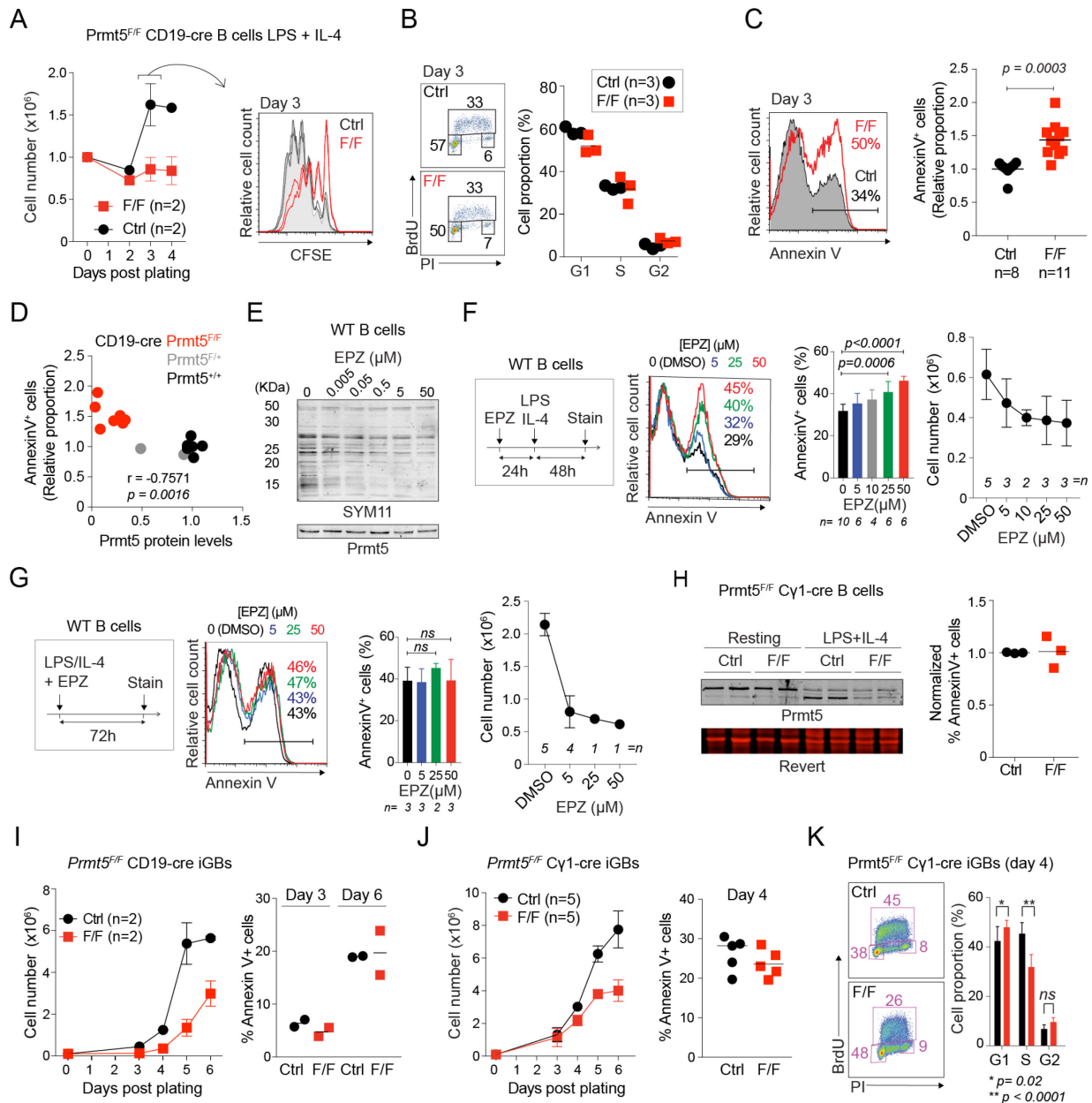


Figure 2.3 – Prmt5 protects B cells from apoptosis and promotes proliferation

A-D) Resting splenic B cells from CD19-cre (Ctrl) and Prmt5^{F/F} CD19-cre (F/F) mice were seeded at 1.10⁶ cells in 24-well plates with LPS (5 μg/mL) + IL-4 (5 ng/mL)

A) Cell expansion was monitored by cell counting over time. Cells were stained with CFSE and analyzed on day 3 by flow cytometry. One experiment, 2 mice per genotype.

B) Cell cycle profile of cell cultures pulsed with BrdU (10 μ M) for 1h at day 3 before staining with anti-BrdU and propidium iodide (PI). Data for 3 mice (symbols) per genotype from one experiment are plotted, with means indicated.

C) Representative histograms monitoring apoptosis by the proportion of Annexin-V⁺ B cells at day 3 post-plating. The proportion of Annexin-V⁺ cells for individual mice (symbols) from 5 experiments are plotted normalized to the Ctrl mean with means shown as bars. P-value from unpaired, two tailed Student's t-test.

D) Proportion of Annexin-V⁺ cells in B cells of each indicated genotype, as a function of Prmt5 protein levels normalized to Actin (measured by WB) at 72 h post-stimulation. Spearman's correlation coefficient (*r*) and p-value (*p*) are indicated.

E) WB for sDMA (SYM11) and Prmt5 in extracts from wt splenic B cells stimulated with LPS (5 μ g/mL) and IL-4 (5 ng/mL) for 72 h in the presence of the indicated concentration of Prmt5 inhibitor (EPZ).

F) Experimental set up and representative flow cytometry histogram of the proportion of Annexin-V⁺ B cells that were plated and treated with the indicated EPZ doses for 24 h before stimulation with LPS (5 μ g/mL) and IL-4 (5 ng/mL). Means + s.d. proportion of Annexin-V⁺ B cells from *n* mice from 5 experiments are plotted. The rightmost plot shows means + s.d. cell counts, except for the 10 μ M dose, for which mean \pm s.e.m was used, of *n* mice from 5 experiments at 72 h post-plating. Significant P-values by one-way ANOVA with Dunnett's correction for multiple comparisons are indicated.

G) Experimental set up for simultaneous Prmt5 inhibition and B cell activation. Apoptosis and cell counts from *n* mice from 2 experiments were measured and plotted as in F).

H) WB of Prmt5 in extracts of splenic B cells from Cy1-cre (Ctrl) and Prmt5^{F/F} Cy1-cre (F/F) mice, stimulated with LPS (5 μ g/mL) and IL-4 (5 ng/mL) for 72 h. Revert protein staining serves as loading control. The normalized proportion of Annexin-V⁺ cells for individual mice (symbols) from 2 experiments and mean values (bars) are plotted.

I) Left, resting splenic B cells from Prmt5^{F/+} CD19-cre (Ctrl) and Prmt5^{F/F} CD19-cre (F/F) mice were plated onto 40LB cells with 1 ng/mL IL-4 to generate GC-like B cells (iGBs). Mean \pm s.e.m. cell counts per day are plotted for 2 mice. Right, proportion of Annexin-V⁺ iGBs for individual mice (symbols) and means (bars) are plotted.

J) B cells from Cy1-cre (Ctrl) and Prmt5^{F/F} Cy1-cre (F/F) mice plated as in I).

K) Representative cell cycle profile of Cy1-cre (Ctrl) and Prmt5^{F/F} Cy1-cre (F/F) iGBs at day 4, done as in B). Means + s.d. of 6 mice per genotype from 3 experiments are plotted. Significant P-values by unpaired, two tailed Student-t test.

2.3.4 Prmt5 promotes activated B cell proliferation independently of apoptosis

Ex vivo activation of purified resting B cells with mitogens only supports limited proliferation (**Fig. 2.3A**). We therefore used a system that permits sustained B cell proliferation, by plating resting B cells onto 40LB feeder cells, which express CD40L and the anti-apoptotic BAFF (Nojima et al., 2011). In the presence of exogenous IL-4, B cells expand exponentially in this system and acquire a GC-like phenotype (iGBs, from now on) in which Prmt5 is the most highly expressed PRMT (**Supplementary Fig. 2.2A**). *Prmt5^{F/F}* CD19-cre iGB cells showed only a small sDMA reduction by day 6 post-plating (**Supplementary Fig. 2.2B**), likely due to inefficient excision and/or selection, which limited the interpretation of the experiment. Yet, these cells showed compromised expansion but no increased apoptosis, compared to controls (**Fig. 2.3I**), suggesting both effects could be separated. Indeed, in *Prmt5^{F/F}* Cγ1-cre iGBs, Prmt5 and sDMA depletion were efficient and sustained (**Supplementary Fig. 2.2C, 2.2D**) and these cells had substantially compromised expansion but no increased apoptosis (**Fig. 2.3J**). Cell cycle analysis revealed significant G1 arrest and reduction in the proportion of cells in S-phase that could explain reduced proliferation (**Fig 2.3K**). We conclude that Prmt5 promotes B cell proliferation by a different mechanism than it protects B cells from apoptosis during activation.

2.3.5 Prmt5 is essential for antibody responses

To examine the pro-proliferation function of Prmt5 in normal B cells *in vivo* without the confounding effect of activation-related apoptosis, we analyzed GC responses in *Prmt5^{F/F}* Cγ1-cre mice, which ablate Prmt5 only after activation. *Prmt5^{F/F}* Cγ1-cre mice immunized with NP-CGG showed a >10-fold reduction in total anti-NP IgG1 at day 14 post-immunization compared to controls (**Fig. 2.4A**), which correlated with a severe deficit in antibody secreting cells (**Fig. 2.4B**). The drastic impairment of the antibody response in *Prmt5^{F/F}* Cγ1-cre mice was consistent at all times post-immunization tested (**Fig. 2.4C**). Furthermore, *Prmt5^{F/F}* Cγ1-cre mice showed a 17-

fold reduction in pre-immune serum IgG1, which is elicited against environmental antigens, indicating that even chronic stimulation could not compensate for the defect (**Fig. 2.4D**). *Prmt5^{F/F}* Cγ1-cre mice immunized with NP-CGG had normal resting splenic B cell populations but showed a 3-fold reduction in GC B cell numbers at day 14 post-immunization (**Fig. 2.4E, 2.4F**). *Prmt5^{F/F}* Cγ1-cre mice infected with *H. polygyrus* exhibited 6-fold reduction in GC B cells in MLN, while total B and T cell numbers were unaffected (**Fig. 2.4G, 2.4H**). Accordingly, IF of MLN from infected *Prmt5^{F/F}* Cγ1-cre mice showed greatly reduced numbers of visible GC compared to the controls (**Fig. 2.4I**). Thus, antigen persistence cannot moderate the GC defect caused by Prmt5-deficiency. The number of total activated CD4⁺ T cells, Th2 or Treg cells was not significantly different between the groups (**Supplementary Fig. 2.3A**). In addition, there was no significant difference in the absolute number or ratio of Tfh and Tfr cells between the groups (**Supplementary Fig. 2.3B**). These data further indicate a B cell-intrinsic role for Prmt5 in GC formation. We conclude that, separate from its function during B cell activation, Prmt5 is essential for the antibody response by promoting GC formation.

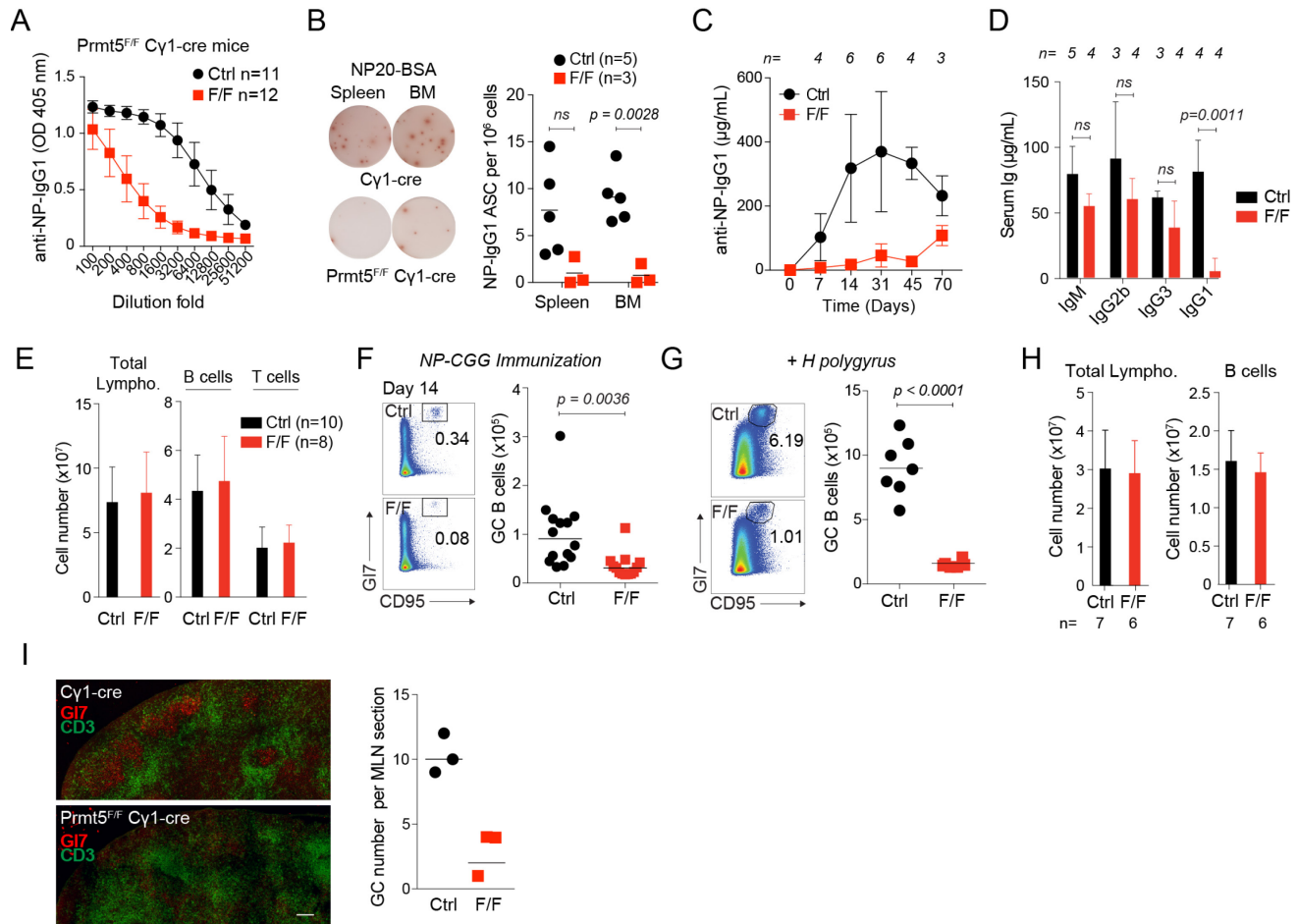


Figure 2.4 – Antibody response and GC defects caused by Prmt5 deficiency

A-I) Cy1-cre (Ctrl) and Prmt5^{F/F} Cy1-cre (F/F) mice were used throughout.

A) Total anti-NP IgG1 in the serum of mice measured by ELISA using NP₂₀-BSA, 14 days after immunization with NP-CGG. Mean ± s.d. OD values for serial dilutions are plotted for n mice from 3 experiments.

B) NP-specific IgG1 antibody secreting cells (ASC) were measured by ELISPOT using NP₂₀-BSA. Representative pictures of ELISPOT wells are shown. The number of ASC of individual mice (symbols) and mean values (bars) are plotted.

C) Anti-NP IgG1 in the serum of mice at various times post-immunization. Antibodies were measured as in A) and converted to mass using a standard curve. Mean ± s.d. values for n mice at each time point from 2 experiments are plotted.

D) Total levels of antibody isotypes in the serum of n non-immunized mice, measured by ELISA.

E) Mean + s.d. number of lymphocytes per spleen enumerated by flow cytometry for *n* mice from 2 experiments.

F) Representative flow cytometry plots (gated on B220⁺) of splenic GC B cell proportions at 14 days post-immunization with NP-CGG. Number of GC B cells per spleen for individual mice (symbol) and mean values (bars) from 3 experiments are plotted.

G) As in F) for MLN of mice infected with *H polygyrus* for 14 days. Data from 2 experiments are plotted.

H) Mean + s.d. number of lymphocytes per MLN in the mice from G).

I) Representative IF in MLN from mice infected with *H polygyrus*, stained for the indicated antigens. Scale bar, 100 μ m. GC number per MLN scored in individual mice (symbols) are plotted to the right.

P-values throughout are indicated for significant differences by unpaired, two tailed Student-*t* test.

2.3.6 Prmt5 is required for GC expansion and dynamics

To pinpoint the GC stage in which Prmt5 played a role, we analyzed GCs at different times after immunizing *Prmt5^{F/F}* C γ 1-cre and C γ 1-cre control mice with SRBC. Both groups showed similar number of GC B cells at day 5 post-immunization (**Fig. 2.5A**). The number of GC per spleen section and their apparent organization was also similar between the groups at this time (**Fig. 2.5B, 2.5C**), despite Prmt5 and sDMA being efficiently depleted in *Prmt5^{F/F}* C γ 1-cre GC (**Fig. 2.5D**). In contrast, by day 8 post-immunization, GC B cell proportion and numbers were severely reduced and there were fewer GCs per spleen in *Prmt5^{F/F}* C γ 1-cre mice (**Fig. 2.5A, 2.5B**), although the GCs we could observe maintained overall organization (i.e. DZ proximal to the T cell zone and CD35⁺ LZ could be distinguished) (**Fig. 2.5C**). Consistent with our *ex vivo* data in iGB cells, GC B cells in *Prmt5^{F/F}* C γ 1-cre mice did not show apoptosis (**Fig. 2.5E**) but were enriched in Ki67^{low} cells (**Fig. 2.5F**), which indicates less cells in S/G2/M (Endl et al., 1997).

To characterize in more detail the GC defect in *Prmt5^{F/F}* C γ 1-cre mice, we examined DZ and LZ B cells. The DZ/LZ ratio in *Prmt5^{F/F}* C γ 1-cre GC was apparently normal (**Fig. 2.5G**), but these mice displayed a Cxcr4⁻ Cd86^{low} GC population at days 8 and 10 post-immunization that was not visible in the controls (**Fig. 2.5G**). This population

was also readily visible in mice infected with *H. polygyrus* (**Fig. 2.5H**), excluding an antigen-dependent effect, and was independent of AID expression (**Fig. 2.5I**), further excluding that it can be caused by reduced SHM and therefore affinity maturation. Further analysis revealed that a large proportion of Cxcr4⁻ Cd86^{low} cells were Ki67^{low} (**Fig. 2.5J**), indicating lower proliferative potential, and that this population did not express AID, as shown using *Prmt5^{F/F}* Cγ1-cre *Aicda-GFP* mice (**Fig. 2.5K**). These reporter mice revealed further alterations in Prmt5-null GC B cells, notably the loss of an AID^{dim} DZ population and there were fewer AID⁺ cells in the LZ, presumably because they converted to the Cxcr4⁻ Cd86^{low} subset (**Fig. 2.5K**).

We conclude that, after the initial requirement for B cell activation, Prmt5 is dispensable for GC initiation but necessary for GC expansion, at least in part by promoting cell proliferation but also by sustaining normal GC dynamics, as shown by accumulation of abnormal Cxcr4⁻ Cd86^{low} Ki67^{low} Aid⁻ B cells in Prmt5-deficient GCs.

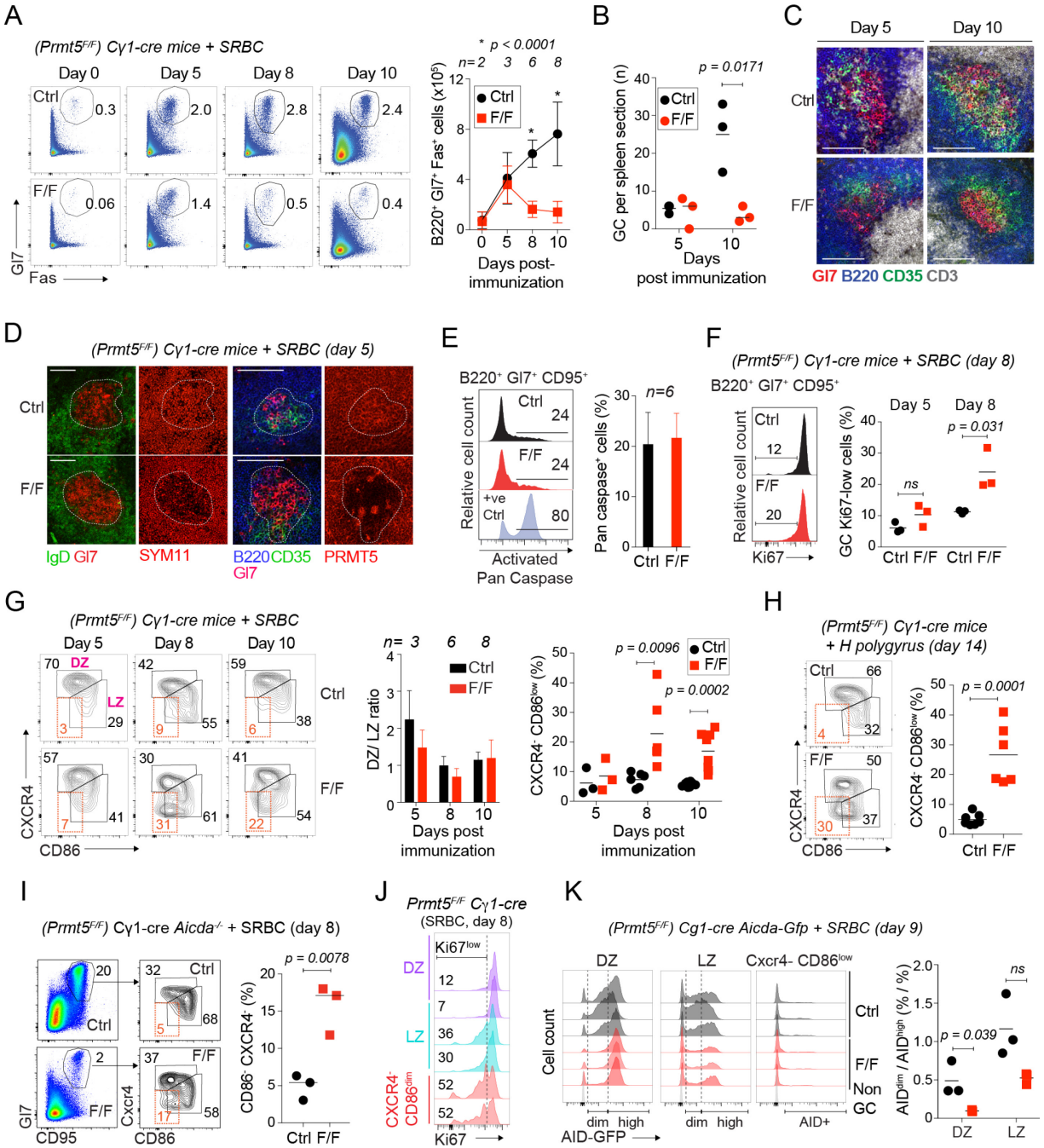


Figure 2.5 – Prmt5 is necessary for GC expansion

A) Representative flow cytometry plots of GC B cells (%) in *Cy1-cre* (Ctrl) or *Prmt5^{F/F}* *Cy1-cre* (F/F) mice at various times post-immunization with SRBC. Mean \pm s.d (except at day 0, s.e.m) of absolute GC B cell numbers from *n* mice from 7 experiments are plotted.

B) Enumeration of GC in spleen from individual *Cy1-cre* (Ctrl) or *Prmt5^{F/F}* *Cy1-cre* (F/F) mice (symbols) at days 5 and 10 post-immunization, analyzed by IF. Mean values are shown by bars.

C) Representative fluorescent microscopy images used for counting GC in B). Antibodies recognized B cells (B220), T cells (CD3), FDCs (CD35) and activated/GC B cells (GL7). Scale bar, 100 μ m.

D) Representative confocal images of IF in splenic sections from immunized mice, stained for the indicated markers as well as *Prmt5* and sDMA (SYM11). GCs are contoured. Scale bar, 100 μ m.

E) Representative histograms showing the frequency of activated pan-caspase⁺ cells in splenic GC B cells from mice analyzed in A) at day 8 post-immunization. The positive gate was set using etoposide (3 μ M) to induce apoptosis. Mean + s.d. proportion of activated pan-caspase⁺ GC B cells for 6 mice per group from 2 independent experiments are plotted.

F) Representative histograms of Ki67 expression in splenic GC B cells from mice as in A), at day 8, with a Ki67^{low} gate indicated. Mean + s.d. proportion of Ki67^{low} GC B cells for individual mice (symbols) at days 5 and 8 post-immunization, from one experiment each.

G) Representative flow cytometry plots of DZ (CXCR4⁺ CD86^{low}), LZ (CXCR4⁻ CD86^{high}) and a third population (CXCR4⁻ CD86^{low}) of GC B cells (B220⁺ GL7⁺ CD95⁺) from *Cy1-cre* (Ctrl) or *Prmt5^{F/F}* *Cy1-cre* (F/F) mice at various times post-immunization with SRBC. Mean + s.d. of DZ/LZ ratios for n mice from 6 independent experiments are plotted, as well as the proportions of (CXCR4⁻ CD86^{low}) GC B cells for individual mice (symbols), with means (bars) indicated.

H) Representative flow cytometry plots and proportion of (CXCR4⁺ CD86^{low}) GC B cells, scored as in G), in *Cy1-cre* (Ctrl) or *Prmt5^{F/F}* *Cy1-cre* (F/F) mice infected with *H. polygyrus* for 14 days. Data compiled from 2 experiments.

I) As in G) for *Aicda*^{-/-} *Cy1-cre* (Ctrl) or *Aicda*^{-/-} *Prmt5^{F/F}* *Cy1-cre* (F/F) mice immunized with SRBC.

J) Representative histograms of Ki67 levels in different GC B cell subsets from *Prmt5^{F/F}* *Cy1-cre* (F/F) immunized with SRBC.

K) Histograms of AID-GFP levels for individual *Aicda-GFPtg* *Cy1-cre* (Ctrl) or *Aicda-GFPtg* *Prmt5^{F/F}* *Cy1-cre* (F/F) mice at 9 days post-immunization with SRBC. Gates distinguishing dim and high AID expression are shown in LZ and DZ. The ratio of AID^{dim}/AID^{high} for individual mice are plotted with (symbols) means indicated (bars).

P-values indicated throughout for significant differences by unpaired, two tailed Student-*t* test.

2.3.7 Prmt5 regulates transcription and affects splicing fidelity in B cells

Since arginine methylation regulates gene expression (Blanc and Richard, 2017), we performed RNA-seq to gain mechanistic insight into the defects of Prmt5-deficient B cells. Given the paucity of GC B cells *in vivo*, we used *Prmt5^{FF}* Cy1-cre and Cy1-cre iGBs at day 4 after plating. At this time, iGB cells are largely CD95⁺ GL7⁺ and Prmt5 deletion and sDMA depletion are complete (**Supplementary Fig. 2.4A, Fig. 2.3J**). Prmt5 ablation induced large transcriptional changes, with 1511 genes differentially expressed in Prmt5-null versus control iGBs (P-adj <0.05, ≥ 1.5 -fold change in either direction) (**Supplementary Table 2.1**). Focusing on genes that changed by ≥ 2 -fold reduced the complexity to 382 genes, with a majority being upregulated and displaying larger changes (**Fig. 2.6A**), in line with the predominant role of Prmt5 as transcriptional repressor (Pal et al., 2007; Wang et al., 2008).

To identify biological processes that were affected by Prmt5 deficiency, we first used functional annotation by gene ontology (GO). No significantly enriched (FDR<5%) GO term was found when we analyzed the downregulated genes, regardless of the fold change in expression (see methods). On the other hand, analyzing all upregulated genes ranked by fold increase showed enrichment in many GO terms, mostly related to cell adhesion and proliferation (**Supplementary Figs. 2.4B, Supplementary Table 2.2**). Restricting the analysis to the 257 genes upregulated by ≥ 2 -fold also showed enrichment in cell adhesion and negative regulators of cell proliferation, which included several p53 target genes (**Fig. 2.6B**). Accordingly, gene set enrichment analysis (GSEA), a more sensitive method to detect gene signatures (Subramanian et al., 2005), revealed the upregulation of a p53 transcriptional signature in Prmt5-null B cells (**Fig. 2.6C, Supplementary Fig. 2.4C**). Additional analysis of a curated gene set composed of 346 genes upregulated by p53 (Fischer, 2017) confirmed a highly significant upregulation of p53 target genes in Prmt5-deficient iGBs, including the cell cycle inhibitor *Cdkn1a* and pro-apoptotic genes (*Perp*, *Bbc3*, *Tnfrsf10b*, *Bax*, *Ei24*, etc) (**Fig. 2.6C**). Thus, in the absence of Prmt5, B cells display a p53 response but

also undergo multiple gene expression changes that affect the proteins composition of the plasma membrane.

Prmt5 also regulates splicing (Bezzi et al., 2013; Blanc and Richard, 2017), which we analyzed from our RNA-seq data (see methods). Splicing of 1518 genes was significantly altered by >10% in Prmt5-deficient B cells (**Supplementary Table 2.3**). Genes affected at the splicing and transcriptional level showed little overlap (**Fig. 2.6D**), indicating that aberrant splicing was not causing the gene expression changes in Prmt5-deficient B cells. There was a clear preference to exclude exons (SE events) and include introns (RI events) in Prmt5-null cells compared to wt (**Fig. 2.6E**), but the genes affected by SE or RI did not overlap (**Supplementary Fig. 2.4D**). In fact, both types of events had the same underlying cause; the skipping of weak 5' splicing donor sites in Prmt5-deficient B cells, while 3' acceptor sites did not differ between used and skipped sites (**Fig. 2.6F, Supplementary Fig. 2.4E**). Functional annotation of the genes affected by splicing showed a predominance of GO terms related to regulation of gene expression and RNA processing whether all or just events with ≥ 0.25 inclusion level difference were analyzed (**Fig. 2.6G, Supplementary Fig. 2.4F, Supplementary Table 2.4**). Splicing was affected for multiple genes encoding chromatin modification factors, including several enzymes involved in histone modification (**Fig. 2.6G**), which is likely to contribute to the observed changes in gene expression. Interestingly, SE events affected several subunits of the Tip60 complex and Hdac6 (**Fig. 2.6G, Supplementary Fig. 2.4G**), both of which participate in DNA repair and regulate the p53 transcriptional response (Ding et al., 2013; Legube et al., 2004). We also found two major SE events resulting in multiple exon exclusions affecting a large proportion of the Mdm4 transcripts (**Fig. 2.6H**). These alternative Mdm4 forms cannot repress the transcriptional activity of p53 (Bezzi et al., 2013), which likely contributes to the p53 gene expression signature observed in Prmt5-deficient B cells.

We conclude that Prmt5 maintains the normal GC transcriptional program, both directly as well as by regulating proper RNA processing of multiple chromatin modifiers by ensuring the use of weak 5' donor sites.

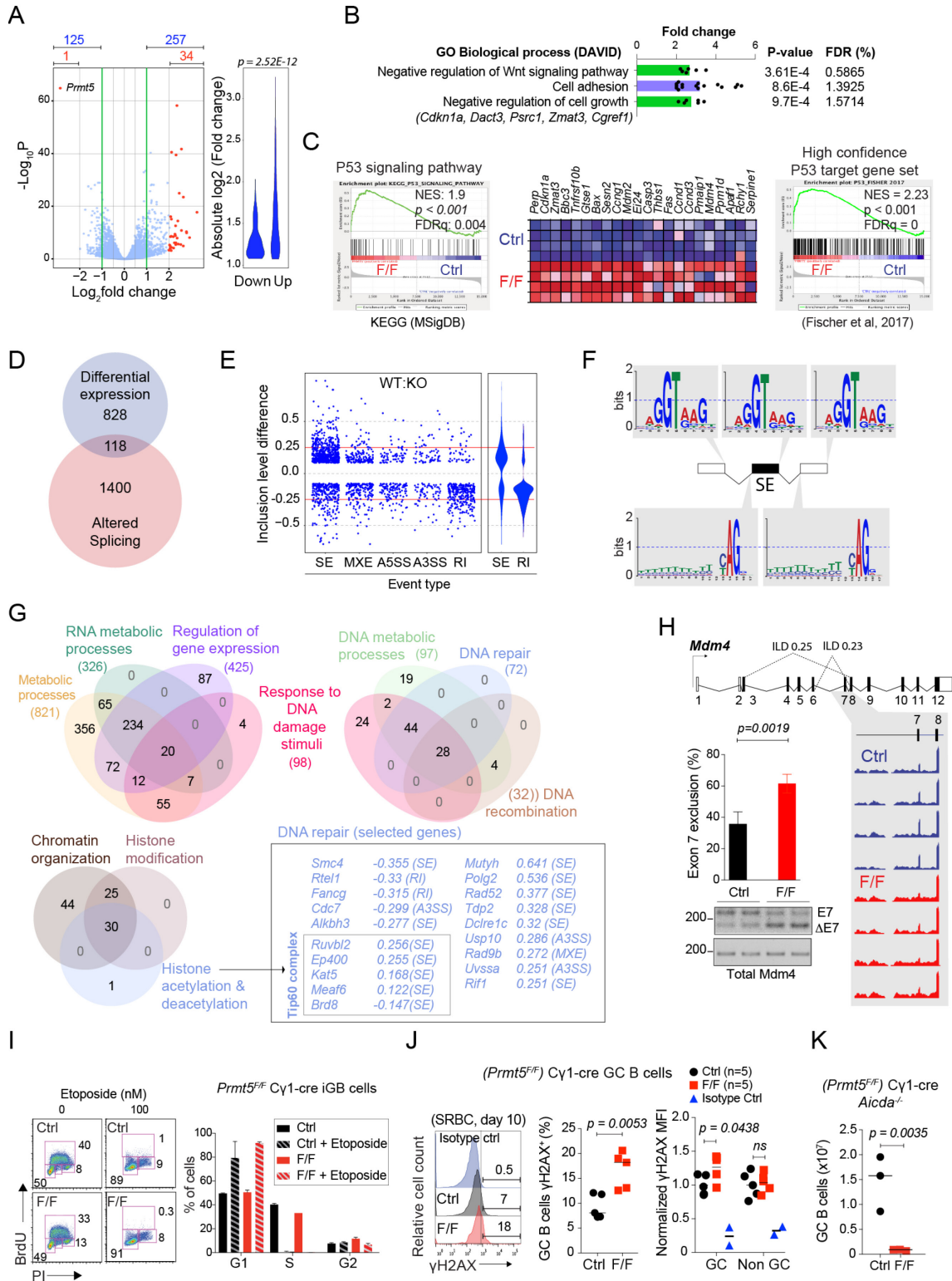


Figure 2.6 – *Prmt5* regulates gene expression and maintains splicing fidelity in B cells

A) Volcano plot of gene expression changes in *Prmt5^{F/F}* *Cy1-cre* versus *Cy1-cre* iGB cells. The number of genes significantly changed by ≥ 2 - or ≥ 4 -fold (in red), are indicated. The violin plot shows the absolute change for the genes changing by ≥ 2 -fold.

B) GO terms significantly enriched in a list of the 257 genes upregulated ≥ 2 -fold in *Prmt5*-null iGBs, as analyzed at the DAVID server against a background list of all expressed genes in iGBs (basemean >0).

C) Gene set enrichment analysis (GSEA) of the KEGG P53 signaling pathway from MSigDB and heat map of genes in the leading edge. GSEA of a curated set of 346 genes that are direct targets of p53 and upregulated in response to p53.

D) Venn diagrams comparing genes differentially expressed by ≥ 1.5 -fold, to genes with at least one splicing alteration. In both cases only significant events (P -value <0.05) and relatively well-expressed genes (basemean >50) were included.

E) Scatter plot of inclusion level difference (ILD) in WT/KO for each significant splicing event (P <0.05 , $\geq 10\%$ ILD) separated by category (SE, skipped exon; MXE, mutually exclusive exons; A5SS and A3SS, altered 5' or 3' splicing site; RI, retained intron). Violin plots for SE and RI are included to highlight the preferential direction of the change in each.

F) Sequence logos of the splicing donor and acceptor sites around SE events of *Prmt5^{F/F}* *Cy1-cre* iGBs. The height represents the probability of each possible letter appearing at that position.

G) Venn diagrams of partially overlapping GO terms grouping the majority of genes with significantly affected splicing in *Prmt5*-null B cells. Names + (ILD) of selected genes involved in DNA repair are indicated.

H) *Mdm4* gene scheme and alignment of RNA-seq data from each sample with the aligned reads for one SE event in each sample. Representative RT-PCR validating the same event and mean + s.d. quantification of exon 7 exclusion for 4 mice are shown.

I) Cell cycle profile of *Cy1-cre* (Ctrl) and *Prmt5^{F/F}* *Cy1-cre* (F/F) iGBs treated or not with 100 nM etoposide on day 3 after plating and analyzed 24 h later. Means + s.e.m of 2 mice per genotype from one experiment are plotted.

J) Representative histograms of γ H2AX staining in GC B cells ($B220^+ Gl7^+ CD95^+$) in *Cy1-cre* (Ctrl) and *Prmt5^{F/F}* *Cy1-cre* (F/F) mice 10 days after SRBC immunization, and compiled data for 5 mice (symbols) per genotype from 2 experiments. Proportion of γ H2AX⁺ and normalized γ H2AX levels estimated from mean fluorescent intensity (MFI) are plotted.

K) Number of GC B cells in the spleen of *Aicda^{-/-}* *Cy1-cre* (Ctrl) and *Aicda^{-/-}* *Prmt5^{F/F}* *Cy1-cre* (F/F) mice (symbols), 10 days after immunization. Data from one experiment.

P-values for significant differences by unpaired, two tailed Student-*t* test in J) and K).

2.3.8 Prmt5 prevents spontaneous DNA damage in GC B cells

Prmt5 promotes homologous recombination repair in human cell lines by methylating Rubv11, with Prmt5 depletion sensitizing cell lines to DNA damaging agents (Clarke et al., 2017). Since GC B cells undergo DNA damage from antibody diversification and high replication rates, we asked if these could cause the p53 response in Prmt5-null B cells and/or growth phenotypes. We confirmed that Prmt5-deficient B cells have an intact G1 checkpoint after DNA damage, indicating that p53 was functional in these cells (**Fig. 2.6I**). Despite a trend towards accumulating more DNA damage in *Prmt5^{F/F}* Cγ1-cre iGBs, these cells were not more sensitive than controls to various DNA damaging agents, including drugs causing replication stress (**Supplementary Fig. 2.4H, 2.4I**). Nonetheless, *in vivo* there was a significant increase in the DNA damage marker γH2AX in GC B cells of immunized *Prmt5^{F/F}* Cγ1-cre mice, which was not seen in control or non-GC B cells (**Fig. 2.6J**). Homologous recombination is important to protect B cells from DNA damage caused by off-target AID activity (Hasham et al., 2010). However, ablating AID did not rescue GC expansion or normal populations in *Aicda^{-/-} Prmt5^{F/F}* Cγ1-cre mice (**Figs. 2.6K, 2.5I**), ruling out AID-induced DNA damage as a cause for the GC defects. Furthermore, antibody class switching per division was normal in *Prmt5^{F/F}* CD19-cre activated B cells (**Supplementary Fig. 2.4J**), indicating that non-homologous end joining repair was functional in Prmt5-null B cells. Several of the chromatin modifiers showing altered splicing also participate in DNA repair, such as the Tip60 complex and Cdh11. Furthermore, there were significant SE and RI events in transcripts of many DNA damage response and repair genes, mostly from the base excision, Fanconi and homologous recombination repair pathways and chromatin modifiers that participate in the DNA damage response, like Tip60 and Cdh11 (**Fig. 2.6G**). Since many of these genes are highly induced in GC B cells according to Immgen, we conclude that Prmt5 prevents the accumulation of spontaneous DNA damage in GC B cells, at least in part by maintaining the splicing fidelity of factors belonging to several but not all DNA repair pathways.

2.3.9 A p53 response eliminates Prmt5-deficient pro-B cells

Based on the RNA-seq analysis, we tested the contribution of the p53 response to the phenotype of Prmt5-deficient B cells *in vivo*. As mentioned, efficient ablation of Prmt5 by Mb1-cre mice (Hobeika et al., 2006) resulted in the absence of mature B cells in the spleen (**Fig. 2.7A**). This was due to a block of B cell development at the pro-B cell stage (Hardy's fraction B) (**Fig. 2.7B**). Progenitor cells initiate VDJ recombination, which evokes a p53 apoptotic response that limits the number of Pro-B cells *in vivo* (Guidos et al., 1996; Lu and Osmond, 2000). However, introducing the prearranged B1-8 V_H allele in *Prmt5^{F/F}* Mb1-cre mice could not rescue the pro-B cell block (**Fig. 2.7C**), ruling out defective VDJ rearrangement or an associated DNA repair defect as the cause. To test the role of p53, we produced *Prmt5^{F/F}* Mb1-cre *Tpr53^{-/-}* mice, which fully recovered pro-B cell numbers and substantially recovered fraction C/C', corresponding to late pro- and large pre-B cell stages, but not the small pre-B cell fraction D (**Fig. 2.7D**). Closer examination of fraction C/C' showed that no pre-BCR⁺ cells were generated in *Prmt5^{F/F}* Mb1-cre *Tpr53^{-/-}* mice (**Fig. 2.7E**). We conclude that Prmt5 is essential for B cell development by dampening the p53 response in Pro-B cells, but also has another essential but p53-independent role in large Pre-B cells.

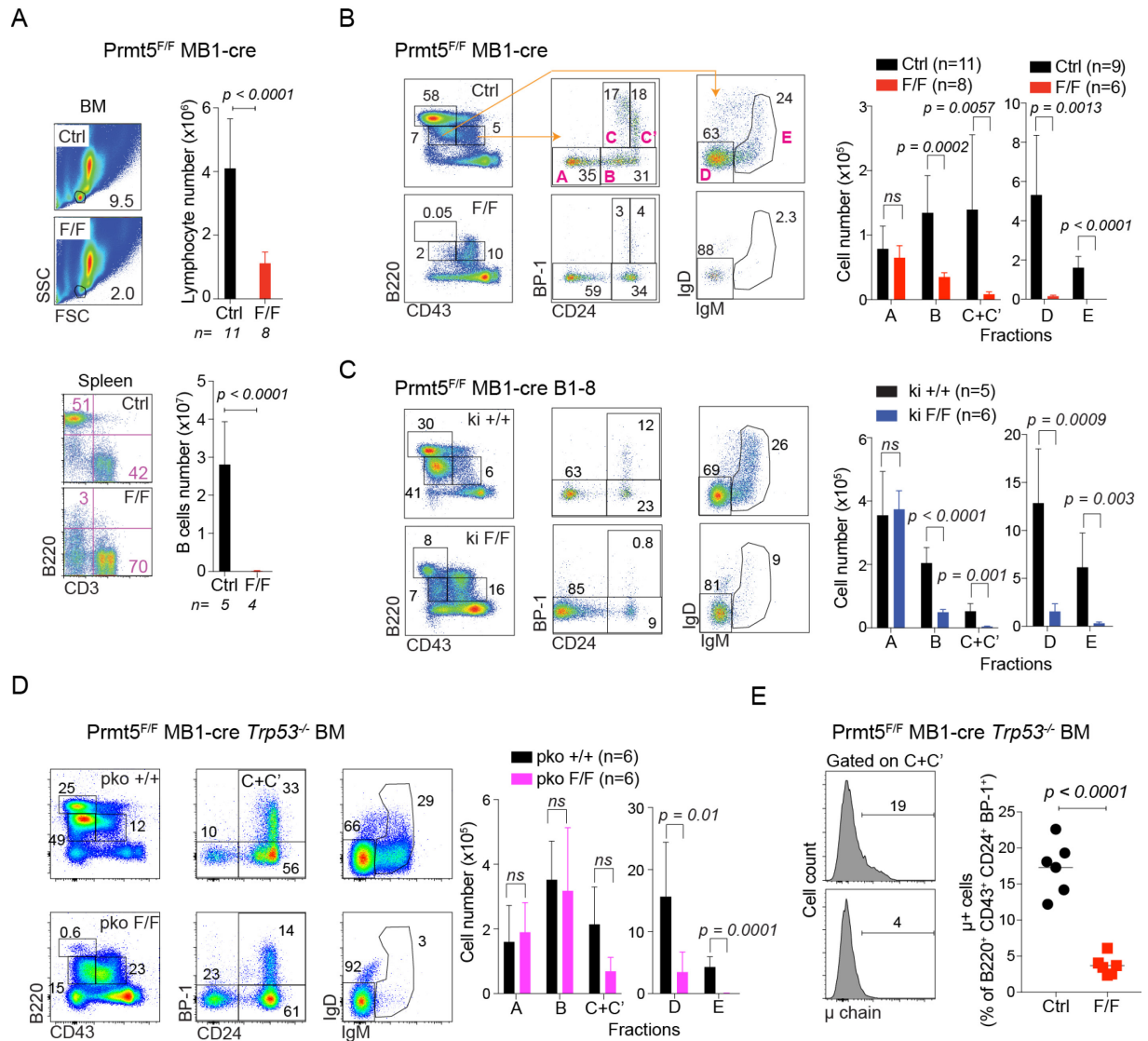


Figure 2.7 – Prmt5 is required for B cell development

A) BM lymphocytes and splenic B cells in MB1-cre (Ctrl) or Prmt5^{F/F} MB1-cre (F/F) mice. Representative flow cytometry plots are shown, indicating cell proportions. Mean + s.d. of absolute lymphocyte counts for n mice from 4 experiments are plotted.

B) Representative flow cytometry plots indicating gating for Hardy fractions A to E used to quantify B cell development in BM from 3-4 months old MB1-cre (Ctrl) and Prmt5^{F/F} MB1-cre (F/F) mice. Means + s.d. absolute cell numbers for each fraction from n of mice from 4 independent experiments are plotted.

C) As in B, for B1-8 MB1-cre (ki +/+) and B1-8 Prmt5^{F/F} MB1-cre (ki F/F) mice, from 3 experiments.

D) As in B, for Trp53^{-/-} MB1-cre (pko +/+) and Trp53^{-/-} Prmt5^{F/F} MB1-cre (pko F/F) mice, from 3 experiments.

E) Proportion of Large Pre-B cells in fractions C+C' estimated by the pre-BCR expression in individual (symbols) *Trp53*^{-/-} MB1-cre (Ctrl) and *Trp53*^{-/-} *Prmt5*^{F/F} MB1-cre (F/F) mice.

P-values throughout are from unpaired, two tailed Student-*t* test.

2.3.10 Prmt5 prevents p53-independent apoptosis during B cell activation

We then asked whether a p53 response might explain the increased apoptosis observed when activating splenic B cells from *Prmt5*^{F/F} CD19-cre mice *ex vivo* (**Fig. 2.3D**). Both p53 protein levels and activation, as verified by phosphorylation of p53 at Ser15, were increased in these cells (**Fig. 2.8A**). Accordingly, the p53 targets *Bax* and *Cdkn1a*, which were upregulated in iGBs, were also upregulated in these cells (**Fig. 2.6C, 2.8B**). Despite this, *Prmt5*^{F/F} CD19-cre *Trp53*^{-/-} B cells still showed apoptosis and reduced proliferation (**Fig. 2.8C**), indicating that these were p53-independent defects. We confirmed this by pharmacological inhibition of Prmt5 24 h before activation in wt and *Trp53*^{-/-} B cells, both of which showed increased apoptosis (**Fig. 2.8D**). On the other hand, Bcl2 overexpression did rescue apoptosis induced by Prmt5 inhibition, as shown in splenic B cells from Bcl2 transgenic mice (**Fig 2.8D**). Interestingly, both p53 deficiency as well as Bcl2 overexpression prevented *Bax* and *Cdkn1a* upregulation (**Fig. 2.8E**). We conclude that Prmt5 is necessary to prevent mitochondrial apoptosis upon B cell activation independently of p53 activation.

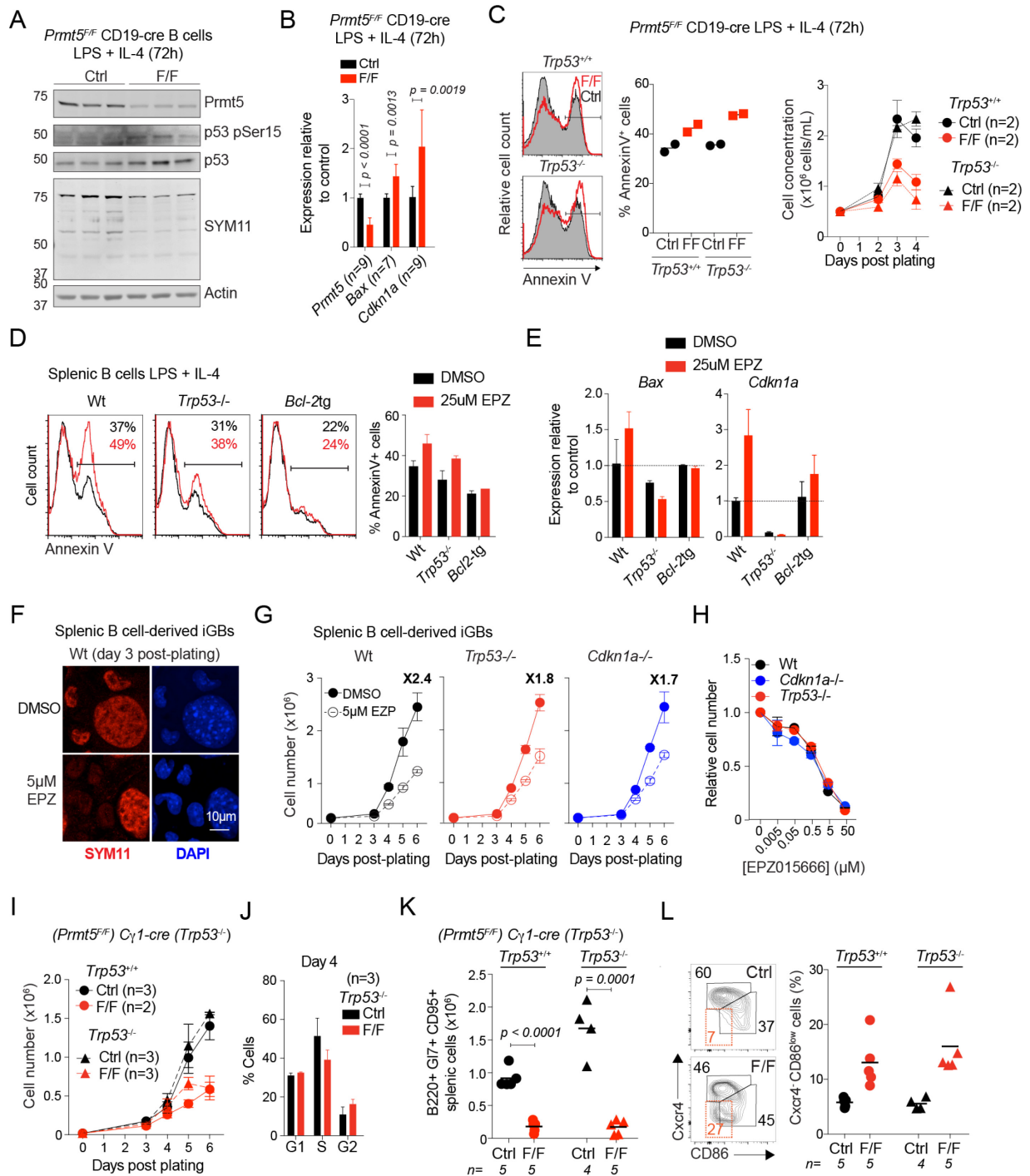


Figure 2.8 – *Prmt5* loss induces p53-independent apoptosis

A) WB probed for the indicated proteins on extracts from CD19-cre (Ctrl) and *Prmt5^{F/F}* CD19-cre (F/F) splenic B cells cultured with LPS (5 μ g/mL) and IL-4 (5 ng/mL) for 3 days.

B) Gene transcript levels estimated by RT-qPCR in splenic B cells as in A). Mean + s.d. mRNA level normalized to Actin for *n* mice are plotted relative to the mean of Ctrl.

C) Representative histograms of Annexin V levels in CD19-cre (Ctrl) and *Prmt5^{F/F}* CD19-cre (F/F) in *Trp53^{+/+}* or *Trp53^{-/-}* background. Mean proportion of Annexin-V⁺ for 2 mice per genotype from one experiment are plotted. Means + s.e.m cell concentrations over time are plotted on the right.

D) Representative histograms of Annexin V levels in wt, *Trp53^{-/-}* and *Bcl-2tg* B cells treated with either DMSO or 25μM EPZ for 24 h, followed by 48 h stimulation with LPS (5 μg/mL) and IL-4 (5 ng/mL). Means + s.e.m proportion of Annexin-V⁺ in 2 mice per genotype from one experiment are plotted.

E) Relative *Bax* and *Cdkn1a* expression by RT-qPCR in B cells from D).

F) Representative confocal microscopy of IF for sDMA (SYM11) in iGB cells from wt mice 3 days post-plating, treated with DMSO or 5 μM EPZ 24 h after plating. The large nuclei are from the feeder cells. Scale bar, 10 μm.

G) Expansion of iGB cells derived from wt, *Trp53^{-/-}* and *Cdkn1a^{-/-}* splenic B cells, treated with DMSO or 5μM EPZ 24h after plating. Means ± s.e.m cell counts of 2 mice from 1 experiment are plotted.

H) Sensitivity of wt, *Trp53^{-/-}* and *Cdkn1a^{-/-}* iGB cells to EPZ. Cells treated with the indicated EPZ doses 24 h after plating and counted 4 days later. Mean ± s.e.m of cell numbers relative to DMSO-treated for each genotype are plotted for 2 mice from 1 experiment.

I) Expansion of iGBs derived from splenic B cells from *Cy1-cre* (Ctrl) and *Prmt5^{F/F}* *Cy1-cre* (F/F) mice (full lines) or *Trp53^{-/-}* *Cy1-cre* (Ctrl) and *Trp53^{-/-}* *Prmt5^{F/F}* *Cy1-cre* (F/F) mice (dotted lines). Mean ± s.d. (except ± s.e.m for *Prmt5^{F/F}* *Cy1-cre*) cell counts for *n* mice are plotted per day.

J) Cell cycle profile of *Trp53^{-/-}* *Cy1-cre* (Ctrl) and *Trp53^{-/-}* *Prmt5^{F/F}* *Cy1-cre* (F/F) iGBs pulsed with BrdU (10μM) for 1h at day 4 post plating before harvesting and staining with anti-BrdU and propidium iodide (PI). Means + s.d. for 3 mice per genotype from 2 independent experiments are plotted.

K) GC B cells in the spleen of *Trp53^{-/-}* *Cy1-cre* (Ctrl) and *Trp53^{-/-}* *Prmt5^{F/F}* *Cy1-cre* (F/F) mice 10 days after immunization with SRBC. Values for individual mice (symbols) and mean (bars) values are plotted from 3 independent experiments.

L) Representative flow cytometry plots and proportion of *Cxcr4⁻* *CD86^{low}* cells in GC from the mice in K).

2.3.11 Prmt5 promotes B cell proliferation independently of p53

The RNA-seq data was obtained from *Prmt5^{F/F}* *Cy1-cre* iGB cells, which do not undergo apoptosis but still fail to expand and show a p53 transcriptional response

with high *Cdkn1a*/p21 expression (**Figs. 2.3J, 2.3K, 2.6B, 2.6C**). We therefore asked whether the non-apoptotic proliferation defect observed in *Prmt5*-deficient B cells was p53- and/or p21-dependent. Pharmacological inhibition of *Prmt5* similarly reduced the proliferation of wt, *Trp53*^{-/-} and *Cdkn1a*^{-/-} iGB cells, without any noticeable difference in their sensitivity to the inhibitor (**Figs. 2.8F-H**). To genetically confirm this, we produced *Prmt5*^{F/F} Cγ1-cre *Trp53*^{-/-} mice. Again, iGBs derived from splenic B cells from these mice showed the same reduced expansion and cell cycle defect as *Prmt5*^{F/F} Cγ1-cre iGBs (**Fig. 2.8I, 2.8J**), demonstrating that these phenotypes were p53-independent. Furthermore, immunized *Prmt5*^{F/F} Cγ1-cre *Trp53*^{-/-} mice displayed the same GC defect as *Prmt5*^{F/F} Cγ1-cre mice, including the accumulation of Cxcr4⁻ CD86^{low} cells (**Fig. 2.8K, 2.8L**). Since *Cdkn1a* is not expressed in p53-deficient cells (**Fig. 2.8E**), these results also ruled out p21 as a cause for the defects in B cell expansion *in vitro* or the GC phenotypes *in vivo*. We conclude that *Prmt5* has a p53- and p21-independent function that promotes B cell proliferation and maintains the GC reaction.

2.3.12 *Prmt5* functions in light zone B cells

To further characterize *Prmt5* in the GC, we analyzed the expression of *Prmt5* in GC B cell subsets. Gene expression data indicated a small but consistent increase in *Prmt5* in centrocytes versus centroblasts (**Supplementary Fig. 2.5A**). Moreover, our IHC suggested polarization of *Prmt5* expression in the GC (**Fig. 2.9A, Supplementary Fig. 2.5B**). IF with the LZ marker CD35 confirmed that *Prmt5* was preferentially expressed in the LZ GC B cells (**Fig. 2.9B**). In line with the polarization of *Prmt5* expression in the GC, *Prmt5*-deficient iGBs were significantly depleted of gene expression signatures characteristic of Cxcr4⁻ LZ B cells (Caron et al., 2009; Victora et al., 2010), as well as genes upregulated by CD40 engagement, while DZ-related gene sets were not significantly affected (FDR>5%) (**Fig 2.9C, Supplementary Fig. 2.5C**). We conclude that *Prmt5* is regulated to favor expression in the LZ and that it contributes to maintain the transcriptional identity of LZ B cells.

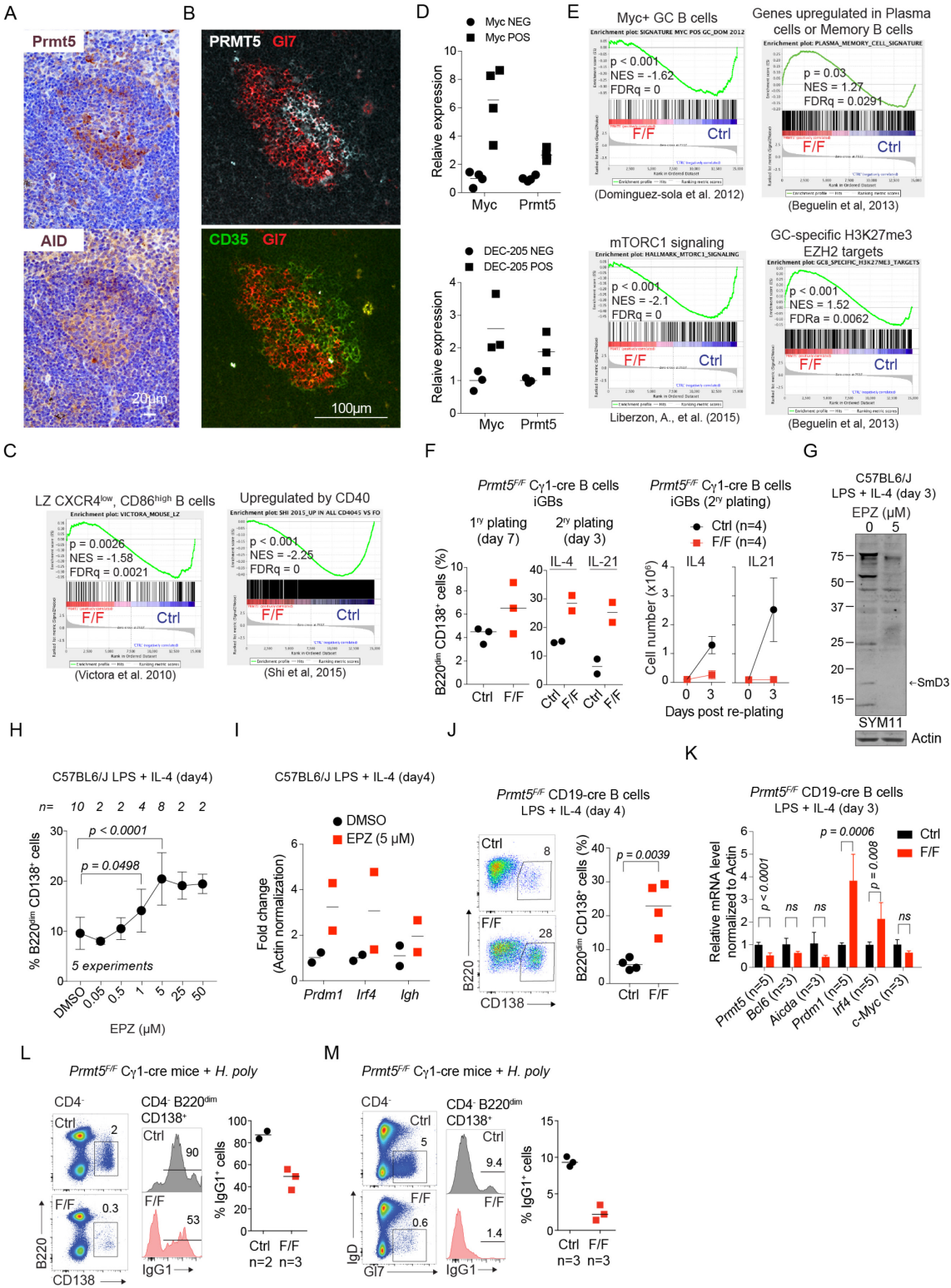


Figure 2.9 – Prmt5 acts in the light zone to prevent B cell differentiation

A) Representative IHC staining for *Prmt5* and AID, as GC marker, on consecutive spleen sections from wt mice 14 days post-immunization with NP-CGG. Images are representative of 3 mice from 2 experiments.

B) Representative IF on spleen from a wt mouse 10 days post-immunization with SRBC, stained for GL7 (GC marker), CD35 (LZ marker) and *Prmt5*.

C) GSEA of transcriptional changes in *Prmt5*^{F/F} *Cy1-cre* (F/F) iGB cells against LZ GC B cell signatures. Enrichment was considered significant when $P < 0.05$ and $FDR < 5\%$.

D) Relative gene expression of *Prmt5* in *Myc*⁺ or positively selected (DEC-205 POS) GC B cells, using *Myc*⁺ as control.

E) GSEA for the indicated gene signatures, as in C).

F) Proportion of plasma cell-like cells (*B200*^{dim} *CD138*⁺) in *Cy1-cre* (Ctrl) or *Prmt5*^{F/F} *Cy1-cre* (F/F) iGB cultures supplemented with 1 ng/mL IL-4 at day 7 post-plating, or upon replating at day 4 on fresh feeder cells supplemented either with 1 ng/mL IL-4 or 10 ng/mL IL-21 and analyzed 3 days later. Individual mice (symbols) and mean (bars) values from one experiment are plotted. The mean \pm s.d. iGB cell count in secondary replating are show on the right. Data from 2 experiments.

G) WB for sDMA (SYM11) and Actin, as a loading control, in extracts from wt splenic B cells stimulated with LPS and IL-4 for 72 h in the presence of 5 μ M EPZ. The position of splicing factor *Smd3* is indicated.

H) Means \pm s.d. (or \pm s.e.m for 0.05, 0.5, 25 and 50 μ M doses) plasma cell (*B200*^{dim} *CD138*⁺) proportion in cultures of wt splenic B cells stimulated with LPS and IL-4 and treated with various EPZ doses, are plotted for *n* mice from 5 experiments.

I) Gene expression by RT-qPCR in B cells treated with 5 μ M EPZ as in G), Individual mice (symbols) and mean (bars) values are plotted.

J) Representative flow cytometry plots of plasma cells (%) from *CD19-cre* (Ctrl) or *Prmt5*^{F/F} *CD19-cre* (F/F) B cells at day 4 after stimulation with LPS (5 μ g/mL) and IL-4 (5 ng/mL). Plasma cell proportion for individual mice (symbols) and mean (bars) values for 4 mice per genotype from 2 independent experiments are plotted

K) Gene expression analysis by RT-qPCR in *Prmt5*^{F/F} *CD19-cre* (F/F) relative to *CD19-cre* (Ctrl) splenic B cells cultured with LPS (5 μ g/mL) and IL-4 (5 ng/mL) for 3 days. Mean + s.d. mRNA levels normalized to Actin for *n* mice from 2 experiments (except for *c-Myc*, one experiment) are plotted relative to Ctrl average.

L) Representative flow cytometry plots of splenic plasma cell (*B200*^{dim} *CD138*⁺) proportions in *Prmt5*^{F/F} *Cy1-cre* (F/F) or *Cy1-cre* (Ctrl) at 14 days post-infection with *H. polygyrus* and histogram of the

proportion of intracellular IgG1 staining in plasma cells. Data for individual mice (symbols) and mean values (bars) from one experiment are plotted

M) Representative flow cytometry plots of GC B cells (IgD⁻ Gl7⁺) and histogram of intracellular IgG1 staining in GC B cells of the mice in L). Data for individual mice (symbols) and mean values (bars) from one experiment are plotted.

P-values throughout by unpaired, two tailed Student-*t* test except for GSEA, in which statistics are indicated.

2.3.13 Prmt5 prevents premature B cell differentiation in the GC

To obtain insight into the dynamics of *Prmt5*^{F/F} Cγ1-cre GC B cells we analyzed additional functional GC B cell subsets. Positively selected LZ GC B cell subpopulations can be defined based on the transient induction of *c-Myc* and mTORC1 activation (Calado et al., 2012; Dominguez-Sola et al., 2012; Ersching et al., 2017). Not only was *Prmt5* preferentially expressed in positively selected cells (**Fig. 2.9D**), but the GC B cell gene signatures associated with *Myc* expression and mTORC1 activation were significantly downregulated in *Prmt5*-null B cells (**Fig. 2.9E**). Moreover, *Prmt5* was preferentially expressed in the high-affinity, *Myc*⁺ and *Irf4*⁺ subset of LZ B cells recently shown to be plasmablast precursors (Ise et al., 2018) (**Supplementary Fig. 2.5D**), suggesting that *Prmt5* was important for this B cell fate.

Additional gene expression analyses suggested that *Prmt5*-null cells were prone to plasma cell differentiation. First, cross-referencing our RNA-seq data with Immgen gene expression data in B cells subsets showed that a significant proportion of the genes encoding cell adhesion and surface membrane proteins overexpressed in *Prmt5*-null iGBs (**Supplementary Figs. 2.4B, 2.4C**) were normally upregulated in memory B cells and/or plasma cells (*Sell*, *Gbp3*, *Itgb7*, *Nid1*, *F11r*, *CD55*, *Il10ra*, *Il2ra*, *CD5*, *Itga4*, *CD2*, *CD38*, etc.) (**Supplementary Fig. 2.5E**). Second, a composite signature made of markers found in terminally differentiated memory B and plasma cells (Beguelin et al., 2013) was significantly enriched among the genes induced in *Prmt5*-deficient B cells (**Fig. 2.9E**). Third, while *Bcl6* signatures, typical of GC B cells,

were not affected (**Supplementary Fig. 2.5C**), Prmt5-null iGB cells showed upregulation of multiple GC-specific targets of EZH2, a transcriptional repressor that opposes B cell differentiation (Beguelin et al., 2013) (**Fig. 2.9E**). More importantly, analyzing *Prmt5^{F/F}* Cy1-cre iGB cells at day 7 after plating revealed a higher proportion of CD138⁺ cells than the controls, which was clearer after re-plating with either IL-4 or IL-21 and coincided with reduced proliferation potential, as expected from differentiated cells (**Fig. 2.9F**).

To further test of whether Prmt5 regulated B cell differentiation, we used splenic B cells stimulated *ex vivo* with LPS + IL-4, a well-accepted model of plasma cell differentiation (Nutt et al., 2015). Pharmacological inhibition of Prmt5 in wt B cells plated in LPS + IL-4, which efficiently reduced sDMA, showed a dose dependent increase in CD138⁺ cells that correlated with reduced proliferation upon treatment and increased *Prdm1*, *Irf4* and *Igh* expression (**Fig. 2.9G-I**). For genetic validation we used B cells from *Prmt5^{F/F}* CD19-cre mice, which also showed much higher generation of CD138⁺ cells and *Prdm1* and *Irf4* upregulation than the control cells (**Fig. 2.9J, 2.9K**). This effect was p53-independent as increased plasma cell differentiation was similar in experiments using *Prmt5^{F/F}* CD19-cre *Trp53^{-/-}* mice, as well as in p21-deficient B cells treated with Prmt5 inhibitor (**Supplementary Figs. 2.5F, 5G**)

To obtain evidence of increased plasma cell differentiation *in vivo* we analyzed *Prmt5^{F/F}* Cy1-cre mice. These mice produce less IgG1⁺ ASC (**Fig. 2.4B**), but since class switch recombination is not affected by Prmt5-deficiency (**Supplementary Fig. 2.4J**), we reasoned that premature differentiation would result in a decreased probability of plasma cells having switched compared to control mice. For this, we analyzed splenic CD138⁺ B cells in *Prmt5^{F/F}* Cy1-cre mice infected with *H polygyrus* for the relative proportion of IgG1⁺ cells. Indeed, while 90% of plasma cells in control mice were IgG1⁺, this proportion was reduced to 50% in *Prmt5^{F/F}* Cy1-cre plasma cells (**Fig. 2.9L**). The reduced proportion of IgG1⁺ cells was also found inside the GC of these mice (**Fig. 2.9M**). We conclude that Prmt5 prevents premature plasma cell

differentiation, which can partly explain the defect in GC expansion *in vivo* in mice with Prmt5-null B cells.

2.4 Discussion

We demonstrate essential roles for Prmt5 in the proliferative stages of normal B cells, both during development as well as for functional competence. Prmt5 ensures cell survival and proliferation at critical B cell stage transitions, strongly influencing GC B cell dynamics and preventing early plasma cell differentiation. The effect of ablating Prmt5 in B cells is pleiotropic, as expected for an enzyme that modifies a large number of substrates (Karkhanis et al., 2011; Yang and Bedford, 2013). Nonetheless, our data helps to delineate Prmt5 functions, some of which stem from the known role of Prmt5 in dampening the p53 response (Jansson et al., 2008), but most of which are in fact p53-independent.

We show that Prmt5 is necessary for B cell development in the BM. At variance with a previous report analyzing the conditional deletion of Prmt5 in all hematopoietic cells, which showed a partial block but increased mature B cells (Liu et al., 2015b), *Prmt5^{F/F}* Mb1-cre have no mature B cells. In these mice, Prmt5 is required to prevent a p53 response, thus allowing the formation of pro-B cells. Prmt5 deficiency also affects T cell development, leading to accumulation of the DN1 stage, at the onset of VDJ recombination (Liu et al., 2015b). We rule out the possibility that the block in B cell development originates from defective VDJ recombination because *Prmt5^{F/F}* Mb1-cre B1-8 mice also fail to produce pro-B cells. Pro-B cells are especially sensitive to p53-dependent apoptosis, as shown by their disproportionate accumulation in *Trp53^{-/-}* mice compared to other stages (Guidos et al., 1996; Lu and Osmond, 2000). Since ablating p53 rescued pro-B cells in *Prmt5^{F/F}* Mb1-cre *Trp53^{-/-}* mice, the developmental blockage is likely due to increased apoptosis. B cell development was subsequently blocked at the pre-B cell stage in those mice, indicating that Prmt5 has a distinct, p53-independent, function required for the generation or survival of pre-B cells, which remains to be investigated. Prmt1 regulates pre-BCR signaling (Infantino et al., 2010) and it would be interesting to determine if this is the case for Prmt5 as well.

All major functions in B cell survival and proliferation in the periphery are p53-independent. This fact distinguishes mature B cells from most other systems in which

the growth and survival phenotypes associated with Prmt5 ablation are to a large extent p53-dependent (Bezzi et al., 2013; Jansson et al., 2008; Li et al., 2015b; Yang et al., 2009). Interestingly, activating B cells that were previously depleted of Prmt5, and therefore of sDMA, leads to p53-independent apoptosis, as shown by combining both deficiencies. Apoptosis independent of p53 had only been described in glioblastoma (Yan et al., 2014) to our knowledge. This mechanism is relevant *in vivo* upon polyclonal B cell activation, as we show for the Alum adjuvant, which is widely used in human vaccines and parasitic infection. Apoptosis upon B cell activation can be avoided by deleting Prmt5 after activation, suggesting the identification of proteins that are premethylated in resting B cells as a way to elucidating the mechanism.

Even after bypassing apoptosis, Prmt5-null B cell proliferation is still compromised, revealing yet another important function of Prmt5 in mature B cell expansion, which is also p53-independent. Thus, it seems that p53 activation is secondary to another defect in Prmt5-null cells, raising the question of what triggers this response. In PRMT5-deficient mouse neural progenitor cells and human B cell lymphoma cells, p53 activation is partly caused by altered splicing producing an unstable form of the negative p53 regulator Mdm4 (Bezzi et al., 2013; Koh et al., 2015b). We have similar findings for Mdm4 splicing in activated Prmt5-null B cells, but there is a larger effect on splicing of DNA damage repair factors, which probably contribute to the p53 activation. Indeed, we detect accumulation of DNA damage in Prmt5-null GC and iGB B cells, which has been observed after deletion of PRMT5 in *C. elegans*, mouse primordial germ cells and human cancer cell lines (Jansson et al., 2008; Kim et al., 2014; Yang and Bedford, 2013). We rule out that this accumulation originates from the activity of antibody diversification and speculate that it may be due to a reduced capacity for DNA repair, as suggested by splicing alterations in components of base excision, Fanconi and homologous recombination pathways, as well as in chromatin modifiers that regulated DNA repair. Interestingly, no core components of the non-homologous end joining pathway were affected, in line with normal class switch recombination per cell division observed in Prmt5-null B cells.

The effect of Prmt5 deficiency in GC in *Prmt5^{F/F}* Cγ1-cre mice and transcriptome analyses point to Prmt5 playing a major role in the GC LZ B cells. Accordingly, we find that Prmt5 protein is polarized in LZ B cells, within which it is most highly expressed in GC B cells undergoing positive selection (Dominguez-Sola et al., 2012; Ersching et al., 2017). Interestingly, the phenotypic definition of these populations overlaps with a subset of GC B cells that are plasma cell precursors (Ise et al., 2018) and Prmt5 prevents premature plasma cell differentiation in the GC, which is supported by *in vitro* differentiation data as well as by the increased ratio of IgM⁺ to IgG1⁺ plasma cells in the spleen and inside the GC *in vivo*. Prmt5-null GC B cells accumulate a population of Cxcr4⁻ CD86^{low} cells that have low proliferation potential and do not express AID. Given the expression pattern of Prmt5 in GC B cells, these cells may represent cells failing positive selection and/or attempting differentiation. While the origin of these cells is uncertain, they indicate a defect in the GC dynamics caused by Prmt5 deficiency. The role of Prmt5 in differentiation is context dependent (Karkhanis et al., 2011; Li et al., 2015c) but Prmt5 deficiency has been shown to cause upregulation of differentiation markers in ES cells (Tee et al., 2010) and promote myeloid differentiation in leukemia cells driven by MLL-fusions (Kaushik et al., 2017). Prmt5 prevents differentiation of leukemia cells by silencing *Cdkn1a/p21* expression (Kaushik et al., 2017). Yet, p21-deficiency did not reduce plasma cell differentiation of Prmt5-null B cells, suggesting another mechanism. Our data suggest that Prmt5 represses at least part of the plasma cell program. Thus, even when RNA-seq was done for day 4 iGBs, when there is no significant increased plasma cell proportions, these *Prmt5^{F/F}* Cγ1-cre iGBs already showed important transcriptional changes associated to plasma cell differentiation, like de-repression of EZH2 targets and upregulation of differentiation markers. At later times, deletion or pharmacological inhibition of Prmt5 results in the expression of CD138, *Irf4*, *Prdm1* and increased *Igh* expression, which are all hallmarks of plasma cell differentiation. Nonetheless, the paucity of plasma cells in Prmt5 deficient mice may reflect incomplete differentiation and/or that Prmt5 has an additional function in plasma cell maintenance.

Mechanistically, we show that Prmt5 regulates transcription but also enforces splicing fidelity in B cells, which probably contributes to the former function. Prmt5 ablation leads to the differential expression of a large number of genes, some of which Prmt5 probably regulates directly. The most likely candidates are those genes that are most highly upregulated in the knockout B cells since H3R8 and H4R3 methylation by PRMT5 are typically transcription repressive marks (Karkhanis et al., 2011). Indeed, we find that Prmt5-dependent sDMA is abundant in the nucleus of GC B cells. We also find that Prmt5 deletion affects splicing fidelity in B cells. Prmt5 ensures spliceosome assembly by methylating SmD proteins (Karkhanis et al., 2011; Koh et al., 2015b), with Prmt5 depletion leading to a defect in donor splice site recognition and usage (Bezzi et al., 2013; Koh et al., 2015b; Sanchez et al., 2010) that we find to be the case in B cells. Since splicing of many histone modifiers is affected it is likely that the splicing defect further contributes to the change in transcriptional program. Dissecting the exact contribution and key players to each phenotype would require first cataloguing those loci directly occupied and methylated by Prmt5, and the dynamics of H3R8 and H4R3 methylation upon B cell activation and in GC B cells. Nonetheless, even if the role of Prmt5 in splicing was known, our data demonstrates a major role for splicing fidelity in B cells that is critical for the antibody response.

Since Prmt5 is mostly cytoplasmic in B cells, it is very likely that cytoplasmic Prmt5 substrates that are not involved in gene expression regulation or splicing, also contribute to the phenotypes observed. Given the effect of Prmt5 in plasma cell differentiation and the determinant role of synergistic BCR and CD40 signaling GC B cell in positive selection (Luo et al., 2018), we speculate that Prmt5 affects these pathways. Unlike other PTM that have long been known to regulate B cell biology, arginine methylation has received much less attention. Our data establish the importance of Prmt5-catalyzed sDMA in multiple normal B cell stages and provide a framework to analyze the contribution of specific substrates to the p53-independent Prmt5 functions in B cells.

2.5 Material and Methods

Animals

Mice were housed at the specific pathogens free facility of the IRCM. *Prmt5^{F/F}* mice from EUCOMM (Bezzi et al., 2013) were backcrossed for >5 generations to C57BL6/J. Cy1-cre (Casola et al., 2006) and B1-8 knock-in (Sonoda et al., 1997) mice, kind gifts of Dr K Rajewsky (MDC, Berlin), were obtained from Dr Hua Gu at IRCM. CD19-cre mice (Rickert et al., 1997) were a gift from Dr Russell Jones (McGill University, Montreal). Mb1-cre mice (Hobeika et al., 2006) were a gift of Dr Michael Reth (MPI, Freiburg). *Trp53^{-/-}* mice (Jacks et al., 1994) were obtained from Jackson labs (Bar Harbour, MN). *Cdkn1a^{-/-}* mice (Brugarolas et al., 1995) and H2K-Bcl2 mice (Kondo et al., 1997) were kind gifts from Dr Tarik Möröy (IRCM, Canada). *Aicda^{-/-}* mice (Muramatsu et al., 2000) were a gift from Dr. T. Honjo (Kyoto University, Japan). *Aicda-GFP* mice (Crouch et al., 2007) were a gift from Dr R Casellas (NCI Bethesda, MD). Lines combining one or more desired alleles were generated by breeding at our animal house. Throughout the paper, *Prmt5^{+/+}* Cre were used as controls, except where indicated that *Prmt5^{+F}* Cre were used. Animal work was reviewed and approved by the animal protection committee at the IRCM (protocols 2013-18 and 2017-08).

Immunization and infection

Age- and sex-matched mice of 40-120 days of age were immunized either intraperitoneally with 50 µg NP₁₈-CGG (Biosearch Technologies) in Imject Alum adjuvant (Thermo Scientific) or intravenous with 10⁹ SRBC in 200 µl PBS (Innovative Research, IC100-0210). Mice were bled and/or sacrificed at various time post-immunization. Infections with *H. polygyrus bakeri* larvae were done by administering 200 L3 by gavage and mice were euthanized 14 days later.

ELISA

Sandwich ELISA for measuring pre-immune sera antibodies were done using anti-isotype-specific antibodies (BD Pharmingen) to capture IgM, IgG1, IgG2b or IgG3, as

described (Zahn et al., 2013). Antigen-specific antibodies were captured from immunized mice sera in ELISA plates coated with NP₂₀-BSA (Biosearch Technologies) followed by the detection of IgG1, as described (Zahn et al., 2013).

ELISPOT

Purified splenocytes or BM cells were added at different dilutions to a 96-well 0.45 µm PVDF membrane (Millipore, cat#MSIPS4W10) previously coated overnight at 4°C with 2 µg/mL NP₂₀BSA and blocked with complete RPMI cell culture media for 2 h at 37°C. Plates with cells were incubated in a humid chamber 12 h at 37°C, 5% CO₂, then washed 6 x with PBS 0.01% Tween-20, followed by incubation with goat anti-mouse IgG1-HRP (A10551, Life Technologies, 1/2000) diluted in culture media for 2 h at RT. Plates were washed and AEC substrate (3' amino-9-ethylcarbazole ; BD Bioscience) was added to reveal the spots. Images were acquired in an Axiophot MZ12 microscope and scored spots were counted from appropriate cell dilutions (2 x 10⁶ cells after primary immunization and 0.5 x 10⁶ cells for recall).

Cell culture

Naïve primary B cells were purified from splenocytes by depleting CD43⁺ cells using anti-CD43 microbeads (Miltenyi, cat# 130-049-801) and an autoMACS (Miltenyi). Primary B cells were cultured at 37°C with 5% (vol vol⁻¹) CO₂ in RPMI 160 media (Wisent), supplemented with 10% fetal bovine serum (Wisent), 1% penicillin/streptomycin (Wisent), 0.1 mM 2-mercaptoethanol (bioshop), 10 mM HEPES, 1 mM sodium pyruvate. Resting B cells were stimulated with lipopolysaccharide (LPS) (5 µg/mL, Sigma) + IL-4 (5 ng/mL, PeproTech). Induced germinal center B cells (iGBs) were generated using 40LB feeder cells (a kind gift from Dr Daisuke Kitamura) (Nojima et al., 2011). Briefly, one day before B cell plating, 40LB cells were irradiated (120 Gy) and plated at 0.3 x 10⁶ cells per well in 2 mL (6-well plate) or 0.13 x 10⁶ cells per well (24-well plate) in 0.5 mL DMEM media supplemented with 10% fetal bovine serum (Wisent) and 1% penicillin/streptomycin (Wisent). Purified naïve B cells were plated on 40LB feeders at 10⁵ cells per well in 4 mL of B cell media (6-well plate), or 2 x 10⁴ cells per well in 1 mL of B cell media (24-

well plate), supplemented with 1 ng/mL IL-4. At day 3 post-plating, the same volume of fresh B cell media was added to the wells, supplemented with either 1 ng/mL IL-4 or 10 ng/mL IL-21 (PeproTech). On subsequent days, half of the volume per well was removed and replaced with fresh B cell media supplemented with cytokines. When re-plated, cells were harvested from the primary culture on day 4 and plated on fresh 40LB feeders in media supplemented with either 1 ng/mL IL-4 or 10 ng/mL IL-21. Re-plated cells were not fed and analyzed 3 days later. The Prmt5 inhibitor EPZ015666 (cayman chemical, cat#17285) was aliquoted and resuspended for long-term storage at -80°C at 50 mM in DMSO. Intermediate dilutions in DMSO (from 25 to 5 mM) were kept at -20°C and frozen/thawed up to three times for individual experiments. DMSO was always diluted 1/1000 in final volume with cells.

Flow cytometry

Mononuclear cells from mouse spleen and MLN were obtained by mashing through a cell strainer with a syringe plunger. Bone marrow cells were obtained by opening and flushing femur and tibia bones from one leg with PBS, using a 1 mL syringe with 23G needle. BM and splenocytes suspensions were washed in PBS and incubated in 1 mL red blood cell lysis buffer (155 mM NH₄Cl, 10mM KHCO₃, 0.1mM EDTA) for 5 min at room temperature to complete lysis before filtering through 40µm nylon cell strainer and resuspending in PBS 1% BSA. Single cell suspensions were stained with combinations of antibodies listed in **Supplementary table 5**. To assess proliferation *in vivo*, splenocytes were surface stained for GC markers and then 3x10⁶ cells were treated with Fixation/permeabilization solution (eBioscience, cat# 00-5123-43) for 1 h at 4°C in the dark, washed twice in Perm buffer (eBioscience), followed by 1 h incubation with anti-Ki67-PECY7 (eBioscience) at 4°C and resuspended in PBS+1% BSA. If necessary, anti-biotin staining was performed following Ki67 stain. To evaluate apoptosis *in vivo*, cells were treated with the FITC conjugated CaspGLOW reagents that detects activated pan-caspases (BioVision, K180) according to the manufacturer's instructions. Briefly, 10⁶ cells were treated with 2 µL FITC-VAD-FMK antibody for 1 h at 37°C in 300 µL warm media, washed, surface stained and analyzed immediately. To assess apoptosis 0.3 - 0.5x10⁶ cultured cells were stained

with 3 μL Annexin V in 100 μL Binding buffer (cat #51-66121E, BD Pharmigen) for 15 min at RT. Then 400 μL of Binding buffer and 5 μL of Propidium Iodide (20 $\mu\text{g}/\text{mL}$) were added prior to flow cytometry acquisition. To assess γH2AX levels *in vivo*, 3×10^6 splenocytes were first surface stained for GC markers then washed twice in PBS 1% FCS 0.09% sodium azide and treated with fixation solution (BD, Cytofix #554655) for 30 min at 4°C in the dark, then washed as previously. Pre-chilled Perm buffer III solution (BD#558050) was then added to the cells drop-wise under constant agitation. Cells were incubated for 30 min on ice in the dark and washed twice as previously before staining with anti- γH2AX (rabbit, 1/50) or anti-His control (rabbit 1/50) in wash solution (final volume 100 μL) for 1 h at 4°C in the dark and washed as previously. Cells were stained with the secondary antibody anti-rabbit Alexa633 (1/8000) in 100 μL wash solution for 1 h at 4°C in the dark, washed and resuspended in PBS + 1% BSA. For intracellular IgG1 staining, cells were stained for GC markers then fixed/permeabilized according to the manufacturers protocol (eBioscience, cat# 00-5123-43) before staining for IgG1. To evaluate cell cycle profile, B cells were incubated with 10 μM BrdU for 1 h at 37°C, fixed in 70% ethanol while vortexing and incubated on ice for 30 min. Then 2N HCl/Triton X-100 0.5% was added to the loosen cell pellet to denature the DNA. Cells were then washed, resuspended in 0.1 M $\text{Na}_2\text{B}_4\text{O}_7$, washed again and resuspended in PBS 0.5% Tween-20 1% BSA. 1×10^6 cells were then stained with anti-BrdU-FITC (1/50) for 30 min at RT in the dark and resuspend cells in PBS 5 $\mu\text{g}/\text{mL}$ PI. Data was acquired using BD LSR Fortessa (BD biosciences) or BD Facscalibur (BD biosciences) and analyzed using FlowJo. For sorting, cells were stained as above and passed through a BD FACSARIA III (BD biosciences).

Immunohistochemistry

Section of 5- μm of paraffin-embedded tissues were deparaffinized in two changes of xylene for 5 min each and then rehydrated in distilled water using graded alcohols. Antigen retrieval was done by steaming the slides for 20 min then cooling for 20 min in either EDTA buffer (1mM EDTA, 0.05% Tween 20, pH 8) for AID and PRMT5; or citrate buffer (10 mM acid citric, 0.05% Tween 20 pH 6.0) for PNA. Endogenous

peroxidase was blocked with a 0.3% hydrogen peroxide solution for 10 min. When needed, endogenous biotin was blocked for 15 min with the blocking buffer provided with the Avidin/Biotin System (#SP2001, Vector Laboratories; Burlingame, CA). For protein block, we used 10% normal goat serum and 1% BSA for 60 min at room temperature or Carbo free buffer (#SP5040, Vector Laboratories). Sections were incubated with anti-AID (1:50, rat Mab mAID-2 eBioscience), anti-PRMT5 (1:250) overnight at 4°C or biotinylated PNA (1:100) for 60 min at room temperature. Biotin-conjugated secondary antibodies were mouse anti-rabbit IgG (1:200, Vector laboratories) to detect anti-PRMT5; mouse anti-rat IgG (1:200, Vector laboratories) to detect anti-AID. Biotinylated reagents were detected with Vectastain ABC kit (PK-6100, Vector laboratories). Peroxidase activity was developed using ImmPACT NovaRED HRP substrate (Vector laboratories). Sections were counterstained with hematoxylin (Sigma cat #MHS32-1L) for 1 min prior to dehydrating and mounting. Antibodies are listed in **Supplementary table 5**.

Immunofluorescence

Tissues were frozen in OCT (VWR #95057-838). Sections of 5- μ m were fixed in PFA 4% for 10 min at RT, washed 3 times in PBS at RT, followed by an incubation in pre-chilled acetone for 10 min at -20°C. Sections were permeabilized in 0.5% Triton X-100 in PBS for 10 min at RT. Sections were then blocked in PBS 5% goat serum 1% BSA 0.3% Triton X-100 for 1 h at RT. Incubations with primary antibodies were performed in blocking solution overnight at 4°C in a humid chamber in the dark. Then, when needed, a secondary antibody was added in blocking solution for 1 h at RT in a humid chamber in the dark. Primary B cells were washed 1x with PBS and then plated on coverslips coated with 0.1 mg/mL poly-L-lysine (Sigma). Cells were centrifuged 5 min at 400 x g, then allowed to adhere at 37°C for 20 min, before fixation with 3.7% formaldehyde (Sigma) for 10 min at room temperature. After 3 washes with PBS, coverslips were blocked for 1 hr with blocking solution (5% goat serum, 1% BSA, 0.5% Triton X-100 in PBS). Cells were then incubated overnight at 4°C with anti-PRMT5 (1:100) or anti-SYM11 (1:500), diluted in blocking solution. After 3x, 5 min washes, with PBS + 0.1% Triton X-100 (PBS-T), cells were incubated for 1

hr at room temperature with anti-Rabbit IgG Alexa-546 (1:500) diluted in blocking solution. After 3x, 5 min washes with PBS-T, cells were incubated with 300 nM Dapi (ThermoFisher) in PBS for 5 min at room temperature. Finally, coverslips were washed with PBS followed by ddH₂O before mounting onto slides using Lerner Aqua-Mount (ThermoFisher). Antibodies are listed in **Supplementary table 5**.

Microscopy and image analysis

Prmt5 and Sym11 immunofluorescence signal in B cells was scored in Volocity (Perkin Elmer), quantifying signal within a dilated mask generated using Dapi. For each experiment, multiple fields were analyzed, excluding cells with saturated signal, abnormal DNA structures or mitotic figures. Quantification of γ H2AX foci was performed on confocal images, using a series of image processing operation to separate B-cell DNA damage from the larger feeder cells. Analysis scripts were programmed using Matlab 2016a (Mathworks Inc.). A total of 42-48 images per genotype per day were automatically analyzed for >900 cells per sample. Cell nuclei were found using the DAPI channel of images, based on an Otsu intensity threshold. Binary images were cleaned of small objects, holes were filled, and edges were smoothed using a morphological closing operation with a 5-pixel-radius circular kernel. Multinuclear cells were removed from this nuclear mask by computing the convex Hull of all objects, and objects where the ratio of their area over their convex Hull area was lower than 0.8 were discarded. Finally, big nuclei, belonging to feeder cells were discarded by only keeping objects of area smaller than 2% of the image size. DNA damage foci were assumed to be fluorescent puncta, most of them of sub-diffraction-limit size. Intensity contrast was enhanced by saturating the bottom 1% and the top1% of all pixels. Fluorescent puncta were detected using a linear band-pass filter that preserved objects of a chosen size and suppressed noise and large structures. After the filter, we chose elements bigger than noise up to twice the diffraction limit. Only foci detected within B-cell nuclei were considered for statistical purposes. In order to consider only foci brighter than in control IF, we quantified the average foci intensity of non-treated cells, and only foci of higher-than-control intensity were considered to compute the number of DNA damage foci per cell.

Western blots

Protein extracts were performed by lysing cells in NP-40 lysis buffer (1% NP-40, 20mM Tris pH 8, 137mM NaCl, 10% glycerol, 2mM EDTA), containing protease and phosphatase inhibitor (Thermo Scientific). Protein extracts were separated by SDS-PAGE and transferred to nitrocellulose membranes (BIO-RAD). In some experiments equal protein loading was controlled by staining the membrane after transfer using REVERT total protein stain solution (LI-COR). Membranes were blocked in TBS 5% milk and probed with primary antibodies overnight, washed 4 x 5 min in TBS + 0.1% Tween before incubating with secondary antibodies conjugated to AlexaFluor680 or IRDye800 for 1 h, washed and read on Odyssey CLx imaging system (LI-COR). Proteins were quantified using ImageStudioLite software. When Revert staining (LI-COR) was used, Revert signal from a whole protein lane was considered for normalization. Antibodies are listed in **Supplementary table 5**.

RT-qPCR

RNA isolated using TRIzol (Life Technologies) was reverse transcribed with ProtoScript™ M-MuLV Taq RT-PCR kit (New England Biolabs). Quantitative PCR using SYBR select master mix (Applied Biosystems) was performed and analyzed in a ViiATM 7 machine and software (Life technologies). Oligos used are listed in **Supplementary table 6**.

RNA-seq

Cy1-cre and *Prmt5^{F/F}* Cy1-cre splenic B cells plated on 40LB cells were separated from the feeder cells by elutriation at day 4 after plating. Total RNA was extracted using RNeasy plus Mini kit (Quiagen) and quality controlled using RNA Pico chip on Bioanalyzer (Agilent). Samples were depleted of rRNA using Ribo-zero Gold rRNA removal kit H/M/R (Illumina Hu Mm Rt). Libraries were constructed using the KAPA stranded RNA-Seq kit (Roche), which included fragmentation, cDNA, dsDNA, ER, ATL, Ligation and PCR enrichment and purified by KAPA magnetic beads (Roche). The mean fragment size obtained was 308bp. QC validation was performed on HSdna chip on Bioanalyzer and Q-PCR titration with NEBnext Library quant Kit for

Illumina (NEB). Sequencing PE125 on HiSeq2500 with v4 chemistry (Illumina) at the Genome Center (Quebec).

RNA-seq analysis

Sequencing reads were trimmed using Trimmomatic (v0.32) (Bolger et al., 2014), removing adaptor and other Illumina-specific sequences as well as the first four bases from the start of each read, and low-quality bases at the end of each read, using a 4 bp sliding window to trim where average window quality fell below 30 (phred33 < 30). An additional 3bp were clipped from the start and end of a read if found of low quality. Trimmed reads < 30 bp were discarded. The resulting clean set of reads were then aligned to the reference mouse genome build mm10 using STAR (v2.3.0e) (Dobin et al., 2013) with default parameters. Reads mapping to more than 10 locations in the genome (MAPQ < 1) were discarded. Gene expression levels were estimated by quantifying uniquely mapped reads to exonic regions (the maximal genomic locus of each gene and its known isoforms) using featureCounts (v1.4.4) (Liao et al., 2014) and the Ensembl gene annotation set. Normalization (mean of ratios) and variance-stabilized transformation of the data were performed using DESeq2 (Love et al., 2014). Differential expression analysis was performed with DESeq2 using the Wald test. Statistically significant (adjusted p value <0.05, Benjamini–Hochberg procedure) genes with large expression changes (absolute fold change ≥ 1.5) that are expressed above a threshold (average normalized expression across samples >50) were considered as differentially expressed genes. Multiple control metrics were obtained using FASTQC (v0.11.2), samtools (v0.1.19), BEDtools (v2.17.0) and custom scripts. For visualization, normalized Bigwig tracks were generated using BEDtools and UCSC tools. Integrative Genomic Viewer was used for data visualization. For splicing analysis, we used rMATS v3.2.5 (Shen et al., 2014) with default parameters to identify alternative splicing (AS) events. Since rMATS requires reads of equal lengths, we performed the analysis on untrimmed reads, using the Mus musculus GRCm38 release 87 Ensembl gtf as exon annotation file. We used both rMATS outputs for analysis: AS events identified using reads mapping to splice junctions and reads on target (JC+ROT), and AS events identified using reads mapped to splice junctions

only (JC). Each of the five types of AS events (skipped exon, SE; mutually exclusive exon, MXE; retained intron, RI; alternative 5' splice site, A5SS and alternative 3' splice site, A3SS) was analyzed separately. A non-redundant list of genes displaying significant AS events was generated by selecting the most statistically significant AS event per gene with more than 10% inclusion level difference. Benjamini-Hochberg correction was applied to this non-redundant set of events. The final list of AS affected genes (**Supplementary table 3**) contains events with FDR <0.05 in genes that pass a minimum expression threshold (normalized mean expression > 50).

Functional annotation

GO terms enrichment was performed using either DAVID (<https://david.ncifcrf.gov/>) (Huang da et al., 2008) or Gorilla (<http://cbl-gorilla.cs.technion.ac.il/>) (Eden et al., 2009) by providing either an unranked gene set and a background list, or a ranked list, as follows. The list of genes differentially expressed by ≥ 2 -fold in either direction with $P_{adj} < 0.05$ were analyzed by DAVID, using the list of all expressed genes (basemean > 0) as background, to identify enriched GO biological process terms. A non-redundant list of aberrantly spliced genes reaching statistical significance was similarly analyzed at Gorilla.

GO or KEGG with FDR < 25% and $P < 0.05$ in adjusted p-value were considered significant. Gorilla permitted the analysis of ranked lists. Two lists were compiled from differential expression analysis, ranking genes according to log₂fold-change, from the most changed to the last unchanged gene in each direction (i.e. the list with upregulated genes excluded downregulated genes and vice versa). Each list was uploaded to Gorilla. In all methods, GO terms with $P < 0.05$ and FDR q-value < 0.05 were considered significant. A list containing gene expression data for each sample for genes with average basemean > 20 was analyzed by Gene Set Enrichment Analysis (GSEA) (Subramanian et al., 2005) using the interface v3.0 provided by the Broad Institute (<http://software.broadinstitute.org/gsea/index.jsp>), using the default KEGG list of gene sets at MsigDB (Liberzon et al., 2011) and gene sets from the literature (Basso et al., 2010; Beguelin et al., 2013; Caron et al., 2009; Dominguez-Sola et al., 2012; Liberzon et al., 2015; Shi et al., 2015; Vitorica et al., 2010). The

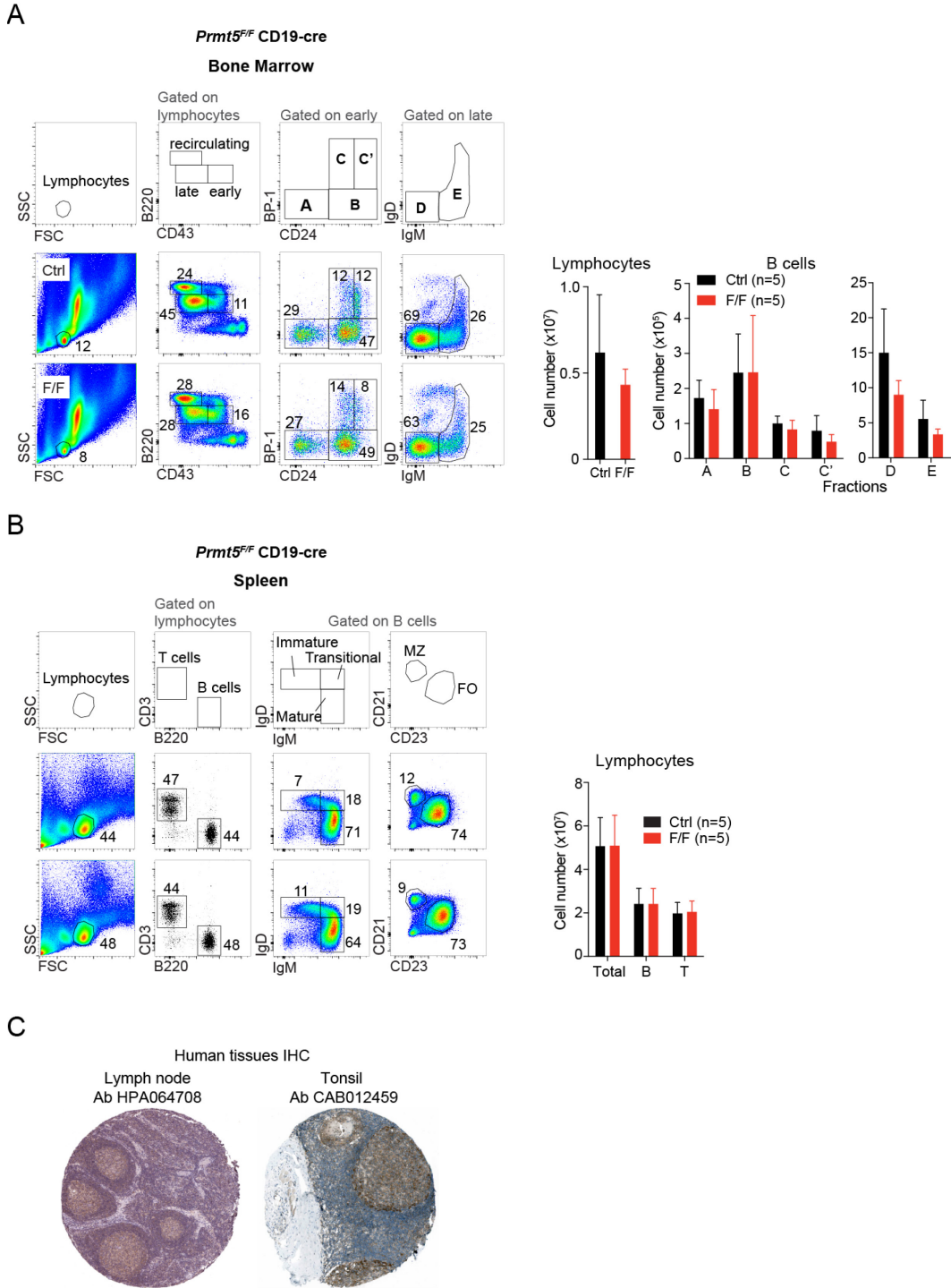
analysis was run with 1000 permutations, excluding gene sets containing more than 1000 and less than 15 genes, ranking genes by Signal2Noise and using weighted enrichment statistic. Specific gene expression signatures for selected candidate pathways to analyze by GSEA were obtained from the literature, as reference in results, and analyzed using the same input data and parameters.

2.6 Acknowledgments

We thank Dr Ari Melnick for discussions. We thank Dr Tarik Moroy, Dan Scott, Jen Fraszczak, Marissa Rashkovan, Charles Vadnais, Mathieu Lapointe for technical help, reagents and advice. We thank Mylène Cawthorn, Eve-Lyne Thivierge, Manon Laprise, Marie Claude Lavallée and Sara Demontigny for animal technical help. We thank Eric Massicote and Julie Lord for help with flow cytometry, Simone Terouz with immunohistochemistry, Dominic Fillion with microscopy imaging, Odile Neyret, Myriam Rondeau, Agnès Dumont with RNA sequencing.

This work was supported by operating grants from the Cancer Research Society to J.M.D.N (#18075 and #20194) and CIHR operating grant (MOP 125991). CIHR operating grant (MOP-130579) to I.L.K. A.P.M is a recipient of a Fonds de recherche du Québec – Santé (FRQ-S) doctoral fellowship. I.L.K. is a Canada Research Chair in Barrier Immunity. L.C.L. and S.P.M were recipients of Cole foundation doctoral fellowships and S.P.M. held a doctoral fellowship from FRQ-S. J.M.D.N was a Canada Research Chair in Genetic Diversity and is a Senior research scholar FRQ-S.

2.7 Supplemental material

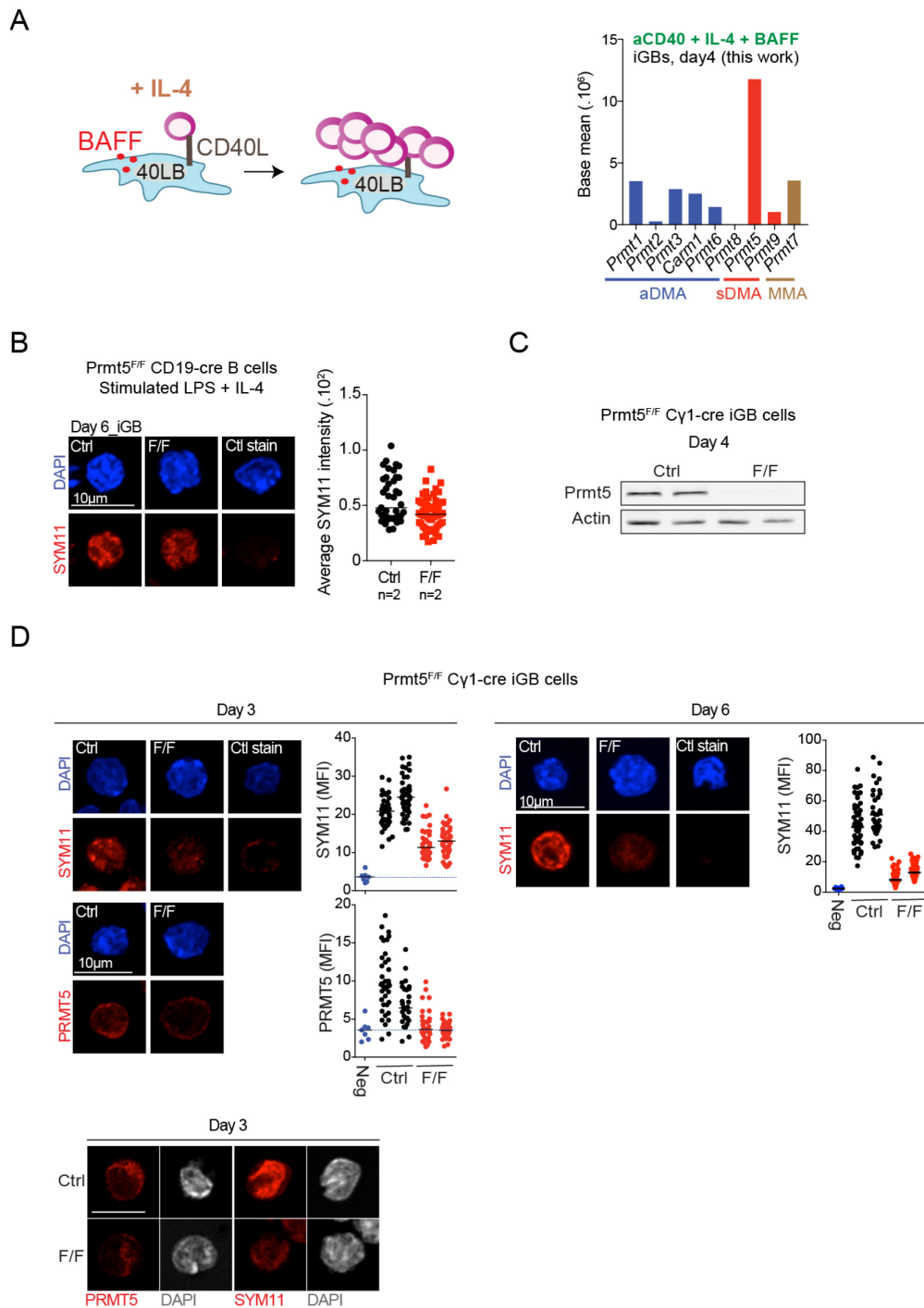


Supplementary Figure 2.1 – Normal B cell development in *Prmt5^{F/F} CD19-cre* mice

A) Left, Representative flow cytometry plots and gating strategy used to quantify BM lymphocytes (based on FSC and SSC) and Hardy's fractions of B cell development in CD19-cre (Ctrl) and Prmt5^{F/F} CD19-cre (F/F) mice. Right, means + s.d. of absolute lymphocyte and B cell fractions counts for 5 mice (3-4 months of age) per genotype from one experiment.

B) Left, Representative flow cytometry plots and gating used to quantify splenic lymphocytes and B cell subpopulations (immature (IgD⁺ IgM⁻), transitional (IgD⁺ IgM⁺), mature (IgD⁻ IgM⁺), follicular (CD21⁺ CD23⁺), marginal zone (CD21⁺ CD23⁻)) in the same mice as in A). Right, Means + s.d. of absolute splenic lymphocyte and B cell subsets counts for the mice in A).

C) Immunohistochemistry pictures taken from a human lymph node (LN) and tonsils, stained for Prmt5 with the indicated antibodies. Data was extracted from the Human protein atlas database (www.proteinatlas.org).



Supplementary Figure 2.2 – Efficiency of Prmt5 depletion over time in Prmt5^{F/F} CD19-cre and Prmt5^{F/F} Cy1-cre iGBs

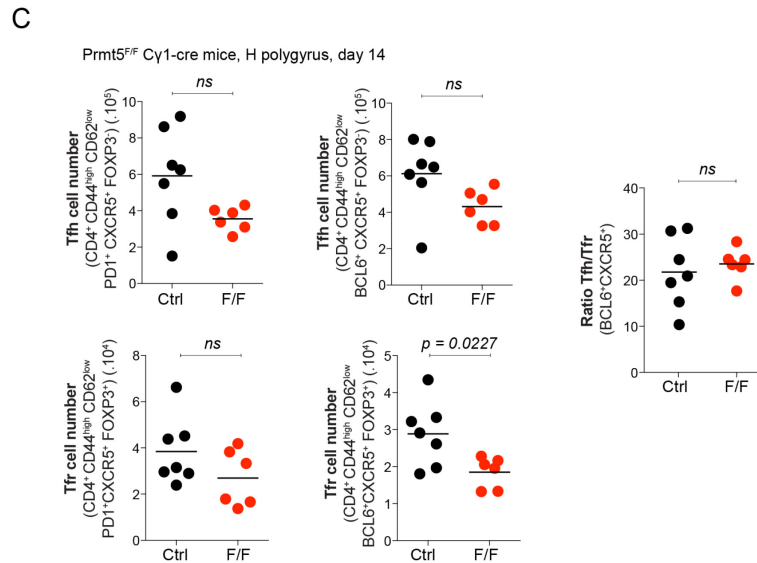
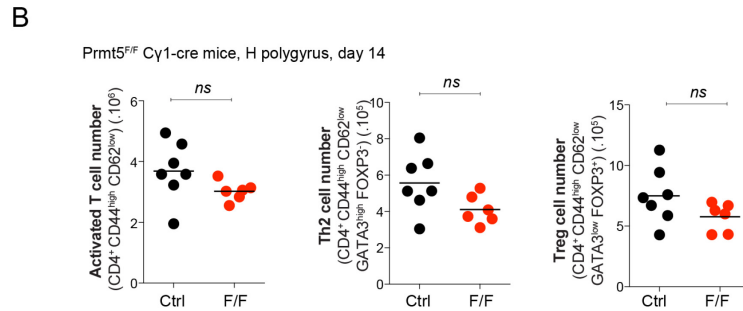
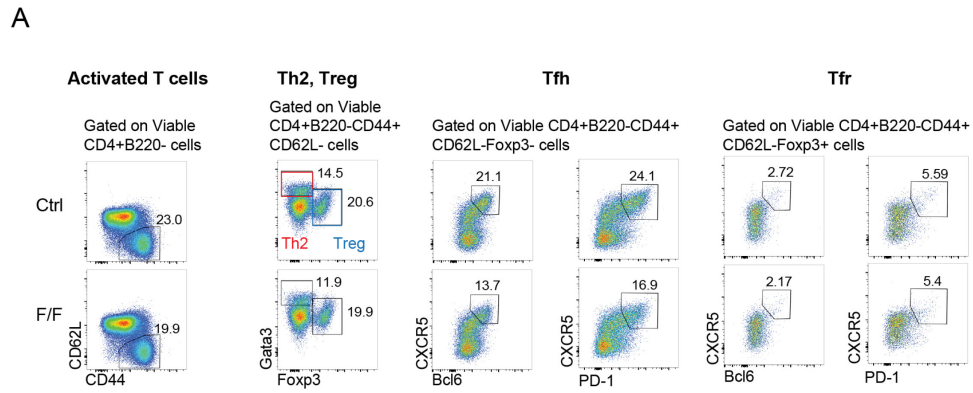
A) Schematic for the induced GC-like B cells (iGBs) system. Resting splenic B cells are plated on 40LB cells (3T3 cells constitutively expressing CD40L and BAFF) and the media supplemented with 1 ng/mL

IL-4. Transcript levels by RNA-seq of each Prmt in iGBs derived from Cy1-cre C57BL6/J resting splenic B cells at day 4 post-plating (see methods).

B) *Representative immunofluorescence of sDMA (SYM11) and DAPI on CD19-cre (Ctrl) and Prmt5^{F/F} CD19-cre (F/F) iGBs at day 6 post-plating. The average SYM11 intensity per cell (symbols) and mean intensity per genotype (bars) are plotted for a pool of 2 mice per genotype.*

C) *Representative WB of Prmt5 and Actin, as a loading control, in extracts of iGB cells from Cy1-cre (Ctrl), Prmt5^{F/F} Cy1-cre mice (F/F), 4 days after plating on 40LB.*

D) *Representative immunofluorescence of sDMA (SYM11), Prmt5 and DAPI on Cy1-cre (Ctrl) and Prmt5^{F/F} Cy1-cre (F/F) iGBs at days 3 and 6 post-plating. The average SYM11 and Prmt5 intensity per cell (symbols) and mean per genotype (bars) are plotted for a pool of 2 mice per genotype.*



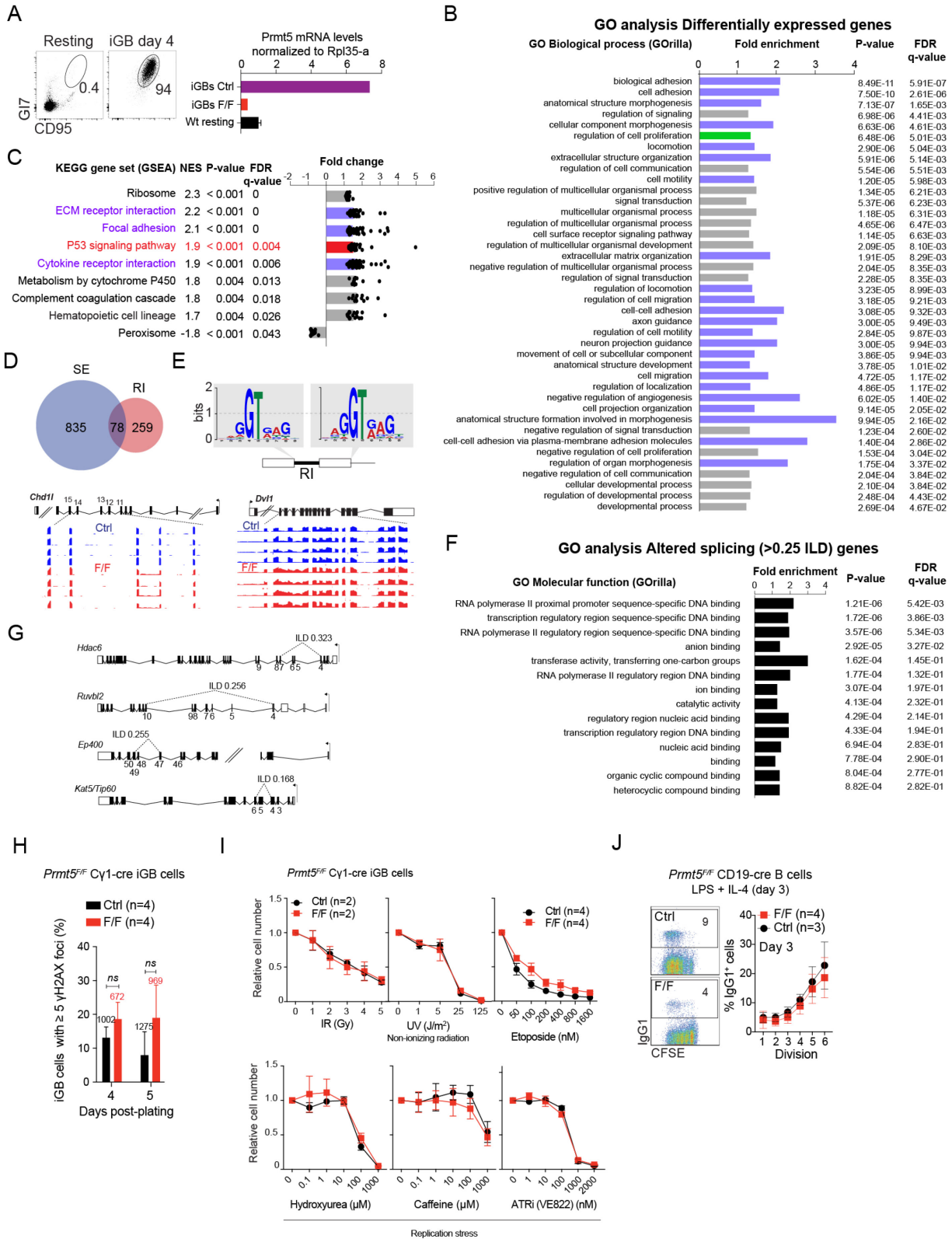
Supplementary Figure 2.3 – T cell populations in mice infected with *H. polygyrus*

A) Gating strategy for analyzing T cell subsets.

B) T cell populations in Cy1-cre (Ctrl) or Prmt5^{F/F} Cy1-cre (F/F) mice 14 days after infection with *H. polygyrus*. Compiled absolute numbers of the indicated T cell populations stained by flow cytometry with the indicated markers. Data from 2 experiments, individual mice (symbols) and mean values (bars) are plotted.

C) *Tfh* and *Tfr* populations in the same mice as in B) were measured using the indicated markers. Two different methods, differing in the use of PD1 or BCL6 staining were used. The ratio of *Tfh*/*Tfr* was calculated using the second method. Data from 2 experiments, individual mice (symbols) and mean values (bars) are plotted.

P-values by unpaired, two tailed Student-*t* test.



Supplementary Figure 2.4 – RNA-seq and p53 response additional analyses

A) Representative flow cytometry plots showing purified resting splenic B cells and iGB cells at day 4 post-plating onto 40LB that were used as source for RNA-seq. *Prmt5* transcript levels in resting wt B cells and in iGBs derived from *Cy1-cre* (Ctrl) or *Prmt5^{F/F} Cy1-cre* (F/F) measured by RT-qPCR are plotted.

B) Functional annotation of differentially expressed genes by GO terms describing biological processes. A list of all genes ranked by fold-change (from f.c. ≥ 0) was analyzed at the GOrilla server. GO terms with $P < 0.05$ and FDRq value < 0.05 were considered significant.

C) Pathways significantly enriched or depleted in *Prmt5*-null iGBs by Gene set enrichment analysis (GSEA) against the MsigDB of KEGG pathways. Normalized enrichment score (NES) of pathways with P -value < 0.05 and false discovery rate $< 5\%$ (FDRq-value < 0.05) are shown. Gene sets related to cell adhesion are in purple. The fold-change of genes in the leading edge (symbols) and the median fold change (bars) of each gene set are plotted.

D) Venn diagram of significant skipped exon (SE) and retained intron (RI) events

E) Sequence logos of the 5' splicing donor sites at introns retained (RI) in *Prmt5*-deficient iGBs, compared to the next site in the same genes, which conforms to the canonical consensus. The aligned sequences showing two examples of retained introns are shown for *Chd1l* and *Dvl1* below the corresponding gene scheme.

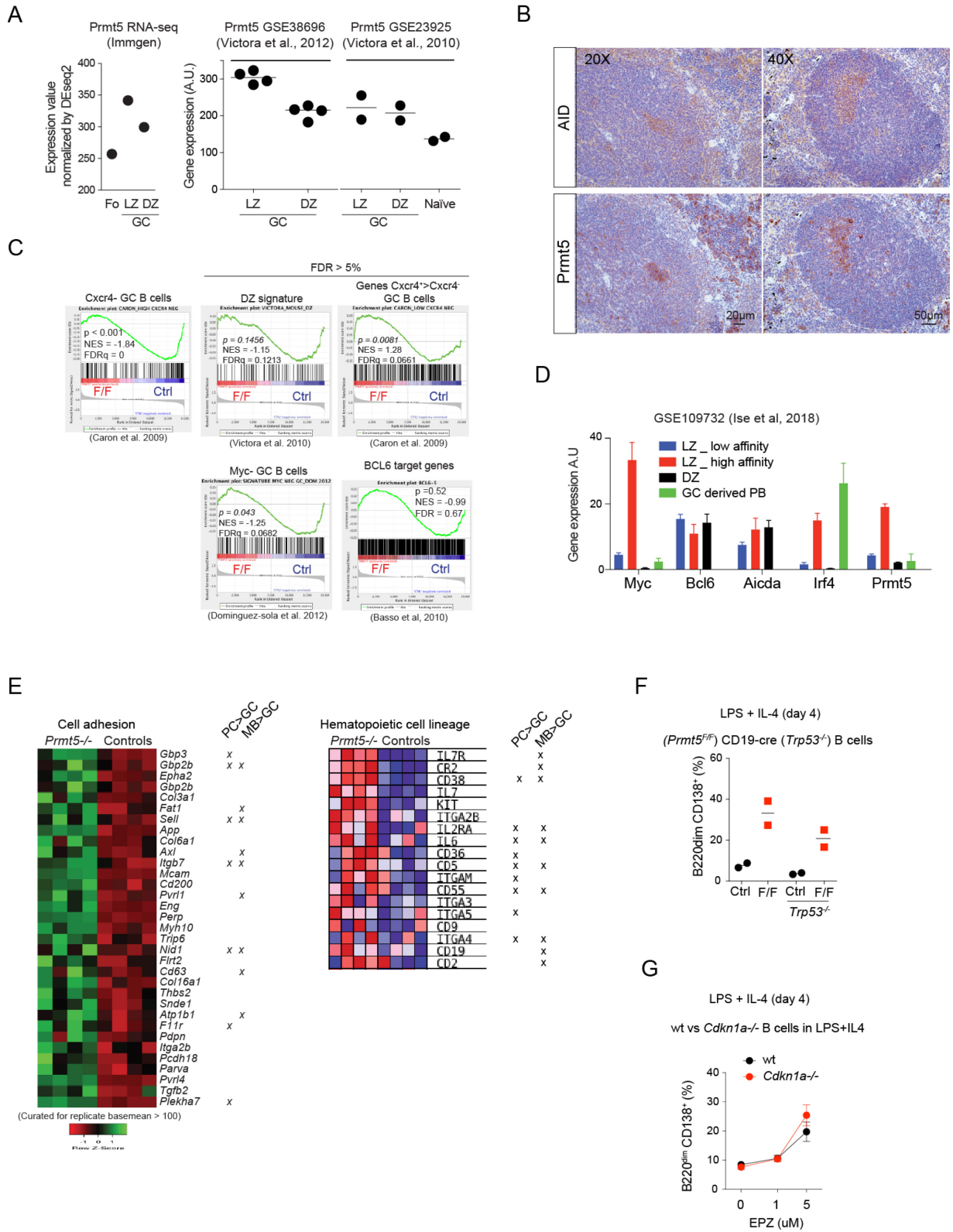
F) Functional annotation for molecular function of the genes showing at least one significant splicing event with ≥ 0.25 inclusion level difference (ILD) in *Prmt5* knockout versus Ctrl iGBs. The unranked list of genes was compared against the background list of all expressed genes at the GOrilla server.

G) Scheme of selected genes with SE, indicating the inclusion level difference of significant events.

H) Mean + s.d. proportion iGB cells with ≥ 5 γ H2AX foci determined by IF at days 4 and 5 after plating. Cells derive from *Cy1-cre* (Ctrl) and *Prmt5^{F/F} Cy1-cre* (F/F) mice, 4 mice per genotype from 2 experiments. The number of cells analyzed and P -values by unpaired, two tailed Student-t test are indicated.

I) DNA damage sensitivity of iGB cells derived from *Cy1-cre* (Ctrl) and *Prmt5^{F/F} Cy1-cre* (F/F) B cells. Cells were treated with different doses of DNA damaging agents at day 3 and counted at day 4 (caffeine and UV) or 5 (other treatments) and normalized to untreated cell numbers. Means \pm s.e.m relative cell numbers from 4 (etoposide) or 2 (others) mice per genotype are plotted.

J) Representative flow cytometry plots showing *Cy1-cre* (Ctrl) or *Prmt5^{F/F} CD19-cre* (F/F) B cells activated ex vivo, stained with CFSE and IgG1. Means \pm s.d. proportions of IgG1⁺ cells per division, determined from CFSE peaks, are plotted from n mice from 2 experiments.



Supplementary Figure 2.5 – Expression of Prmt5 in GC light zone B cells

- A)** *Relative Prmt5 transcript expression between GC light zone (LZ) and dark zone (DZ) in microarray data obtained from the indicated sources. Fo, follicular; and naïve B cell data is shown for comparison.*
- B)** *Additional IHC of consecutive splenic sections stained with anti-AID and anti-Prmt5, from immunized C57BL6/J mice.*
- C)** *Additional GSEA of transcriptional changes in Prmt5^{F/F} Cγ1-cre (F/F) iGB cells obtained from the indicated references. Enrichment was considered significant when $P < 0.05$ and $FDR < 5\%$.*
- D)** *Relative transcript levels of Prmt5 and other genes between GC subsets obtained from RNA-seq data from the indicated source.*
- E)** *Heat map of the top expressed genes (basemean >100) included in the cell adhesion category significantly enriched in Prmt5^{F/F} Cγ1-cre (F/F) compared to Cγ1-cre (Ctrl) iGB cells by Gorilla (F) or leading-edge genes included in the hematopoietic cell lineage KEGG pathway gene set from GSEA MsigDB (G) (see Figure 6C and supplementary table 2). Genes that are induced in plasma cells (PC) and/or memory cells (MC) compared to GC cells according to Immgen microarray data are indicated by a cross.*
- F)** *Plasma cell proportion in cultures of splenic B cells from individual mice (symbols) of the indicated genotypes and mean (bars) from 1 experiments are plotted*
- G)** *Mean + s.d. of plasma cell proportion in cultures of splenic B cells from wt or p21-deficient mice treated with DMSO or doses of Prmt5 inhibitor EZH.*

Supplementary Table 2.5 - Antibodies

Antibodies for flow cytometry

Anti-	TAG	CATALOGUE	CLONE	VENDOR	DILUTION
CD45R (B220)	APC	553092	RA3-6B2	BD Pharmingen	1/200
CD45R (B220)	PercP-Cy5.5	552771	RA3-6B2	BD Pharmingen	1/50
CD45R (B220)	Alexa Fluor 700	103232	RA3-6B2	BioLegend	1/50
CD45R (B220)	FITC	11-0452-85	RA3-6B2	Invitrogen	1/200
CD3e	PE	553063	145-2C11	BD Pharmingen	1/150
CD3e	biotin	553239	500-A2	BD Pharmingen	1/130
CD4	biotin	553045	RM4-5	BD Pharmingen	18 µl
IgD	biotin	13-5993-81	11-26c	eBioscience	18 µl
GL7	BV421	562967	GL7	BD Pharmingen	1/200
GL7	Alexa Fluor 647	561529	GL7	BD Pharmingen	1/200
Fas (CD95)	FITC	554257	Jo2	BD Pharmingen	1/200
Fas (CD95)	BV421	562633	Jo2	BD Pharmingen	1/130
CXCR4 (CD184)	PE	12-9991	2B11	eBioscience	1/100
CD86	biotin	13-0862	GL1	eBioscience	1/100
Streptavidin IgD	BV605	405229	-	BioLegend	1/100
IgD	FITC	553439	11-26c.2a	BD Pharmingen	1/150
IgM	BV605	563003	11-26c.2a	BD Pharmingen	1/50
IgM	BV421	562595	R6-60.2	BD Pharmingen	1/50
CD21/CD35	APC	558658	7G6	BD Pharmingen	1/200
CD23	PE-Cy7	562825	B3B4	BD Pharmingen	1/200
CD138	APC	561705	281-2	BD Pharmingen	1/150
Ki67	PE-Cy7	25-5698-82	SolA15	eBioscience	1/1000
CD24	FITC	11-0241-82	30-F1	eBioscience	1/50
BP-1	PE	553735	BP-1	BD Pharmingen	1/50
CD43	PE-Cy7	562866	S7	BD Pharmingen	1/50
IgG1	PE	550083	A85-1	BD Pharmingen	1/1000
IgG1	biotin	553441	A85-1	BD Pharmingen	1/200
BrdU	FITC	347583	B44	BD Pharmingen	20 µl
Annexin-V	APC	550474	-	BD Pharmingen	1/33
VAD-FMK	FITC	K180	-	BioVision	1/50
Phospho-histone H2AX (ser139)	-	2577	-	Cell signaling	1/50
His (used as isotype control)	-	710286	-	Invitrogen	1/50
Rabbit	Alexa 633	A21070	-	Invitrogen	1/8000
CXCR5	Biotin	13-7185-80	SPRCL5	Invitrogen	1/25
Bcl6	PE	91561522	K112-91	BD Pharmingen	1/20
CD62L	APC-Cy7	47-0621-82	MEL-14	Invitrogen	1/100
PD-1	PE-Cy7	25-9985-82	J43	Invitrogen	1/100
CD44	BV421	563970	IM7	BD Pharmingen	1/800
Foxp3	Alexa Fluor 700	56-5773-82	FJK-16s	Invitrogen	1/100
Gata-3	PerCP-eFluor 710	46-9966-42	TWAJ	Invitrogen	1/20
CD4	BUV 395	563790	GK1.5	BD Pharmingen	1/100

Antibodies for immunohistochemistry

Anti-	TAG	CATALOGUE	CLONE	VENDOR	DILUTION	Raised in
PRMT5	-	Ab109451	EPR5772	Abcam	1/250	Rabbit
PNA (not an antibody)	biotin	B-1075		Vector	1/100	
AID	-	14-5959-82	mAID-2	eBioscience	1/50	Rat
Rabbit-IgG	biotin			Vector	1/200	
Rat-IgG	biotin			Vector	1/200	

Antibodies for immunofluorescence

Anti-	TAG	CATALOGUE	CLONE	VENDOR	DILUTION
GL7	BV421	562967	GL7	BD Pharmingen	1/100
CD45R (B220)	APC	553092	RA3-6B2	BD Pharmingen	1/100
CD21/CD35	FITC	553818	7G6	BD Pharmingen	1/100
IgD	FITC	553439	11-26c.2a	BD Pharmingen	1/100

Antibodies for Western blots

Anti-	TAG	CATALOGUE	CLONE	VENDOR	DILUTION	Raised in
PRMT5	-	07-405		Millipore	1:2000	Rabbit
SYM11	-	Gift from SR			1:1000	Rabbit
SYM10	-	Gift from SR			1:1000	Rabbit
Rabbit	AlexaFluor 680	A10043		Invitrogen	1:20 000	Donkey
Mouse	AlexaFluor 680	A21057		Invitrogen	1:20 000	Goat
Rabbit	IRDye800	925-32211		LI-COR	1:20 000	Goat
Mouse	IRDye800	925-32210		LI-COR	1:20 000	Goat
Actin	-	A2066		Sigma	1:3000	Rabbit
p53	-	2524S	1C12	Cell Signaling	1:1000	Mouse
P-p53 (serine 15)	-	12571S	D4S1H	Cell Signaling	1:1000	Rabbit

Supplementary Table 2.6 - Primers

Primers for RT-qPCR

Gene	Type	Sequences	Product size (bp)	Lab name	Reference
<i>Prmt5</i>	Forward	CCCCATTAAGCAGCCCATCA	96	OJ 863	-
	Reverse	GCCCACTCGTACCACACTTT		OJ 864	
<i>Actin</i>	Forward	CTCTGGCTCCTAGCACCATGAAGA	200	OJ 897	-
	Reverse	GTA AAAACGCAGCTCAGTAACAGTCCG		OJ 898	
<i>Bcl2</i>	Forward	GAGCGTCAACAGGGAGATGT			
	Reverse	CTGGGGCCATATAGTTCCACAA			
<i>Mcl-1</i>	Forward	CCCCTCCCCATCCTAATCA			
	Reverse	CAATCCCTGGTCACTGTCTCGG			
<i>Bcl-XL</i>	Forward	AGTAAACTGGGGTCCGATCG			
	Reverse	GCCATCCA AACTGCAATCCG			
<i>Bax</i>	Forward	CAGGATGCGTCCACCAAGAA		-	Li, T., et al. (2012)
	Reverse	AGTCCGTGTCCACGTCAGCA		-	
<i>Bbc3</i>	Forward	ACGACCTCAACGCGCAGTACG			Li, T., et al. (2012)
	Reverse	GAGGAGTCCCATG AAGAGATTG			
<i>Pmaip1</i>	Forward	TCGCAAAAAGAGCAGGATGAG			Li, T., et al. (2012)
	Reverse	CACTTTGTCTCCAATCCTCCG			
<i>Bad</i>	Forward	CAGCAGCCCAGAGTATGTTCC			
	Reverse	CGTCCCTGCTGATGAATGTTG			
<i>Trp53</i>	Forward	AAGACAGGCAGACTTTTTCGCC			Hattangadi, S. M., et al. (2010)
	Reverse	CGGGTGGCTCATAAGGTACC			
<i>Cdkn1a</i>	Forward	AGATCCACAGCGATATCCAGAC		-	Li, T., et al. (2012)
	Reverse	ACCGAAGAGACAACGGCACACT		-	
<i>Bcl6</i>	Forward	CACACCCGTCCATCATTGAA		-	Nurieva, R. I., et al. (2008)
	Reverse	TGTCCTACGGTGCCTTTTT		-	
<i>Aicda</i>	Forward	GCCACCTTCGCAACAAGTCT	137	OJ 844	-
	Reverse	CCGGGCACAGTCATAGCAC		OJ 845	
<i>Prdm1</i>	Forward	GGAGGATCTGACCCGAAT			Todd, D. J., et al. (2009)
	Reverse	TCCTCAAGACGGTCTGCA			
<i>Irf4</i>	Forward	CTCTCAAGGCTTGGGCATT			Todd, D. J., et al. (2009)
	Reverse	TGCTCCTTTTTTGGCTCCCT			
<i>Myc</i>	Forward	TTTGTCTATTTGGGGACAGTGTT			Wolf, E., et al. (2013)
	Reverse	CATCGTCGTGGCTGTCTG			
<i>Rpl35a</i>	Forward	CGTGCCAAATCCGAAGCAA	70	OJ 1074	-
	Reverse	ATGGGTACAGCATCACACGG		OJ 1075	
<i>Igh</i>	Forward	AGCTCACACCTTGACCTTTCA		OJ 1621	Minnich, M., et al. (2016)
	Reverse	TGGTGGGACGAACACATTTA		OJ 1622	

Primers for RT-PCR

Gene	Type	Sequences	Product size (bp)	Lab name	Reference
<i>Mdm4 total</i>	Forward	AGTCAGGTGCGGCCAAAA	173	OJ 1617	Bezzi, M., et al. (2013)
	Reverse	CCCAAAAGATCTCCACCACA		OJ 1618	
<i>Mdm4 splicing</i>	Forward	TGTGGTGGAGATCTTTTGGG	Short: 159 Long: 227	OJ 1613	Bezzi, M., et al. (2013)
	Reverse	TCAGTTCTTTTTCTGGGATTGG		OJ 1614	
<i>Gapdh</i>	Forward	ACTCCACTCACGGCAAATTCA		OJ 651	
	Reverse	GCCTCACCCCATTTGATGTT		OJ 652	

3 Chapter III

Prmt1 supports antibody affinity maturation and represses plasma cell differentiation

Ludivine C. Litzler ^{1,2}, Adrien Sprumont ¹, Astrid Zahn ¹, Stephen P Methot ^{1,+}, Anne-Marie Patenaude ^{1,++}, Seolkyoung Jung ³, Stéphane Richard ^{4,5,6}, Javier M Di Noia ^{1,2,6,7}

¹ Institut de Recherches Cliniques de Montréal, 110 av. des Pins Ouest, Montréal, QC, Canada H2W 1R7.

² Department of Biochemistry and molecular medicine, 2900 boul. Édouard-Montpetit, bureau D-360, Montréal, QC, Canada, H3T 1J4

³ Lymphocyte Nuclear Biology, NIAMS, National Institutes of Health, 10 Center Drive, Bethesda, MD 20892, USA.

⁴ Segal Cancer Center, Bloomfield Center for Research on Aging, Lady Davis Institute for Medical Research, Montréal, Québec, Canada H3T 1E2.

⁵ Departments of Oncology and Medicine, McGill University, 5100 Maisonneuve Blvd West, Suite 720; Montreal, QC, Canada H4A3T2

⁶ Department of Medicine, Division of Experimental Medicine, McGill University, 1001 boul Decarie, Montreal, QC, Canada H4A 3J1.

⁷ Department of Medicine, Université de Montréal, C.P. 6128, succ. Centre-ville, Montréal, QC, Canada, H3C 3J7.

⁺ *Present address: Friedrich Miescher Institute for Biomedical Research, Maulbeerstrasse 66, R-1066.2.58. P.O. Box 3775. 4002 Basel, Switzerland.*

⁺⁺ *Present address: Genos, BioCentar Borongajska cesta 83H, 10000 Zagreb, Croatia.*

3.1 Abstract

High affinity antibodies are generated during the germinal center (GC) reaction, in which B cells go through cycles of somatic hypermutation and selection before differentiating into plasma B cells. The mechanisms defining GC dynamics are incompletely understood. Protein arginine methyltransferase 1 (Prmt1) is necessary for B cell development and activation but its function during the GC reaction is unknown. Here, we show that Prmt1 depletion in GC B cells strongly compromises the magnitude and affinity of the antibody response to protein antigens, while permitting normal titers but generating affinity-compromised antibodies to a conjugated hapten that elicits a clonally-restricted response. This defect originates from an impaired GC reaction, characterized by expansion failure and abnormal B cell subsets. *Ex vivo*, Prmt1 deficiency or inhibition leads to reduced B cell proliferation and drastically increases plasma cell differentiation. *In vivo*, the absence of Prmt1 leads to premature GC B cell differentiation, although Prmt1 is required afterwards for plasma cell maintenance. Our data provides new insight into the impact of arginine methylation on the dynamics and B cell fate choice in the GC.

3.2 Introduction

High affinity antibody responses depend on the cooperation between B lymphocytes that can recognize invading antigen and cognate T cells, to form germinal centers (GC). The GC is a transient structure formed upon infection or immunization within the B cell follicles of secondary lymphoid organs, wherein the antibody genes of antigen-activated B cells undergo somatic hypermutation (SHM). This process generates antibody variants that are selected for their affinity by interactions between the B cells and T follicular helper (Tfh) cells (Mesin et al., 2016; Rajewsky, 1996). GCs acquire spatial organization, including the division into a dark zone (DZ) and a

light zone (LZ), in which B cells undergo distinct phases of functional differentiation. In the DZ, B cells have a centroblast phenotype, express Activation induced deaminase (AID) and undergo SHM. When centroblasts move into the LZ, they acquire another identity, as centrocytes. LZ B cells are selected based on their ability to acquire antigen from follicular dendritic cells and present it to Tfh cells. Positively selected centrocytes can re-enter the DZ and undergo further cycles of mutation and selection that underpin the generation of high affinity antibodies. Alternatively, once GC B cells reach a certain threshold of affinity, and/or in a stochastic manner, they can differentiate to plasma or memory B cells (Nutt et al., 2015; Zotos and Tarlinton, 2012). The affinity of the antibody, acting as B cell receptor (BCR), influences GC B cell fate. High affinity BCR typically induces plasma cell differentiation (Krautler et al., 2017). CD40 signaling strength, enhanced by long T-B interactions, also influences B cell fate, as reducing CD40 protein levels favors DZ re-entry over differentiation (Ise et al., 2018). In fact, BCR and CD40 signaling synergize in centrocytes to induce *c-Myc* expression (Luo et al., 2018), which is highly expressed in positively selected cells that re-enter the DZ (Calado et al., 2012; Dominguez-Sola et al., 2012), as well as in plasma cell-committed centrocytes (Ise et al., 2018). Thus, additional factors that remain to be identified must modulate the underlying mechanisms deciding centrocyte fate in the GC.

Post-translational modifications (PTM) regulate signaling cascades and gene expression. While the study of PTM in B cell biology has focused on phosphorylation and ubiquitination, important roles for less traditional PTM, such as O-GlcNAcylation (Wu et al., 2017) and arginine methylation (Hata and Mizuguchi, 2013; Infantino et al., 2010; Ying et al., 2015), are emerging. Arginine methylation is catalyzed by a family of protein arginine methyltransferases (PRMTs) that transfer methyl groups to the guanidino group in the side chain of arginine residues (Blanc and Richard, 2017; Yang and Bedford, 2013). Depending on whether the two methyl groups are added to the same or a different nitrogen atom of the guanidino group, PRMTs produce either asymmetrical or symmetrical dimethyl arginine (aDMA or sDMA), respectively. PRMT1 is the main enzyme catalyzing aDMA modification in most mammalian cell types, methylating a large repertoire of substrates (Blanc and Richard, 2017).

Accordingly, PRMT1 can have multiple cellular functions, notably acting as coactivator of many transcription factors, but also regulating translation and participating in signaling pathways (Blanc and Richard, 2017), including lymphocyte antigen receptors signaling (Infantino et al., 2010; Mowen and David, 2014).

PRMT1 is essential for embryogenesis and its loss leads to cell cycle arrest in mouse embryo fibroblasts (Yu et al., 2009). Conditional ablation has shown that Prmt1 is necessary for mouse B cell development, by promoting the differentiation of pre-B cells (Dolezal et al., 2017; Hata et al., 2016; Infantino et al., 2010). Reflecting the multiplicity of PRMT1 substrates, this is achieved by at least two mechanisms. Firstly, aDMA of the Ig α subunit of the pre-B cell receptor (BCR) complex dampens PI3K/Akt signaling, thus favoring differentiation (Infantino et al., 2010). Secondly, Prmt1 activity, enhanced by its association with Btg2, reduces pre-B cell proliferation by methylating CDK4 to prevent its interaction with cyclin D3, thus leading to G1 arrest, Rag2 expression and *IgL* rearrangement (Dolezal et al., 2017). While there is consensus about the requirement for Prmt1 for B cell development, the analysis of the T-cell dependent antibody response in mice lacking Prmt1 in mature B cells has yielded contradictory findings. While one group found GC defects, and accordingly greatly reduced antibody responses (Infantino et al., 2017), another group found normal antibody responses, although they did not analyze GC (Hata et al., 2016). These reports differed also in the response of purified Prmt1-deficient mature B cells to stimulation with anti-IgM, CD40L or LPS *in vitro*, showing either reduced (Infantino et al., 2017) or increased proliferation (Hata et al., 2016). The discrepant results between these two reports might be explained by differences in excision efficiency and ontogeny of B cells devoid of Prmt1, as they used different Cre drivers to delete *Prmt1*. Nevertheless, they stress the need for further scrutiny to clarify the role of Prmt1 in antibody responses. Moreover, since Prmt1-deficient B cells show activation defects and reduced expression of anti-apoptotic genes *in vitro* following BCR cross-linking (Infantino et al., 2017), little could be concluded about the role of Prmt1 in GC as any phenotype would be influenced by defects during B cell activation.

Here we have analyzed GC function in mice in which Prmt1 is conditionally deleted at the onset of the GC reaction but after B cell activation. We find that these mice have compromised GC expansion, yet respond well to antigens that elicit a clonally restricted antibody response. However, the magnitude and affinity of a response against protein antigens is compromised. *In vitro* and *in vivo* analysis of Prmt1-deficient B cells provide evidence of altered GC dynamics compatible with a defect in LZ B cells, most likely during positive selection. We finally show that Prmt1 inhibition or ablation *ex vivo* results in greatly enhanced plasma cell differentiation. Our data establishes Prmt1 as a fundamental factor in sustaining GC dynamics and negatively regulating plasma cell differentiation.

3.3 Results

3.3.1 Prmt1 is upregulated in activated and GC B cells

A systematic survey to determine Prmt1 expression in B cell stages showed that it was regulated during B cell development but decreased and remained unchanged in immature and resting mature B cells (**Fig. 3.1A**). Prmt1 gene expression was increased in activated and GC B cells (**Fig. 3.1A**). Moreover, comparing the RNA levels of all nine murine PRMTs in activated and GC B cells, showed that Prmt1 is the most expressed PRMT in both B cell types (**Fig. 3.1B**). In agreement with RNA levels, Prmt1 protein levels increased and were sustained for 4 days after stimulating splenic B cells with LPS and IL-4 (**Fig. 3.1C**). Similarly, in mouse spleen, Prmt1 was highly expressed in the red pulp and in GC B cells, predominantly in the nucleus, and was much less abundant in follicular (FO) B cells (**Fig. 3.1D**). Prmt1 protein expression also distinguished GC from FO B cells in human lymph node and tonsil (**Fig. 3.1E**). These results suggested that Prmt1 was particularly relevant at B cell activation and in the GC.

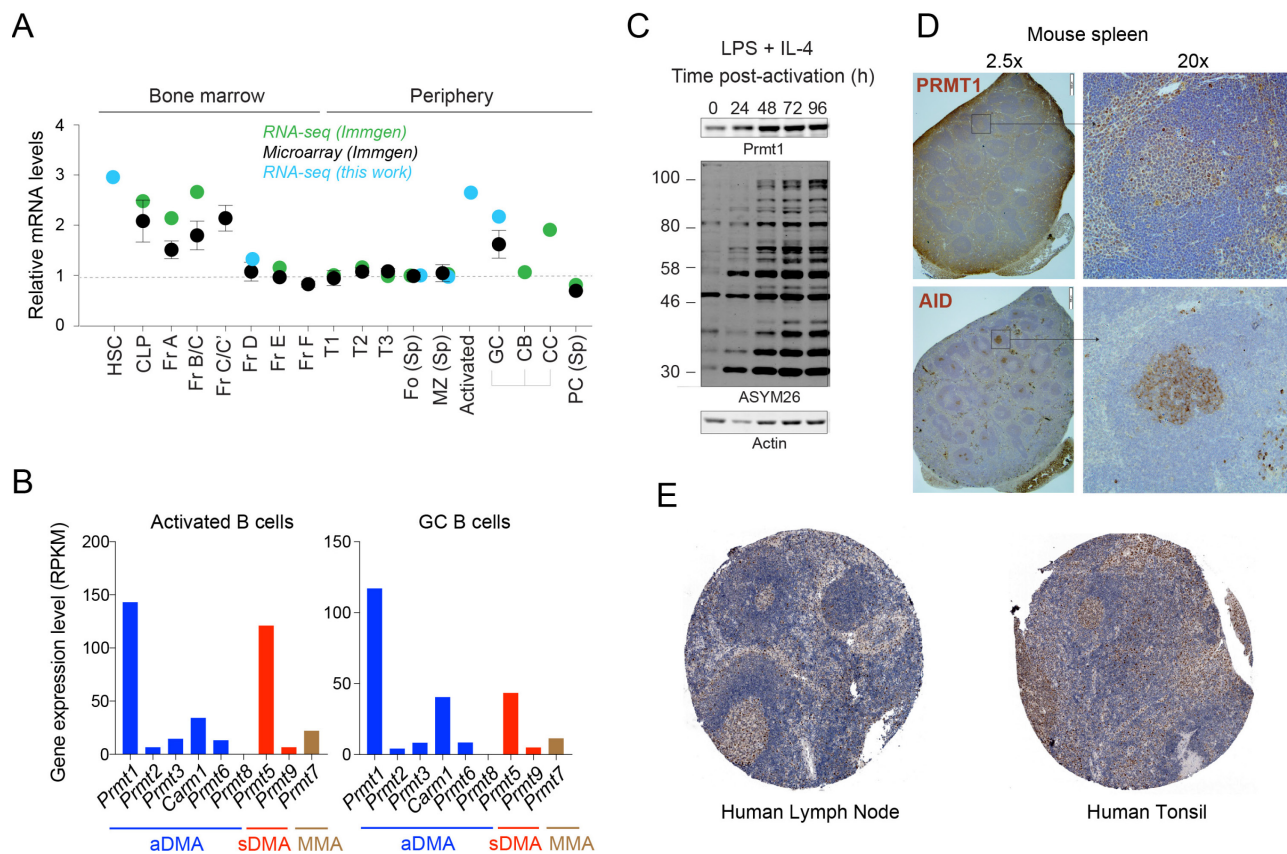


Figure 3.1 – Prmt1 expression in B cells

A) Prmt1 mRNA levels in B cell populations from each indicated source were normalized to resting mature follicular (Fo) B cells. CLP, common lymphoid progenitor; FrA to F, Hardy's fractions of B cell development; T1-T3, transitional B cell types; MZ, marginal zone B cells; GC, germinal center; CB, centroblasts; CC, centrocytes; PC, plasma cells; (Sp), spleen.

B) Expression level of Prmts in wt mouse splenic B cells activated with LPS (50 $\mu\text{g}/\text{mL}$) + IL-4 (2.5 ng/mL) for 72 h and in GC B cells sorted from lymph nodes of immunized mice. Average reads per kilobase per million mapped reads (RPKM), from two biological replicates.

C) Prmt1, aDMA-modified proteins and Actin (as loading control) were probed by WB with anti-Prmt1 and ASYM26 antibody, respectively, in extracts of splenic B cells stimulated with LPS (5 $\mu\text{g}/\text{mL}$) + IL-4 (5 ng/mL) for various times.

D) Representative pictures of immunohistochemical staining for Prmt1 and AID, as GC marker, on consecutive spleen sections from an immunized mouse.

E) Representative pictures of PRMT1 immunohistochemical staining with antibody CAB022550 in human lymph node and tonsil, obtained from the Human protein atlas database.

3.3.2 Prmt1 is required for GC formation

We initially analyzed *Prmt1^{F/F}* CD21-cre mice, which excise *Prmt1* in marginal zone (MZ) and FO B cells (Kraus et al., 2004), to produce Prmt1-deficient mature B cells. Prmt1 was efficiently deleted in resting splenic B cells from *Prmt1^{F/F}* CD21-cre mice, which were also depleted of aDMA (**Fig. 3.2A**). Most splenic B cells populations were normal in *Prmt1^{F/F}* CD21-cre mice, except for MZ B cells that were reduced (**Fig. 3.2B**). To test the effect of Prmt1 deficiency on GC formation we resorted to bone marrow (BM) chimeras, to avoid confounding effects from deletion in CD21⁺ follicular dendritic cells (Schmidt-Supprian and Rajewsky, 2007). We transplanted a 1:1 mixture of BM cells from either *Prmt1^{F/F}* CD21-cre or CD21-cre control mice together with BM from μ MT mice, which cannot produce B cells (Kitamura et al., 1991), into lethally irradiated wt mice. The chimeric mice were immunized with the hapten 4-hydroxy-3-nitrophenyl conjugated to chicken gamma globulin (NP-CGG) two months after BM reconstitution and analyzed 10 days later. We verified a significant deficiency in MZ B cells in splenic resting B cell populations, confirming this was a B cell intrinsic defect, but FO B cell proportions were normal (**Fig. 3.2C**). GCs were reduced by ~3-fold in *Prmt1^{F/F}* CD21-cre : μ MT BM chimeras compared to control chimeric mice (**Fig. 3.2D**), in line with published data using *Prmt1^{F/F}* CD23-cre mice (Infantino et al., 2017). Thus, Prmt1 in peripheral B cells is required for MZ B cells, dispensable for the homeostasis of FO B cells and necessary for GC formation.

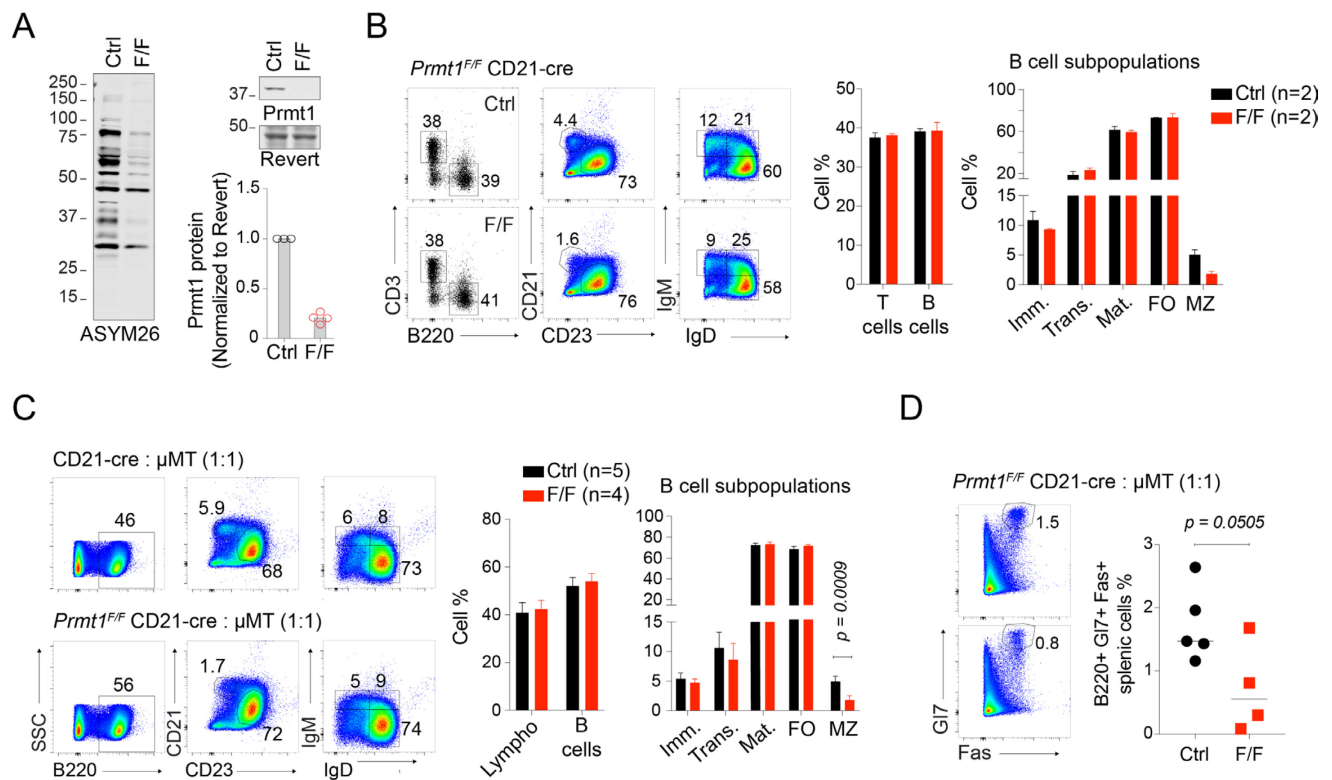


Figure 3.2 – Prmt1 is required for GC formation

A) WB for Prmt1 and aDMA (ASYM26) in purified resting B cells from the spleen of CD21-cre (Ctrl) and Prmt1^{F/F} CD21-cre (F/F). Revert is used as a loading control. Mean (bars) and individual mice (circles) values are indicated, from 2 experiments, normalized to revert.

B) Representative flow cytometry plots used to analyze splenic T cells and B cell subpopulations in CD21-cre (Ctrl) and Prmt1^{F/F} CD21-cre (F/F) mice. B cells were gated on B220⁺ and subpopulations are defined as immature (IgD⁻ IgM⁺), transitional (IgD⁺ IgM⁺), mature (IgD⁺ IgM⁻), follicular (CD21⁺ CD23⁺) or marginal zone (CD21⁺ CD23⁻). Mean + s.e.m. proportions for 2 mice from one experiment.

C) As in B for mixed BM chimera of either CD21-cre (Ctrl) or Prmt1^{F/F} CD21-cre (F/F) and μMT BM cells (1:1 ratio). Reconstituted mice were immunized with NP-CGG and splenocytes analyzed 10 days later.

D) Representative flow cytometry plots of B220⁺ cells showing GC B cell proportions in the spleen of chimeric mice from C). Values for individual mice are plotted.

3.3.3 Prmt1 in GC B cells is required for the antibody response to complex antigen

The *Prmt1^{F/F}* CD21-cre mice, as well as previous work analyzing Prmt1 in B cells (Hata et al., 2016; Infantino et al., 2017), ablated the enzyme in mature resting B cells. Given that Prmt1 is induced both in activated as well as GC B cells, potential defects upon B cell activation might obscure additional functions of Prmt1 in GC B cells. To bypass any effect of Prmt1 deficiency prior to activation, we generated *Prmt1^{F/F}* C γ 1-cre mice, which delete *Prmt1* following B cell activation (Casola et al., 2006). *Prmt1^{F/F}* C γ 1-cre mice showed normal numbers of T and B lymphocytes, as well as resting B cell subsets (**Fig. 3.3A**). Basal serum Ig in *Prmt1^{F/F}* C γ 1-cre mice showed a significant and specific decrease of circulating IgG1 (**Fig. 3.3B**), indicating a defect of Prmt1-deficient B cells for generating antibody responses. It was therefore surprising that after immunization with NP-CGG, these mice produced normal IgG1 responses against NP (**Fig. 3.3C**). However, the response against NP is heavily biased towards using the λ light chain and Ig VH186.1, in which relatively high affinity can be reached through a single point mutation (Allen et al., 1988). This clonal restriction leads to a response dominated by intraclonal competition (Jacob et al., 1993). In contrast, pre-immune serum IgG1 reflects polyclonal antibody responses against environmental antigens that likely undergo interclonal competition in the GC (Bannard and Cyster, 2017). Since proteins are complex antigenic entities (Benjamin et al., 1984), we then analyzed the serum IgG1 against the CGG protein carrier in the immunized *Prmt1^{F/F}* C γ 1-cre mice. Anti-CGG IgG1 was significantly decreased after immunization, despite a normal anti-NP response in the same mice (**Fig. 3.3D**). Upon recall immunization 18 weeks after primary immunization, anti-CGG IgG1 was still strongly reduced compared to wt and the anti-NP response was still very similar to the controls (**Fig. 3.3E**). The distinct defects in antibody responses against each antigen were not easily explained by GC or plasma cell phenotypes. Thus, *Prmt1^{F/F}* C γ 1-cre mice displayed a 3.6-fold decrease in mean GC B cell numbers in the spleen 14 days after immunization (**Fig. 3.3F**) but the difference in GC B cell numbers was no longer significant for GC formed after recall (**Fig. 3.3G**). The latter results,

suggested that memory B cells generated from the primary GC had compensated for the initial defect. Moreover, even if NP-specific IgG1⁺ antibody secreting cells (ASC) were readily detectable in the spleen of *Prmt1^{F/F}* C γ 1-cre mice after primary response and at recall, they were still fewer than in the control (**Fig. 3.3G**). The reduction in ASC was consistently larger in bone marrow (BM), suggesting an additional defect caused by Prmt1 deficiency in plasma cells. We therefore hypothesized that not only GC B cell numbers, but also GC function were affected by Prmt1-deficiency. To glean information about GC function we studied affinity maturation in *Prmt1^{F/F}* C γ 1-cre mice by comparing the affinity of antigen-specific antibodies using NaSCN displacement ELISA (Luxton and Thompson, 1990; Zahn et al., 2013). This method revealed affinity maturation defects for both responses but still showed differences depending on the antigen. Thus, there was no significant difference in the affinity of the primary anti-NP response of the *Prmt1^{F/F}* C γ 1-cre compared to control mice, but the recall response had reduced affinity (**Fig. 3.3H**). Meanwhile, the affinity of anti-CGG IgG1 was significantly reduced at both primary and recall immunizations in *Prmt1^{F/F}* C γ 1-cre mice (**Fig. 3.3I**).

Thus, Prmt1 is much more critical for mounting high affinity antibody responses against complex antigens, such as CGG, than to elicit antibodies against antigens that evoke a clonally restricted responses, such as NP. We conclude that Prmt1 expression in GC B cells is necessary for GC homeostasis as well as for affinity maturation, strongly suggesting a functional GC defect.

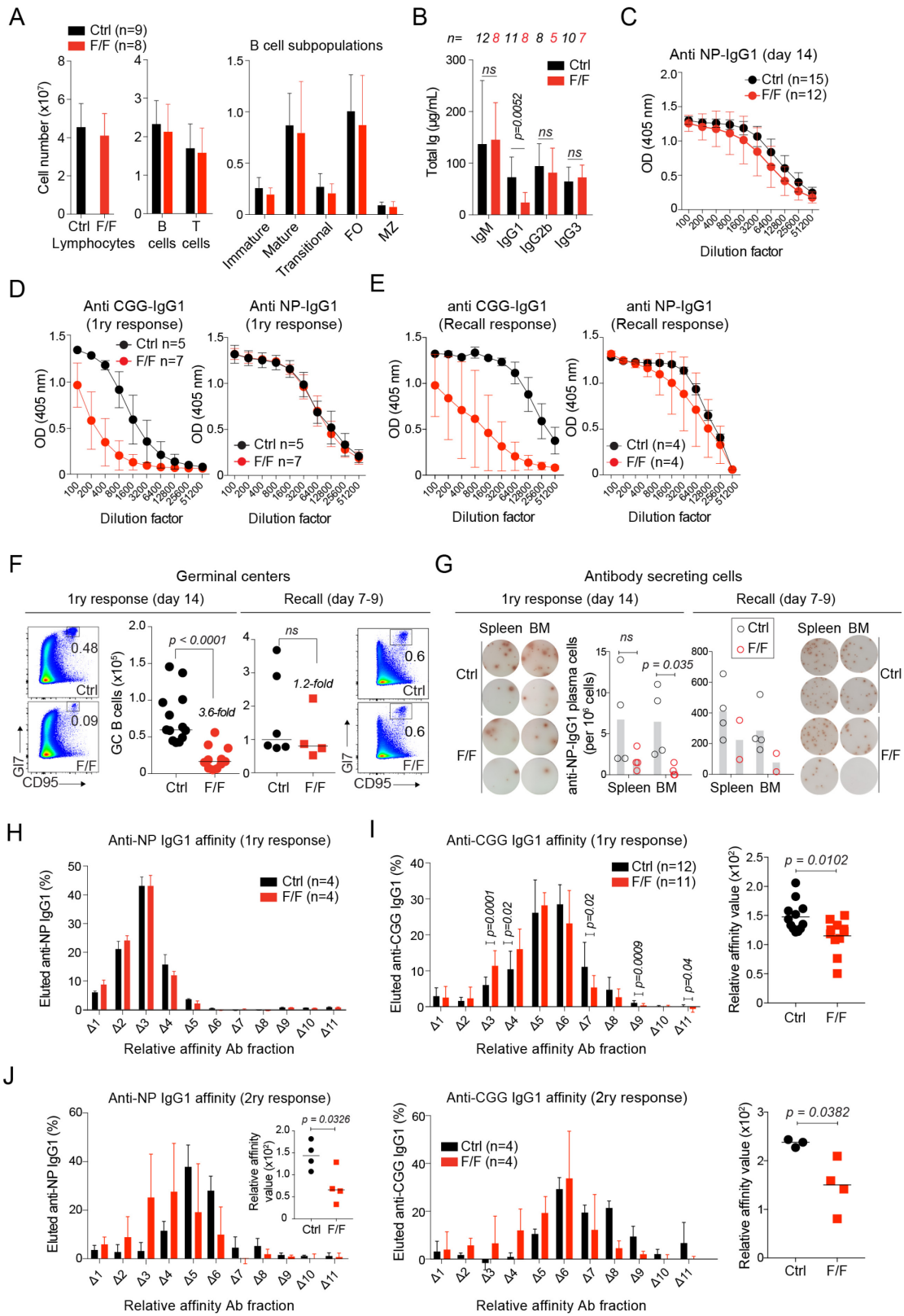


Figure 3.3 – Prmt1 is necessary for humoral response against complex antigen

A) Mean + s.d. number of lymphocytes and B cell subpopulations per spleen for n C γ 1-cre (Ctrl) or Prmt1^{F/F} C γ 1-cre (F/F) mice from 3 independent experiments.

B) Total levels of antibody isotypes in the pre-immune sera from n C γ 1-cre (Ctrl) or Prmt1^{F/F} C γ 1-cre (F/F) mice, measured by ELISA.

C) Anti-NP-specific IgG1 in the sera of C γ 1-cre (Ctrl) or Prmt1^{F/F} C γ 1-cre (F/F) mice at day 14 after immunization with NP-CGG in Alum, measured by ELISA using NP₂₀-BSA for capture. Mean \pm s.d. of OD values for n mice per group are plotted for serial dilutions, compiled from 5 independent experiments.

D) Anti-CGG-specific IgG1 in the serum of a subset of mice from C), measured by ELISA. The anti-NP IgG1 measured in the same sera are shown. Mean \pm s.d. of OD values from n mice are plotted for serum serial dilutions.

E) C γ 1-cre (Ctrl) or Prmt1^{F/F} C γ 1-cre (F/F) mice were immunized as in C) and a recall immunization performed 18 weeks later. Anti-CGG- and anti-NP- specific IgG1 was measured at day 7 post recall as in D). Mean \pm s.e.m. OD values for n mice are plotted for various dilutions, from 2 independent experiments.

F) Representative flow cytometry plots gated on B220⁺ cells showing GC cell (G17^{high} CD95⁺) proportions in the spleen of C γ 1-cre (Ctrl) or Prmt1^{F/F} C γ 1-cre (F/F) mice, 14 days post-immunization with NP-CGG. Data for individual mice (dots) are plotted to the right with means (bars) shown. Similar data from mice at 7-9 days after recall immunization is shown to the right. Data from individual mice (dots) and means (bars) from 2 experiments are indicated.

G) Number of NP-specific IgG1 antibody secreting cells (ASC) per 10⁶ cells in the spleen or BM of C γ 1-cre (Ctrl) or Prmt1^{F/F} C γ 1-cre (F/F) mice, measured by ELISPOT using NP₂₀-BSA for capture. Data for 14 days post primary immunization and at 9 days after recall are shown for individual mice (circles) with means (bars). Representative images for each are shown next to the corresponding graph.

P-values throughout are indicated for significant differences by unpaired, two-tailed Student-t test.

H, I) Affinity of NP-specific or CGG-specific IgG1 from C γ 1-cre (Ctrl) or Prmt1^{F/F} C γ 1-cre (F/F) mice at day 14 post-immunization with NP-CGG, measured by NaSCN displacement affinity ELISA using either NP₂₀-BSA- or CGG-coated plates, respectively. Mean + s.d of the fraction

of antigen-specific IgG1 eluted at each stepwise increasing concentration of NaSCN (Δn) is plotted for n mice from at least 2 independent experiments. Relative affinity values of anti-CGG IgG1 were calculated (see methods) and plotted for individual mice, with means (bars) shown.

J) Affinity measured as in H) for anti-NP and anti-CGG IgG1 after recall immunization.

3.3.4 Prmt1 is required for GC expansion and LZ homeostasis

To gain insight into the function of Prmt1 in GC, we characterized GCs in *Prmt1^{F/F}* $C\gamma 1$ -cre mice in more detail. We followed the kinetics of GC formation after immunization with sheep red blood cells (SRBC). GC B cell proportions and numbers were similar to control at day 5 (**Fig. 3.4A, 3.4B**), despite efficient Prmt1 depletion evidenced by the loss of aDMA specifically in GC B cells (**Fig. 3.4C**). However, by days 8 and 15 after immunization GC B cell proportion and numbers were significantly lower in *Prmt1^{F/F}* $C\gamma 1$ -cre mice (**Fig. 3.4A, 3.4B**). We did not observe increased apoptosis (**Fig 3.4D**), but we detected a larger fraction of Ki67^{low} cells at day 8 (**Fig 3.4E**), indicative of reduced proliferation *in vivo* (Endl et al., 1997). The DZ to LZ ratio, calculated from the Cxcr4^{low} CD86^{high} versus Cxcr4^{high} CD86^{low} staining (Victoria et al., 2010), appeared normal (**Fig. 3.4F**). However, there were indications that the B cell subsets dynamics were affected. Indeed, the *Prmt1^{F/F}* $C\gamma 1$ -cre mice showed the accumulation of a Cxcr4⁻ CD86^{low} population in the gate corresponding to the LZ (**Fig. 3.4F, 3.4G**). This population could be detected at day 5 but was most evident at days 8 and 15 post-immunization (**Fig. 3.4G**). Cxcr4⁻ CD86^{low} GC B cells were less proliferative, as shown by a lower proportion of Ki67⁺ cells compared to centroblasts and centrocytes (**Fig. 3.4H**). Immunizing *Prmt1^{F/F}* $C\gamma 1$ -cre *Aicda*-GFP mice, which express an AID reporter (Crouch et al., 2007), recapitulated phenotypes of reduced GC B cells and Cxcr4⁻ CD86^{low} B cell accumulation and showed that this population did not express AID (**Fig. 3.4I, 3.4J**). The AID-GFP reporter revealed further GC abnormalities in *Prmt1^{F/F}* $C\gamma 1$ -cre mice: a population of AID^{dim} cells visible in control DZ and LZ was absent and the overall proportion of AID⁺ centrocytes was

reduced in these mice (**Fig. 3.4J**), which we posit reflects alterations in the normal GC dynamics.

We conclude that *Prmt1* is necessary for the GC homeostasis and normal dynamics.

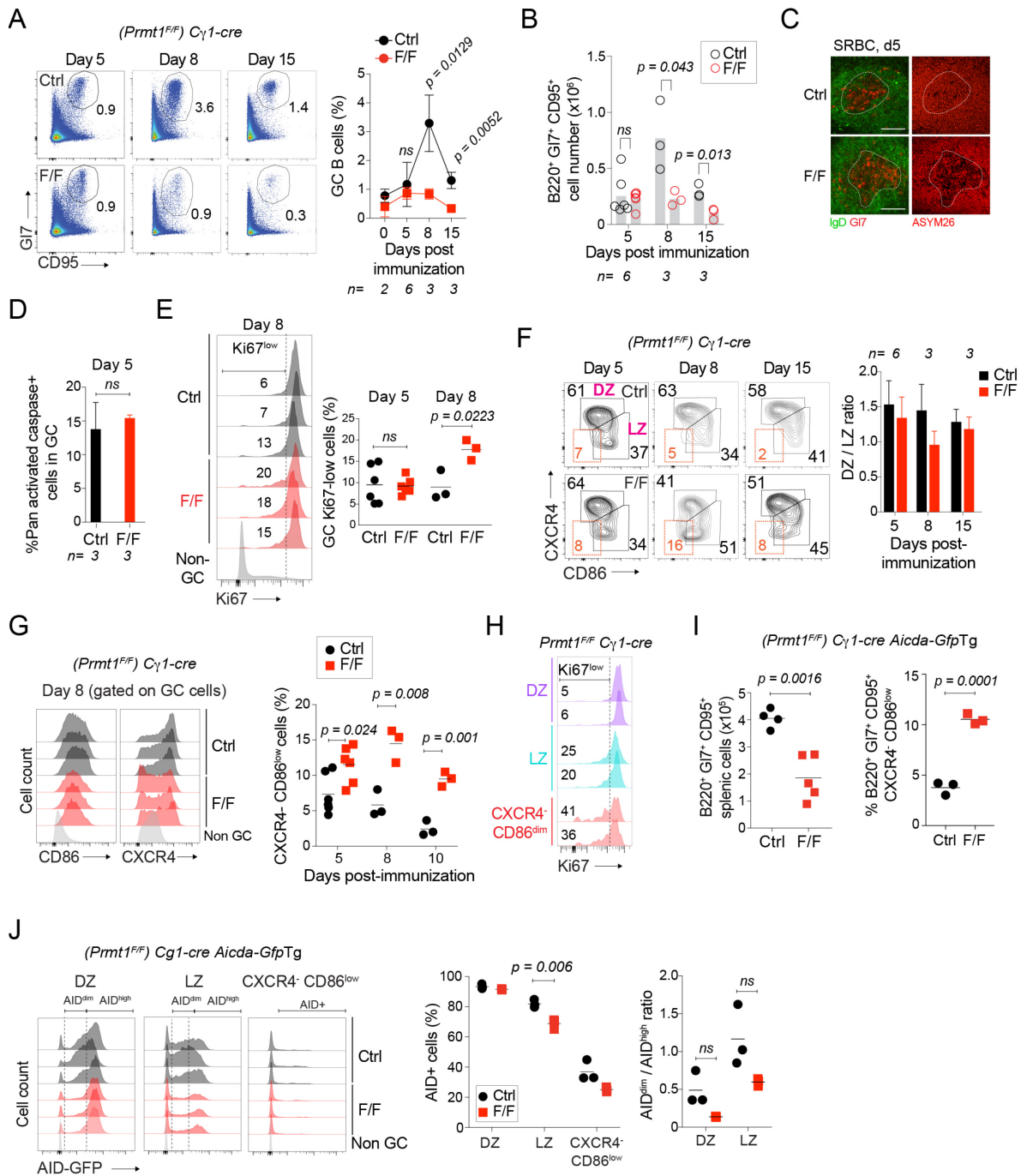


Figure 3.4 – *Prmt1* is necessary for GC expansion and dynamics

A) Representative flow cytometry plots of the proportion of GC B cells in the spleen of $C\gamma 1$ -cre (Ctrl) or $Prmt1^{F/F}$ $C\gamma 1$ -cre (F/F) mice at various times post-immunization with SRBC. Mean \pm s.d (except at day 0, s.e.m) of GC B cells proportion for n mice from 5 independent experiments are plotted.

B) Mean (bars) GC B cell numbers for individual mice (circles) from A) from 2 independent experiments at day 5 and one experiment at days 8 and 15.

C) Representative confocal images of immunofluorescence in splenic sections from $C\gamma 1$ -cre (Ctrl) or $Prmt1^{F/F}$ $C\gamma 1$ -cre (F/F) mice at day 5 after SRBC immunization, stained with antibodies against aDMA (ASYM26). GCs (IgD^- $Gl7^+$) are contoured by dashed lines. Scale bar 100 μ m.

D) Apoptosis measured with pan-activated caspase staining by flow cytometry in GC B cells of $C\gamma 1$ -cre (Ctrl) and $Prmt1^{F/F}$ $C\gamma 1$ -cre (F/F) mice at day 5 post-immunization with SRBC. Mean + s.d. proportion of activated caspase⁺ cells in GC B cells for 3 mice from one experiment.

E) Representative histograms of Ki67 staining in splenic GC B cells ($B220^+$, $Gl7^{high}$ $CD95^+$) from $C\gamma 1$ -cre (Ctrl) and $Prmt1^{F/F}$ $C\gamma 1$ -cre (F/F) mice 8 days post-immunization with SRBC. Means \pm s.d. proportion of $Ki67^{low}$ GC B cells for 3 mice from 2 experiments at day 5 and one experiment at day 8 are shown.

F) Representative flow cytometry plots of GC B cells ($B220^+$ $Gl7^+$ $CD95^+$) from $C\gamma 1$ -cre (Ctrl) or $Prmt1^{F/F}$ $C\gamma 1$ -cre (F/F) mice showing the proportion of DZ ($Cxcr4^+$ $CD86^{low}$), LZ ($Cxcr4^-$ $CD86^{high}$) and $Cxcr4^-$ $CD86^{low}$ cells at various times post-immunization with SRBC. Mean + s.d. DZ/LZ ratios for n mice, from 4 independent experiments.

G) Representative histograms of CD86 and $Cxcr4$ staining in GC B cells from $C\gamma 1$ -cre (Ctrl) or $Prmt1^{F/F}$ $C\gamma 1$ -cre (F/F) mice. The proportions of $Cxcr4^-$ $CD86^{low}$ cells in individual mice (symbols) and mean values (bars) are plotted.

H) Representative histograms of Ki67 staining with proportions of $Ki67^{low}$ cells in DZ ($Cxcr4$ $CD86^{low}$), LZ ($Cxcr4$ $CD86^{high}$) and $Cxcr4^-$ $CD86^{low}$ cells from 2 $Prmt1^{F/F}$ $C\gamma 1$ -cre (F/F) mice at 8 days post-immunization with SRBC.

I) Proportion of GC B cells at 9 days after SRBC immunization in $C\gamma 1$ -cre $Aicda$ -GFPTg (Ctrl) or $Prmt1^{F/F}$ $C\gamma 1$ -cre $Aicda$ -GFPTg (F/F) mice (symbols) and means (bars) are plotted for n mice (dots) from 2 independent experiments. The proportion of $Cxcr4^-$ $CD86^{low}$ GC B cells for a subset of the mice is plotted on the right.

J) Left, histograms of AID-GFP levels in DZ ($Cxcr4^-$ $CD86^{low}$), LZ ($CXCR4^{low}$ $CD86^{high}$) and $CXCR4^-$ $CD86^{low}$ B cells in GCs ($B220^+$, $Gl7^+$ $CD95^+$) of the mice analyzed in I). The gates shown in the histogram were used to calculate the proportion of AID⁺ cells in each population (Middle) and the ratio

of AID^{dim} to AID^{high} B cells in the DZ and LZ (right). Individual mice (symbols) and mean values (bars) are shown, from one experiment.

P-values throughout are indicated for significant differences by unpaired, two tailed Student-*t* test.

3.3.5 Prmt1 promotes B cell proliferation but is dispensable for isotype switching

For further insight into the B cell function of Prmt1 we analyzed the effect of ablating Prmt1 *ex vivo* in co-cultures with 40LB cells, which express CD40L and BAFF. B cells plated onto 40LB cells in the presence of IL-4 acquire a GC B cell-like phenotype (or iGBs heretofore) (Nojima et al., 2011). Resting B cells from $C\gamma 1$ -cre control mice plated onto 40LB briskly expanded for up to 6 days while $Prmt1^{F/F}$ $C\gamma 1$ -cre iGBs showed similar expansion up to day 5 but collapsed at day 6 (**Fig. 3.5A**). In fact, the expansion potential of $Prmt1^{F/F}$ $C\gamma 1$ -cre iGBs was compromised by day 4, as revealed by replating cells from this time point onto fresh 40LB (**Fig. 3.5A**). Importantly, $Prmt1^{F/F}$ $C\gamma 1$ -cre iGBs were depleted of aDMA by day 3 post-plating, demonstrating efficient *Prmt1* ablation, which was maintained at day 6, indicating there was no counter selection of Prmt1-deficient B cells (**Fig 3.5B**). We did not detect any consistent increase in apoptosis in $Prmt1^{F/F}$ $C\gamma 1$ -cre iGBs compared to controls (**Fig 3.5C**). On the other hand, cell cycle analysis revealed G1 arrest and reduced S phase in these cells at day 4 (**Fig 3.5D**), consistent with a proliferation defect and in line with reduced Ki67 staining *in vivo*.

Because PRMT1 has been shown to regulate the function of Mre11 and 53BP1 (Adams et al., 2005; Boisvert et al., 2005a; Yu et al., 2012), DNA repair factors that are important for antibody class switch recombination (CSR) (Stavnezer and Schrader, 2014), we analyzed CSR in the Prmt1-deficient iGBs. Isotype switching to IgG1 was modestly reduced at days 6 and 7 in the $Prmt1^{F/F}$ $C\gamma 1$ -cre iGBs (**Fig. 3.5E**). However, this reduction could be explained by reduced proliferation, as it coincided with the time points when cell expansion was more affected. To rule out a direct role of Prmt1 in the CSR mechanism, we depleted Prmt1 in the CH12F3 B cell line, which

switches from IgM to IgA upon cytokine stimulation (Nakamura et al., 1996) and constitutively expresses Prmt1 (**Supplementary Fig. 3.1A**). Knockdown of Prmt1 was efficient (**Fig. 3.5F, Supplementary Fig. 3.1B-E**) and did not significantly affect AID expression levels or germline transcripts (**Supplementary Fig. 3.1F-G**). Prmt1-deficient CH12F3 B cells showed reduced proliferation, as measured by CFSE, but had no CSR defects (**Fig. 3.5G, 3.5H**). These data show that the reduced IgG1 levels observed in the serum of *Prmt1^{F/F}* C γ 1-cre mice (**Fig. 3.3B**) could not be explained by an intrinsic defect in the CSR mechanism.

We conclude that Prmt1 is necessary for activated B cell proliferation but dispensable for CSR.

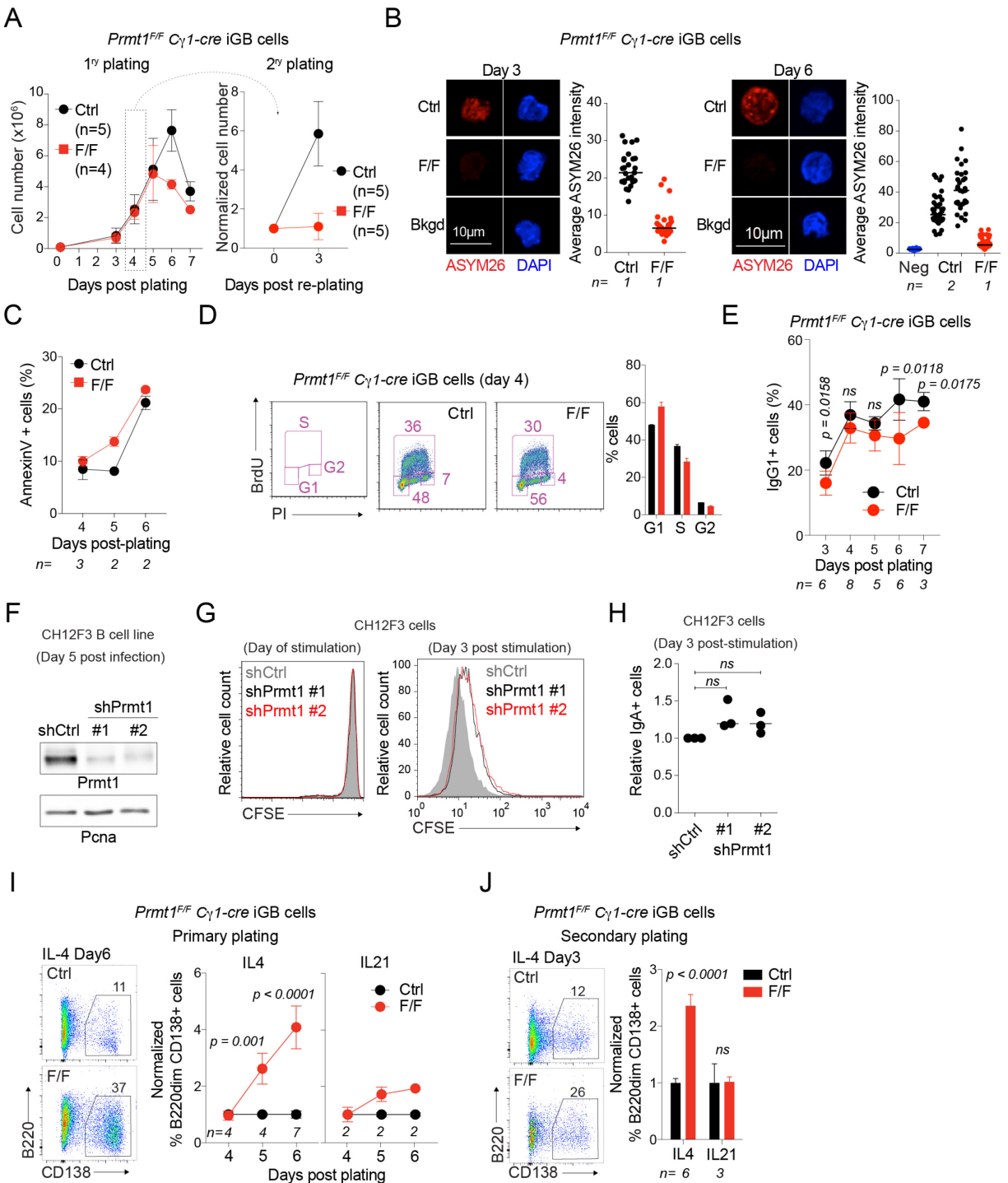


Figure 3.5 – Prmt1 is necessary for GC homeostasis

A) iGB cell counting over time from resting splenic B cells from *C γ 1-cre* (Ctrl) and *Prmt1^{F/F} C γ 1-cre* (F/F) mice plated on 40LB feeder cells supplemented with 1 ng/mL IL-4 (primary plating). At day 4 post-plating, cells were re-plated onto fresh 40LB feeders and maintained in culture for 3 days in identical conditions (secondary plating). Compilation of *n* mice from 2 experiments.

B) Representative confocal pictures of immunofluorescence of aDMA (ASYM26) on C γ 1-cre (Ctrl) and Prmt1^{F/F} C γ 1-cre (F/F) iGBs at 3 and 6 days post plating. Nuclei were stained with DAPI. Bkgd, no primary antibody control. Average ASYM26 signal per cell is plotted. Scale bar 10 μ m.

C) Mean \pm s.e.m. proportion of Annexin-V⁺ C γ 1-cre (Ctrl) and Prmt1^{F/F} C γ 1-cre (F/F) iGB cells at various days after primary plating for *n* mice, from 2 experiments.

D) Cell cycle profile of C γ 1-cre (Ctrl) and Prmt1^{F/F} C γ 1-cre (F/F) splenic B cells cultured as in A) and pulsed with BrdU (10 μ M) for 1 h at day 4 post plating before harvesting and staining with anti-BrdU and propidium iodide (PI). The plot shows mean + s.e.m. values for 2 mice per genotype from one experiment.

E) Mean \pm s.d. proportion of IgG1⁺ C γ 1-cre (Ctrl) and Prmt1^{F/F} C γ 1-cre (F/F) iGB cells at various days post primary plating for *n* mice from 5 experiments.

F) Prmt1 and PcnA (loading control) levels measured by WB in CH12F3 B cells expressing scramble shRNA (shCtrl) or shRNAs against Prmt1 (#1, #2).

G) CH12F3 B cells expressing shRNAs as in F) were stained with CFSE and stimulated with 1 ng/mL TGF β , 10 ng/mL IL-4, 1 μ g/mL α -CD40. Representative histogram showing CFSE levels at the day of staining and after 3 days in culture, from 3 independent experiments.

H) Proportion of IgA⁺ in CH12F3 cells expressing shRNAs as in F) at day 3 post stimulation. Three independent experiments (dots) and mean values (bars) are shown, normalized to shCtrl cells.

I) Left, Representative flow cytometry plots showing the proportion of plasma cells (B200^{dim} CD138⁺) arising from C γ 1-cre (Ctrl) or Prmt1^{F/F} C γ 1-cre (F/F) iGBs at day 6 post primary plating on 40LB cells. Mean \pm s.d. proportion of plasma cells, normalized to Ctrl average values, in cultures with either 1 ng/mL IL-4 (from *n* mice from 3 experiments) or additionally supplemented with 10 ng/mL IL-21 (from *n* mice from 1 experiment).

J) Left, Representative flow cytometry plots as in I) for B200^{dim} CD138⁺ plasma cells derived from C γ 1-cre (Ctrl) or Prmt1^{F/F} C γ 1-cre (F/F) iGBs at day 3 of secondary plating on 40LB cells supplemented with 1 ng/mL IL-4 or 10 ng/mL IL-21 at re-plating. Data from *n* mice from 3 experiments.

P-values throughout are indicated for significant differences by unpaired, two-tailed Student-*t* test.

3.3.6 Prmt1 represses plasma cell differentiation

Unexpectedly, we observed a large increase in the proportion of CD138⁺ cells in Prmt1^{F/F} C γ 1-cre iGB cultures. This was visible in primary as well as secondary

plating and relatively specific for cells supplemented with IL-4 rather than IL-21 (**Fig. 3.5I, 3.5J**). This result contrasted with a previous report in which *Prmt1^{F/F}* CD23-cre B cells stimulated *in vitro* with mitogen and cytokines, a classical assay to monitor plasma cell differentiation (Nutt et al., 2015), generated reduced proportions of plasma cells (Infantino et al., 2017). The kinetics of Prmt1 deletion of *Prmt1^{F/F}* C γ 1-cre cells when activated in this fashion were slow, and deletion inefficient (not shown). Therefore, to further study plasma cell differentiation *in vitro* we used splenic B cells from *Prmt1^{F/F}* CD21-cre mice stimulated *in vitro*. CD21-cre control B cells cultured in LPS + IL-4 showed >2-fold Prmt1 protein up-regulation and increased aDMA, while activated *Prmt1^{F/F}* CD21-cre B cells were depleted of both (**Fig 3.6A**). There was no significant difference in apoptosis or cell counts up to day 3 post-stimulation with LPS + IL-4 (**Supplementary Figs. 3.2A, 3.2B**). However, by day 4 reduced proliferation was visible by cell proliferation dye staining and cell counting (**Fig 3.6B, 3.6C**). The activated *Prmt1^{F/F}* CD21-cre B cells showed decreased CSR to IgG1 and concomitantly increased CD138⁺ plasma cell differentiation per division (**Fig. 3.6B, Supplementary Fig. 3.2C**). Increased differentiation in Prmt1-null B cells was confirmed by increased expression of the plasma cell specification genes *Prdm1* and *Irf4* and augmented *Igh* transcription (**Fig. 3.6D**). Prmt1-deficient B cells showed proliferation defects after LPS or CD40 + IL4 stimulation but the largest defect was observed after CD40 stimulation (Compare **Figs. 3.6B, 3.6E 3.6F**). Nonetheless, all stimulations of *Prmt1^{F/F}* CD21-cre B cells consistently enhanced plasma cell differentiation and reduced isotype switching per division (**Figs. 3.6E, 3.6F, Supplementary Fig. 3.2D, 3.2E**). As an orthogonal approach, we tested the effect of pharmacological inhibition of Prmt1 on plasma cell differentiation in stimulated wt B cells, using the type I PRMT inhibitor MS023 (Eram et al., 2016). Since Prmt1 is >4-fold more expressed than other type I PRMTs in activated B cells (**Fig. 3.1B**), any effects are most likely to originate from reduced Prmt1 activity. Accordingly, the pattern of proteins with reduced aDMA modification was very similar between MS023-treated and Prmt1-deficient activated B cells (**Figs. 3.6A, 3.6G**). MS023 caused a dose-responsive increase in B cell differentiation in activated wt B cells, judged both by the increase in CD138 surface expression and induction of *Prdm1* and *Irf4* (**Figs.**

3.6H, 3.6I), ruling out any influence of cre system in the results. We conclude that Prmt1 limits B cell differentiation into plasma cells *in vitro*.

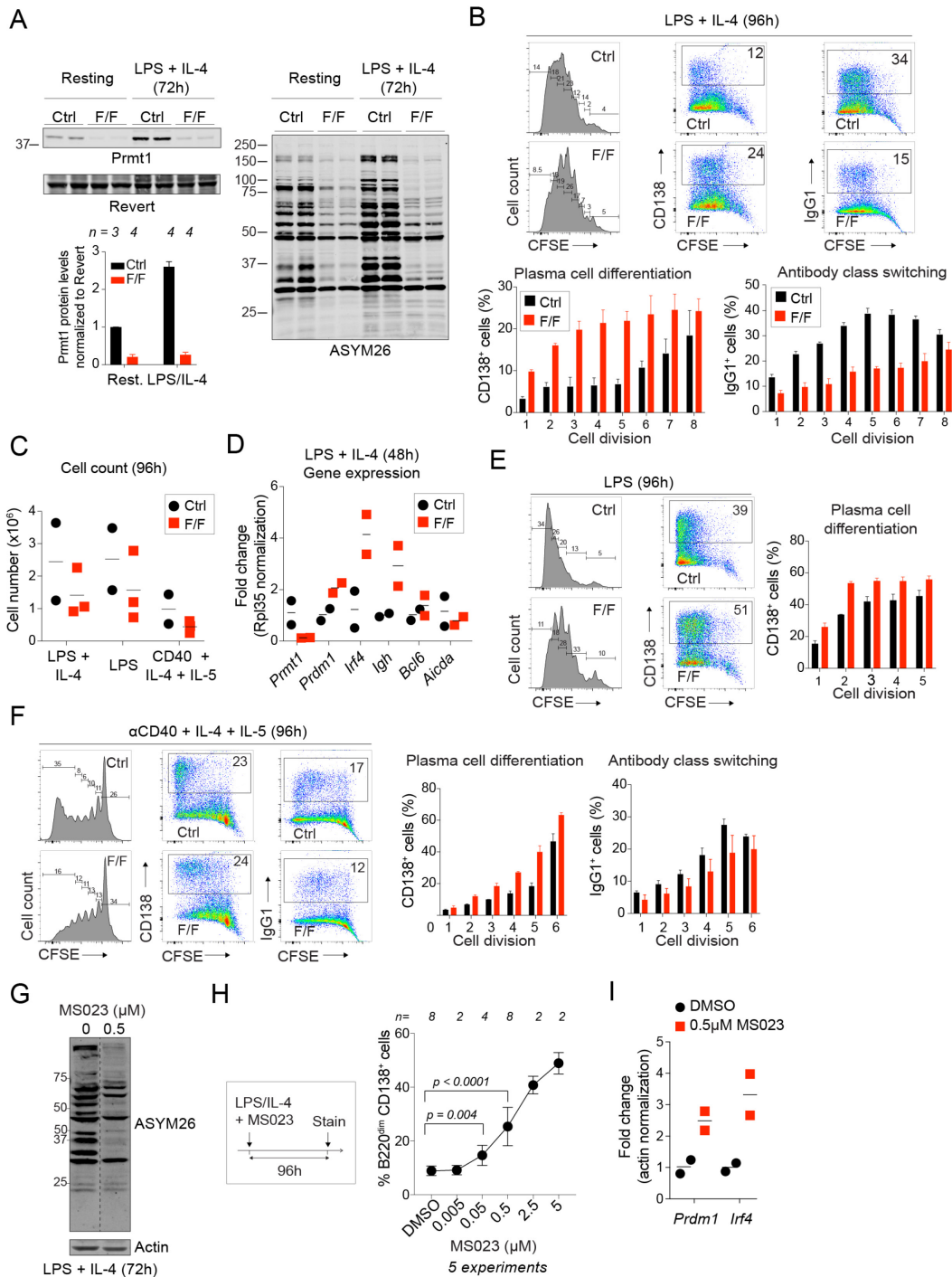


Figure 3.6 – Prmt1 limits B cell differentiation per division

A) WB for Prmt1 and aDMA (ASYM26) in extracts from CD21-cre (Ctrl) and Prmt1^{F/F} CD21-cre (F/F) purified naïve B cells, either resting or 72 h post stimulation with LPS (5 µg/mL) and IL-4 (5 ng/mL). Revert is used as a loading control. The plot shows mean + s.d. quantification of Prmt1 levels for n mice, normalized to revert.

B) Naïve CD21-cre (Ctrl) and Prmt1^{F/F} CD21-cre (F/F) B cells were purified and stained with CFSE previous to activation with LPS (5 µg/mL) and IL-4 (5 ng/mL). Representative flow cytometry plots of CFSE levels at 96 h indicating proportion of cells in each division, as well as plots of the proportion of plasma cells (CD138⁺) class-switched (IgG1⁺) B cells are shown. Means + s.e.m proportion of CD138⁺ or IgG1⁺ cells for each cell division for 2 mice per genotype of a representative experiment are shown.

C) Number of CD21-cre (Ctrl) and Prmt1^{F/F} CD21-cre (F/F) cells per well from naïve B cells cultures stained with CFSE and activated for 96 h with either LPS (5 µg/mL) and IL-4 (5 ng/mL), LPS (25 µg/mL) or agonist anti-CD40 (10 µg/mL), IL-4 (10 ng/mL) and IL-5 (5 ng/mL). Means (bars) and individual mice (dots) values from 2 experiments are shown.

D) Transcript levels of the indicated genes in Prmt1^{F/F} CD21-cre (F/F) relative to CD21-cre (Ctrl) measured by RT-qPCR in purified splenic B cells activated with LPS (5 µg/mL) and IL-4 (5 ng/mL) for 2 days. All mRNA levels were normalized to Rpl35 expression. Means (bars) are indicated, 2 mice were analyzed from one experiment per condition.

E) Purified naïve CD21-cre (Ctrl) and Prmt1^{F/F} CD21-cre (F/F) B cells were stained with CFSE and activated with LPS (25 µg/mL) for 96 h. Representative CFSE histograms and CD138⁺ cells at 96 h. Means ± s.e.m proportions of CD138⁺ cells per division from two mice from one representative experiment.

F) Purified naïve CD21-cre (Ctrl) and Prmt1^{F/F} CD21-cre (F/F) B cells were stained with CFSE and activated with agonist anti-CD40 (10 µg/mL), IL-4 (10 ng/mL) and IL-5 (5 ng/mL) for 96 h. Representative flow cytometry plots and mean + s.e.m proportions of CD138⁺ and IgG1⁺ cells per cell division for 2 mice per genotype from one representative experiment.

G) WB for aDMA (ASYM26) in extracts from wt purified naïve B cells stimulated as in A), treated or not with the Type I PRMT inhibitor MS023.

H) Scheme of the experimental set up and quantitation of plasma cells (B220^{dim} CD138⁺) in cultures of wt naïve B cells purified and stimulated as in A) and treated with the indicated concentrations of MS023. Mean ± s.d. for n mice from 5 experiments are plotted.

I) Expression of Prmd1 and Irf4 determined by RT-qPCR in cultures as in H treated with MS023. Two mice from one experiment.

3.3.7 Synergistic effect of Prmt1 and Prmt5 on plasma cell differentiation

PRMT1 substrate scavenging has been described, whereby in the absence of PRMT1 other PRMTs can methylate the orphaned substrates (Dhar et al., 2013) and scavenging of Prmt1 substrates by Prmt5, thus replacing aDMA by sDMA, could have unpredictable functional consequences. Indeed, WB revealed PRMTs substrate scavenging in mouse wt activated B cells, as shown by specific increases in sDMA-containing bands when Prmt1 was inhibited, in addition to reduction in some specific sDMA bands upon Prmt1 inhibition suggesting enzyme cooperation (**Fig. 3.7A**). On the other hand, we have found that ablating Prmt5, a type II PRMT that is highly expressed in activated B cells (**Fig. 3.1B**), also leads to increased plasma cell differentiation (Litzler et al, in preparation). We therefore asked whether Prmt5 and Prmt1 might collaborate or compete during plasma cell differentiation. We found that Prmt5 inhibition, in conjunction with Prmt1 genetic deficiency or inhibition, potentiated plasma cell differentiation. Indeed, even at low doses of PRMT1 and PRMT5 inhibitors, which alone barely affected plasma cell differentiation of wt B cells compared to DMSO control, showed a synergistic effect when combined, increasing differentiation and concomitantly decreasing proliferation (**Figs. 3.7B, 3.7C**). We confirmed this effect in the iGB system, by treating *Prmt1^{F/F}* C γ 1-cre iGBs with PRMT5 inhibitor, which increased plasma cell differentiation upon replating with IL-4, but not IL-21 (**Fig. 3.7D, 3.7E**), consistent with our results above. We conclude that Prmt1 and Prmt5 negatively regulate plasma cell differentiation by non-epistatic mechanisms.

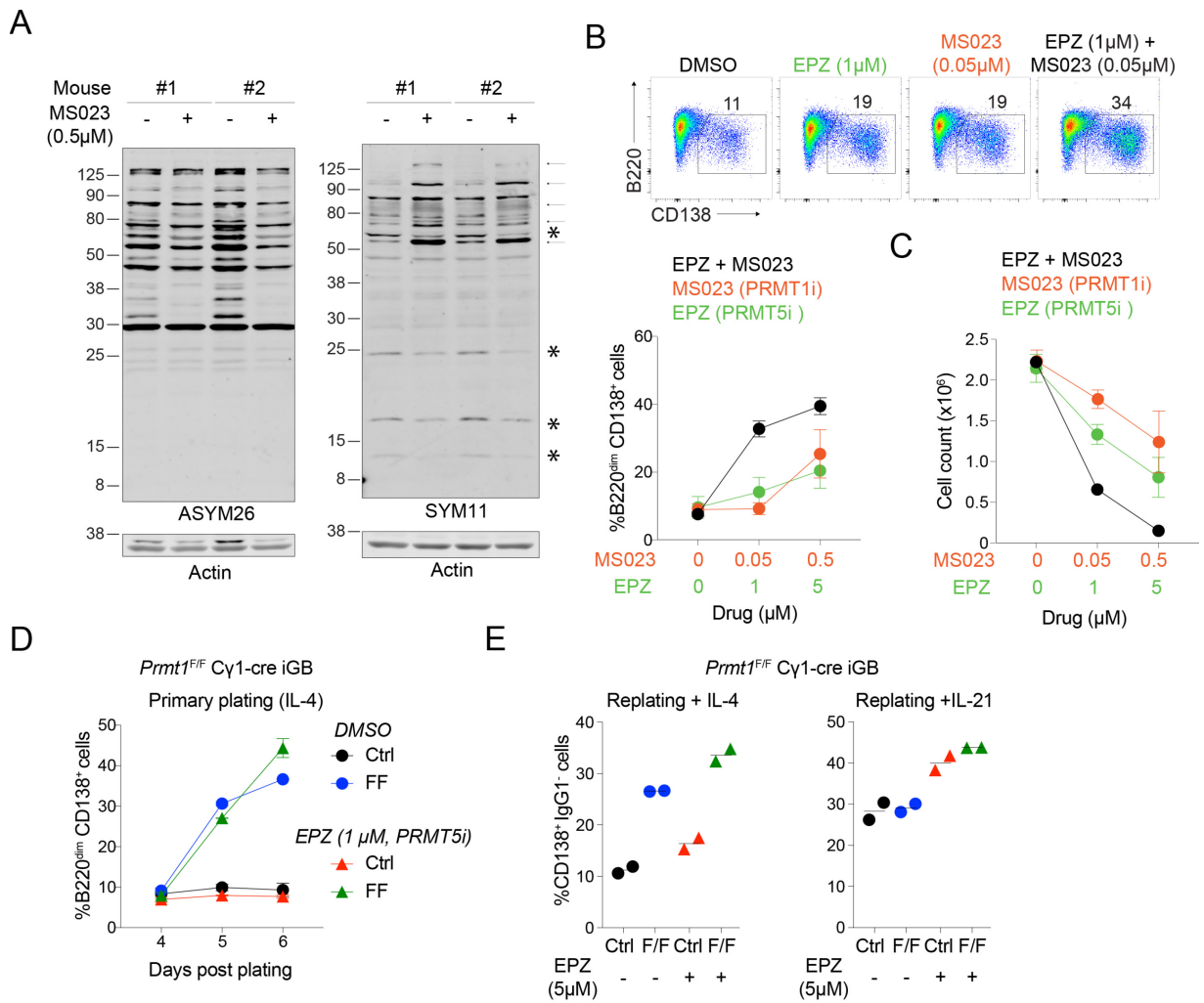


Figure 3.7 – Prmt1 cooperates with Prmt5 to restrict plasma cell differentiation

A) WB for aDMA (ASYM26) and sDMA (SYM11) in extracts from purified naive wt B cells cultured in LPS (5 μ g/mL) IL-4 (5 ng/mL) and treated with either 0.5 μ M MS023 or DMSO for 72 h. Actin WB is a loading control. Arrows indicate proteins bands with increased sDMA after MS023 treatment, asterisk indicate proteins bands with reduced sDMA upon MS023 treatment.

B) Representative flow cytometry plots showing proportions of plasma cells in cultures of purified naive wt B stimulated with LPS (5 μ g/mL) IL-4 (5 ng/mL) and treated with the indicated PRMT1 (MS023) or PRMT5 (EPZ015666) inhibitors, alone or in combination for 4 days. Mean \pm s.e.m plasma cell proportions for 2 mice from one experiment are plotted.

C) Mean \pm s.e.m cell counts in the cultures from B) are plotted.

D) Proportion of B200^{dim} CD138⁺ plasma cells derived from C γ 1-cre (Ctrl) or Prmt1^{F/F} C γ 1-cre (F/F) iGBs plated on 40LB cells supplemented with 1 ng/mL IL-4 and treated with EPZ015666 or DMSO 24 h post plating. Data from 2 mice from one experiment are plotted.

E) Proportion of B200^{dim} CD138⁺ plasma cells derived after replating the cells in D) onto fresh 40LB supplemented with either 1 ng/mL IL-4 or 10 ng/mL IL-21, in the presence of the indicated inhibitors. Data from 2 mice from one experiment.

3.3.8 Prmt1 prevents premature plasma cell differentiation *in vivo*

While the *ex vivo* data clearly indicated that Prmt1-deficiency promoted plasma cell differentiation, Prmt1^{F/F} C γ 1-cre mice still showed reduced number of plasma cells after immunization (**Fig. 3.3G**). It was conceivable that Prmt1-deficient plasma cells might have additional defects in survival and/or migration, which would prevent their accumulation *in vivo*, without precluding that Prmt1 negatively regulated their generation from GC B cells. In fact, Prmt1 was most highly expressed in positively selected Myc⁺ GC LZ B cells, which can either reenter the DZ or differentiate into plasma cells (Dominguez-Sola et al., 2012; Ise et al., 2018) (**Fig. 3.8A, 3.8B**). Thus, we asked whether Prmt1 might be influencing that choice. To obtain evidence that Prmt1 deficiency would favour plasma cell differentiation *in vivo*, we analyzed the proportion of GC B cells and plasma cells that had switched isotype in the spleen of immunized Prmt1^{F/F} C γ 1-cre mice. Since Prmt1 deficiency did not affect the CSR mechanism, as shown above, we reasoned that premature differentiation would result in an increased ratio of IgM⁺ to IgG1⁺ GC B cells. Indeed, while IgG1⁺ GC B cells were readily detectable in the GC of control mice, they were very rare in Prmt1^{F/F} C γ 1-cre mice (**Fig. 3.8C**). When the total splenic plasma cell population was analyzed, the Prmt1^{F/F} C γ 1-cre mice showed a trend to have fewer plasma cells (**Fig. 3.8D**), in line with results above (**Fig. 3.3G**). Nonetheless, the proportion of IgG1⁺ CD138⁺ plasma cells was lower in Prmt1^{F/F} C γ 1-cre mice than in controls (**Fig. 3.8E**). We conclude that Prmt1 negatively regulates plasma cell differentiation from GC B cells *in vivo*.

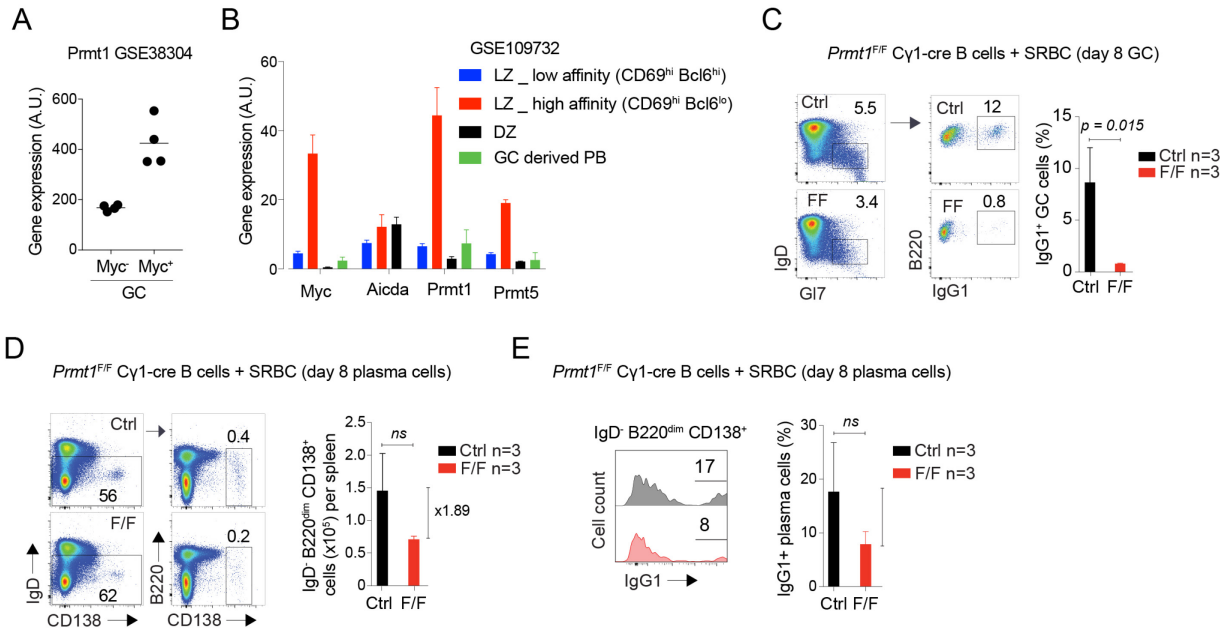


Figure 3.8 – Prmt1 limits B cell differentiation in vivo

A) Prmt1 gene expression in GC B cells stratified by c-Myc expression. Microarray data from (Dominguez-Sola et al., 2012).

B) Expression of the indicated genes in various GC B cell subsets, with LZ B cells classified by antibody affinity. RNA-seq data from (Ise et al., 2018). The group of Ise et al, sorted centrocytes based on CD69 and Bcl6 expression, followed by sequencing of their IgH variable region, revealing that CD69⁺ Bcl6^{high} cells expressed lower affinity IgH than CD69⁺ Bcl6^{low}.

Centrocytes were sorted based on

C) Representative flow cytometry plots showing the proportions of IgG1⁺ cells from GC (IgD⁻ GI7⁺) of splenocytes from Cγ1-cre (Ctrl) or Prmt1^{F/F} Cγ1-cre (F/F) mice immunized with SRBC for 8 days. Means + s.d. IgG1⁺ GC B cell proportions for 3 mice from one experiment are plotted.

D) Representative flow cytometry plots showing the proportion of plasma cells (IgD⁻B220^{dim}CD138⁺) from mice immunized as in C). Means + s.d. plasma cell numbers for 3 mice from one experiment are plotted.

E) Representative histograms showing the proportions of IgG1⁺ cells from plasma cells gated in D). Means + s.d. IgG1⁺ plasma cell proportions for 3 mice from one experiment are plotted.

P-values throughout are indicated for significant differences by unpaired, two-tailed Student-t test.

3.4 Discussion

We reveal critical functions for Prmt1 during the GC reaction. Previous work had analyzed mice in which resting mature B cells were deficient in Prmt1 (Hata et al., 2016; Infantino et al., 2017), showing that Prmt1-deficient B cells have activation defects, as we confirmed here. Because of this, the role of Prmt1 during the GC reaction was not clear, as B cells were compromised prior to GC formation. Using C γ 1-cre mice allowed us to address this point (Casola et al., 2006). Our data establishes roles for Prmt1 in maintaining the homeostasis and dynamics of the GC. We show that Prmt1 is necessary for affinity maturation, particularly for the antibody response against complex antigens, but even for simple antigens like NP at recall immunization. These underlying defects in GC dynamics can be explained at least in part by premature plasma cell differentiation.

We find that Prmt1 is dispensable for homeostasis of resting FO B cells, which had been suggested in *Prmt1^{F/F}* CD19-cre mice (Hata et al., 2016) and demonstrated in *Prmt1^{F/F}* CD23-cre mice (Infantino et al., 2017). We additionally find that *Prmt1^{F/F}* CD21-cre mice have reduced MZ B cell numbers, a defect that is B cell intrinsic as shown by BM chimeras. This defect may contribute to the reduced T-independent response seen in *Prmt1^{F/F}* CD19-cre and *Prmt1^{F/F}* CD23-cre mice (Hata et al., 2016; Infantino et al., 2017). *Prmt1^{F/F}* CD19-cre mice showed less MZ B cells (Hata et al., 2016), which could be a consequence of B cell development defects. Instead, *Prmt1^{F/F}* CD23-cre mice did not show a MZ B cell defect (Infantino et al., 2017). However, CD23-cre is not as efficient in MZ as in FO B cells (Kwon et al., 2008), while CD21 is highly expressed in MZ B cells, which can explain the different results. The differential requirement for Prmt1 in MZ versus FO B cells would be worth exploring. While we cannot discriminate at which stage of MZ formation or maintenance Prmt1 is most important, we speculate that it reflects an emerging role of Prmt1 in B cell differentiation processes (see below).

Discrepant results have been reported regarding the effect of ablating Prmt1 in B cells on T-dependent antibody responses using NP as a model antigen. A severe defect

was described in *Prmt1^{F/F}* CD23-cre mice (Infantino et al., 2017) while no defect was found in *Prmt1^{F/F}* CD19-cre (Hata et al., 2016). In both cases Prmt1 was absent in resting mature B cells. Since Prmt1 is required for B cell development (Dolezal et al., 2017) and CD19-cre is active from early B cell development but inefficient (Hobeika et al., 2006; Rickert et al., 1997), compensatory mechanism might have masked the defect in *Prmt1^{F/F}* CD19-cre mice. On the other hand, CD23-cre is active only in peripheral resting B cells (Kwon et al., 2008) and efficiently excised Prmt1 (Infantino et al., 2017). The large defect seen in the anti-NP response in *Prmt1^{F/F}* CD23-cre mice could be a combination of defects during B cell activation, which would compromise GC formation, as we find in *Prmt1^{F/F}* CD21-cre mice. To be able to bypass the function of Prmt1 during B cell activation and study its contribution to GC homeostasis, we used *Prmt1^{F/F}* C γ 1-cre mice in which GCs are normal 5 days after immunization. Since C γ 1-cre is active soon after B cell activation (Casola et al., 2006), we posit that the time it takes for Prmt1 and/or the relevant aDMA substrates to turn over, permits GC initiation. Indeed, at day 5 most aDMA was gone from *Prmt1^{F/F}* C γ 1-cre GCs, indicating that Prmt1-deficient GC B cells can migrate to the B cell follicle and proliferate to some extent but cannot sustain the GC reaction, which fails to expand. Despite this defect in GC, *Prmt1^{F/F}* C γ 1-cre mice could mount efficient IgG1 antibody titers against NP, which has little clonal diversity (Bannard and Cyster, 2017; Jacob et al., 1993), while the response against the carrier protein was severely reduced. However, while anti-NP antibodies achieved similar affinity to the control in the primary response, the secondary response was of lower affinity, revealing a defect. Moreover, the affinity of the anti-CGG antibodies was compromised in the primary and secondary responses. These results reveal another instance of GC biology that is regulated by Prmt1, strongly suggesting its implication in affinity maturation, especially for polyclonal antibody responses.

We reveal yet another function of Prmt1 in repressing plasma cell differentiation. Our results *ex vivo* differ from those reported for *Prmt1^{F/F}* CD23-cre B cells stimulated with LPS/IL-4, which showed reduced plasma cell differentiation (Infantino et al., 2017). Importantly, the discrepancy is not due to the system or excision timing, as we see

increased differentiation irrespective of whether Prmt1 is deleted prior or after activation (i.e. *Prmt1^{F/F}* C γ 1-cre and *Prmt1^{F/F}* CD21-cre). Moreover we confirmed our results in wt mouse B cells after pharmacological inhibition of Prmt1. The only difference we find between the assays is the magnitude of proliferation achieved post-stimulation, as measured by cell division dye, which was visibly higher in our system. CSR and plasma cell differentiation are linked to cell division (Hasbold et al., 2004; Hodgkin et al., 1996) and we verified an inverse correlation per cell division for these two processes in Prmt1-deficient B cells. It is possible that more robust proliferation, which allows scoring a larger number of cells per division, might allow us to reveal the phenotype. While this difference will need to be explained, our results are supported by multiple genetic and pharmacological approaches.

We propose that reduced isotype switching and reduced proliferation of Prmt1-deficient B cells are secondary to accrued differentiation. The normal isotype switching activity in Prmt1-depleted CH12F3 B cells and in *Prmt1^{F/F}* C γ 1-cre iGBs support this notion. Our data indicates that methylation of 53BP1 or Mre11 is not necessary for CSR, as suggested by the normal CSR in B cells from a mouse in which Mre11 lacked the Prmt1 target residues and could not be methylated (Yu et al., 2012). Yet, we cannot rule out that another PRMT might complement for Prmt1 deficiency in B cells for this function. In any case, several results suggest that enhanced plasma cell differentiation contributes at least in part to the defect in GC expansion in *Prmt1^{F/F}* C γ 1-cre mice. Firstly, a normal primary response against NP and compromised but readily detectable response against CGG, which was responsive to recall, indicate that ASC are generated. Secondly, the magnitude of the defect on anti-NP ASC is lower than on GC B cell numbers. Thirdly, a fraction of GC B cells in *Prmt1^{F/F}* C γ 1-cre mice acquire differentiation traits, such as lower Ki67 and AID expression. More conclusive, *Prmt1^{F/F}* C γ 1-cre mice showed a reduced proportion of IgG1⁺ GC and plasma cells *in vivo*, which is consistent with early exit of IgM B cells from the GC reaction before isotype switching. Finally, whilst we did not analyze memory B cells, the normalization of GC B cell numbers at recall immunization suggested that memory B cells had been generated, raising the

possibility that the anti-differentiation function of Prmt1 extends to this B cell compartment as well. Altogether, our results, both *in vitro* and *in vivo*, support the conclusion that Prmt1 negatively regulates plasma cell differentiation, as additionally suggested by the upregulation of *Prdm1* and *Irf4* in Prmt1-deficient and MS023-treated cells. In other systems, PRMT1 seems to have a context-dependent function in cellular differentiation processes. For instance, Prmt1 promotes differentiation of oligodendrocytes (Hashimoto et al., 2016) and muscle stem cells (Blanc and Richard, 2017) while it opposes differentiation of epidermal progenitor cells (Bao et al., 2017), megakaryocytes (Jin et al., 2018) or acute myeloid leukemia cells (Cheung et al., 2016). It is interesting that in the B cell lineage PRMT1 has both activities depending on the compartment. Thus, while Prmt1 ablation blocks the differentiation of pre-B cells in the bone marrow (Dolezal et al., 2017), we find that it promotes plasma cell differentiation of activated B cells in the periphery.

The loss of AID-intermediate LZ B cells and appearance of a Cxcr4⁻ CD86^{low} Ki67^{low} B population in GC *Prmt1^{F/F}* C γ 1-cre mice was also observed in Prmt5-deficient GC B cells, which also limits plasma cell differentiation (Litzler et al, in preparation). Thus, while our data shows that Prmt5 and Prmt1 synergize to limit differentiation by distinct mechanisms, the similar GC phenotypes may reflect a common defective stage. Accordingly, the highest expression of both *Prmts* coincides with *c-Myc* expression in the GC B cell subset that give rise to plasma cells (Ise et al., 2018). Taking together the defective GC expansion and altered cellular composition, compromised affinity maturation and enhanced differentiation, it is likely that Prmt1 functions during GC B cell selection and/or fate decision in the LZ. In line with this, the accrued plasma cell differentiation of Prmt1-deficient B cells was particularly enhanced by the presence of IL-4, a key cytokine provided by LZ Tfh cells for plasma cell differentiation (Weinstein et al., 2016). Prmt1 dampens pre-BCR and BCR signaling (Infantino et al., 2010; Infantino et al., 2017), and we see a defect in Prmt1-deficient B cells stimulated via CD40. CD40 stimulation and BCR signaling act synergistically for inducing *c-Myc* and driving positive selection in GC LZ B cells (Luo et al., 2018). Prmt1 may thus act as a sensor of CD40 signaling strength, with signaling imbalance promoting differentiation

instead of positive selection to sustain the GC reaction, in line with the reduced affinity maturation for polyclonal responses. Identifying the relevant targets mediating each of Prmt1 functions will not be trivial but is an exciting future perspective although the mechanism may involve multiple Prmt1 substrates.

3.5 Material and Methods

Mice

Prmt1^{ff} mice (Yu et al., 2009) were backcrossed to C57BL6/J background and bred with *C γ 1-cre* mice (Casola et al., 2006), a kind gift of Dr K Rajewsky (MDC, Germany), or *CD21-cre* mice (Kraus et al., 2004), obtained from Jackson labs (Bar Harbour, MN), at the IRCM. *Aicda-GFP* mice (Crouch et al., 2007) were a gift from Dr R Casellas (NCI Bethesda, MD). B cell-deficient μ MT mice (Kitamura et al., 1991) were obtained from Dr A Veillette (IRCM). *Cre⁺* mice were used as controls throughout the work. Mice were housed in a specific pathogens-free animal house. All work was reviewed and approved by the animal protection committee at the IRCM (protocols 2013-18 and 2017-08).

Immunization

Age- and sex-matched mice of 40-120 days of age were immunized either intraperitoneally with 50 μ g NP₁₈-CGG (Biosearch Technologies) in Imject Alum adjuvant (Thermo Scientific) or intravenous with 10⁹ sheep red blood cells in 200 μ L PBS (Innovative Research, IC100-0210). Recall immunizations were done ~18 weeks after the primary immunization with 50 μ g NP₁₈-CGG. Mice were bled and/or sacrificed at various time post-immunization to analyze antibody responses and lymphocyte populations.

BM chimeras

C57BL6/J females were irradiated with 9 Gy and transplanted with a 1:1 mixture of BM cells purified from 50 μ MT and either *CD21-cre* (Control) or *Prmt1^{F/F}* *CD21-cre*.

Mice were bled 4 weeks post-transplantation to confirm reconstitution and chimerism. Mice were immunized with 100 µg NP₁₈-CGG in Imject Alum adjuvant 6 weeks after transplantation and analyzed 10 days later.

Flow cytometry

Mononuclear cells from mouse spleen were obtained by mashing through a 40 µm cell strainer with a syringe plunger. Cells suspensions were washed in PBS and resuspended in 1mL of red blood cell lysis (155 mM NH₄Cl, 10mM KHCO₃, 0.1mM EDTA) for 5 min at room temperature before filtering using a 40 µm nylon cell strainer. After washing, cells were resuspended in PBS 1% BSA and stained with combinations of antibodies listed in **Supplementary table 1** for analysis of different lymphocyte populations. Data was acquired using BD LSR Fortessa (BD biosciences) or BD FACSibur (BD biosciences) and analyzed using FlowJo. For sorting, cells were stained as above and passed through a BD FACSARIA III (BD biosciences).

Cell proliferation

Growth curves of primary B cells, cell concentrations were calculated using 123count eBeads (Invitrogen) according to manufacturer's instructions: 200 µL of cells were mixed with 20 µL of beads and 5 µL propidium iodide (20 µg/mL). 1000 beads were acquired at the FACScalibur for accurate counting. To assess proliferation *in vivo*, 3 x 10⁶ splenocytes were first surface-stained for GC markers and then treated with fixation/permeabilization solution (eBioscience, cat# 00-5523) for 1 h at 4°C in the dark, washed twice in Perm buffer (eBioscience), followed by 1 h incubation with anti-Ki67-PECY7 (eBioscience) at 4°C and resuspended in PBS+1% BSA. When necessary, anti-biotin staining was performed following Ki67 staining. Primary B cells in culture were stained with 1 µM CFSE (Invitrogen) on the day of plating, as described in the manufacturer's protocol, and stimulated with cytokines. CH12 cells were stained with 5 µM CFSE (Invitrogen) 4 days post-infection (2 days post puro selection), as described in the manufacturer's protocol and stimulated with CIT [1 µg/mL rat-antiCD40 (clone 1C10, eBioscience), 10 ng/mL interleukin IL-4 and 1

ng/mL transforming growth factor- β 1 (R&D Systems)] in the presence of 1 μ g/mL puromycin.

Apoptosis and cell cycle

To evaluate apoptosis *in vivo*, cells were treated with the FITC conjugated CaspGLOW reagent that detects activated pan-caspases (BioVision, K180) according to the manufacturer's instructions with minor alterations. Briefly, 10^6 cells were treated with 2 μ L of FITC-VAD-FMK antibody for 1 h at 37°C in 300 μ L warm media, washed according to the manufacturer's instructions, then surface stained and assessed immediately via flow cytometry. To assess apoptosis *ex vivo* $0.3-0.5 \times 10^6$ cells were stained with 3 μ L Annexin V-FITC (cat #51-66121E, BD Pharmigen) in 100 μ L of the provided Binding buffer (x1) for 15 min at RT. Then 400 μ L of Binding buffer (x1) and 5 μ L of propidium iodide (20 μ g/mL) were added prior to flow cytometry acquisition. For cell cycle analysis, B cells were incubated with 10 μ M BrdU for 1 h at 37°C in complete RPMI medium, then washed and resuspended in 200 μ L cold PBS before fixing by adding the cells to pre-chilled 70% ethanol drop-wise under constant agitation and incubated on ice for 30 min. Then, 2N HCl 0.5% Triton X-100 was added to the loosen cell pellet to denature the DNA, washed, resuspended in 0.1M $\text{Na}_2\text{B}_4\text{O}_7$, washed again and resuspended in PBS 0.5% Tween-20 1% BSA. 10^6 cells were then stained with anti-BrdU-FITC (1/50) for 30 min at RT in the dark before resuspending in PBS containing 5 μ g/mL propidium iodide. Cells were analyzed by flow cytometry as above.

Cell culture

Naïve primary B cells were purified from splenocytes by depleting CD43⁺ cells using anti-CD43 microbeads (Miltenyi, cat# 130-049-801) and an autoMACS (Miltenyi). Primary B cells were cultured at 37°C with 5% (vol vol⁻¹) CO₂ in RPMI 160 media (Wisent), supplemented with 10% fetal bovine serum (Wisent), 1% penicillin/streptomycin (Wisent), 0.1 mM 2-mercaptoethanol (bioshop), 10 mM HEPES, 1 mM sodium pyruvate. Resting B cells were stimulated either with lipopolysaccharide (LPS) (5 μ g/mL, Sigma) + IL-4 (5 ng/mL, PeproTech), LPS (25

µg/mL), or anti-CD40 (10 µg/mL, clone 1C10, eBioscience) + IL-4 (10 ng/mL, R&D Systems) + IL-5 (5 ng/mL, R&D Systems). Induced germinal center B cells (iGBs) were generated using 40LB feeder cells (a kind gift from Dr Daisuke Kitamura) (Nojima et al., 2011). Briefly, one day before B cell plating, 40LB cells were irradiated (120 Gy) and plated at 0.3×10^6 cells per well in 2 mL (6-well plate) or 0.13×10^6 cells per well (24-well plate) in 0.5 mL DMEM media supplemented with 10% fetal bovine serum (Wisent) and 1% penicillin/streptomycin (Wisent). Purified naïve B cells were plated on 40LB feeders at 10^5 cells per well in 4 mL of B cell media (6-well plate), or 2×10^4 cells per well in 1 mL of B cell media (24-well plate), supplemented with 1 ng/mL IL-4. At day 3 post-plating, the same volume of fresh B cell media was added to the wells, supplemented with either 1 ng/mL IL-4 or 10 ng/mL IL-21 (PeproTech). On subsequent days, half of the volume per well was removed and replaced with fresh B cell media supplemented with cytokines. When re-plated, cells were harvested from the primary culture on day 4 and plated on fresh 40LB feeders in media supplemented with either 1 ng/mL IL-4 or 10 ng/mL IL-21. Re-plated cells were not fed and analyzed 3 days later.

The CH12F3 mouse B cell lymphoma cell line (Nakamura et al., 1996) (a kind gift from Dr T Honjo, Kyoto University, Japan) was cultured at 37°C with 5% (vol vol⁻¹) CO₂ in RPMI 160 media (Wisent), supplemented with 10% fetal bovine serum (Wisent), 5% NCTC 109 (Sigma), 1% penicillin/streptomycin (Wisent), 0.1 mM 2-mercaptoethanol (bioshop). Prmt1 depletion was achieved by retroviral transduction of shRNAs cloned in pLKO.1 (Sigma), #1: TRCN000018491 (CCGGGCTGAGGACATGACATCCAAACTCGAGTTTGGATGTCATGTCCTCAGCTTTT), #2: TRCN000018493 (CCGGGCAAGTGAAGAGGAACGACTACTCGAGTAGTCGTTTCTTCACTTGCTTTT). Briefly, VSV-G, PAX2 and pLKO vectors (at 1:2.5:3.25 ratio, 1.35 µg DNA total) were transfected into HEK293 cells using Trans-IT LT-1 (Mirus Bio, Cat.# MIR 2305). Two days post-transfection, 1 mL of HEK293 supernatant was added to 24-well plates coated already with Retronectin (Takara) according to manufacturer's protocol and spun at $2000 \times g$ for 90 min at 32 °C. After removing the virus, 10^5 CH12F3 cells

were added per well in 1mL and spun at 600 × g for 30 min at 32 °C. The next day, 1mL of fresh media was added and one day 1 µg/mL puromycin was added for selection.

Inhibitors

Prmt1 inhibitor MS023 (cayman chemical, cat#18361) and Prmt5 inhibitor EPZ015666 (cayman chemical, cat#17285) were resuspended at 50 mM in DMSO and aliquoted for long-term storage at -80°C. Working dilutions in DMSO were kept at -20°C and thawed up to 3 times for experiments. DMSO represented at most 1/1000 of the media.

Immunohistochemistry

Section of 5-µm of paraffin-embedded tissues were deparaffinized in two changes of xylene for 5 min each and then rehydrated in distilled water using graded alcohols. Antigen retrieval was done by steaming the slides for 20 min then cooling for 20 min in EDTA buffer (1mM EDTA, 0.05% Tween 20, pH 8) for AID and PRMT1. Endogenous peroxidase was blocked with a 0.3% hydrogen peroxide solution for 10 min. Endogenous biotin was blocked for 15 min with the blocking buffer provided with the Avidin/Biotin System (#SP2001, Vector Laboratories; Burlingame, CA). For protein block, we used 10% normal goat serum and 1% BSA for 60 min at room temperature. Sections were incubated with anti-AID (1:50, rat Mab mAID-2 eBioscience), anti-PRMT1 (1:100) overnight at 4°C. Biotin-conjugated secondary antibodies were mouse anti-rabbit IgG (1:200, Vector laboratories) to detect anti-PRMT1; mouse anti-rat IgG (1:200, Vector laboratories) to detect anti-AID. Biotinylated reagents were detected with Vectastain ABC kit (PK-6100, Vector laboratories). Peroxidase activity was developed using ImmPACT NovaRED HRP substrate (Vector laboratories). Sections were counterstained with hematoxylin (Sigma cat #MHS32-1L) for 1 min prior to dehydrating and mounting for imaging on a bright field microscope.

Immunofluorescence

For tissue IF, tissues were frozen in OCT (VWR #95057-838). Sections of 10 μ m were fixed in PFA 4% for 10 min at RT, washed 3 times in PBS at RT, followed by an incubation in pre-chilled acetone for 10 min at -20°C. Sections were permeabilized in 0.5% Triton X-100 in PBS for 10 min at RT, blocked in PBS 5% goat serum 1% BSA 0.3% Triton X-100 for 1 h at RT. Incubations with primary antibodies were performed in blocking solution overnight at 4°C in a humid chamber. When needed, secondary antibody was added in blocking solution for 1 h at RT in a humid chamber in the dark. Purified B cells were washed with PBS and then plated on coverslips coated with 0.1 mg/mL poly-L-lysine (Sigma). For single cell IF, cells were centrifuged 5 min at 400 x g, then allowed to adhere at 37°C for 20 min, before fixation with 3.7% formaldehyde (Sigma) for 10 min at RT. After 3 washes with PBS, coverslips were blocked for 1 h with blocking solution (5% goat serum, 1 % BSA, 0.5% Triton X-100 in PBS). Cells were then incubated overnight at 4°C with anti-aDMA ASYM26 antibody (1:500), diluted in blocking solution. After 3 x 5 min washes, with PBS + 0.1% Triton X-100 (PBS-T), cells were incubated for 1 hr at room temperature with anti-Rabbit IgG Alexa-546 (1:500) diluted in blocking solution. After 3 x 5 min washes with PBS-T, cells were incubated with 300 nM Dapi (ThermoFisher) in PBS for 5 min at room temperature. Finally, coverslips were washed with PBS followed by ddH₂O before mounting onto slides using Lerner Aqua-Mount (ThermoFisher) before imaging. Antibodies are listed in **Supplementary table 1**.

Microscopy

Images were acquired at RT using a Leica DM6 upright microscope (tissues), or a Zeiss LSM700 confocal microscope (tissues and single cells). For the LSM700, excitation lasers were 405 nM (Dapi and BV-421), 488 nM (Fitc and Alexa488), 543 nM (R-PE and Alexa546), and 633 nM (Alex-680), with either 40x/1.3 or 63x/1.4 oil immersion objectives and collected using a Hamamatsu PMT. Quantifications were done using Volocity (Perkin Elmer). For each experiment, multiple fields were analyzed, excluding cells with saturated signal, abnormal DNA structure or mitotic figures. To make figures, images were transferred to Photoshop for cropping and adjusting contrast throughout the whole image when necessary to enhance visibility.

ELISPOT

Purified splenocytes or BM cells were added at different dilutions to a 96-well 0.45 μm PVDF membrane (Millipore, cat#MSIPS4W10) previously coated overnight at 4°C with 2 $\mu\text{g}/\text{mL}$ NP₂₀BSA and blocked with complete RPMI cell culture media for 2 h at 37°C. Plates with cells were incubated in a humid chamber 12 h at 37°C, 5% CO₂, then washed 6 x with PBS 0.01% Tween-20, followed by incubation with goat anti-mouse IgG1-HRP (A10551, Life Technologies, 1/2000) diluted in culture media for 2 h at RT. Plates were washed and AEC substrate (3' amino-9-ethylcarbazole ; BD Bioscience) was added to reveal the spots. Images were acquired in an Axiophot MZ12 microscope and scored spots were counted from appropriate cell dilutions (2 x 10⁶ cells after primary immunization and 0.5 x 10⁶ cells for recall).

ELISAS

Sandwich ELISA for measuring pre-immune sera antibodies using anti-isotype-specific antibodies (BD Pharmingen) to capture IgM, IgG1, IgG2b or IgG3 were done as described (Zahn et al., 2013). Antigen-specific antibodies were captured from immunized mice sera by coating ELISA plates with NP₂₀-BSA (Biosearch Technologies) or CGG (100 ng/well) (Biosearch Technologies) followed by the detection of IgG1, as described (Zahn et al., 2013). Sodium thiocyanate NaSCN displacement ELISA to measure antibody affinity / avidity was performed as described (Zahn et al., 2013) on plates coated as above. Sera were previously titrated by antigen-specific ELISA to choose a working dilution that ensured similar levels of antigen-specific antibodies across samples. Relative affinity values (RAV) were calculated as described (Zahn et al., 2013).

Western blots

For protein extracts, cells were lysed in NP-40 lysis buffer (1% NP-40, 20mM Tris pH 8, 137mM NaCl, 10% glycerol, 2mM EDTA), containing protease and phosphatase inhibitor (Thermo Scientific). Extracts separated by SDS-PAGE were transferred to nitrocellulose membranes (BIO-RAD) by western blotting. Membranes were blocked in TBS 5% milk and probed with primary antibodies overnight, washed 4 x 5 min in

TBS 0.1% Tween-20 before incubating with secondary antibodies conjugated to AlexaFluor680 or IRDye800 for 1 h, washed and read on Odyssey CLx imaging system (LI-COR). Proteins were quantified using ImageStudiolite software. In some experiments, equal protein loading was controlled for by staining the membrane after transfer using REVERT total protein stain solution (LI-COR) before probing and the Revert signal from a whole lane was used for normalization. Antibodies used for WB are listed in **Supplementary table 1**.

RT-qPCR

RNA isolated using TRIzol (Life Technologies) was reverse transcribed with ProtoScript™ M-MuLV Taq RT-PCR kit (New England Biolabs). Quantitative PCR using SYBR select master mix (Applied Biosystems) was performed and analyzed in a ViiATM 7 machine and software (Life technologies). Oligos used are listed in **Supplementary table 2**

RNA sequencing data

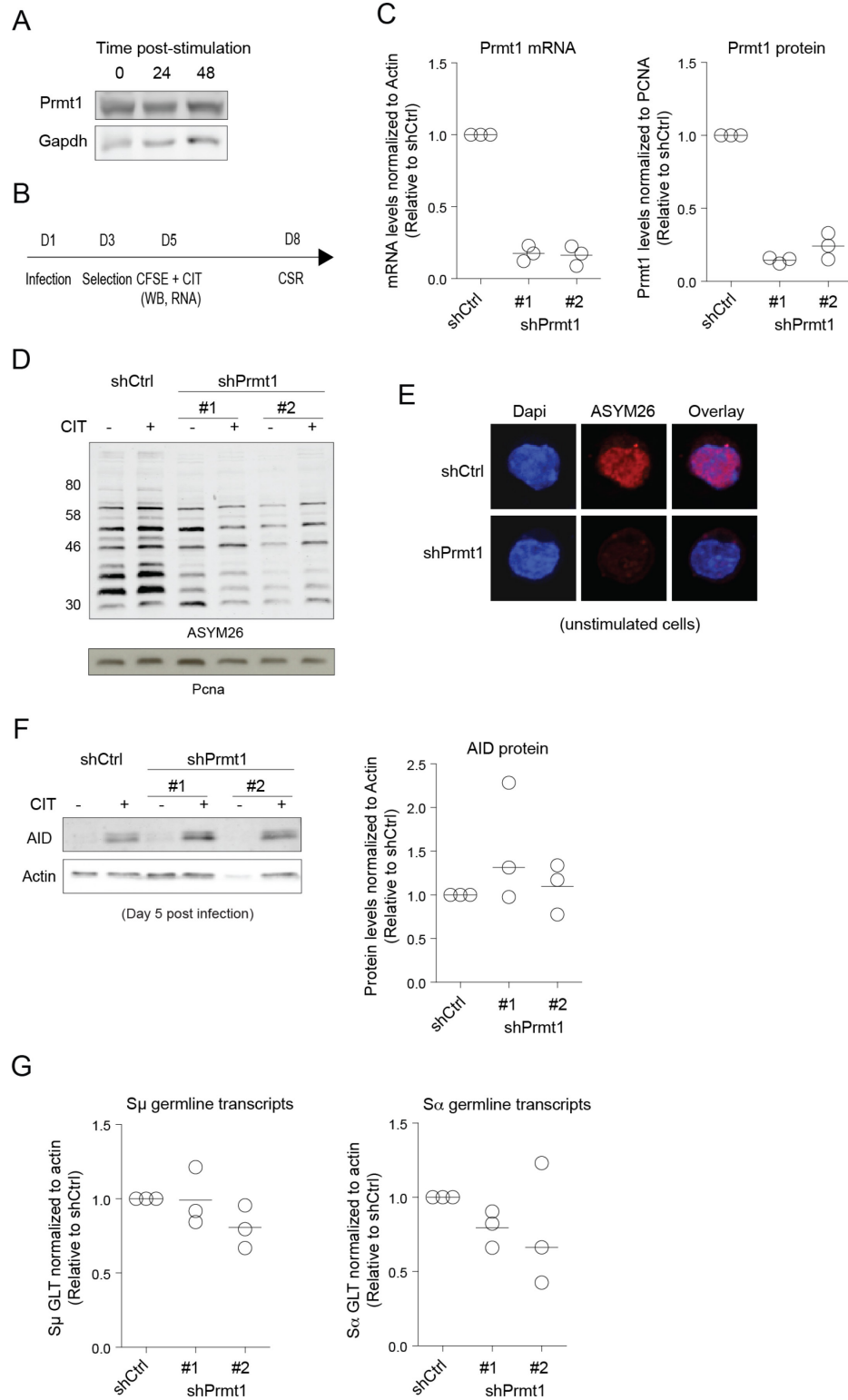
Data was obtained from previously available B cell stages samples obtained by sorting. Sample processing, preparation and paired end sequencing have been described (Kuchen et al., 2010). Additional data for activated B cell and GC B cell were sequenced as single end with 50bp read length. Reads were aligned to the mouse genome (mm9) with gsnap without detecting splice junctions *de novo* (`--novelsplicing=0`). Existing splice junctions from RefSeq annotation were taken into account (`--use-splicing=/path/to/mm9.splices.iit`). Output files were filtered to remove unaligned reads and any alignments with a mapping quality less than 20. Reads were mapped to RefSeq genes with `htseq-count -m intersection-nonempty` and rpk value were calculated from the counts. Density bed files were generated by using `bedtools genomecov` program with a normalizing scale factor to calculate rpm and converted into bigwig files by using ucsc toolkit `bedGraphToBigWig`. Data is available under accession number GSE112420.

3.6 Acknowledgments

We thank Dr Daisuke Kitamura for 40LB cells. Dr Tarik Möröy for qPCR primers, and Dr Rafael Casellas for RNA-seq data. We thank Dr Irah King and Alexandre Melli for critical reading of the manuscript. We thank the technical assistance of Eve-Lyne Thivierge, Manon Laprise, Marie Claude Lavallée and Sara Demontigny with animal work, Eric Massicote and Julie Lord with flow cytometry, Simone Terouz with immunohistochemistry, Dominic Filion with microscopy imaging, Gustavo Gutierrez for sequencing assistance. RNA-seq analysis used the high-performance computational capabilities of NIH Helix Systems (<http://helix.nih.gov>). This work was supported by operating grants from the Cancer Research Society and Bergeron-Jetté Foundation and the Canadian Institutes of Health Research (MOP-125991) to J.M.D.N.

S.P.M. was a recipient of a doctoral fellowship from FRQ-S and L.C.L. of a Cole foundation doctoral fellowship. J.M.D.N was partially supported by the Canada Research Chair in Genetic Diversity.

3.7 Supplemental material



Supplementary Figure 3.1 – Prmt1 depletion in CH12F3 B cells

A) WB for Prmt1 and Gapdh as loading control in CH12F3 B cells at various times of stimulation with CIT (1 ng/mL TGF β , 10 ng/mL interleukin IL-4 and 1 μ g/mL antiCD40).

B) Schematics of the experiment.

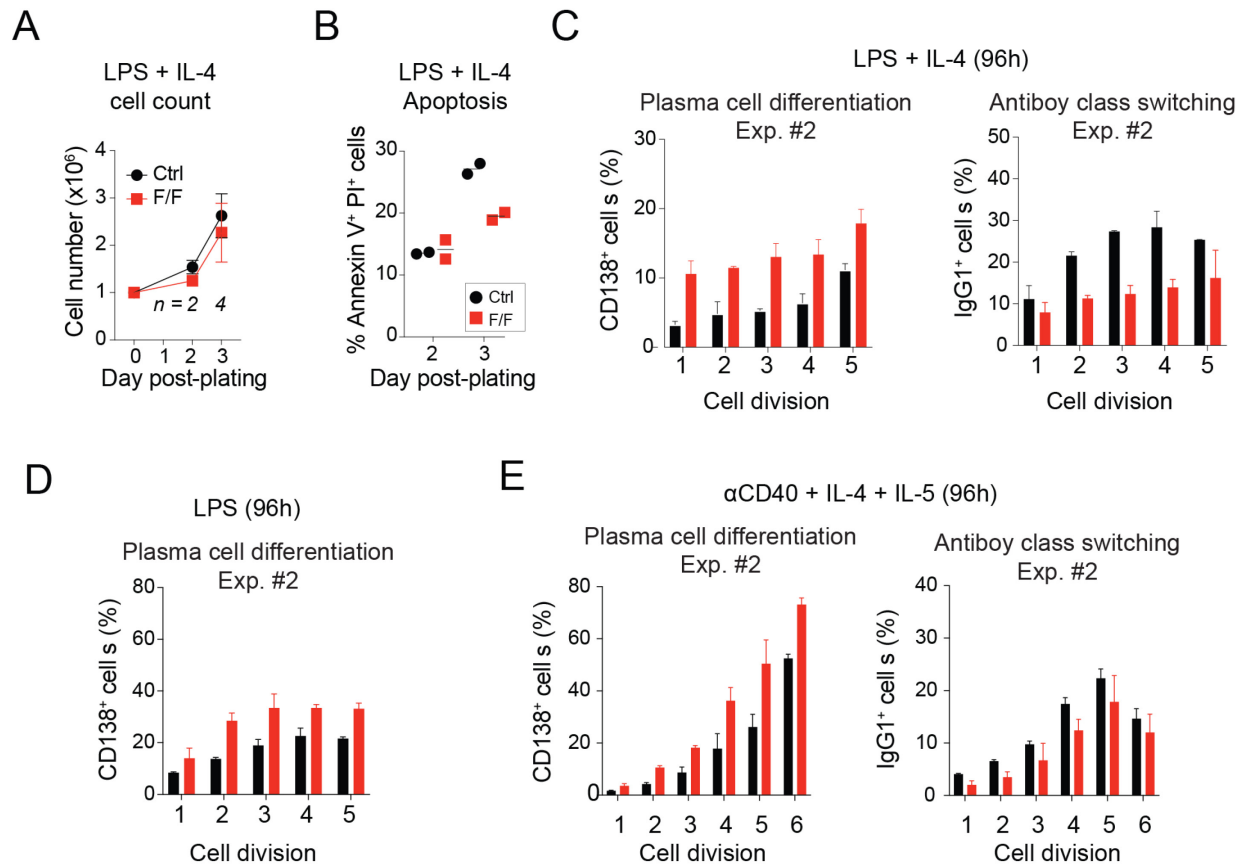
C) Prmt1 mRNA levels measured by RT-qPCR and of Prmt1 protein levels from WB quantified by densitometry in CH12F3 cells expressing shRNA control (shCtrl) or against Prmt1 (#1 and #2). Values are normalized to the control for 3 independent experiments.

D) Effect of Prmt1 depletion on aDMA (ASYM26) in CH12F3 cells expressing the indicated shRNAs as in C) and stimulated or not with CIT.

E) Representative confocal pictures of CH12F3 cells expressing the indicated shRNAs and probed by IF with anti aDMA antibody ASYM26 and DAPI to stain the nucleus.

F) Expression of AID measured by WB, in CH12F3 cells expressing the indicated shRNAs and activated or not with CIT. Actin is loading control. A plot with AID levels quantified for 3 independent experiments is shown.

G) Germline transcripts at the S μ and S α regions of CH12F3 cells expressing the indicated shRNAs, measured by RT-qPCR, normalized to actin transcript levels and plotted relative to CH12F3 cells expressing control shRNA.



Supplementary Figure 3.2 – Plasma cell differentiation ex vivo

A) Naïve CD21-cre (Ctrl) and Prmt1^{F/F} CD21-cre (F/F) B cells were activated with LPS (5 µg/mL) and IL-4 (5 ng/mL) and counted at various times. Means ± s.e.m data from *n* mice per genotype from a representative experiment.

B) Proportion of Annexin-V⁺ CD21-cre (Ctrl) and Prmt1^{F/F} CD21-cre (F/F) B cells at days 2 and 3 after activation with LPS and IL-4 for 2 mice from one experiment.

C) Means ± s.e.m proportion of CD138⁺ or IgG1⁺ cells per cell division identified from CFSE peaks from a second experiment on naïve CD21-cre (Ctrl) and Prmt1^{F/F} CD21-cre (F/F) B cells activated with LPS (5 µg/mL) and IL-4 (5 ng/mL).

D) Means + s.e.m proportion of CD138⁺ cells per cell division identified from CFSE peaks from a second experiment on naïve CD21-cre (Ctrl) and Prmt1^{F/F} CD21-cre (F/F) B cells at 96 h, activated with LPS (25 µg/mL).

E) Means + s.e.m proportion of CD138⁺ or IgG1⁺ cells per cell division identified from CFSE peaks from a second experiment on naïve CD21-cre (Ctrl) and Prmt1^{F/F} CD21-cre (F/F) B cells at 96 h, activated with anti-CD40 (10 µg/mL), IL-4 (10 ng/mL) and IL-5 (5 ng/mL).

Supplementary Table 3.1 - Antibodies

Antibodies for flow cytometry

Anti-	TAG	CATALOGUE	CLONE	VENDOR
CD45R (B220)	APC	553092	RA3-6B2	BD Pharmingen
CD45R (B220)	PercP-Cy5.5	552771	RA3-6B2	BD Pharmingen
CD45R (B220)	Alexa Fluor 700	103232	RA3-6B2	BioLegend
CD3e	PE	553063	145-2C11	BD Pharmingen
CD3e	biotin	553239	500-A2	BD Pharmingen
CD4	biotin	553045	RM4-5	BD Pharmingen
IgD	biotin	13-5993-81	11-26c	eBioscience
GL7	BV421	562967	GL7	BD Pharmingen
Fas (CD95)	FITC	554257	Jo2	BD Pharmingen
Fas (CD95)	BV421	562633	Jo2	BD Pharmingen
CXCR4 (CD184)	PE	12-9991	2B11	eBioscience
CD86	biotin	13-0862	GL1	eBioscience
Streptavidin	BV605	405229	-	BioLegend
IgD	FITC	553439	11-26c.2a	BD Pharmingen
IgM	BV421	562595	R6-60.2	BD Pharmingen
CD21/CD35	APC	558658	7G6	BD Pharmingen
CD23	PE-Cy7	562825	B3B4	BD Pharmingen
CD138	APC	561705	281-2	BD Pharmingen
CD138	BV605	563147	281-2	BD Pharmingen
Ki67	PE-Cy7	25-5698-82	SolA15	eBioscience
IgG1	PE	550083	A85-1	BD Pharmingen
IgG1	biotin	553441	A85-1	BD Pharmingen
BrdU	FITC	347583	B44	BD Pharmingen
Annexin-V	APC	550474	-	BD Pharmingen
VAD-FMK	FITC	K180	-	BioVision
IgA	PE	12-5994-81	11-44-2	eBioscience

Antibodies for immunohistochemistry

Anti-	TAG	CATALOGUE	CLONE	VENDOR
PRMT1	-	Ab3768	-	Abcam
AID	-	14-5959-82	mAID-2	eBioscience
Rabbit-IgG	biotin			Vector
Rat-IgG	biotin			Vector

Antibodies for immunofluorescence

Anti-	TAG	CATALOGUE	CLONE	VENDOR
GL7	BV421	562967	GL7	BD Pharmingen
IgD	FITC	553439	11-26c.2a	BD Pharmingen
ASYM26	-	13-0011		EpiCypher
Rabbit IgG	Alexa 546	A11010		Invitrogen

Antibodies for Western blots

Anti-	TAG	CATLOGUE	CLONE	VENDOR
PRMT1	-	MABE431		Millipore
ASYM26	-	13-0011		EpiCypher
Rabbit IgG	AlexaFluor 680	A10043		Invitrogen
Rat IgG	AlexaFluor 680	A21096		Invitrogen
Rabbit IgG	IRDye800	925-32211		LI-COR
Actin	-	A2066		Sigma

Supplementary Table 3.2 - Primers

Primers for RT-qPCR

Gene	Type	Sequences	Product size (bp)	Lab name	Reference
<i>Prmt1</i>	Forward	TTGGGATTGAGTGTCCAGT	90	OJ 867	-
	Reverse	TGCCCTTGATGATGGTCACC		OJ 868	
<i>Actin</i>	Forward	CTCTGGCTCCTAGCACCATGAAGA	200	OJ 897	-
	Reverse	GTAAAACGCAGCTCAGTAACAGTCCG		OJ 898	
<i>Bcl6</i>	Forward	CACACCCGTCCATCATTGAA	-	-	Nurieva, R. I., et al. (2008)
	Reverse	TGTCCTCACGGTGCCTTTTT		-	
<i>Aicda</i>	Forward	GCCACCTTCGCAACAAGTCT	137	OJ 844	-
	Reverse	CCGGGCACAGTCATAGCAC		OJ 845	
<i>Prdm1</i>	Forward	GGAGGATCTGACCCGAAT	-	-	Todd, D. J., et al. (2009)
	Reverse	TCCTCAAGACGGTCTGCA		-	
<i>Irf4</i>	Forward	CTCTTCAAGGCTTGGGCATT	-	-	Todd, D. J., et al. (2009)
	Reverse	TGCTCCTTTTTTGGCTCCCT		-	
<i>Rpl35a</i>	Forward	CGTGCCAAATTCCGAAGCAA	70	OJ 1074	-
	Reverse	ATGGGTACAGCATCACACGG		OJ 1075	
<i>Igh</i>	Forward	AGCTCACACCTTGACCTTTCA	-	OJ 1621	Minnich, M., et al. (2016)
	Reverse	TGGTGGGACGAACACATTTA		OJ 1622	

4 Chapter IV: DISCUSSION

Humoral immunity relies on B cell fitness that depends on complex mechanisms involving a large number of factors and signalling pathways along B cell life, which is essential for adaptive immunity. Arginine methylation is emerging as an important PTM in B cell biology. During my thesis we investigated the effects of depleting the two main PRMTs expressed in B cells: PRMT1 and PRMT5 at different stages of B cell development. Our results show that PRMT1 and/or PRMT5 regulate B cell proliferation, survival and differentiation at different stages of B cell life, through different mechanisms. Some of these results are in agreement with recent publications (Hata et al., 2016; Infantino et al., 2017), but most observations are novel and others differ from previous results (Hata et al., 2016; Infantino et al., 2017), as I discussed in Chapter III and I will further discuss below. Interestingly, despite the fact that they deposit different marks, depleting either PRMT1 or PRMT5 results in similar phenotypes. For instance, both PRMTs promote B cell development in the BM, GC expansion in the periphery, and limit plasma cell differentiation in the periphery. Moreover, in mature B cells, both Prmt proteins are upregulated upon activation *in vitro* (**Fig. 2.1B, 3.1B**) and *in vivo* (**Fig. 2.1G, 3.1D**). In addition, they are both induced in the same GC compartments (c-Myc⁺ cells) at the mRNA level (**Fig. 2.9D, 3.8A**). On the other hand, I also found that Prmt1 and Prmt5 have different roles regarding MZ B cells homeostasis and the antibody response. In the next section, I am going to recapitulate the importance of either PRMT at every B cell stage studied, highlighting similarities and differences.

4.1 Expression of Prmts and their substrates

Prmt1 and *Prmt5* are both induced in BM B cells during development and in *in vitro* activated B cells. Interestingly, *Prmt1* and *Prmt5* mRNA levels in GCs are comparable to resting B cells (**Fig 2.1A, 3.1A**), even though both proteins are highly induced in GCs. This suggests that post-transcriptional regulation of both genes may occur in GCs, possibly through mi-RNA expression, as has been described for *Prmt5* in B cell lymphomas (Alinari et al., 2015b; Pal et al., 2007; Wang et al., 2008). Such regulation

allows rapid protein expression when needed, suggesting that Prmts have to be quickly expressed upon B cell activation. Nonetheless, RNAseq data from c-Myc⁺ and c-Myc⁻ GC B cells (Dominguez-Sola et al., 2012), positively selected centrocytes (Ersching et al., 2017), and high affinity CD69⁺ LZ (Ise et al., 2018) as well as our immunofluorescences for Prmt5, suggest that Prmt1 and Prmt5 are preferentially expressed in the positively selected centrocytes of the LZ (**Fig. 2.9A-D, 2.S5D, 3.8A,B**). This polarized expression of Prmts is consistent with a role in GC dynamics that will be discussed further. Of note, Prmt1 and Prmt5 are the most expressed in high affinity centrocytes among the other Prmts (**Fig. 4.1**) (Ise et al., 2018).

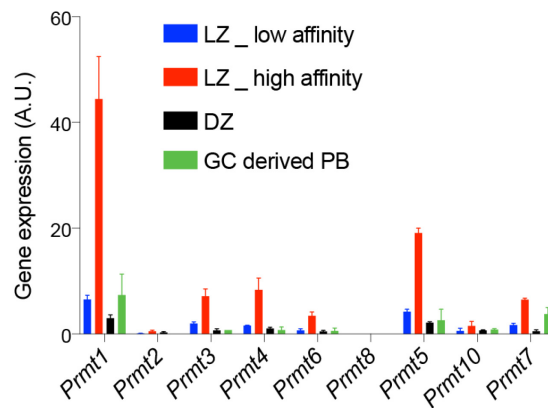


Figure 4.1 - Prmts expression in GC B cell subsets

Prmts transcripts levels obtained from RNA seq data generated by (Ise et al., 2018). Centrocytes were sorted based on CD69 and *Bcl6* expression (LZ_low affinity: CD69⁺ *Bcl6*^{high}, LZ_high affinity: CD69⁺ *Bcl6*^{low}). LZ: light zone, DZ: dark zone, PB: plasmablast.

It is possible that Prmt expression varies throughout the course of the GC response. The output of the GC changes with time from memory B cells early on to plasma cells later (Weisel et al., 2016). We could imagine for instance that Prmt1 is induced early during the GC reaction, to limit premature plasma cell differentiation. We would need to perform GC kinetics and evaluate Prmt1 and Prmt5 mRNA as well as protein levels to investigate this point. Prmt regulation may also vary depending on the B cell stimuli. Indeed, Prmt1 regulation seems to be different depending on the type of

activation, as RNAseq indicated that Prmt1 was the main type I PRMT induced upon LPS + IL-4 (**Fig. 3.1B**), while Prmt1, Prmt3, Carm1 and Prmt6 were induced to the same extent, but much less than Prmt5, after CD40 activation (**Fig. 2.S2A**). It would be interesting to evaluate the contribution of every Prmt to the methylated-protein pool in B cells upon different stimuli. *Prmt1*^{-/-} iGBs, stimulated via CD40, show a milder growth defect than *Prmt5*^{-/-} iGBs (**Fig. 2.3J, 3.5A**). This is in accordance with the few changes in methylation that are observed upon CD40 stimulation in *Prmt1*^{-/-} compared to wt B cells (Infantino et al., 2017). More experiments need to be performed to understand the relevance of each enzyme downstream of various B cell stimuli.

Immunofluorescence images for sDMA and aDMA marks in activated B cells at day 3 showed high levels of both methylation types in the nucleus (**Fig. 2.S2D, 3.5B**). Methylated histones, which are very abundant in the nucleus, are the most likely nuclear signal for the SYM11 and ASYM26 antibodies at this time. Interestingly, Prmt1 is largely nuclear in GC B cells while Prmt5 is mostly cytoplasmic. At later times in culture, on day 6, we detected sDMA and aDMA signals in the cytoplasm as well, suggesting that arginine methylation is a dynamic process that changes during the B cell reaction. Thus it will be important to consider timing and stimulation conditions when pursuing Prmt methylation targets by mass spectrometry.

4.2 Roles of Prmt1 and Prmt5 along the B cell lifespan

4.2.1 BM development

PRMT1 plays important roles in BM B cell development at multiple stages (**Fig. 1.10**). First Prmt1 was found to be required for pro-B cells via an unknown mechanism (Dolezal et al., 2017). Second, Prmt1 methylation of Cdk4 is required for large pre-B cell exit of the cell cycle so that they develop into small resting pre-B cells (Dolezal et al., 2017). Third, Prmt1 is necessary for pre-B cell development into immature B cells *in vitro*, via direct methylation of the BCR (Infantino et al., 2010).

We uncovered that PRMT5 is required for at least two stages of BM B cell development. First, we believe that PRMT5 is required for the survival of pro-B cells. In *Prmt5^{F/F}* Mb1-cre mice, *Prmt5* depletion resulted in loss of B cells from fraction B (**Fig. 2.7B**). Crossing *Prmt5^{F/F}* Mb1-cre mice with mice bearing a pre-arranged IgVH (B1-8 mice) did not rescue this BM development block, suggesting that the defect did not originate from a defect in D-J rearrangement (**Fig. 2.7C**). On the other hand, crossing *Prmt5^{F/F}* Mb1-cre mice with *Trp53^{-/-}* mice rescued pro-B cells (**Fig. 2.7D**). As p53 is responsible for pro-B cell death (Guidos et al., 1996; Lu and Osmond, 2000), the most likely explanation is that *Prmt5* is involved in repressing the pro-apoptotic activity of p53, as has been shown in other cell types (Bezzi et al., 2013). However, *Prmt5*-deficient mature activated B cells also show a p53 response, but this is not the cause of apoptosis (**Fig. 2.6C**). To confirm that *Prmt5* promotes pro-B cell survival by preventing apoptosis, we should check the levels of apoptosis in fraction B in *Prmt5^{F/F}* Mb1-cre compared to Mb1-cre mice.

We also found that PRMT5 is required in pre-B cells. Indeed, *Prmt5^{F/F}* Mb1-cre *Trp53^{-/-}* mice presented an additional block at the pre-B cell stage, as they showed a clear B cells loss in fraction D. Analysis of Ig μ expression on B220⁺ CD43⁻ (early B cells) showed that *Prmt5^{F/F}* Mb1-cre *Trp53^{-/-}* mice were depleted for cells expressing the pre-B cell receptor (**Fig. 2.7E**). Many possibilities could lead to such a phenotype. It is possible that *Prmt5*, like *Prmt1*, is involved in pre-BCR signalling, which is required to overcome the pre-BCR checkpoint. *Prmt5* has been shown to induce expression of certain receptors during hematopoiesis (Liu et al., 2015b). By contrast we have found that *Prmt5^{-/-}* mature activated B cells (iGBs) had increased expression of genes involved in cytokine-receptor interaction, notably a 3-fold increase in IL7R expression (**Fig. 4.2**). Despite iGBs not being the optimal system to investigate IL7R levels, as its expression is restricted to BM B cells, we can speculate that IL7R levels may be upregulated in BM B cells from *Prmt5^{F/F}* Mb1-cre *Trp53^{-/-}* mice, which could disrupt proper B cell differentiation given the interplay between IL7R and pre-BCR during development (Clark et al., 2014). We could test this hypothesis by flow cytometry, analysing IL7R levels at the membrane of pre-B cells. We could also culture the pro-B

cells *ex vivo* on the feeder OP9 cells allowing us to analyze Prmt5-depleted pro-B survival and proliferation in more detail (Cho et al., 1999).

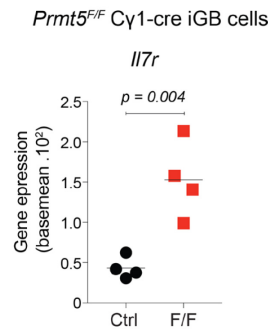


Figure 4.2 - *Il7r* expression level

Il7r expression levels obtained from RNAseq performed in *Cy1-cre* (Ctrl) and *Prmt5^{F/F} Cy1-cre* (F/F) iGBs, 4 days post plating.

Overall, genetic depletion of Prmt1/5 has uncovered the importance of arginine dimethylation at different stages of BM B cell development (**Fig. 4.3**). Our work has further shown that the role of Prmt5 involves p53 at only certain B cell stages, but more work is needed to understand the underlying mechanisms.

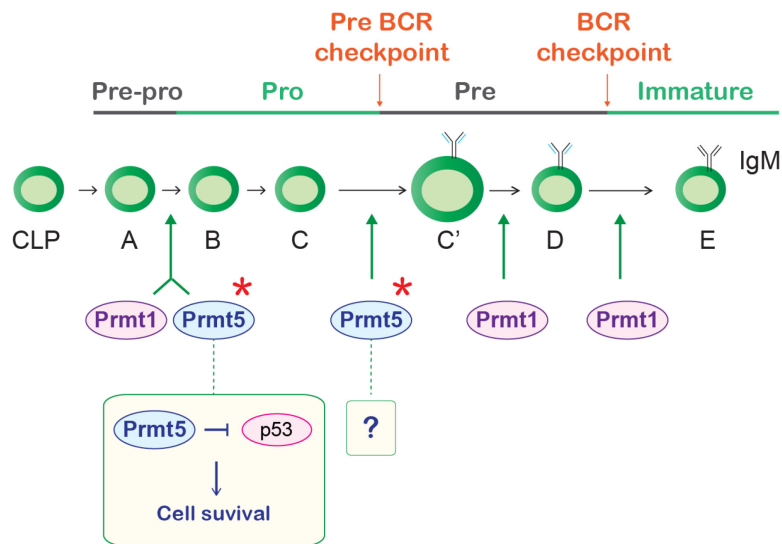


Figure 4.3 - Stages regulated by Prmt1 and Prmt5 during B cell development

Schematic of bone marrow B cell development. The critical stages where *Prmt1/5* are required are indicated with green arrows. Our work demonstrated the importance of *Prmt5* during BM B cell development, indicated by a red star. This figure is complementary to **Fig 1.10**.

4.2.2 Mature B cells homeostasis

While depleting *Prmt5* in mature B cells using CD19-cre did not affect splenic B cell subpopulations (**Fig. 2.1C**), we have found that *Prmt1* deletion results in loss of MZ B cells using *Prmt1^{F/F}* CD21-cre (**Fig. 3.2B**). The requirement for *Prmt1* in MZ B cells was already observed in *Prmt1^{F/F}* CD19-cre mice (Hata et al., 2016). Interestingly loss of MZ B cells was also detected following *Prmt7* depletion (Ying et al., 2015), highlighting the importance of mono- and asymmetric di-methylation for mature B cell homeostasis. Surprisingly, *Prmt1^{F/F}* CD23-cre mice had normal numbers of MZ B cells (Infantino et al., 2017), which could originate from a difference in the excision efficiency of *Prmt1* by the two Cre-drivers CD21-cre and CD23-cre mice.

Mice in which the BCR component *Igα* was truncated using the CD21-cre have reduced numbers of MZ and FO B cells, suggesting that BCR signalling is important for mature B cell survival (Allman and Pillai, 2008; Kraus et al., 2004). Indeed, modulating BCR signaling *in vivo* has shown that the strength of BCR signaling is inversely correlated to MZ B cell generation (Cariappa et al., 2001). As *Prmt1* can dampen BCR signalling (Infantino et al., 2010; Infantino et al., 2017), it is possible that its depletion causes sustained BCR signaling, leading to MZ B cell loss in the periphery. To demonstrate this, we could try to rescue the MZ population by inhibiting a BCR signalling effector, downstream of *Igα* methylation by *Prmt1*. One possibility would be to inhibit Syk. Although complete Syk depletion leads to MZ loss (Hobeika et al., 2015), partial Syk inhibition by entospletinib (Liu and Mamorska-Dyga, 2017) may restore normal levels of BCR signaling and the MZ B cell population in *Prmt1^{F/F}* CD21-cre mice.

The cyclin D3 (*Ccnd3*) was found to negatively regulate MZ formation, as *Ccnd3*^{-/-} mice showed a significant increase in the MZ B cell population (Peled et al., 2010).

Since Prmt1 limits pre-B cell proliferation by disrupting the Ccnd3-Cdk4 complex, via Cdk4 methylation (Dolezal et al., 2017), it is also possible that Prmt1 depletion promotes Ccnd3 activity, which may lead to MZ B cell loss.

4.2.3 B cell activation

Upon activation, mature B cells undergo massive transcriptional and signaling changes (Kouzine et al., 2013; Luo et al., 2018) that sustain rapid proliferation and survival. Similar type of changes, later determine plasma cell differentiation for antibody production (Nutt et al., 2015; Shi et al., 2015). Our experiments allowed us to dissect the importance of Prmt1 and Prmt5 in promoting B cell proliferation, B cell survival and for limiting plasma cell differentiation contributing to a growing body of work on these enzymes in B cells (Hata et al., 2016; Infantino et al., 2017; Koh et al., 2015b).

4.2.3.1 Arginine dimethylation and B cell proliferation

The two main pathways that promote B cell activation at the onset of the GC response are the BCR and CD40 signaling pathways, which promote B cell proliferation (Niiro and Clark, 2002; Rickert et al., 2011). These two pathways have also been shown to synergize in GCs to induce c-Myc expression (Luo et al., 2018). CD40 signaling induces NFκB activation, while the BCR activates the PI3K-AKT-Foxo1 axis (Niiro and Clark, 2002; Rickert et al., 2011). Both can result in MAPK activation (Batlle et al., 2009; Niiro and Clark, 2002). In the next section, I will discuss the roles of Prmt1 and Prmt5 downstream of these signaling pathways. Interestingly, while dimethylation by Prmt1/5 promotes GC proliferation, monomethylation by Prmt7 negatively regulates GC proliferation, as Prmt7-deficient mice have larger GCs (Ying et al., 2015), illustrating the variety of processes arginine methylation regulates.

Role of arginine methylation upon BCR engagement

Prmt1 was shown to be required for mature B cell proliferation upon BCR stimulation (Infantino et al., 2017). It is possible that BCR methylation by Prmt1, shown to

dampen BCR signaling in pre-B cells (Infantino et al., 2010), also occurs in mature B cells and regulates the B cell response to antigens. Indeed, *Prmt1*^{-/-} B cells stimulated with anti-IgM reveal that several downstream BCR effectors remain activated longer than in wt cells, causing increased levels of total phospho-tyrosine, phospho-ERK and phospho-Foxo1 (Infantino et al., 2017). In addition to potentially affecting B cell expansion, increased phospho-Foxo1 could alter GC dynamics (Sander et al., 2015), which will be discussed below. Knowing that the BCR signalling may be compromised, and that BCR signalling promotes Foxo1 degradation resulting in *c-Myc* upregulation (Luo et al., 2018), it would be important to know whether *c-Myc* is still induced in *Prmt1*^{-/-} GC B cells. On the other hand, we still do not know whether Prmt5 plays a role in BCR signaling, so we should assess the growth and survival capacity of *Prmt5*^{-/-} B cells following BCR engagement, as well as the activation of downstream BCR effectors by western blot and monitoring Ca²⁺ signaling. Prmt5 can regulate receptor turn over (Calabretta et al., 2018) so it would be interesting to test whether it affects BCR internalization capacity of *Prmt5*^{-/-} B cells, which could affect antigen presentation for instance.

Role of arginine methylation upon CD40 engagement

Prmt1 depletion *ex vivo* caused various degrees of growth defect depending on the stimulus. Indeed, while *Prmt1*^{F/F} CD21-cre cells showed a clear proliferation defect upon CD40 stimulation, the effect was milder upon TLR stimulation with LPS (**Fig. 3.6**). Experiments to evaluate CD40 signaling in *Prmt1*^{F/F} CD21-cre B cells would be necessary to understand the role of Prmt1 downstream of CD40 engagement. One of the major consequences of CD40 engagement is NFκB activation (Rickert et al., 2011). We could verify the activation of NFκB transcription factors by checking their nuclear translocation and the induction of NFκB targets by qRT-PCR. Defective growth upon CD40 stimulation was also observed in *Prmt1*^{F/F} Cγ1-cre iGB cells, however the proliferation defect was more pronounced in *Prmt5*^{F/F} Cγ1-cre iGBs (**Fig. 2.3J**). Interestingly, both systems exhibited an efficient aDMA/sDMA reduction by day 3, suggesting that the difference in growth does not result from differences in excision

efficiency or methylation mark stability (**Fig. 2.S2D, 3.5B**). Thus, it is likely that Prmt1 and Prmt5 regulate B cell proliferation via distinct mechanisms. Accordingly, both *Prmt1*^{-/-} and *Prmt5*^{-/-} iGBs accumulate in G1 and show a reduced proportion of cells in S-phase (**Fig. 2.3K, 3.5D**). Interestingly, we found that *Prmt5*^{-/-} iGB cells have reduced expression of genes involved in CD40 signaling by GSEA analysis, suggesting that Prmt5 may be involved in signaling downstream of CD40 (**Fig. 2.9A**).

There are a number of mechanisms by which Prmt5 could promote B cell proliferation:

- Prmt5 has been shown repress the cell cycle inhibitor *Cdkn1a* by repressing p53 activity (Bezzi et al., 2013; Li et al., 2015b) as well as through p53-independent mechanism (Zhang et al., 2015b). Although we observed an upregulation of *Cdkn1a* transcripts in *Prmt5*^{-/-} iGBs, we found that Prmt5 promotes B cell growth in a p21-independent manner (**Fig. 2.8G,H**).

- Prmt5 was shown to methylate the transcription factor E2F1 (Cho et al., 2012; Zheng et al., 2013), which is required to promote GC development (Beguelin et al., 2017). Interestingly, GSEA analysis revealed that *Prmt5*^{-/-} iGBs significantly upregulate genes that are normally repressed by E2F1 in mouse fibroblasts (**Fig. 4.4A**). This result is consistent with the fact that Prmt5 methylation of E2F1 directs it towards gene repression (Cho et al., 2012; Zheng et al., 2013). Therefore Prmt5 regulation of E2F1 may contribute to the proliferation defect in iGBs.

- Prmt5 has also been shown to induce c-Myc translation in mouse embryonic fibroblasts (Gao et al., 2017). It remains to be seen whether Prmt5 regulates c-Myc protein levels in B cells, since a reduction of c-Myc would correlate with reduced proliferation (Heinzel et al., 2017). GSEA analysis shows that c-Myc targets are downregulated in *Prmt5*^{-/-} iGBs (**Fig. 4.4C**), supporting the possibility that *Prmt5*^{-/-} iGBs express less c-Myc protein. As c-Myc is critical for DZ re-entry in GCs, diminished c-Myc levels would have important consequences on GC B cell dynamics, which will be discussed further.

Despite clear growth differences between *Prmt1*^{-/-} and *Prmt5*^{-/-} iGBs *ex vivo*, GC proliferation from *Prmt1*^{F/F} Cγ1-cre and *Prmt5*^{F/F} Cγ1-cre mice, assessed by Ki67 levels, does not differ (**Fig. 2.5F, 3.4E**). In accordance, the kinetics of GC B cells following SRBC immunization is similar between *Prmt1*^{F/F} Cγ1-cre and *Prmt5*^{F/F} Cγ1-cre mice (**Fig. 2.5A, 3.4A**). These results demonstrate that *in vivo* phenotypes are more complex to interpret, as GC growth defects reflects the sum of many mechanisms involving different signaling pathways that can be regulated by arginine methylation. Accordingly, the effect of Prmt5 deficiency on the antibody response is much more pronounced than that of Prmt1 deficiency, highlighting their different contribution to the function of the GC beyond their similar role in B cell proliferation.

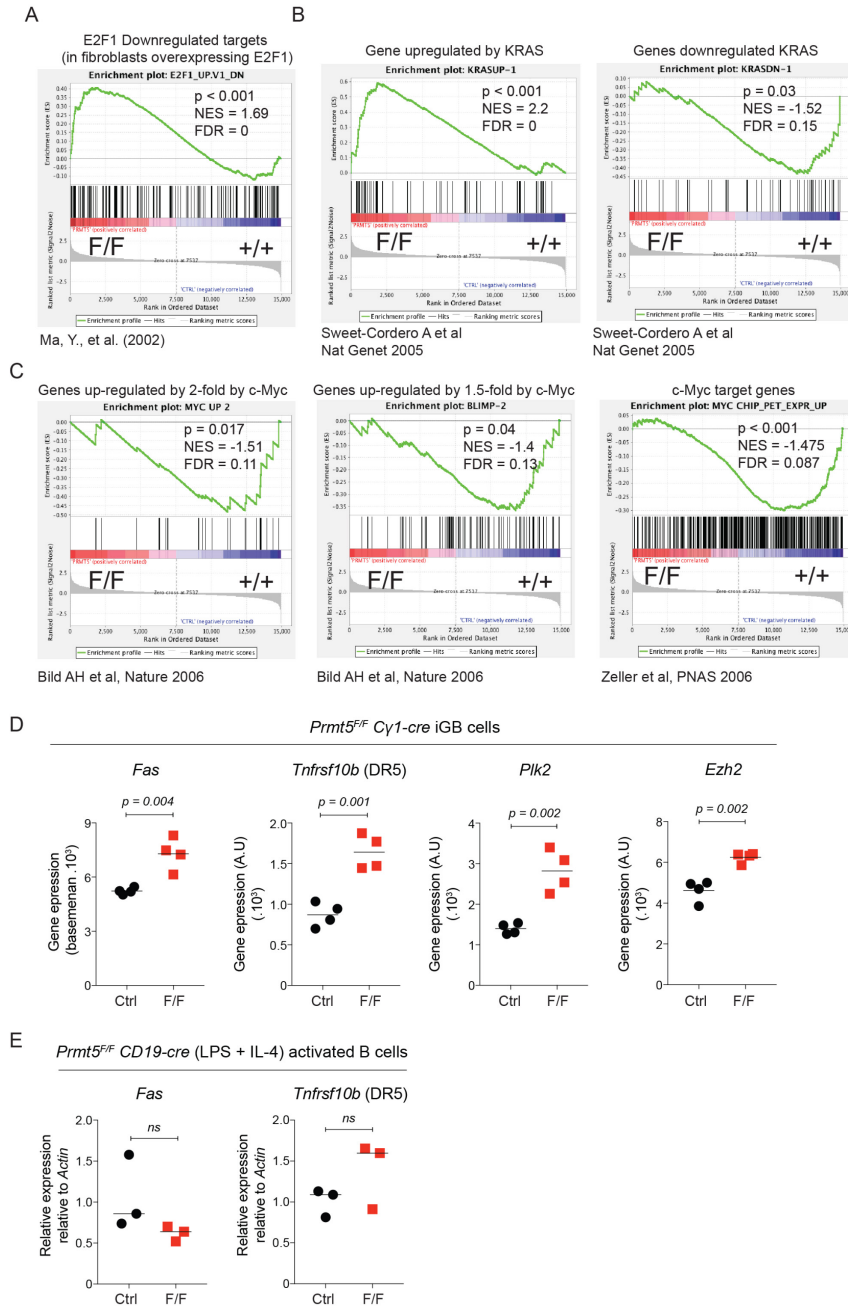


Figure 4.4 - Gene expression upon *Prmt5*-depletion

A)-C) GSEA of transcriptional changes in *Prmt5^{F/F} Cy1-cre* (F/F) iGBs against the indicated gene sets (Bild et al., 2006; Ma et al., 2002; Sweet-Cordero et al., 2005; Zeller et al., 2006). P values, normalized enrichment score (NES) and fold-discovery rates (FDR) are indicated.

D) Expression levels of the indicated genes obtained from RNAseq performed in *Cy1-cre* (Ctrl) and *Prmt5^{F/F} Cy1-cre* (F/F) iGBs, 4 days post plating.

E) Expression levels of the indicated genes measured by RTqPCR in CD19-cre (Ctrl) and *Prmt5^{F/F}* CD19-cre (F/F) LPS + IL-4 activated B cells for 3 days.

4.2.3.2 Arginine dimethylation and B cell survival

Apoptosis was not induced in GCs from mice depleted of either *Prmt1* or *Prmt5* in B cells, suggesting that arginine methylation mostly contributes to GC B cell proliferation, rather than survival (**Fig. 2.5E, 3.4D**). However, arginine methylation does seem to be critical for cell survival upon activation at the onset of the T-dependant antibody response.

Prmt1 was found to promote B cell survival following BCR stimulation by maintaining normal levels of anti-apoptotic proteins (Infantino et al., 2017), possibly via BCR signaling (Infantino et al., 2010). We did not detect increased cell death upon CD40 activation in *Prmt1^{F/F}* Cγ1-cre iGBs or following LPS + IL-4 activation in *Prmt1^{F/F}* CD21-cre cells (**Fig 2.5C, 3.S2B**). This further confirms that *Prmt1* may play distinct roles in activated B cells, depending on the stimuli.

By contrast, we established that *Prmt5* was essential for activated B cell survival *in vitro* upon LPS + IL-4 stimulation as well as *in vivo* following polyclonal B cell activation (**Fig 2.3C, 2.2F,G**). While we observed that *Prmt5*-depleted B cells expressed non-functional forms of the p53 inhibitor Mdm4, due to splicing defects, that in other systems has been shown to partly explain the enhanced p53 response (Bezzi et al., 2013; Koh et al., 2015b), we have found that increased cell death of *Prmt5^{F/F}* CD19-cre cells was p53-independent. Indeed, we still detected apoptosis in *Trp53^{-/-}* B cells treated with the *Prmt5* inhibitor EPZ150666 and in *Prmt5^{F/F}* CD19-cre *Trp53^{-/-}* cells, suggesting that *Prmt5* promotes B cell survival via a different mechanism(s) (**Fig. 2.8C,D**). Furthermore, B cells do not undergo apoptosis if *Prmt5* is depleted following B cell activation, suggesting that one or more *Prmt5* substrate(s) need(s) to be methylated at the time of activation to quickly respond and promote survival. Of note, as p53 signaling was upregulated in *Prmt5^{-/-}* B cells irrespectively of the activation timing or the stimulation type, we believe that p53 activation is a general consequence of *Prmt5* loss that is independent of B cell stimulation. In fact,

increased p53 signaling has been detected in multiple tissues depleted for Prmt5 *in vivo* (Bezzi et al., 2013; Koh et al., 2015b).

There are multiple mechanisms by which Prmt5 could promote B cell survival:

- An important factor triggering apoptosis in mature B cells is the Fas/CD95 receptor, which was upregulated in *Prmt5*^{-/-} iGBs, but not in *Prmt5*^{F/F} CD19-cre cells (**Fig. 4.4D,E**). We also did not detect increased CD95 levels at the B cell membrane *in vivo* by flow cytometry in *Prmt5*^{F/F} CD19-cre mice (**Fig. 2.2F**). Thus, it is highly unlikely that apoptosis is triggered due to abnormal Fas expression in *Prmt5*^{-/-} cells. However, it is a possibility that Fas signalling is enhanced in these cells, which we could test by treating them with an inhibitor of caspase 8 that is downstream of Fas. Prmt5 has been shown to antagonize TRAIL-induced apoptosis in some cancer cells by activating NFκB signaling (Tanaka et al., 2009). We found increased expression of the TRAIL-receptor DR5 in *Prmt5*^{-/-} iGBs (**Fig. 4.4D**), as well as in *Prmt5*^{F/F} CD19-cre cells by qRT-PCR (**Fig. 4.4E**). However, TRAIL-dependant apoptosis is not normally induced in activated B cells (Ursini-Siegel et al., 2002), making this possibility unlikely.

- As discussed above, we observed increased expression of E2F1-regulated genes in *Prmt5*^{-/-} iGBs (**Fig. 4.4A**). One of these, *Polo-like kinase 2* (*Plk2*) was induced by 2-fold (**Fig. 4.4D**). Interestingly, *Plk2* was reported to be silenced in B cell lymphomas, and *Plk2* over-expression in B-cell lymphoma lines causes increased apoptosis (Smith et al., 2006). Likewise, it is possible that *Plk2* expression is partly responsible for increased death of *Prmt5*^{F/F} CD19-cre cells. It would be worth testing *Plk2* expression levels in these cells and testing whether knocking-down *Plk2* can partially rescue apoptosis.

- Prmt5 was shown to enhance the canonical NFκB pathway (Tanaka et al., 2009; Wei et al., 2013), which is downstream from CD40 signaling. As CD40 signaling provides survival signals to B cells, Prmt5 loss could prompt B cells to apoptosis *in vivo*. This could be tested by monitoring apoptosis of *Prmt5*^{F/F} CD19-cre B cells stimulated with various doses of anti-CD40 + IL-4 to determine their relative

sensitivity. Interestingly, *Prmt5^{F/F}* CD19-cre iGBs do not show increased apoptosis (**Fig. 2.3I**). This could result from BAFF expression by 40LB feeder cells. BAFF-R signals via the non-canonical NFκB pathway and induces the pro-survival genes *Bcl-xL* and *Bcl2* (Rickert et al., 2011). Thus, the BAFF-R pathway could compensate for a defect in CD40 signaling.

4.2.3.3 Arginine dimethylation and B cell differentiation

Both Prmt1 and Prmt5 prevent plasma cell differentiation (**Fig. 2.9J, 3.6B**), although Prmt1 loss seems to induce higher levels of B cell differentiation into plasma cells compared to Prmt5 loss (**Fig. 2.9F, 3.5I**). Interestingly, inhibition of both Prmt1 and Prmt5 together, resulted in more than additive differentiation compared to inhibition of either alone, suggesting that Prmt1 and Prmt5 act synergistically (**Fig. 3.7B,D,E**). Synergy suggests that each act via a different mechanism.

Prmt5 and B cell differentiation

We found that Prmt5 loss in LPS + IL-4 activated B cells leads to increased expression of *Prdm1* that codes for Blimp-1. This could be a consequence of increased differentiation. However, it is also possible that Prmt5 represses *Prdm1* directly by methylating histones, which can be assessed by CHIP for Prmt5, H3R8me2s and H3R4me2s at the *Prdm1* locus. Another interesting possibility is that Prmt5 indirectly regulates *Prdm1*. Indeed, Prmt5 was shown to regulate NFκB signalling by methylating RelA (Wei et al., 2013), and RelA depletion is associated with reduced plasma cell production, accompanied by reduced *Prdm1* expression (Heise et al., 2014). If this were true, reconstituting *Rela^{F/F}* CD19-cre B cells with a “Rela arginine mutant” should lead to the same phenotype as in *Prmt5^{F/F}* CD19-cre. Prmt5 could also be involved in co-repressing a subset of Ezh2-repressed bivalent genes, involved in plasma cell differentiation (Beguelin et al., 2013). Indeed, we found that *Prmt5^{-/-}* iGBs were enriched for the expression of Ezh2 target genes. As *Ezh2* expression is not affected in *Prmt5^{-/-}* iGBs (**Fig. 4.4D**), we could imagine that Prmt5 cooperates with Ezh2 by methylating histones at bivalent genes loci, thus helping to maintain the GC program. This hypothesis is supported by the fact that mice depleted

for *Ezh2* in B cells exhibit the same GC defects as *Prmt5^{F/F}* Cγ1-cre mice (Beguelin et al., 2013). Also, Prmt5 and PRC2 co-occupancy at some promoters in human B cell lines has been reported (Tae et al., 2011). Thus, both testing the interaction between Prmt5 and PRC2, as well as a genome wide ChIP for Prmt5, H3R8me2s and H3R4me2s in B cells, which could be compared to EZH2 targets, would allow a better understanding of whether Prmt5 and Ezh2 interact in activated B cells but also help in discriminating which genes might be directly regulated by Prmt5 at the transcriptional level by comparing to our RNA-seq.

Prmt5 was shown to regulate the MAPK pathway by methylating Raf proteins, resulting in reduced Erk1/2 phosphorylation and enhanced proliferation (Andreu-Perez et al., 2011). By contrast, Prmt5 depletion reduced Erk1/2 phosphorylation in hematopoietic cells (Liu et al., 2015b). By GSEA analysis, we found that *Prmt5^{-/-}* iGBs have increased levels of genes that are up-regulated in cells expressing an active mutant form of Ras (Kras), and have reduced levels of genes that are down-regulated in cells expressing Kras, suggesting that the MAPK pathway is enhanced in *Prmt5^{-/-}* cells (**Fig. 4.4B**). Interestingly, Erk1/2 activity was found to induce mature B cell differentiation by promoting *Prdm1* expression (Allman and Cancro, 2011; Yasuda et al., 2011). Thus, it is possible that Prmt5 activity represses the MAPK pathway in mature B cells to limit plasma cell differentiation. To investigate this hypothesis further, we should first verify the levels of Erk1/2 phosphorylation in *Prmt5^{-/-}* iGBs and in *Prmt5^{F/F}* CD19-cre, where we see a strong induction of differentiation (**Fig. 2.9J**).

Interestingly, while apoptosis was only detected when Prmt5 was inhibited before B cell activation, we observed increased differentiation irrespective of Prmt5 inhibition timing: before or after activation (data not shown). This result demonstrates that increased apoptosis and differentiation are triggered by distinct mechanisms.

In summary, there are several potential mechanisms, including transcription and signaling pathways, by which Prmt5 could limit plasma cell differentiation. These mechanisms are not mutually exclusive and are a challenging but interesting future direction.

Prmt1 and B cell differentiation

The effect of Prmt1 for limiting B cell differentiation is more striking than Prmt5 in all the systems and stimuli used. Yet, we found that Prmt1 limits differentiation to a much lesser extent when in the presence of IL-21 than with IL-4 stimulation (**Fig. 3.5I**). Interestingly, Tfh cells produce IL-21 and IL-4 in a sequential manner in GCs (Weinstein et al., 2016). In early GCs, a higher proportion of Tfh cells produce IL-21, sustaining the GC reaction, while in mature GCs they mostly express IL-4, which promotes plasma cell differentiation (Weinstein et al., 2016). This suggests that Prmt1 is required to repress plasma cell differentiation in mature GCs, in order to prevent premature B cell exit and incomplete affinity maturation. As is the case with Prmt5, there are several potential mechanisms by which Prmt1 could play this role. Prmt1 regulates gene expression (Blanc and Richard, 2017). We have not analyzed the transcriptome of Prmt1-deficient B cells but, in combination with ChIP-seq, it would be an informative future direction. Another possibility is that Prmt1 inhibits the plasma cell program indirectly because of a function downstream of IL-4 signaling. Interestingly, enhanced PI3K-AKT signaling, by depleting *Pten* (which antagonizes PI3K), can enhance plasma cell differentiation *in vitro* (Omori et al., 2006). Enhanced AKT activity promotes Foxo1 degradation (Greer and Brunet, 2005), and we suspect that *Prmt1* depletion could have the same effect, as Prmt1 antagonizes Foxo1 phosphorylation by AKT in human epithelial cells (Yamagata et al., 2008). Moreover, Foxo1 is expressed and localized in the nucleus in DZ B cells, promoting the GC program and inhibiting the plasma cell program via *Prdm1* repression (Dominguez-Sola et al., 2015; Luo et al., 2018; Sander et al., 2015). As we found increased *Prdm1* expression in *Prmt1*-depleted B cells, we hypothesize that Prmt1 limits plasma cell differentiation by stabilizing Foxo1. To confirm that hypothesis, it would be important to analyze CD40 signaling, as well as measure phospho-AKT levels in GCs of *Prmt1^{F/F}* Cγ1-cre mice by flow cytometry and evaluate phospho-Foxo1 levels and localization by immunofluorescence in spleens.

It is possible that additional type I PRMTs are involved in limiting plasma cell differentiation. Indeed, while we found that MS023 treatments recapitulate genetic

ablation of *Prmt1* in B cells, this compound also inhibits Prmt6 (Hu et al., 2016) (**Fig. 3.6B,H**). In order to confirm the synergistic role of Prmt1 and Prmt5 in repressing plasma cell differentiation we could perform the reciprocal experiment, treating activated *Prmt1^{F/F}*-CD21 B cells with the specific Prmt5 inhibitor EPZ150666 (Hu et al., 2016). To rule out any potential off-target effects of the inhibitors, we could also test the differentiation potential of *Prmt1^{F/+} Prmt5^{F/+}* Cy1-cre compared to *Prmt1^{F/+} Prmt5^{+/+}* Cy1-cre and *Prmt1^{+/+} Prmt5^{F/+}* Cy1-cre controls. Of note, treating *Prmt1^{F/F}*-Cy1 iGBs with EPZ150666 caused a slight increase in plasma cell differentiation, though inhibiting Prmt5 alone in iGBs did not show much effect, supporting Prmt1 and Prmt5 synergy (**Fig. 3.7D**).

4.2.4 Arginine methylation influences GC dynamics and GC output

Ex vivo experiments allowed us to dissect the importance of arginine methylation upon B cell activation. We found that Prmt1 and Prmt5 likely regulate different pathways downstream of various stimuli, with Prmt1 overall playing a major role in limiting plasma cell differentiation in GCs and Prmt5 in promoting cell proliferation. However, when immunized, both *Prmt1^{F/F}* Cy1-cre and *Prmt5^{F/F}* Cy1-cre mice exhibit the same GC defects in expansion, as well as the appearance of an abnormal GC cell population that shows reduced proliferation while downregulating CD86, CXCR4 and AID (**Fig. 2.5, 3.4**). As discussed, Prmt1 may regulate Foxo1 levels, and Prmt5 may modulate c-Myc expression (Luo et al., 2018; Sander et al., 2015). Such effects could explain the altered GC dynamics in knock-out mice. The exact identity and origin of this abnormal populations remains to be identified. However, these cells present reduced proliferation and AID levels, which are features of plasma cells. As we found Prmt1 and Prmt5 to limit plasma cell differentiation *in vitro*, one possibility is that this new population represents abnormal plasma cells that exit the GC reaction prematurely. To test this hypothesis, we could perform an intracellular staining for Irf4 by flow cytometry, to see whether this population indeed contains plasma cell precursors. Regardless of whether this population is or not related to plasma cells,

the premature differentiation into plasma cells is supported by our observation that a reduced proportion of *Prmt1*- and *Prmt5*-null GCs and plasma cells express IgG1, suggesting that their GC residency was shorter than controls and differentiated before undergoing class switch recombination (**Fig 2. 9L,M, 3.8C,E**).

Interestingly, *Prmt1* and *Prmt5* were found to be induced in positively selected centrocytes bearing high affinity BCRs, along with the “pro-GC” factors *Aicda*, *Foxo1* and *c-Myc* (Ise et al., 2018) (**Fig. 4.5**). Even though these cells expressed a transcription profile resembling plasmablasts and were suggested to be plasma cell precursors (Ise et al., 2018), it is possible that a proportion of these cells, expressing high levels of *Prmt1/5* would re-enter the DZ and be maintained in the GC reaction, thus improving affinity maturation (**Fig. 4.6**).

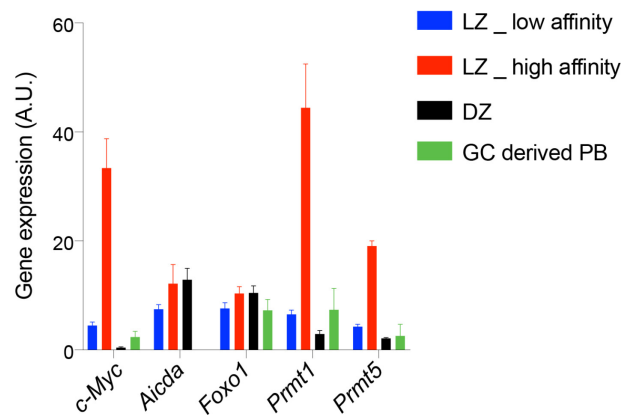


Figure 4.5 - Pro-GC genes are induced in high affinity centrocytes

Transcripts levels of the indicated genes obtained from RNA seq data generated by (Ise et al., 2018). Centrocytes were sorted based on CD69 and *Bcl6* expression (LZ_low affinity: CD69⁺ *Bcl6*^{low}, LZ_high affinity: CD69⁺ *Bcl6*^{low}). LZ: light zone, DZ: dark zone, PB: plasmablast.

Despite the apparent similarities, *Prmt5*^{F/F} Cy1-cre mice have a much more compromised antibody response compared to *Prmt1*^{F/F} Cy1-cre, at least against NP after NP-CGG immunization. Indeed, *Prmt5*^{F/F} Cy1-cre mice showed a dramatic and consistent defect, while *Prmt1*^{F/F} Cy1-cre mice produced comparable amounts of NP-

IgG1 antibodies relative to control mice, even if of lower affinity in the secondary response (**Fig. 2.4A,C, 3.3C**). This divergence could be explained by the different roles of each Prmts. If Prmt5 primarily promotes GC B cell expansion, a Prmt5 deficiency would result in a more profound effect, as it would compromise the whole GC reaction. In contrast, if Prmt1 regulates plasma cell differentiation later in the GC response, the effect of knocking-out Prmt1 would have a milder effect early in the antibody response.

Because *Prmt1^{F/F}* Cγ1-cre mice produce normal anti-NP-IgG1 levels by day 14, we suspect these mice may generate normal levels of ASCs at the peak of the extrafollicular response, at day 7 (Smith et al., 1996), which we need to test. Later in the GC response, at day 14, we found that *Prmt1^{F/F}* Cγ1-cre mice produce less ASCs, suggesting a late GC specific defect in plasma cell differentiation (**Fig. 3.3G**). Another possibility is that the premature plasma cells are IgM+, and as we measured IgG1 ASC, we are not detecting the overall increase. We will measure IgM+ ASC in the future. Interestingly, we observed a reduction in the IgG1 response against the complex antigen CGG at day 14 and after re-call (**Fig. 3.3D,E**). Since this is a more complex antigen, generating CGG-specific antibodies requires longer GC residence time than NP-specific antibodies. Moreover, because of the higher number of epitopes that CGG contains, B cells against different CGG epitopes must compete with each other in the GC, while anti-NP responses are dominated by one type of clone (Bannard and Cyster, 2017). Thus, we could explain the milder antibody response defect in *Prmt1^{F/F}* Cγ1-cre mice for two reasons: (i) the function of Prmt1 in cell proliferation is not as important as Prmt5 and (ii) the predominant role for Prmt1 in regulating differentiation late in the GC response, and showing normal extrafollicular antibody response against NP. Nonetheless, the defect is revealed in the secondary response that shows anti-NP IgG1 of reduced affinity. Because GC B cells directed against complex antigen require a longer time in the GC to improve affinity, we observe an exacerbated defect in the antibodies produced against CGG in *Prmt1^{F/F}* Cγ1-cre.

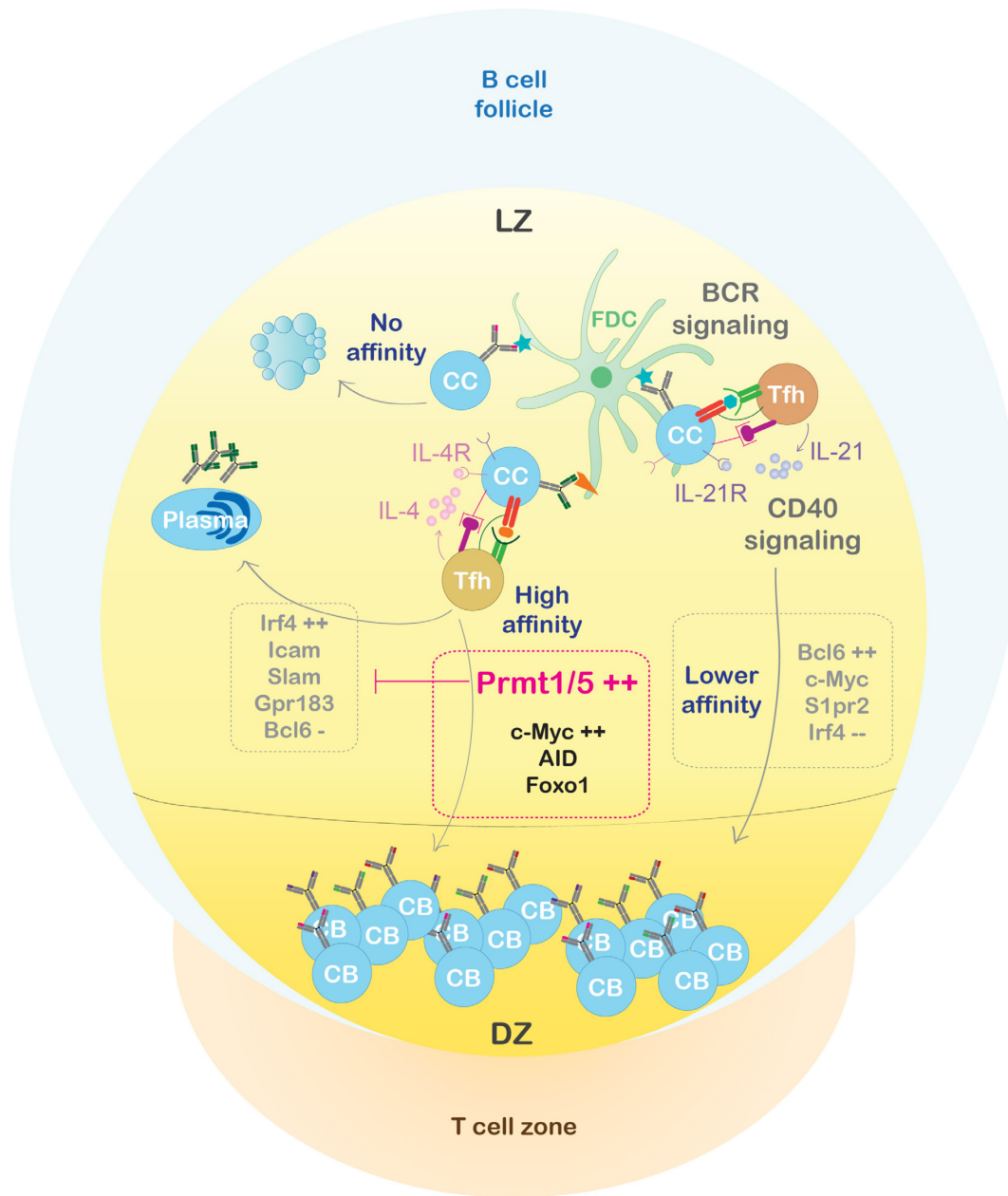


Figure 4.6 - Prmt1 and Prmt5 influence GC B cell fate

This figure is a model that complements Fig. 1.6, showing the role for Prmt1 and Prmt5 in promoting GC maintenance and repressing premature plasma cell differentiation.

5 Conclusion

We discovered distinct roles for Prmt1 and Prmt5 in regulating B cell development. Both enzymes promote B cell activation, support the GC reaction and limit plasma cell differentiation, although most likely by different mechanisms. Our work revealed the intrinsic importance of arginine methylation in B cells for T-dependent antibody responses and particularly the GC reaction. Overall, our data suggests that Prmt1 and Prm5 influence GC B cell fate by sustaining DZ re-entry and repressing premature B cell differentiation by different mechanisms (**Fig. 4.6**). We propose that the high affinity centrocytes that are positively selected in the LZ can follow two fates depending on the expression of *Prmt1* and *Prmt5*. Cells with reduced *Prmt1/5* expression exit the GC and differentiate into plasma cells, while cells expressing high *Prmt1/5* are maintained in the GC reaction and re-enter the DZ. This work furthers our understanding of the complex mechanisms influencing B cell fate. Future efforts will be required to understand the signalling pathways inducing Prmt1 and Prmt5 in GCs, as well as exploring the mechanisms by which Prmt1 and Prmt5 sustain GC B cell proliferation and differentiation. This work will also help in understanding the development of B cell malignancies, most of which display elevated levels of Prmt5.

Bibliographie

- Adams, M.M., B. Wang, Z. Xia, J.C. Morales, X. Lu, L.A. Donehower, D.A. Bochar, S.J. Elledge, and P.B. Carpenter. 2005. 53BP1 oligomerization is independent of its methylation by PRMT1. *Cell cycle* 4:1854-1861.
- Adem, J., A. Hamalainen, A. Ropponen, J. Eeva, M. Eray, U. Nuutinen, and J. Pelkonen. 2015. ERK1/2 has an essential role in B cell receptor- and CD40-induced signaling in an in vitro model of germinal center B cell selection. *Molecular immunology* 67:240-247.
- Aggarwal, P., L.P. Vaites, J.K. Kim, H. Mellert, B. Gurung, H. Nakagawa, M. Herlyn, X. Hua, A.K. Rustgi, S.B. McMahon, and J.A. Diehl. 2010. Nuclear cyclin D1/CDK4 kinase regulates CUL4 expression and triggers neoplastic growth via activation of the PRMT5 methyltransferase. *Cancer cell* 18:329-340.
- Aguzzi, A., J. Kranich, and N.J. Krautler. 2014. Follicular dendritic cells: origin, phenotype, and function in health and disease. *Trends in immunology* 35:105-113.
- Alinari, L., K.V. Mahasenan, F. Yan, V. Karkhanis, J.H. Chung, E.M. Smith, C. Quinion, P.L. Smith, L. Kim, J.T. Patton, R. Lapalombella, B. Yu, Y. Wu, S. Roy, A. De Leo, S. Pileri, C. Agostinelli, L. Ayers, J.E. Bradner, S. Chen-Kiang, O. Elemento, T. Motiwala, S. Majumder, J.C. Byrd, S. Jacob, S. Sif, C. Li, and R.A. Baiocchi. 2015a. Selective inhibition of protein arginine methyltransferase 5 blocks initiation and maintenance of B-cell transformation. *Blood* 125:2530-2543.
- Alinari, L., K.V. Mahasenan, F. Yan, V. Karkhanis, J.H. Chung, E.M. Smith, C. Quinion, P.L. Smith, L. Kim, J.T. Patton, R. Lapalombella, B. Yu, Y. Wu, S. Roy, A. De Leo, S. Pileri, C. Agostinelli, L. Ayers, J.E. Bradner, S. Chen-Kiang, O. Elemento, T. Motiwala, S. Majumder, J.C. Byrd, S. Jacob, S. Sif, C. Li, and R.A. Baiocchi. 2015b. Selective inhibition of protein arginine methyltransferase 5 blocks initiation and maintenance of B-cell transformation. *Blood*
- Allen, C.D., K.M. Ansel, C. Low, R. Lesley, H. Tamamura, N. Fujii, and J.G. Cyster. 2004. Germinal center dark and light zone organization is mediated by CXCR4 and CXCR5. *Nature immunology* 5:943-952.
- Allen, D., T. Simon, F. Sablitzky, K. Rajewsky, and A. Cumano. 1988. Antibody engineering for the analysis of affinity maturation of an anti-hapten response. *The EMBO journal* 7:1995-2001.
- Allman, D., and S. Pillai. 2008. Peripheral B cell subsets. *Current opinion in immunology* 20:149-157.
- Allman, D.M., and M.P. Cancro. 2011. pERKing up the BLIMP in plasma cell differentiation. *Sci Signal* 4:pe21.
- Amzel, L.M., and R.J. Poljak. 1979. Three-dimensional structure of immunoglobulins. *Annual review of biochemistry* 48:961-997.
- Ancelin, K., U.C. Lange, P. Hajkova, R. Schneider, A.J. Bannister, T. Kouzarides, and M.A. Surani. 2006. Blimp1 associates with Prmt5 and directs histone arginine methylation in mouse germ cells. *Nature cell biology* 8:623-630.
- Anderson, S.M., A. Khalil, M. Uduman, U. Hershberg, Y. Louzoun, A.M. Haberman, S.H. Kleinstein, and M.J. Shlomchik. 2009. Taking advantage: high-affinity B cells in the

- germinal center have lower death rates, but similar rates of division, compared to low-affinity cells. *Journal of immunology* 183:7314-7325.
- Andreu-Perez, P., R. Esteve-Puig, C. de Torre-Minguela, M. Lopez-Fauqued, J.J. Bech-Serra, S. Tenbaum, E.R. Garcia-Trevijano, F. Canals, G. Merlino, M.A. Avila, and J.A. Recio. 2011. Protein arginine methyltransferase 5 regulates ERK1/2 signal transduction amplitude and cell fate through CRAF. *Sci Signal* 4:ra58.
- Antonyasamy, S., Z. Bonday, R.M. Campbell, B. Doyle, Z. Druzina, T. Gheyi, B. Han, L.N. Jungheim, Y. Qian, C. Rauch, M. Russell, J.M. Sauder, S.R. Wasserman, K. Weichert, F.S. Willard, A. Zhang, and S. Emtage. 2012. Crystal structure of the human PRMT5:MEP50 complex. *Proceedings of the National Academy of Sciences of the United States of America* 109:17960-17965.
- Avalos, A.M., and H.L. Ploegh. 2014. Early BCR Events and Antigen Capture, Processing, and Loading on MHC Class II on B Cells. *Frontiers in immunology* 5:92.
- Avery, D.T., E.K. Deenick, C.S. Ma, S. Suryani, N. Simpson, G.Y. Chew, T.D. Chan, U. Palendira, J. Bustamante, S. Boisson-Dupuis, S. Choo, K.E. Bleasel, J. Peake, C. King, M.A. French, D. Engelhard, S. Al-Hajjar, S. Al-Muhsen, K. Magdorf, J. Roesler, P.D. Arkwright, P. Hissaria, D.S. Riminton, M. Wong, R. Brink, D.A. Fulcher, J.L. Casanova, M.C. Cook, and S.G. Tangye. 2010. B cell-intrinsic signaling through IL-21 receptor and STAT3 is required for establishing long-lived antibody responses in humans. *The Journal of experimental medicine* 207:155-171.
- Bachand, F. 2007. Protein arginine methyltransferases: from unicellular eukaryotes to humans. *Eukaryot Cell* 6:889-898.
- Baldwin, R.M., A. Moretton, G. Paris, I. Goulet, and J. Cote. 2012. Alternatively spliced protein arginine methyltransferase 1 isoform PRMT1v2 promotes the survival and invasiveness of breast cancer cells. *Cell cycle* 11:4597-4612.
- Banasavadi-Siddegowda, Y.K., L. Russell, E. Frair, V.A. Karkhanis, T. Relation, J.Y. Yoo, J. Zhang, S. Sif, J. Imitola, R. Baiocchi, and B. Kaur. 2017. PRMT5-PTEN molecular pathway regulates senescence and self-renewal of primary glioblastoma neurosphere cells. *Oncogene* 36:263-274.
- Bannard, O., and J.G. Cyster. 2017. Germinal centers: programmed for affinity maturation and antibody diversification. *Current opinion in immunology* 45:21-30.
- Bannard, O., R.M. Horton, C.D. Allen, J. An, T. Nagasawa, and J.G. Cyster. 2013. Germinal center centroblasts transition to a centrocyte phenotype according to a timed program and depend on the dark zone for effective selection. *Immunity* 39:912-924.
- Bannard, O., S.J. McGowan, J. Ersching, S. Ishido, G.D. Victora, J.S. Shin, and J.G. Cyster. 2016. Ubiquitin-mediated fluctuations in MHC class II facilitate efficient germinal center B cell responses. *The Journal of experimental medicine* 213:993-1009.
- Bao, X., Z. Siplashvili, B.J. Zarnegar, R.M. Shenoy, E.J. Rios, N. Nady, K. Qu, A. Mah, D.E. Webster, A.J. Rubin, G.G. Wozniak, S. Tao, J. Wysocka, and P.A. Khavari. 2017. CSNK1a1 Regulates PRMT1 to Maintain the Progenitor State in Self-Renewing Somatic Tissue. *Dev Cell* 43:227-239 e225.
- Basso, K., U. Klein, H. Niu, G.A. Stolovitzky, Y. Tu, A. Califano, G. Cattoretti, and R. Dalla-Favera. 2004. Tracking CD40 signaling during germinal center development. *Blood* 104:4088-4096.
- Basso, K., M. Saito, P. Sumazin, A.A. Margolin, K. Wang, W.K. Lim, Y. Kitagawa, C. Schneider, M.J. Alvarez, A. Califano, and R. Dalla-Favera. 2010. Integrated

- biochemical and computational approach identifies BCL6 direct target genes controlling multiple pathways in normal germinal center B cells. *Blood* 115:975-984.
- Basso, K., C. Schneider, Q. Shen, A.B. Holmes, M. Setty, C. Leslie, and R. Dalla-Favera. 2012. BCL6 positively regulates AID and germinal center gene expression via repression of miR-155. *The Journal of experimental medicine* 209:2455-2465.
- Batista, F.D., and N.E. Harwood. 2009. The who, how and where of antigen presentation to B cells. *Nature reviews. Immunology* 9:15-27.
- Batista, F.D., and M.S. Neuberger. 2000. B cells extract and present immobilized antigen: implications for affinity discrimination. *The EMBO journal* 19:513-520.
- Battle, A., V. Papadopoulou, A.R. Gomes, S. Willimott, J.V. Melo, K. Naresh, E.W. Lam, and S.D. Wagner. 2009. CD40 and B-cell receptor signalling induce MAPK family members that can either induce or repress Bcl-6 expression. *Molecular immunology* 46:1727-1735.
- Bedford, M.T., and S.G. Clarke. 2009. Protein arginine methylation in mammals: who, what, and why. *Molecular cell* 33:1-13.
- Bedford, M.T., and S. Richard. 2005. Arginine methylation an emerging regulator of protein function. *Molecular cell* 18:263-272.
- Beguelin, W., R. Popovic, M. Teater, Y. Jiang, K.L. Bunting, M. Rosen, H. Shen, S.N. Yang, L. Wang, T. Ezponda, E. Martinez-Garcia, H. Zhang, Y. Zheng, S.K. Verma, M.T. McCabe, H.M. Ott, G.S. Van Aller, R.G. Kruger, Y. Liu, C.F. McHugh, D.W. Scott, Y.R. Chung, N. Kelleher, R. Shaknovich, C.L. Creasy, R.D. Gascoyne, K.K. Wong, L. Cerchietti, R.L. Levine, O. Abdel-Wahab, J.D. Licht, O. Elemento, and A.M. Melnick. 2013. EZH2 is required for germinal center formation and somatic EZH2 mutations promote lymphoid transformation. *Cancer cell* 23:677-692.
- Beguelin, W., M.A. Rivas, M.T. Calvo Fernandez, M. Teater, A. Purwada, D. Redmond, H. Shen, M.F. Challman, O. Elemento, A. Singh, and A.M. Melnick. 2017. EZH2 enables germinal centre formation through epigenetic silencing of CDKN1A and an Rb-E2F1 feedback loop. *Nature communications* 8:877.
- Bekeredjian-Ding, I., and G. Jengo. 2009. Toll-like receptors--sentries in the B-cell response. *Immunology* 128:311-323.
- Benjamin, D.C., J.A. Berzofsky, I.J. East, F.R. Gurd, C. Hannum, S.J. Leach, E. Margoliash, J.G. Michael, A. Miller, E.M. Prager, and et al. 1984. The antigenic structure of proteins: a reappraisal. *Annual review of immunology* 2:67-101.
- Bergtold, A., D.D. Desai, A. Gavhane, and R. Clynes. 2005. Cell surface recycling of internalized antigen permits dendritic cell priming of B cells. *Immunity* 23:503-514.
- Bernstein, B.E., T.S. Mikkelsen, X. Xie, M. Kamal, D.J. Huebert, J. Cuff, B. Fry, A. Meissner, M. Wernig, K. Plath, R. Jaenisch, A. Wagschal, R. Feil, S.L. Schreiber, and E.S. Lander. 2006. A bivalent chromatin structure marks key developmental genes in embryonic stem cells. *Cell* 125:315-326.
- Berthet, C., F. Guehenneux, V. Revol, C. Samarut, A. Lukaszewicz, C. Dehay, C. Dumontet, J.P. Magaud, and J.P. Rouault. 2002. Interaction of PRMT1 with BTG/TOB proteins in cell signalling: molecular analysis and functional aspects. *Genes to cells : devoted to molecular & cellular mechanisms* 7:29-39.
- Bezzi, M., S.X. Teo, J. Muller, W.C. Mok, S.K. Sahu, L.A. Vardy, Z.Q. Bonday, and E. Guccione. 2013. Regulation of constitutive and alternative splicing by PRMT5 reveals

- a role for Mdm4 pre-mRNA in sensing defects in the spliceosomal machinery. *Genes & development* 27:1903-1916.
- Bild, A.H., G. Yao, J.T. Chang, Q. Wang, A. Potti, D. Chasse, M.B. Joshi, D. Harpole, J.M. Lancaster, A. Berchuck, J.A. Olson, Jr., J.R. Marks, H.K. Dressman, M. West, and J.R. Nevins. 2006. Oncogenic pathway signatures in human cancers as a guide to targeted therapies. *Nature* 439:353-357.
- Blanc, R.S., and S. Richard. 2017. Arginine Methylation: The Coming of Age. *Molecular cell* 65:8-24.
- Blanc, R.S., G. Vogel, X. Li, Z. Yu, S. Li, and S. Richard. 2017. Arginine Methylation by PRMT1 Regulates Muscle Stem Cell Fate. *Molecular and cellular biology* 37:
- Blanchet, F., A. Cardona, F.A. Letimier, M.S. Hershfield, and O. Acuto. 2005. CD28 costimulatory signal induces protein arginine methylation in T cells. *The Journal of experimental medicine* 202:371-377.
- Blink, E.J., A. Light, A. Kallies, S.L. Nutt, P.D. Hodgkin, and D.M. Tarlinton. 2005. Early appearance of germinal center-derived memory B cells and plasma cells in blood after primary immunization. *The Journal of experimental medicine* 201:545-554.
- Boehm, T., and J.B. Swann. 2014. Origin and evolution of adaptive immunity. *Annu Rev Anim Biosci* 2:259-283.
- Boisvert, F.M., U. Dery, J.Y. Masson, and S. Richard. 2005a. Arginine methylation of MRE11 by PRMT1 is required for DNA damage checkpoint control. *Genes & development* 19:671-676.
- Boisvert, F.M., M.J. Hendzel, J.Y. Masson, and S. Richard. 2005b. Methylation of MRE11 regulates its nuclear compartmentalization. *Cell cycle* 4:981-989.
- Bolger, A.M., M. Lohse, and B. Usadel. 2014. Trimmomatic: a flexible trimmer for Illumina sequence data. *Bioinformatics* 30:2114-2120.
- Bonizzi, G., and M. Karin. 2004. The two NF-kappaB activation pathways and their role in innate and adaptive immunity. *Trends in immunology* 25:280-288.
- Boulianne, B., O.L. Rojas, D. Haddad, A. Zaheen, A. Kapelnikov, T. Nguyen, C. Li, R. Hakem, J.L. Gommerman, and A. Martin. 2013. AID and caspase 8 shape the germinal center response through apoptosis. *Journal of immunology* 191:5840-5847.
- Brandtzaeg, P. 2009. Mucosal immunity: induction, dissemination, and effector functions. *Scand J Immunol* 70:505-515.
- Bremang, M., A. Cuomo, A.M. Agresta, M. Stugiewicz, V. Spadotto, and T. Bonaldi. 2013. Mass spectrometry-based identification and characterisation of lysine and arginine methylation in the human proteome. *Mol Biosyst* 9:2231-2247.
- Brenner, D., and T.W. Mak. 2009. Mitochondrial cell death effectors. *Curr Opin Cell Biol* 21:871-877.
- Brugarolas, J., C. Chandrasekaran, J.I. Gordon, D. Beach, T. Jacks, and G.J. Hannon. 1995. Radiation-induced cell cycle arrest compromised by p21 deficiency. *Nature* 377:552-557.
- Butt, D., T.D. Chan, K. Bourne, J.R. Hermes, A. Nguyen, A. Statham, L.A. O'Reilly, A. Strasser, S. Price, P. Schofield, D. Christ, A. Basten, C.S. Ma, S.G. Tangye, T.G. Phan, V.K. Rao, and R. Brink. 2015. FAS Inactivation Releases Unconventional Germinal Center B Cells that Escape Antigen Control and Drive IgE and Autoantibody Production. *Immunity* 42:890-902.

- Calabretta, S., G. Vogel, Z. Yu, K. Choquet, L. Darbelli, T.B. Nicholson, C.L. Kleinman, and S. Richard. 2018. Loss of PRMT5 promotes PDGFRa degradation during oligodendrocyte differentiation and myelination. *Bio Archive*
- Calado, D.P., Y. Sasaki, S.A. Godinho, A. Pellerin, K. Kochert, B.P. Sleckman, I.M. de Alboran, M. Janz, S. Rodig, and K. Rajewsky. 2012. The cell-cycle regulator c-Myc is essential for the formation and maintenance of germinal centers. *Nature immunology* 13:1092-1100.
- Cariappa, A., M. Tang, C. Parng, E. Nebelitskiy, M. Carroll, K. Georgopoulos, and S. Pillai. 2001. The follicular versus marginal zone B lymphocyte cell fate decision is regulated by Aiolos, Btk, and CD21. *Immunity* 14:603-615.
- Caron, G., S. Le Gallou, T. Lamy, K. Tarte, and T. Fest. 2009. CXCR4 expression functionally discriminates centroblasts versus centrocytes within human germinal center B cells. *Journal of immunology* 182:7595-7602.
- Carrington, E.M., Y. Zhan, J.L. Brady, J.G. Zhang, R.M. Sutherland, N.S. Anstee, R.L. Schenk, I.B. Vikstrom, R.B. Delconte, D. Segal, N.D. Huntington, P. Bouillet, D.M. Tarlinton, D.C. Huang, A. Strasser, S. Cory, M.J. Herold, and A.M. Lew. 2017. Anti-apoptotic proteins BCL-2, MCL-1 and A1 summate collectively to maintain survival of immune cell populations both in vitro and in vivo. *Cell death and differentiation* 24:878-888.
- Casola, S., G. Cattoretti, N. Uyttersprot, S.B. Koralov, J. Seagal, Z. Hao, A. Waisman, A. Egert, D. Ghitza, and K. Rajewsky. 2006. Tracking germinal center B cells expressing germ-line immunoglobulin gamma transcripts by conditional gene targeting. *Proceedings of the National Academy of Sciences of the United States of America* 103:7396-7401.
- Cattoretti, G., M. Buttner, R. Shaknovich, E. Kremmer, B. Alobeid, and G. Niedobitek. 2006. Nuclear and cytoplasmic AID in extrafollicular and germinal center B cells. *Blood* 107:3967-3975.
- Chan-Penebre, E., K.G. Kuplast, C.R. Majer, P.A. Boriack-Sjodin, T.J. Wigle, L.D. Johnston, N. Rioux, M.J. Munchhof, L. Jin, S.L. Jacques, K.A. West, T. Lingaraj, K. Stickland, S.A. Ribich, A. Raimondi, M.P. Scott, N.J. Waters, R.M. Pollock, J.J. Smith, O. Barbash, M. Pappalardi, T.F. Ho, K. Nurse, K.P. Oza, K.T. Gallagher, R. Kruger, M.P. Moyer, R.A. Copeland, R. Chesworth, and K.W. Duncan. 2015. A selective inhibitor of PRMT5 with in vivo and in vitro potency in MCL models. *Nat Chem Biol* 11:432-437.
- Chen, C., T.J. Nott, J. Jin, and T. Pawson. 2011. Deciphering arginine methylation: Tudor tells the tale. *Nature reviews. Molecular cell biology* 12:629-642.
- Chen, H.Z., S.Y. Tsai, and G. Leone. 2009. Emerging roles of E2Fs in cancer: an exit from cell cycle control. *Nature reviews. Cancer* 9:785-797.
- Cheng, D., J. Cote, S. Shaaban, and M.T. Bedford. 2007. The arginine methyltransferase CARM1 regulates the coupling of transcription and mRNA processing. *Molecular cell* 25:71-83.
- Cheung, N., T.K. Fung, B.B. Zeisig, K. Holmes, J.K. Rane, K.A. Mowen, M.G. Finn, B. Lenhard, L.C. Chan, and C.W. So. 2016. Targeting Aberrant Epigenetic Networks Mediated by PRMT1 and KDM4C in Acute Myeloid Leukemia. *Cancer cell* 29:32-48.
- Cho, E.C., S. Zheng, S. Munro, G. Liu, S.M. Carr, J. Moehlenbrink, Y.C. Lu, L. Stimson, O. Khan, R. Konietzny, J. McGouran, A.S. Coutts, B. Kessler, D.J. Kerr, and N.B.

- Thangue. 2012. Arginine methylation controls growth regulation by E2F-1. *The EMBO journal* 31:1785-1797.
- Cho, S.K., T.D. Webber, J.R. Carlyle, T. Nakano, S.M. Lewis, and J.C. Zuniga-Pflucker. 1999. Functional characterization of B lymphocytes generated in vitro from embryonic stem cells. *Proceedings of the National Academy of Sciences of the United States of America* 96:9797-9802.
- Chu, Z., B. Niu, H. Zhu, X. He, C. Bai, G. Li, and J. Hua. 2015. PRMT5 enhances generation of induced pluripotent stem cells from dairy goat embryonic fibroblasts via down-regulation of p53. *Cell Prolif* 48:29-38.
- Chung, E., and M. Kondo. 2011. Role of Ras/Raf/MEK/ERK signaling in physiological hematopoiesis and leukemia development. *Immunol Res* 49:248-268.
- Chung, J., V. Karkhanis, S. Tae, F. Yan, P. Smith, L.W. Ayers, C. Agostinelli, S. Pileri, G.V. Denis, R.A. Baiocchi, and S. Sif. 2013. Protein arginine methyltransferase 5 (PRMT5) inhibition induces lymphoma cell death through reactivation of the retinoblastoma tumor suppressor pathway and polycomb repressor complex 2 (PRC2) silencing. *The Journal of biological chemistry* 288:35534-35547.
- Clark, M.R., M. Mandal, K. Ochiai, and H. Singh. 2014. Orchestrating B cell lymphopoiesis through interplay of IL-7 receptor and pre-B cell receptor signalling. *Nature reviews. Immunology* 14:69-80.
- Clarke, T.L., M.P. Sanchez-Bailon, K. Chiang, J.J. Reynolds, J. Herrero-Ruiz, T.M. Bandejas, P.M. Matias, S.L. Maslen, J.M. Skehel, G.S. Stewart, and C.C. Davies. 2017. PRMT5-Dependent Methylation of the TIP60 Coactivator RUVBL1 Is a Key Regulator of Homologous Recombination. *Molecular cell* 65:900-916 e907.
- Coffey, F., B. Alabyev, and T. Manser. 2009. Initial clonal expansion of germinal center B cells takes place at the perimeter of follicles. *Immunity* 30:599-609.
- Crouch, E.E., Z. Li, M. Takizawa, S. Fichtner-Feigl, P. Gourzi, C. Montano, L. Feigenbaum, P. Wilson, S. Janz, F.N. Papavasiliou, and R. Casellas. 2007. Regulation of AID expression in the immune response. *The Journal of experimental medicine* 204:1145-1156.
- Crowder, R.N., H. Zhao, W.W. Chatham, T. Zhou, and R.H. Carter. 2011. B lymphocytes are resistant to death receptor 5-induced apoptosis. *Clin Immunol* 139:21-31.
- Cyster, J.G. 2010. B cell follicles and antigen encounters of the third kind. *Nature immunology* 11:989-996.
- Cyster, J.G., K.M. Ansel, K. Reif, E.H. Ekland, P.L. Hyman, H.L. Tang, S.A. Luther, and V.N. Ngo. 2000. Follicular stromal cells and lymphocyte homing to follicles. *Immunological reviews* 176:181-193.
- Dalla-Favera, K.B.a.R. 2015. Germinal centres and B cell lymphomagenesis. *nature reviews immunology* 15:172-184.
- Davies, D.R., and H. Metzger. 1983. Structural basis of antibody function. *Annual review of immunology* 1:87-117.
- De Silva, N.S., and U. Klein. 2015. Dynamics of B cells in germinal centres. *Nature reviews. Immunology* 15:137-148.
- Dhar, S., V. Vemulapalli, A.N. Patananan, G.L. Huang, A. Di Lorenzo, S. Richard, M.J. Comb, A. Guo, S.G. Clarke, and M.T. Bedford. 2013. Loss of the major Type I arginine methyltransferase PRMT1 causes substrate scavenging by other PRMTs. *Scientific reports* 3:1311.

- Di Lorenzo, A., and M.T. Bedford. 2011. Histone arginine methylation. *FEBS letters* 585:2024-2031.
- Di Noia, J.M., and M.S. Neuberger. 2007. Molecular mechanisms of antibody somatic hypermutation. *Annual review of biochemistry* 76:1-22.
- Diaz-Munoz, M.D., V.Y. Kiselev, N. Le Novere, T. Curk, J. Ule, and M. Turner. 2017. Tial dependent regulation of mRNA subcellular location and translation controls p53 expression in B cells. *Nature communications* 8:530.
- Ding, G., H.D. Liu, Q. Huang, H.X. Liang, Z.H. Ding, Z.J. Liao, and G. Huang. 2013. HDAC6 promotes hepatocellular carcinoma progression by inhibiting P53 transcriptional activity. *FEBS letters* 587:880-886.
- Do, R.K., E. Hatada, H. Lee, M.R. Tourigny, D. Hilbert, and S. Chen-Kiang. 2000. Attenuation of apoptosis underlies B lymphocyte stimulator enhancement of humoral immune response. *The Journal of experimental medicine* 192:953-964.
- Dobin, A., C.A. Davis, F. Schlesinger, J. Drenkow, C. Zaleski, S. Jha, P. Batut, M. Chaisson, and T.R. Gingeras. 2013. STAR: ultrafast universal RNA-seq aligner. *Bioinformatics* 29:15-21.
- Dolezal, E., S. Infantino, F. Drepper, T. Borsig, A. Singh, T. Wossning, G.J. Fiala, S. Minguet, B. Warscheid, D.M. Tarlinton, H. Jumaa, D. Medgyesi, and M. Reth. 2017. The BTG2-PRMT1 module limits pre-B cell expansion by regulating the CDK4-Cyclin-D3 complex. *Nature immunology* 18:911-920.
- Dominguez-Sola, D., J. Kung, A.B. Holmes, V.A. Wells, T. Mo, K. Basso, and R. Dalla-Favera. 2015. The FOXO1 Transcription Factor Instructs the Germinal Center Dark Zone Program. *Immunity* 43:1064-1074.
- Dominguez-Sola, D., G.D. Victora, C.Y. Ying, R.T. Phan, M. Saito, M.C. Nussenzweig, and R. Dalla-Favera. 2012. The proto-oncogene MYC is required for selection in the germinal center and cyclic reentry. *Nature immunology* 13:1083-1091.
- Eden, E., R. Navon, I. Steinfeld, D. Lipson, and Z. Yakhini. 2009. GOrilla: a tool for discovery and visualization of enriched GO terms in ranked gene lists. *BMC Bioinformatics* 10:48.
- Elakoum, R., G. Gauchotte, A. Oussalah, M.P. Wissler, C. Clement-Duchene, J.M. Vignaud, J.L. Gueant, and F. Namour. 2014. CARM1 and PRMT1 are dysregulated in lung cancer without hierarchical features. *Biochimie* 97:210-218.
- Elmore, S. 2007. Apoptosis: a review of programmed cell death. *Toxicol Pathol* 35:495-516.
- Endl, E., P. Steinbach, R. Knuchel, and F. Hofstadter. 1997. Analysis of cell cycle-related Ki-67 and p120 expression by flow cytometric BrdUrd-Hoechst/7AAD and immunolabeling technique. *Cytometry* 29:233-241.
- Eram, M.S., Y. Shen, M. Szewczyk, H. Wu, G. Senisterra, F. Li, K.V. Butler, H.U. Kaniskan, B.A. Speed, C. Dela Sena, A. Dong, H. Zeng, M. Schapira, P.J. Brown, C.H. Arrowsmith, D. Barsyte-Lovejoy, J. Liu, M. Vedadi, and J. Jin. 2016. A Potent, Selective, and Cell-Active Inhibitor of Human Type I Protein Arginine Methyltransferases. *ACS chemical biology* 11:772-781.
- Ersching, J., A. Efeyan, L. Mesin, J.T. Jacobsen, G. Pasqual, B.C. Grabiner, D. Dominguez-Sola, D.M. Sabatini, and G.D. Victora. 2017. Germinal Center Selection and Affinity Maturation Require Dynamic Regulation of mTORC1 Kinase. *Immunity* 46:1045-1058 e1046.
- Fischer, M. 2017. Census and evaluation of p53 target genes. *Oncogene* 36:3943-3956.

- Fischer, U., and R. Luhrmann. 1990. An essential signaling role for the m3G cap in the transport of U1 snRNP to the nucleus. *Science* 249:786-790.
- Friesen, W.J., S. Paushkin, A. Wyce, S. Massenet, G.S. Pesiridis, G. Van Duyne, J. Rappsilber, M. Mann, and G. Dreyfuss. 2001. The methylosome, a 20S complex containing JBP1 and pICln, produces dimethylarginine-modified Sm proteins. *Molecular and cellular biology* 21:8289-8300.
- Friesen, W.J., A. Wyce, S. Paushkin, L. Abel, J. Rappsilber, M. Mann, and G. Dreyfuss. 2002. A novel WD repeat protein component of the methylosome binds Sm proteins. *The Journal of biological chemistry* 277:8243-8247.
- Gao, G., S. Dhar, and M.T. Bedford. 2017. PRMT5 regulates IRES-dependent translation via methylation of hnRNP A1. *Nucleic acids research* 45:4359-4369.
- Gao, Y., Y. Zhao, J. Zhang, Y. Lu, X. Liu, P. Geng, B. Huang, Y. Zhang, and J. Lu. 2016. The dual function of PRMT1 in modulating epithelial-mesenchymal transition and cellular senescence in breast cancer cells through regulation of ZEB1. *Scientific reports* 6:19874.
- Gary, J.D., and S. Clarke. 1998. RNA and protein interactions modulated by protein arginine methylation. *Prog Nucleic Acid Res Mol Biol* 61:65-131.
- Gass, J.N., K.E. Gunn, R. Sriburi, and J.W. Brewer. 2004. Stressed-out B cells? Plasma-cell differentiation and the unfolded protein response. *Trends in immunology* 25:17-24.
- Gayatri, S., and M.T. Bedford. 2014. Readers of histone methylarginine marks. *Biochimica et biophysica acta* 1839:702-710.
- Genestier, L., M. Taillardet, P. Mondiere, H. Gheit, C. Bella, and T. Defrance. 2007. TLR agonists selectively promote terminal plasma cell differentiation of B cell subsets specialized in thymus-independent responses. *Journal of immunology* 178:7779-7786.
- Geoghegan, V., A. Guo, D. Trudgian, B. Thomas, and O. Acuto. 2015. Comprehensive identification of arginine methylation in primary T cells reveals regulatory roles in cell signalling. *Nature communications* 6:6758.
- Gitlin, A.D., Z. Shulman, and M.C. Nussenzweig. 2014. Clonal selection in the germinal centre by regulated proliferation and hypermutation. *Nature* 509:637-640.
- Gkountela, S., Z. Li, C.J. Chin, S.A. Lee, and A.T. Clark. 2014. PRMT5 is required for human embryonic stem cell proliferation but not pluripotency. *Stem Cell Rev* 10:230-239.
- Goenka, R., A.H. Matthews, B. Zhang, P.J. O'Neill, J.L. Scholz, T.S. Migone, W.J. Leonard, W. Stohl, U. Hershberg, and M.P. Cancro. 2014. Local BLyS production by T follicular cells mediates retention of high affinity B cells during affinity maturation. *The Journal of experimental medicine* 211:45-56.
- Good-Jacobson, K.L., Y. Chen, A.K. Voss, G.K. Smyth, T. Thomas, and D. Tarlinton. 2014. Regulation of germinal center responses and B-cell memory by the chromatin modifier MOZ. *Proceedings of the National Academy of Sciences of the United States of America* 111:9585-9590.
- Gostissa, M., J.M. Bianco, D.J. Malkin, J.L. Kutok, S.J. Rodig, H.C. Morse, 3rd, C.H. Bassing, and F.W. Alt. 2013. Conditional inactivation of p53 in mature B cells promotes generation of nongerminal center-derived B-cell lymphomas. *Proceedings of the National Academy of Sciences of the United States of America* 110:2934-2939.
- Goulet, I., G. Gauvin, S. Boisvenue, and J. Cote. 2007. Alternative splicing yields protein arginine methyltransferase 1 isoforms with distinct activity, substrate specificity, and subcellular localization. *The Journal of biological chemistry* 282:33009-33021.

- Greer, E.L., and A. Brunet. 2005. FOXO transcription factors at the interface between longevity and tumor suppression. *Oncogene* 24:7410-7425.
- Gu, Z., S. Gao, F. Zhang, Z. Wang, W. Ma, R.E. Davis, and Z. Wang. 2012a. Protein arginine methyltransferase 5 is essential for growth of lung cancer cells. *The Biochemical journal* 446:235-241.
- Gu, Z., Y. Li, P. Lee, T. Liu, C. Wan, and Z. Wang. 2012b. Protein arginine methyltransferase 5 functions in opposite ways in the cytoplasm and nucleus of prostate cancer cells. *PloS one* 7:e44033.
- Guderian, G., C. Peter, J. Wiesner, A. Sickmann, K. Schulze-Osthoff, U. Fischer, and M. Grimm. 2011. RioK1, a new interactor of protein arginine methyltransferase 5 (PRMT5), competes with pICln for binding and modulates PRMT5 complex composition and substrate specificity. *The Journal of biological chemistry* 286:1976-1986.
- Guidos, C.J., C.J. Williams, I. Grandal, G. Knowles, M.T. Huang, and J.S. Danska. 1996. V(D)J recombination activates a p53-dependent DNA damage checkpoint in scid lymphocyte precursors. *Genes & development* 10:2038-2054.
- Hardy, R.R., and K. Hayakawa. 2001. B cell development pathways. *Annual review of immunology* 19:595-621.
- Harris, D.P., S. Bandyopadhyay, T.J. Maxwell, B. Willard, and P.E. DiCorleto. 2014. Tumor necrosis factor (TNF)-alpha induction of CXCL10 in endothelial cells requires protein arginine methyltransferase 5 (PRMT5)-mediated nuclear factor (NF)-kappaB p65 methylation. *The Journal of biological chemistry* 289:15328-15339.
- Harris, L.J., S.B. Larson, K.W. Hasel, J. Day, A. Greenwood, and A. McPherson. 1992. The three-dimensional structure of an intact monoclonal antibody for canine lymphoma. *Nature* 360:369-372.
- Hasbold, J., L.M. Corcoran, D.M. Tarlinton, S.G. Tangye, and P.D. Hodgkin. 2004. Evidence from the generation of immunoglobulin G-secreting cells that stochastic mechanisms regulate lymphocyte differentiation. *Nature immunology* 5:55-63.
- Hasham, M.G., N.M. Donghia, E. Coffey, J. Maynard, K.J. Snow, J. Ames, R.Y. Wilpan, Y. He, B.L. King, and K.D. Mills. 2010. Widespread genomic breaks generated by activation-induced cytidine deaminase are prevented by homologous recombination. *Nature immunology* 11:820-826.
- Hashimoto, M., K. Murata, J. Ishida, A. Kanou, Y. Kasuya, and A. Fukamizu. 2016. Severe Hypomyelination and Developmental Defects Are Caused in Mice Lacking Protein Arginine Methyltransferase 1 (PRMT1) in the Central Nervous System. *The Journal of biological chemistry* 291:2237-2245.
- Hata, K., and J. Mizuguchi. 2013. Arginine methylation regulates antibody responses through modulating cell division and isotype switching in B cells. *Microbiology and immunology* 57:185-192.
- Hata, K., N. Yanase, K. Sudo, H. Kiyonari, Y. Mukumoto, J. Mizuguchi, and T. Yokosuka. 2016. Differential regulation of T-cell dependent and T-cell independent antibody responses through arginine methyltransferase PRMT1 in vivo. *FEBS letters* 590:1200-1210.
- Heinz, S., C. Benner, N. Spann, E. Bertolino, Y.C. Lin, P. Laslo, J.X. Cheng, C. Murre, H. Singh, and C.K. Glass. 2010. Simple combinations of lineage-determining

- transcription factors prime cis-regulatory elements required for macrophage and B cell identities. *Molecular cell* 38:576-589.
- Heinzel, S., T. Binh Giang, A. Kan, J.M. Marchingo, B.K. Lye, L.M. Corcoran, and P.D. Hodgkin. 2017. A Myc-dependent division timer complements a cell-death timer to regulate T cell and B cell responses. *Nature immunology* 18:96-103.
- Heise, N., N.S. De Silva, K. Silva, A. Carette, G. Simonetti, M. Pasparakis, and U. Klein. 2014. Germinal center B cell maintenance and differentiation are controlled by distinct NF-kappaB transcription factor subunits. *The Journal of experimental medicine* 211:2103-2118.
- Hennino, A., M. Berard, P.H. Krammer, and T. Defrance. 2001. FLICE-inhibitory protein is a key regulator of germinal center B cell apoptosis. *The Journal of experimental medicine* 193:447-458.
- Hobeika, E., E. Levit-Zerdoun, V. Anastasopoulou, R. Pohlmeier, S. Altmeier, A. Alsadeq, M.W. Dobenecker, R. Pelanda, and M. Reth. 2015. CD19 and BAFF-R can signal to promote B-cell survival in the absence of Syk. *The EMBO journal* 34:925-939.
- Hobeika, E., S. Thiemann, B. Storch, H. Jumaa, P.J. Nielsen, R. Pelanda, and M. Reth. 2006. Testing gene function early in the B cell lineage in mb1-cre mice. *Proceedings of the National Academy of Sciences of the United States of America* 103:13789-13794.
- Hodgkin, P.D., J.H. Lee, and A.B. Lyons. 1996. B cell differentiation and isotype switching is related to division cycle number. *The Journal of experimental medicine* 184:277-281.
- Hoek, K.L., L.E. Gordy, P.L. Collins, V.V. Parekh, T.M. Aune, S. Joyce, J.W. Thomas, L. Van Kaer, and E. Sebzda. 2010. Follicular B cell trafficking within the spleen actively restricts humoral immune responses. *Immunity* 33:254-265.
- Hsu, J.M., C.T. Chen, C.K. Chou, H.P. Kuo, L.Y. Li, C.Y. Lin, H.J. Lee, Y.N. Wang, M. Liu, H.W. Liao, B. Shi, C.C. Lai, M.T. Bedford, C.H. Tsai, and M.C. Hung. 2011. Crosstalk between Arg 1175 methylation and Tyr 1173 phosphorylation negatively modulates EGFR-mediated ERK activation. *Nature cell biology* 13:174-181.
- Hu, D., M. Gur, Z. Zhou, A. Gamper, M.C. Hung, N. Fujita, L. Lan, I. Bahar, and Y. Wan. 2015. Interplay between arginine methylation and ubiquitylation regulates KLF4-mediated genome stability and carcinogenesis. *Nature communications* 6:8419.
- Hu, H., K. Qian, M.C. Ho, and Y.G. Zheng. 2016. Small Molecule Inhibitors of Protein Arginine Methyltransferases. *Expert Opin Investig Drugs* 25:335-358.
- Huang da, W., B.T. Sherman, R. Stephens, M.W. Baseler, H.C. Lane, and R.A. Lempicki. 2008. DAVID gene ID conversion tool. *Bioinformatics* 24:428-430.
- Huang, J., G. Vogel, Z. Yu, G. Almazan, and S. Richard. 2011. Type II arginine methyltransferase PRMT5 regulates gene expression of inhibitors of differentiation/DNA binding Id2 and Id4 during glial cell differentiation. *The Journal of biological chemistry* 286:44424-44432.
- Igarashi, H., K. Kuwahara, M. Yoshida, Y. Xing, K. Maeda, K. Nakajima, and N. Sakaguchi. 2009. GANP suppresses the arginine methyltransferase PRMT5 regulating IL-4-mediated STAT6-signaling to IgE production in B cells. *Molecular immunology* 46:1031-1041.
- Infantino, S., B. Benz, T. Waldmann, M. Jung, R. Schneider, and M. Reth. 2010. Arginine methylation of the B cell antigen receptor promotes differentiation. *The Journal of experimental medicine* 207:711-719.

- Infantino, S., A. Light, K. O'Donnell, V. Bryant, D.T. Avery, M. Elliott, S.G. Tangye, G. Belz, F. Mackay, S. Richard, and D. Tarlinton. 2017. Arginine methylation catalyzed by PRMT1 is required for B cell activation and differentiation. *Nature communications* 8:891.
- Ise, W., K. Fujii, K. Shiroguchi, A. Ito, K. Kometani, K. Takeda, E. Kawakami, K. Yamashita, K. Suzuki, T. Okada, and T. Kurosaki. 2018. T Follicular Helper Cell-Germinal Center B Cell Interaction Strength Regulates Entry into Plasma Cell or Recycling Germinal Center Cell Fate. *Immunity* 48:702-715 e704.
- Jacks, T., L. Remington, B.O. Williams, E.M. Schmitt, S. Halachmi, R.T. Bronson, and R.A. Weinberg. 1994. Tumor spectrum analysis in p53-mutant mice. *Current biology : CB* 4:1-7.
- Jacob, A., D. Cooney, M. Pradhan, and K.M. Coggeshall. 2002. Convergence of signaling pathways on the activation of ERK in B cells. *The Journal of biological chemistry* 277:23420-23426.
- Jacob, J., J. Przylepa, C. Miller, and G. Kelsoe. 1993. In situ studies of the primary immune response to (4-hydroxy-3-nitrophenyl)acetyl. III. The kinetics of V region mutation and selection in germinal center B cells. *The Journal of experimental medicine* 178:1293-1307.
- Jansson, M., S.T. Durant, E.C. Cho, S. Sheahan, M. Edelmann, B. Kessler, and N.B. La Thangue. 2008. Arginine methylation regulates the p53 response. *Nature cell biology* 10:1431-1439.
- Jiang, H., M.B. Harris, and P. Rothman. 2000. IL-4/IL-13 signaling beyond JAK/STAT. *The Journal of allergy and clinical immunology* 105:1063-1070.
- Jin, S., Y. Mi, J. Song, P. Zhang, and Y. Liu. 2018. PRMT1-RBM15 axis regulates megakaryocytic differentiation of human umbilical cord blood CD34(+) cells. *Exp Ther Med* 15:2563-2568.
- Jin, Y., J. Zhou, F. Xu, B. Jin, L. Cui, Y. Wang, X. Du, J. Li, P. Li, R. Ren, and J. Pan. 2016. Targeting methyltransferase PRMT5 eliminates leukemia stem cells in chronic myelogenous leukemia. *The Journal of clinical investigation* 126:3961-3980.
- Kallies, A., J. Hasbold, D.M. Tarlinton, W. Dietrich, L.M. Corcoran, P.D. Hodgkin, and S.L. Nutt. 2004. Plasma cell ontogeny defined by quantitative changes in blimp-1 expression. *The Journal of experimental medicine* 200:967-977.
- Kaniskan, H.U., M.L. Martini, and J. Jin. 2018. Inhibitors of Protein Methyltransferases and Demethylases. *Chem Rev* 118:989-1068.
- Karkhanis, V., Y.J. Hu, R.A. Baiocchi, A.N. Imbalzano, and S. Sif. 2011. Versatility of PRMT5-induced methylation in growth control and development. *Trends in biochemical sciences* 36:633-641.
- Kaushik, S., F. Liu, K.J. Veazey, G. Gao, P. Das, L.F. Neves, K. Lin, Y. Zhong, Y. Lu, V. Giuliani, M.T. Bedford, S.D. Nimer, and M.A. Santos. 2017. Genetic deletion or small-molecule inhibition of the arginine methyltransferase PRMT5 exhibit anti-tumoral activity in mouse models of MLL-rearranged AML. *Leukemia*
- Kedersha, N., and P. Anderson. 2002. Stress granules: sites of mRNA triage that regulate mRNA stability and translatability. *Biochem Soc Trans* 30:963-969.
- Kerfoot, S.M., G. Yaari, J.R. Patel, K.L. Johnson, D.G. Gonzalez, S.H. Kleinstein, and A.M. Haberman. 2011. Germinal center B cell and T follicular helper cell development initiates in the interfollicular zone. *Immunity* 34:947-960.

- Kim, S., U. Gunesdogan, J.J. Zylitz, J.A. Hackett, D. Cougot, S. Bao, C. Lee, S. Dietmann, G.E. Allen, R. Sengupta, and M.A. Surani. 2014. PRMT5 protects genomic integrity during global DNA demethylation in primordial germ cells and preimplantation embryos. *Molecular cell* 56:564-579.
- King, I.L., and M. Mohrs. 2009. IL-4-producing CD4⁺ T cells in reactive lymph nodes during helminth infection are T follicular helper cells. *The Journal of experimental medicine* 206:1001-1007.
- Kischkel, F.C., D.A. Lawrence, A. Chuntharapai, P. Schow, K.J. Kim, and A. Ashkenazi. 2000. Apo2L/TRAIL-dependent recruitment of endogenous FADD and caspase-8 to death receptors 4 and 5. *Immunity* 12:611-620.
- Kitamura, D., J. Roes, R. Kuhn, and K. Rajewsky. 1991. A B cell-deficient mouse by targeted disruption of the membrane exon of the immunoglobulin mu chain gene. *Nature* 350:423-426.
- Kitano, M., S. Moriyama, Y. Ando, M. Hikida, Y. Mori, T. Kurosaki, and T. Okada. 2011. Bcl6 protein expression shapes pre-germinal center B cell dynamics and follicular helper T cell heterogeneity. *Immunity* 34:961-972.
- Klaewsongkram, J., Y. Yang, S. Golech, J. Katz, K.H. Kaestner, and N.P. Weng. 2007. Kruppel-like factor 4 regulates B cell number and activation-induced B cell proliferation. *Journal of immunology* 179:4679-4684.
- Klein, U., and N. Heise. 2015. Unexpected functions of nuclear factor-kappaB during germinal center B-cell development: implications for lymphomagenesis. *Curr Opin Hematol* 22:379-387.
- Koh, C.M., M. Bezzi, and E. Guccione. 2015a. The where and how of PRMT5. *Current molecular biology reports* 1:19-28.
- Koh, C.M., M. Bezzi, D.H. Low, W.X. Ang, S.X. Teo, F.P. Gay, M. Al-Haddawi, S.Y. Tan, M. Osato, A. Sabo, B. Amati, K.B. Wee, and E. Guccione. 2015b. MYC regulates the core pre-mRNA splicing machinery as an essential step in lymphomagenesis. *Nature* 523:96-100.
- Kondo, M., K. Akashi, J. Domen, K. Sugamura, and I.L. Weissman. 1997. Bcl-2 rescues T lymphopoiesis, but not B or NK cell development, in common gamma chain-deficient mice. *Immunity* 7:155-162.
- Kouzine, F., D. Wojtowicz, A. Yamane, W. Resch, K.R. Kieffer-Kwon, R. Bandle, S. Nelson, H. Nakahashi, P. Awasthi, L. Feigenbaum, H. Menoni, J. Hoeijmakers, W. Vermeulen, H. Ge, T.M. Przytycka, D. Levens, and R. Casellas. 2013. Global regulation of promoter melting in naive lymphocytes. *Cell* 153:988-999.
- Kraus, M., M.B. Alimzhanov, N. Rajewsky, and K. Rajewsky. 2004. Survival of resting mature B lymphocytes depends on BCR signaling via the Igalphabeta heterodimer. *Cell* 117:787-800.
- Krautler, N.J., D. Suan, D. Butt, K. Bourne, J.R. Hermes, T.D. Chan, C. Sundling, W. Kaplan, P. Schofield, J. Jackson, A. Basten, D. Christ, and R. Brink. 2017. Differentiation of germinal center B cells into plasma cells is initiated by high-affinity antigen and completed by Tfh cells. *The Journal of experimental medicine* 214:1259-1267.
- Kruse, J.P., and W. Gu. 2009. Modes of p53 regulation. *Cell* 137:609-622.
- Kryukov, G.V., F.H. Wilson, J.R. Ruth, J. Paulk, A. Tsherniak, S.E. Marlow, F. Vazquez, B.A. Weir, M.E. Fitzgerald, M. Tanaka, C.M. Bielski, J.M. Scott, C. Dennis, G.S. Cowley, J.S. Boehm, D.E. Root, T.R. Golub, C.B. Clish, J.E. Bradner, W.C. Hahn, and

- L.A. Garraway. 2016. MTAP deletion confers enhanced dependency on the PRMT5 arginine methyltransferase in cancer cells. *Science* 351:1214-1218.
- Kuchen, S., W. Resch, A. Yamane, N. Kuo, Z. Li, T. Chakraborty, L. Wei, A. Laurence, T. Yasuda, S. Peng, J. Hu-Li, K. Lu, W. Dubois, Y. Kitamura, N. Charles, H.W. Sun, S. Muljo, P.L. Schwartzberg, W.E. Paul, J. O'Shea, K. Rajewsky, and R. Casellas. 2010. Regulation of microRNA expression and abundance during lymphopoiesis. *Immunity* 32:828-839.
- Kuhn, R., F. Schwenk, M. Aguet, and K. Rajewsky. 1995. Inducible gene targeting in mice. *Science* 269:1427-1429.
- Kuppers, R., and R. Dalla-Favera. 2001. Mechanisms of chromosomal translocations in B cell lymphomas. *Oncogene* 20:5580-5594.
- Kuppers, R., U. Klein, M.L. Hansmann, and K. Rajewsky. 1999. Cellular origin of human B-cell lymphomas. *N Engl J Med* 341:1520-1529.
- Kuraoka, M., A.G. Schmidt, T. Nojima, F. Feng, A. Watanabe, D. Kitamura, S.C. Harrison, T.B. Kepler, and G. Kelsoe. 2016. Complex Antigens Drive Permissive Clonal Selection in Germinal Centers. *Immunity* 44:542-552.
- Kurosaki, T., K. Kometani, and W. Ise. 2015. Memory B cells. *Nature reviews. Immunology* 15:149-159.
- Kurosaki, T., H. Shinohara, and Y. Baba. 2010. B cell signaling and fate decision. *Annual review of immunology* 28:21-55.
- Kuwahara, K., M. Yoshida, E. Kondo, A. Sakata, Y. Watanabe, E. Abe, Y. Kouno, S. Tomiyasu, S. Fujimura, T. Tokuhisa, H. Kimura, T. Ezaki, and N. Sakaguchi. 2000. A novel nuclear phosphoprotein, GANP, is up-regulated in centrocytes of the germinal center and associated with MCM3, a protein essential for DNA replication. *Blood* 95:2321-2328.
- Kwak, Y.T., J. Guo, S. Prajapati, K.J. Park, R.M. Surabhi, B. Miller, P. Gehrig, and R.B. Gaynor. 2003. Methylation of SPT5 regulates its interaction with RNA polymerase II and transcriptional elongation properties. *Molecular cell* 11:1055-1066.
- Kwon, H., D. Thierry-Mieg, J. Thierry-Mieg, H.P. Kim, J. Oh, C. Tunyaplin, S. Carotta, C.E. Donovan, M.L. Goldman, P. Taylor, K. Ozato, D.E. Levy, S.L. Nutt, K. Calame, and W.J. Leonard. 2009. Analysis of interleukin-21-induced Prdm1 gene regulation reveals functional cooperation of STAT3 and IRF4 transcription factors. *Immunity* 31:941-952.
- Kwon, K., C. Hutter, Q. Sun, I. Bilic, C. Cobaleda, S. Malin, and M. Busslinger. 2008. Instructive role of the transcription factor E2A in early B lymphopoiesis and germinal center B cell development. *Immunity* 28:751-762.
- Lacroix, M., S. El Messaoudi, G. Rodier, A. Le Cam, C. Sardet, and E. Fabbrizio. 2008. The histone-binding protein COPR5 is required for nuclear functions of the protein arginine methyltransferase PRMT5. *EMBO reports* 9:452-458.
- Lai, A.Y., and M. Kondo. 2008. T and B lymphocyte differentiation from hematopoietic stem cell. *Seminars in immunology* 20:207-212.
- Lai, A.Y., and P.A. Wade. 2011. Cancer biology and NuRD: a multifaceted chromatin remodelling complex. *Nature reviews. Cancer* 11:588-596.
- Lanzavecchia, A. 1985. Antigen-specific interaction between T and B cells. *Nature* 314:537-539.

- Le Guezennec, X., M. Vermeulen, A.B. Brinkman, W.A. Hoeijmakers, A. Cohen, E. Lasonder, and H.G. Stunnenberg. 2006. MBD2/NuRD and MBD3/NuRD, two distinct complexes with different biochemical and functional properties. *Molecular and cellular biology* 26:843-851.
- Lee, J., and S. Desiderio. 1999. Cyclin A/CDK2 regulates V(D)J recombination by coordinating RAG-2 accumulation and DNA repair. *Immunity* 11:771-781.
- Legube, G., L.K. Linares, S. Tyteca, C. Caron, M. Scheffner, M. Chevillard-Briet, and D. Trouche. 2004. Role of the histone acetyl transferase Tip60 in the p53 pathway. *The Journal of biological chemistry* 279:44825-44833.
- Li, B., L. Liu, X. Li, and L. Wu. 2015a. miR-503 suppresses metastasis of hepatocellular carcinoma cell by targeting PRMT1. *Biochemical and biophysical research communications* 464:982-987.
- Li, Y., N. Chitnis, H. Nakagawa, Y. Kita, S. Natsugoe, Y. Yang, Z. Li, M.A. Wasik, A.J. Klein-Szanto, A.K. Rustgi, and J.A. Diehl. 2015b. PRMT5 is required for lymphomagenesis triggered by multiple oncogenic drivers. *Cancer discovery*
- Li, Z., J. Yu, L. Hosohama, K. Nee, S. Gkountela, S. Chaudhari, A.A. Cass, X. Xiao, and A.T. Clark. 2015c. The Sm protein methyltransferase PRMT5 is not required for primordial germ cell specification in mice. *The EMBO journal* 34:748-758.
- Liao, H.W., J.M. Hsu, W. Xia, H.L. Wang, Y.N. Wang, W.C. Chang, S.T. Arold, C.K. Chou, P.H. Tsou, H. Yamaguchi, Y.F. Fang, H.J. Lee, H.H. Lee, S.K. Tai, M.H. Yang, M.P. Morelli, M. Sen, J.E. Ladbury, C.H. Chen, J.R. Grandis, S. Kopetz, and M.C. Hung. 2015. PRMT1-mediated methylation of the EGF receptor regulates signaling and cetuximab response. *The Journal of clinical investigation* 125:4529-4543.
- Liao, Y., G.K. Smyth, and W. Shi. 2014. featureCounts: an efficient general purpose program for assigning sequence reads to genomic features. *Bioinformatics* 30:923-930.
- Liberzon, A., C. Birger, H. Thorvaldsdottir, M. Ghandi, J.P. Mesirov, and P. Tamayo. 2015. The Molecular Signatures Database (MSigDB) hallmark gene set collection. *Cell Syst* 1:417-425.
- Liberzon, A., A. Subramanian, R. Pinchback, H. Thorvaldsdottir, P. Tamayo, and J.P. Mesirov. 2011. Molecular signatures database (MSigDB) 3.0. *Bioinformatics* 27:1739-1740.
- Lin, K.I., Y. Lin, and K. Calame. 2000. Repression of c-myc is necessary but not sufficient for terminal differentiation of B lymphocytes in vitro. *Molecular and cellular biology* 20:8684-8695.
- Lin, W.C., and S. Desiderio. 1994. Cell cycle regulation of V(D)J recombination-activating protein RAG-2. *Proceedings of the National Academy of Sciences of the United States of America* 91:2733-2737.
- Lin, W.J., J.D. Gary, M.C. Yang, S. Clarke, and H.R. Herschman. 1996. The mammalian immediate-early TIS21 protein and the leukemia-associated BTG1 protein interact with a protein-arginine N-methyltransferase. *The Journal of biological chemistry* 271:15034-15044.
- Lin, Y., K. Wong, and K. Calame. 1997. Repression of c-myc transcription by Blimp-1, an inducer of terminal B cell differentiation. *Science* 276:596-599.
- Link, A., T.K. Vogt, S. Favre, M.R. Britschgi, H. Acha-Orbea, B. Hinz, J.G. Cyster, and S.A. Luther. 2007. Fibroblastic reticular cells in lymph nodes regulate the homeostasis of naive T cells. *Nature immunology* 8:1255-1265.

- Linterman, M.A., L. Beaton, D. Yu, R.R. Ramiscal, M. Srivastava, J.J. Hogan, N.K. Verma, M.J. Smyth, R.J. Rigby, and C.G. Vinuesa. 2010. IL-21 acts directly on B cells to regulate Bcl-6 expression and germinal center responses. *The Journal of experimental medicine* 207:353-363.
- Liu, D., and A. Mamorska-Dyga. 2017. Syk inhibitors in clinical development for hematological malignancies. *Journal of hematology & oncology* 10:145.
- Liu, D., H. Xu, C. Shih, Z. Wan, X. Ma, W. Ma, D. Luo, and H. Qi. 2015a. T-B-cell entanglement and ICOSL-driven feed-forward regulation of germinal centre reaction. *Nature* 517:214-218.
- Liu, F., G. Cheng, P.J. Hamard, S. Greenblatt, L. Wang, N. Man, F. Perna, H. Xu, M. Tadi, L. Luciani, and S.D. Nimer. 2015b. Arginine methyltransferase PRMT5 is essential for sustaining normal adult hematopoiesis. *The Journal of clinical investigation* 125:3532-3544.
- Liu, F., X. Zhao, F. Perna, L. Wang, P. Koppikar, O. Abdel-Wahab, M.W. Harr, R.L. Levine, H. Xu, A. Tefferi, A. Deblasio, M. Hatlen, S. Menendez, and S.D. Nimer. 2011. JAK2V617F-mediated phosphorylation of PRMT5 downregulates its methyltransferase activity and promotes myeloproliferation. *Cancer cell* 19:283-294.
- Love, M.I., W. Huber, and S. Anders. 2014. Moderated estimation of fold change and dispersion for RNA-seq data with DESeq2. *Genome biology* 15:550.
- Lu, L., D. Lejtenyi, and D.G. Osmond. 1999. Regulation of cell survival during B lymphopoiesis: suppressed apoptosis of pro-B cells in P53-deficient mouse bone marrow. *Eur J Immunol* 29:2484-2490.
- Lu, L., and D.G. Osmond. 2000. Apoptosis and its modulation during B lymphopoiesis in mouse bone marrow. *Immunological reviews* 175:158-174.
- Lu, M., D.A. Lawrence, S. Marsters, D. Acosta-Alvear, P. Kimmig, A.S. Mendez, A.W. Paton, J.C. Paton, P. Walter, and A. Ashkenazi. 2014. Opposing unfolded-protein-response signals converge on death receptor 5 to control apoptosis. *Science* 345:98-101.
- Lundberg, A.S., and R.A. Weinberg. 1998. Functional inactivation of the retinoblastoma protein requires sequential modification by at least two distinct cyclin-cdk complexes. *Molecular and cellular biology* 18:753-761.
- Luo, W., F. Weisel, and M.J. Shlomchik. 2018. B Cell Receptor and CD40 Signaling Are Rewired for Synergistic Induction of the c-Myc Transcription Factor in Germinal Center B Cells. *Immunity*
- Lutzker, S., P. Rothman, R. Pollock, R. Coffman, and F.W. Alt. 1988. Mitogen- and IL-4-regulated expression of germ-line Ig gamma 2b transcripts: evidence for directed heavy chain class switching. *Cell* 53:177-184.
- Luxton, R.W., and E.J. Thompson. 1990. Affinity distributions of antigen-specific IgG in patients with multiple sclerosis and in patients with viral encephalitis. *Journal of immunological methods* 131:277-282.
- Ma, Y., R. Croxton, R.L. Moorer, Jr., and W.D. Cress. 2002. Identification of novel E2F1-regulated genes by microarray. *Archives of biochemistry and biophysics* 399:212-224.
- Maloney, A., P.A. Clarke, S. Naaby-Hansen, R. Stein, J.O. Koopman, A. Akpan, A. Yang, M. Zvelebil, R. Cramer, L. Stimson, W. Aherne, U. Banerji, I. Judson, S. Sharp, M. Powers, E. deBilly, J. Salmons, M. Walton, A. Burlingame, M. Waterfield, and P. Workman. 2007. Gene and protein expression profiling of human ovarian cancer cells

- treated with the heat shock protein 90 inhibitor 17-allylamino-17-demethoxygeldanamycin. *Cancer research* 67:3239-3253.
- Marichal, T., K. Ohata, D. Bedoret, C. Mesnil, C. Sabatel, K. Kobiyama, P. Lekeux, C. Coban, S. Akira, K.J. Ishii, F. Bureau, and C.J. Desmet. 2011. DNA released from dying host cells mediates aluminum adjuvant activity. *Nature medicine* 17:996-1002.
- Matera, A.G., and Z. Wang. 2014. A day in the life of the spliceosome. *Nature reviews. Molecular cell biology* 15:108-121.
- Matsuoka, M. 1972. [Epsilon-N-methylated lysine and guanidine-N-methylated arginine of proteins. 3. Presence and distribution in nature and mammals]. *Seikagaku* 44:364-370.
- Matthews, A.J., S. Zheng, L.J. DiMenna, and J. Chaudhuri. 2014. Regulation of immunoglobulin class-switch recombination: choreography of noncoding transcription, targeted DNA deamination, and long-range DNA repair. *Advances in immunology* 122:1-57.
- Mavrakis, K.J., E.R. McDonald, 3rd, M.R. Schlabach, E. Billy, G.R. Hoffman, A. deWeck, D.A. Ruddy, K. Venkatesan, J. Yu, G. McAllister, M. Stump, R. deBeaumont, S. Ho, Y. Yue, Y. Liu, Y. Yan-Neale, G. Yang, F. Lin, H. Yin, H. Gao, D.R. Kipp, S. Zhao, J.T. McNamara, E.R. Sprague, B. Zheng, Y. Lin, Y.S. Cho, J. Gu, K. Crawford, D. Ciccone, A.C. Vitari, A. Lai, V. Capka, K. Hurov, J.A. Porter, J. Tallarico, C. Mickanin, E. Lees, R. Pagliarini, N. Keen, T. Schmelzle, F. Hofmann, F. Stegmeier, and W.R. Sellers. 2016. Disordered methionine metabolism in MTAP/CDKN2A-deleted cancers leads to dependence on PRMT5. *Science* 351:1208-1213.
- Mayer, C.T., A. Gazumyan, E.E. Kara, A.D. Gitlin, J. Golijanin, C. Viant, J. Pai, T.Y. Oliveira, Q. Wang, A. Escolano, M. Medina-Ramirez, R.W. Sanders, and M.C. Nussenzweig. 2017. The microanatomic segregation of selection by apoptosis in the germinal center. *Science* 358:
- McCoy, K.D., M. Stoel, R. Stettler, P. Merky, K. Fink, B.M. Senn, C. Schaer, J. Massacand, B. Odermatt, H.C. Oettgen, R.M. Zinkernagel, N.A. Bos, H. Hengartner, A.J. Macpherson, and N.L. Harris. 2008. Polyclonal and specific antibodies mediate protective immunity against enteric helminth infection. *Cell Host Microbe* 4:362-373.
- Meister, G., C. Eggert, D. Buhler, H. Brahms, C. Kambach, and U. Fischer. 2001. Methylation of Sm proteins by a complex containing PRMT5 and the putative U snRNP assembly factor pICln. *Current biology : CB* 11:1990-1994.
- Melchers, F. 2015. Checkpoints that control B cell development. *The Journal of clinical investigation* 125:2203-2210.
- Meli, A.P., G. Fontes, C. Leung Soo, and I.L. King. 2017. T Follicular Helper Cell-Derived IL-4 Is Required for IgE Production during Intestinal Helminth Infection. *Journal of immunology* 199:244-252.
- Mesin, L., J. Ersching, and G.D. Victora. 2016. Germinal Center B Cell Dynamics. *Immunity* 45:471-482.
- Meyer-Hermann, M., E. Mohr, N. Pelletier, Y. Zhang, G.D. Victora, and K.M. Toellner. 2012. A theory of germinal center B cell selection, division, and exit. *Cell reports* 2:162-174.
- Minnich, M., H. Tagoh, P. Bonelt, E. Axelsson, M. Fischer, B. Cebolla, A. Tarakhovsky, S.L. Nutt, M. Jaritz, and M. Busslinger. 2016. Multifunctional role of the transcription factor Blimp-1 in coordinating plasma cell differentiation. *Nature immunology* 17:331-343.

- Mittrucker, H.W., T. Matsuyama, A. Grossman, T.M. Kundig, J. Potter, A. Shahinian, A. Wakeham, B. Patterson, P.S. Ohashi, and T.W. Mak. 1997. Requirement for the transcription factor LSIRF/IRF4 for mature B and T lymphocyte function. *Science* 275:540-543.
- Mizuno, T., and T.L. Rothstein. 2005. B cell receptor (BCR) cross-talk: CD40 engagement enhances BCR-induced ERK activation. *Journal of immunology* 174:3369-3376.
- Mongiardi, M.P., M. Savino, L. Bartoli, S. Beji, S. Nanni, F. Scagnoli, M.L. Falchetti, A. Favia, A. Farsetti, A. Levi, S. Nasi, and B. Illi. 2015. Myc and Omomyc functionally associate with the Protein Arginine Methyltransferase 5 (PRMT5) in glioblastoma cells. *Scientific reports* 5:15494.
- Monroe, J.G. 2006. ITAM-mediated tonic signalling through pre-BCR and BCR complexes. *Nature reviews. Immunology* 6:283-294.
- Morales, Y., D.V. Nitzel, O.M. Price, S. Gui, J. Li, J. Qu, and J.M. Hevel. 2015. Redox Control of Protein Arginine Methyltransferase 1 (PRMT1) Activity. *The Journal of biological chemistry* 290:14915-14926.
- Morin, R.D., N.A. Johnson, T.M. Severson, A.J. Mungall, J. An, R. Goya, J.E. Paul, M. Boyle, B.W. Woolcock, F. Kuchenbauer, D. Yap, R.K. Humphries, O.L. Griffith, S. Shah, H. Zhu, M. Kimbara, P. Shashkin, J.F. Charlot, M. Tcherpakov, R. Corbett, A. Tam, R. Varhol, D. Smailus, M. Moksa, Y. Zhao, A. Delaney, H. Qian, I. Birol, J. Schein, R. Moore, R. Holt, D.E. Horsman, J.M. Connors, S. Jones, S. Aparicio, M. Hirst, R.D. Gascoyne, and M.A. Marra. 2010. Somatic mutations altering EZH2 (Tyr641) in follicular and diffuse large B-cell lymphomas of germinal-center origin. *Nature genetics* 42:181-185.
- Morin, R.D., M. Mendez-Lago, A.J. Mungall, R. Goya, K.L. Mungall, R.D. Corbett, N.A. Johnson, T.M. Severson, R. Chiu, M. Field, S. Jackman, M. Krzywinski, D.W. Scott, D.L. Trinh, J. Tamura-Wells, S. Li, M.R. Firme, S. Rogic, M. Griffith, S. Chan, O. Yakovenko, I.M. Meyer, E.Y. Zhao, D. Smailus, M. Moksa, S. Chittaranjan, L. Rimsza, A. Brooks-Wilson, J.J. Spinelli, S. Ben-Neriah, B. Meissner, B. Woolcock, M. Boyle, H. McDonald, A. Tam, Y. Zhao, A. Delaney, T. Zeng, K. Tse, Y. Butterfield, I. Birol, R. Holt, J. Schein, D.E. Horsman, R. Moore, S.J. Jones, J.M. Connors, M. Hirst, R.D. Gascoyne, and M.A. Marra. 2011. Frequent mutation of histone-modifying genes in non-Hodgkin lymphoma. *Nature* 476:298-303.
- Mowen, K.A., and M. David. 2014. Unconventional post-translational modifications in immunological signaling. *Nature immunology* 15:512-520.
- Mowen, K.A., B.T. Schurter, J.W. Fathman, M. David, and L.H. Glimcher. 2004. Arginine methylation of NIP45 modulates cytokine gene expression in effector T lymphocytes. *Molecular cell* 15:559-571.
- Muramatsu, M., K. Kinoshita, S. Fagarasan, S. Yamada, Y. Shinkai, and T. Honjo. 2000. Class switch recombination and hypermutation require activation-induced cytidine deaminase (AID), a potential RNA editing enzyme. *Cell* 102:553-563.
- Murphy, K., P. Travers, M. Walport, and C. Janeway. 2012. Janeway's immunobiology. Garland Science, New York. xix, 868 p. pp.
- Nagamatsu, G., T. Kosaka, M. Kawasumi, T. Kinoshita, K. Takubo, H. Akiyama, T. Sudo, T. Kobayashi, M. Oya, and T. Suda. 2011. A germ cell-specific gene, Prmt5, works in somatic cell reprogramming. *The Journal of biological chemistry* 286:10641-10648.

- Nakamura, M., S. Kondo, M. Sugai, M. Nazarea, S. Imamura, and T. Honjo. 1996. High frequency class switching of an IgM⁺ B lymphoma clone CH12F3 to IgA⁺ cells. *International immunology* 8:193-201.
- Niiro, H., and E.A. Clark. 2002. Regulation of B-cell fate by antigen-receptor signals. *Nature reviews. Immunology* 2:945-956.
- Nojima, T., K. Haniuda, T. Moutai, M. Matsudaira, S. Mizokawa, I. Shiratori, T. Azuma, and D. Kitamura. 2011. In-vitro derived germinal centre B cells differentially generate memory B or plasma cells in vivo. *Nature communications* 2:465.
- Nutt, S.L., P.D. Hodgkin, D.M. Tarlinton, and L.M. Corcoran. 2015. The generation of antibody-secreting plasma cells. *Nature reviews. Immunology* 15:160-171.
- Ochiai, K., M. Maienschein-Cline, G. Simonetti, J. Chen, R. Rosenthal, R. Brink, A.S. Chong, U. Klein, A.R. Dinner, H. Singh, and R. Sciammas. 2013. Transcriptional regulation of germinal center B and plasma cell fates by dynamical control of IRF4. *Immunity* 38:918-929.
- Odendahl, M., H. Mei, B.F. Hoyer, A.M. Jacobi, A. Hansen, G. Muehlinghaus, C. Berek, F. Hiepe, R. Manz, A. Radbruch, and T. Dorner. 2005. Generation of migratory antigen-specific plasma blasts and mobilization of resident plasma cells in a secondary immune response. *Blood* 105:1614-1621.
- Okada, T., M.J. Miller, I. Parker, M.F. Krummel, M. Neighbors, S.B. Hartley, A. O'Garra, M.D. Cahalan, and J.G. Cyster. 2005. Antigen-engaged B cells undergo chemotaxis toward the T zone and form motile conjugates with helper T cells. *PLoS biology* 3:e150.
- Omori, S.A., M.H. Cato, A. Anzelon-Mills, K.D. Puri, M. Shapiro-Shelef, K. Calame, and R.C. Rickert. 2006. Regulation of class-switch recombination and plasma cell differentiation by phosphatidylinositol 3-kinase signaling. *Immunity* 25:545-557.
- Orthwein, A., and J.M. Di Noia. 2012. Activation induced deaminase: how much and where? *Seminars in immunology* 24:246-254.
- Osmond, D.G. 1991. Proliferation kinetics and the lifespan of B cells in central and peripheral lymphoid organs. *Current opinion in immunology* 3:179-185.
- Pal, S., R.A. Baiocchi, J.C. Byrd, M.R. Grever, S.T. Jacob, and S. Sif. 2007. Low levels of miR-92b/96 induce PRMT5 translation and H3R8/H4R3 methylation in mantle cell lymphoma. *The EMBO journal* 26:3558-3569.
- Pal, S., and S. Sif. 2007. Interplay between chromatin remodelers and protein arginine methyltransferases. *J Cell Physiol* 213:306-315.
- Pal, S., S.N. Vishwanath, H. Erdjument-Bromage, P. Tempst, and S. Sif. 2004. Human SWI/SNF-associated PRMT5 methylates histone H3 arginine 8 and negatively regulates expression of ST7 and NM23 tumor suppressor genes. *Molecular and cellular biology* 24:9630-9645.
- Palaniraja Thandapani, T.R.O.C., Timothy L. Bailey, and Stephane Richard. 2013. Defining the RGG/RG Motif. *Molecular cell review* 50:
- Papadokostopoulou, A., K. Mathioudaki, A. Scorilas, D. Xynopoulos, A. Ardavanis, E. Kouroumalis, and M. Talieri. 2009. Colon cancer and protein arginine methyltransferase 1 gene expression. *Anticancer Res* 29:1361-1366.
- Pappas, L., M. Foglierini, L. Piccoli, N.L. Kallewaard, F. Turrini, C. Silacci, B. Fernandez-Rodriguez, G. Agatic, I. Giacchetto-Sasselli, G. Pellicciotta, F. Sallusto, Q. Zhu, E.

- Vicenzi, D. Corti, and A. Lanzavecchia. 2014. Rapid development of broadly influenza neutralizing antibodies through redundant mutations. *Nature* 516:418-422.
- Parkin, J., and B. Cohen. 2001. An overview of the immune system. *Lancet* 357:1777-1789.
- Paus, D., T.G. Phan, T.D. Chan, S. Gardam, A. Basten, and R. Brink. 2006. Antigen recognition strength regulates the choice between extrafollicular plasma cell and germinal center B cell differentiation. *The Journal of experimental medicine* 203:1081-1091.
- Pawlak, M.R., C.A. Scherer, J. Chen, M.J. Roshon, and H.E. Ruley. 2000. Arginine N-methyltransferase 1 is required for early postimplantation mouse development, but cells deficient in the enzyme are viable. *Molecular and cellular biology* 20:4859-4869.
- Peled, J.U., J.J. Yu, J. Venkatesh, E. Bi, B.B. Ding, M. Krupski-Downs, R. Shaknovich, P. Sicinski, B. Diamond, M.D. Scharff, and B.H. Ye. 2010. Requirement for cyclin D3 in germinal center formation and function. *Cell Res* 20:631-646.
- Peperzak, V., I. Vikstrom, J. Walker, S.P. Glaser, M. LePage, C.M. Coquery, L.D. Erickson, K. Fairfax, F. Mackay, A. Strasser, S.L. Nutt, and D.M. Tarlinton. 2013. Mcl-1 is essential for the survival of plasma cells. *Nature immunology* 14:290-297.
- Phan, R.T., and R. Dalla-Favera. 2004. The BCL6 proto-oncogene suppresses p53 expression in germinal-centre B cells. *Nature* 432:635-639.
- Phan, R.T., M. Saito, K. Basso, H. Niu, and R. Dalla-Favera. 2005. BCL6 interacts with the transcription factor Miz-1 to suppress the cyclin-dependent kinase inhibitor p21 and cell cycle arrest in germinal center B cells. *Nature immunology* 6:1054-1060.
- Phan, T.G., I. Grigorova, T. Okada, and J.G. Cyster. 2007. Subcapsular encounter and complement-dependent transport of immune complexes by lymph node B cells. *Nature immunology* 8:992-1000.
- Pollack, B.P., S.V. Kotenko, W. He, L.S. Izotova, B.L. Barnoski, and S. Pestka. 1999. The human homologue of the yeast proteins Skb1 and Hsl7p interacts with Jak kinases and contains protein methyltransferase activity. *The Journal of biological chemistry* 274:31531-31542.
- Prieyl, J.A., and T.W. LeBien. 1996. Interleukin 7 independent development of human B cells. *Proceedings of the National Academy of Sciences of the United States of America* 93:10348-10353.
- Qin, D., J. Wu, K.A. Vora, J.V. Ravetch, A.K. Szakal, T. Manser, and J.G. Tew. 2000. Fc gamma receptor IIB on follicular dendritic cells regulates the B cell recall response. *Journal of immunology* 164:6268-6275.
- Rajewsky, K. 1996. Clonal selection and learning in the antibody system. *Nature* 381:751-758.
- Raman, B., C. Guarnaccia, K. Nadassy, S. Zakhariyev, A. Pintar, F. Zanuttin, D. Frigyes, C. Acatrinei, A. Vindigni, G. Pongor, and S. Pongor. 2001. N(omega)-arginine dimethylation modulates the interaction between a Gly/Arg-rich peptide from human nucleolin and nucleic acids. *Nucleic acids research* 29:3377-3384.
- Ranuncolo, S.M., J.M. Polo, J. Dierov, M. Singer, T. Kuo, J. Greally, R. Green, M. Carroll, and A. Melnick. 2007. Bcl-6 mediates the germinal center B cell phenotype and lymphomagenesis through transcriptional repression of the DNA-damage sensor ATR. *Nature immunology* 8:705-714.

- Reimold, A.M., N.N. Iwakoshi, J. Manis, P. Vallabhajosyula, E. Szomolanyi-Tsuda, E.M. Gravallesse, D. Friend, M.J. Grusby, F. Alt, and L.H. Glimcher. 2001. Plasma cell differentiation requires the transcription factor XBP-1. *Nature* 412:300-307.
- Ren, J., Y. Wang, Y. Liang, Y. Zhang, S. Bao, and Z. Xu. 2010. Methylation of ribosomal protein S10 by protein-arginine methyltransferase 5 regulates ribosome biogenesis. *The Journal of biological chemistry* 285:12695-12705.
- Rickert, R.C., J. Jellusova, and A.V. Miletic. 2011. Signaling by the tumor necrosis factor receptor superfamily in B-cell biology and disease. *Immunological reviews* 244:115-133.
- Rickert, R.C., J. Roes, and K. Rajewsky. 1997. B lymphocyte-specific, Cre-mediated mutagenesis in mice. *Nucleic acids research* 25:1317-1318.
- Robbiani, D.F., S. Bunting, N. Feldhahn, A. Bothmer, J. Camps, S. Deroubaix, K.M. McBride, I.A. Klein, G. Stone, T.R. Eisenreich, T. Ried, A. Nussenzweig, and M.C. Nussenzweig. 2009. AID produces DNA double-strand breaks in non-Ig genes and mature B cell lymphomas with reciprocal chromosome translocations. *Molecular cell* 36:631-641.
- Robbiani, D.F., S. Deroubaix, N. Feldhahn, T.Y. Oliveira, E. Callen, Q. Wang, M. Jankovic, I.T. Silva, P.C. Rommel, D. Bosque, T. Eisenreich, A. Nussenzweig, and M.C. Nussenzweig. 2015. Plasmodium Infection Promotes Genomic Instability and AID-Dependent B Cell Lymphoma. *Cell* 162:727-737.
- Robbiani, D.F., and M.C. Nussenzweig. 2013. Chromosome translocation, B cell lymphoma, and activation-induced cytidine deaminase. *Annual review of pathology* 8:79-103.
- Robin-Lespinasse, Y., S. Sentis, C. Kolytcheff, M.C. Rostan, L. Corbo, and M. Le Romancer. 2007. hCAF1, a new regulator of PRMT1-dependent arginine methylation. *Journal of cell science* 120:638-647.
- Rodda, L.B., O. Bannard, B. Ludewig, T. Nagasawa, and J.G. Cyster. 2015. Phenotypic and Morphological Properties of Germinal Center Dark Zone Cxcl12-Expressing Reticular Cells. *Journal of immunology* 195:4781-4791.
- Rolink, A.G., F. Melchers, and J. Andersson. 1999. The transition from immature to mature B cells. *Curr Top Microbiol Immunol* 246:39-43; discussion 44.
- Rolink, A.G., C. Schaniel, J. Andersson, and F. Melchers. 2001. Selection events operating at various stages in B cell development. *Current opinion in immunology* 13:202-207.
- Roth, D.B. 2014. V(D)J Recombination: Mechanism, Errors, and Fidelity. *Microbiol Spectr* 2:
- Rowland, B.D., and D.S. Peeper. 2006. KLF4, p21 and context-dependent opposing forces in cancer. *Nature reviews. Cancer* 6:11-23.
- Rust, H.L., V. Subramanian, G.M. West, D.D. Young, P.G. Schultz, and P.R. Thompson. 2014. Using unnatural amino acid mutagenesis to probe the regulation of PRMT1. *ACS chemical biology* 9:649-655.
- Saito, M., J. Gao, K. Basso, Y. Kitagawa, P.M. Smith, G. Bhagat, A. Pernis, L. Pasqualucci, and R. Dalla-Favera. 2007. A signaling pathway mediating downregulation of BCL6 in germinal center B cells is blocked by BCL6 gene alterations in B cell lymphoma. *Cancer cell* 12:280-292.
- Saito, M., U. Novak, E. Piovan, K. Basso, P. Sumazin, C. Schneider, M. Crespo, Q. Shen, G. Bhagat, A. Califano, A. Chadburn, L. Pasqualucci, and R. Dalla-Favera. 2009. BCL6 suppression of BCL2 via Miz1 and its disruption in diffuse large B cell lymphoma.

- Proceedings of the National Academy of Sciences of the United States of America* 106:11294-11299.
- Sakamaki, J., H. Daitoku, K. Ueno, A. Hagiwara, K. Yamagata, and A. Fukamizu. 2011. Arginine methylation of BCL-2 antagonist of cell death (BAD) counteracts its phosphorylation and inactivation by Akt. *Proceedings of the National Academy of Sciences of the United States of America* 108:6085-6090.
- Sanchez, S.E., E. Petrillo, E.J. Beckwith, X. Zhang, M.L. Rognone, C.E. Hernando, J.C. Cuevas, M.A. Godoy Herz, A. Depetris-Chauvin, C.G. Simpson, J.W. Brown, P.D. Cerdan, J.O. Borevitz, P. Mas, M.F. Ceriani, A.R. Kornblihtt, and M.J. Yanovsky. 2010. A methyl transferase links the circadian clock to the regulation of alternative splicing. *Nature* 468:112-116.
- Sander, S., V.T. Chu, T. Yasuda, A. Franklin, R. Graf, D.P. Calado, S. Li, K. Imami, M. Selbach, M. Di Virgilio, L. Bullinger, and K. Rajewsky. 2015. PI3 Kinase and FOXO1 Transcription Factor Activity Differentially Control B Cells in the Germinal Center Light and Dark Zones. *Immunity* 43:1075-1086.
- Sayegh, J., K. Webb, D. Cheng, M.T. Bedford, and S.G. Clarke. 2007. Regulation of protein arginine methyltransferase 8 (PRMT8) activity by its N-terminal domain. *The Journal of biological chemistry* 282:36444-36453.
- Schmidt-Suprian, M., and K. Rajewsky. 2007. Vagaries of conditional gene targeting. *Nature immunology* 8:665-668.
- Schoenhals, M., M. Jourdan, A. Seckinger, V. Pantesco, D. Hose, A. Kassambara, J. Moreaux, and B. Klein. 2016. Forced KLF4 expression increases the generation of mature plasma cells and uncovers a network linked with plasma cell stage. *Cell cycle* 15:1919-1928.
- Schwickert, T.A., G.D. Victora, D.R. Fooksman, A.O. Kamphorst, M.R. Mugnier, A.D. Gitlin, M.L. Dustin, and M.C. Nussenzweig. 2011. A dynamic T cell-limited checkpoint regulates affinity-dependent B cell entry into the germinal center. *The Journal of experimental medicine* 208:1243-1252.
- Sciammas, R., A.L. Shaffer, J.H. Schatz, H. Zhao, L.M. Staudt, and H. Singh. 2006. Graded expression of interferon regulatory factor-4 coordinates isotype switching with plasma cell differentiation. *Immunity* 25:225-236.
- Seo, W., T. Ikawa, H. Kawamoto, and I. Taniuchi. 2012. Runx1-Cbfbeta facilitates early B lymphocyte development by regulating expression of Ebf1. *The Journal of experimental medicine* 209:1255-1262.
- Shapiro-Shelef, M., K.I. Lin, L.J. McHeyzer-Williams, J. Liao, M.G. McHeyzer-Williams, and K. Calame. 2003. Blimp-1 is required for the formation of immunoglobulin secreting plasma cells and pre-plasma memory B cells. *Immunity* 19:607-620.
- Shen, S., J.W. Park, Z.X. Lu, L. Lin, M.D. Henry, Y.N. Wu, Q. Zhou, and Y. Xing. 2014. rMATS: robust and flexible detection of differential alternative splicing from replicate RNA-Seq data. *Proceedings of the National Academy of Sciences of the United States of America* 111:E5593-5601.
- Shi, W., Y. Liao, S.N. Willis, N. Taubenheim, M. Inouye, D.M. Tarlinton, G.K. Smyth, P.D. Hodgkin, S.L. Nutt, and L.M. Corcoran. 2015. Transcriptional profiling of mouse B cell terminal differentiation defines a signature for antibody-secreting plasma cells. *Nature immunology* 16:663-673.

- Shinnakasu, R., T. Inoue, K. Kometani, S. Moriyama, Y. Adachi, M. Nakayama, Y. Takahashi, H. Fukuyama, T. Okada, and T. Kurosaki. 2016. Regulated selection of germinal-center cells into the memory B cell compartment. *Nature immunology* 17:861-869.
- Shulman, Z., A.D. Gitlin, J.S. Weinstein, B. Lainez, E. Esplugues, R.A. Flavell, J.E. Craft, and M.C. Nussenzweig. 2014. Dynamic signaling by T follicular helper cells during germinal center B cell selection. *Science* 345:1058-1062.
- Slifka, M.K., R. Antia, J.K. Whitmire, and R. Ahmed. 1998. Humoral immunity due to long-lived plasma cells. *Immunity* 8:363-372.
- Smith, K.G., T.D. Hewitson, G.J. Nossal, and D.M. Tarlinton. 1996. The phenotype and fate of the antibody-forming cells of the splenic foci. *Eur J Immunol* 26:444-448.
- Smith, P., N. Syed, and T. Crook. 2006. Epigenetic inactivation implies a tumor suppressor function in hematologic malignancies for Polo-like kinase 2 but not Polo-like kinase 3. *Cell cycle* 5:1262-1264.
- Sonoda, E., Y. Pewzner-Jung, S. Schwerts, S. Taki, S. Jung, D. Eilat, and K. Rajewsky. 1997. B cell development under the condition of allelic inclusion. *Immunity* 6:225-233.
- Stavnezer, J., and C.E. Schrader. 2014. IgH chain class switch recombination: mechanism and regulation. *Journal of immunology* 193:5370-5378.
- Stone, K.D., C. Prussin, and D.D. Metcalfe. 2010. IgE, mast cells, basophils, and eosinophils. *The Journal of allergy and clinical immunology* 125:S73-80.
- Subramanian, A., P. Tamayo, V.K. Mootha, S. Mukherjee, B.L. Ebert, M.A. Gillette, A. Paulovich, S.L. Pomeroy, T.R. Golub, E.S. Lander, and J.P. Mesirov. 2005. Gene set enrichment analysis: a knowledge-based approach for interpreting genome-wide expression profiles. *Proceedings of the National Academy of Sciences of the United States of America* 102:15545-15550.
- Sun, L., M. Wang, Z. Lv, N. Yang, Y. Liu, S. Bao, W. Gong, and R.M. Xu. 2011. Structural insights into protein arginine symmetric dimethylation by PRMT5. *Proceedings of the National Academy of Sciences of the United States of America* 108:20538-20543.
- Sweet-Cordero, A., S. Mukherjee, A. Subramanian, H. You, J.J. Roix, C. Ladd-Acosta, J. Mesirov, T.R. Golub, and T. Jacks. 2005. An oncogenic KRAS2 expression signature identified by cross-species gene-expression analysis. *Nature genetics* 37:48-55.
- Tae, S., V. Karkhanis, K. Velasco, M. Yaneva, H. Erdjument-Bromage, P. Tempst, and S. Sif. 2011. Bromodomain protein 7 interacts with PRMT5 and PRC2, and is involved in transcriptional repression of their target genes. *Nucleic acids research* 39:5424-5438.
- Tanaka, H., Y. Hoshikawa, T. Oh-hara, S. Koike, M. Naito, T. Noda, H. Arai, T. Tsuruo, and N. Fujita. 2009. PRMT5, a novel TRAIL receptor-binding protein, inhibits TRAIL-induced apoptosis via nuclear factor-kappaB activation. *Mol Cancer Res* 7:557-569.
- Tang, J., A. Frankel, R.J. Cook, S. Kim, W.K. Paik, K.R. Williams, S. Clarke, and H.R. Herschman. 2000. PRMT1 is the predominant type I protein arginine methyltransferase in mammalian cells. *The Journal of biological chemistry* 275:7723-7730.
- Tang, L., E. Nogales, and C. Ciferri. 2010. Structure and function of SWI/SNF chromatin remodeling complexes and mechanistic implications for transcription. *Prog Biophys Mol Biol* 102:122-128.
- Tangye, S.G. 2011. Staying alive: regulation of plasma cell survival. *Trends in immunology* 32:595-602.

- Tarighat, S.S., R. Santhanam, D. Frankhouser, H.S. Radomska, H. Lai, M. Anghelina, H. Wang, X. Huang, L. Alinari, A. Walker, M.A. Caligiuri, C.M. Croce, L. Li, R. Garzon, C. Li, R.A. Baiocchi, and G. Marcucci. 2016. The dual epigenetic role of PRMT5 in acute myeloid leukemia: gene activation and repression via histone arginine methylation. *Leukemia* 30:789-799.
- Tas, J.M., L. Mesin, G. Pasqual, S. Targ, J.T. Jacobsen, Y.M. Mano, C.S. Chen, J.C. Weill, C.A. Reynaud, E.P. Browne, M. Meyer-Hermann, and G.D. Victora. 2016. Visualizing antibody affinity maturation in germinal centers. *Science* 351:1048-1054.
- Tee, W.W., M. Pardo, T.W. Theunissen, L. Yu, J.S. Choudhary, P. Hajkova, and M.A. Surani. 2010. Prmt5 is essential for early mouse development and acts in the cytoplasm to maintain ES cell pluripotency. *Genes & development* 24:2772-2777.
- Thandapani, P., J. Song, V. Gandin, Y. Cai, S.G. Rouleau, J.M. Garant, F.M. Boisvert, Z. Yu, J.P. Perreault, I. Topisirovic, and S. Richard. 2015. Aven recognition of RNA G-quadruplexes regulates translation of the mixed lineage leukemia protooncogenes. *Elife* 4:
- Tokoyoda, K., T. Egawa, T. Sugiyama, B.I. Choi, and T. Nagasawa. 2004. Cellular niches controlling B lymphocyte behavior within bone marrow during development. *Immunity* 20:707-718.
- Tourriere, H., K. Chebli, L. Zekri, B. Courselaud, J.M. Blanchard, E. Bertrand, and J. Tazi. 2003. The RasGAP-associated endoribonuclease G3BP assembles stress granules. *The Journal of cell biology* 160:823-831.
- Tsai, W.C., S. Gayatri, L.C. Reineke, G. Sbardella, M.T. Bedford, and R.E. Lloyd. 2016. Arginine Demethylation of G3BP1 Promotes Stress Granule Assembly. *The Journal of biological chemistry* 291:22671-22685.
- Tunayaplin, C., A.L. Shaffer, C.D. Angelin-Duclos, X. Yu, L.M. Staudt, and K.L. Calame. 2004. Direct repression of prdm1 by Bcl-6 inhibits plasmacytic differentiation. *Journal of immunology* 173:1158-1165.
- Ursini-Siegel, J., W. Zhang, A. Altmeyer, E.N. Hatada, R.K. Do, H. Yagita, and S. Chen-Kiang. 2002. TRAIL/Apo-2 ligand induces primary plasma cell apoptosis. *Journal of immunology* 169:5505-5513.
- van Galen, J.C., D.F. Dukers, C. Giroth, R.G. Sewalt, A.P. Otte, C.J. Meijer, and F.M. Raaphorst. 2004. Distinct expression patterns of polycomb oncoproteins and their binding partners during the germinal center reaction. *Eur J Immunol* 34:1870-1881.
- Velichutina, I., R. Shaknovich, H. Geng, N.A. Johnson, R.D. Gascoyne, A.M. Melnick, and O. Elemento. 2010. EZH2-mediated epigenetic silencing in germinal center B cells contributes to proliferation and lymphomagenesis. *Blood* 116:5247-5255.
- Ventura, A., D.G. Kirsch, M.E. McLaughlin, D.A. Tuveson, J. Grimm, L. Lintault, J. Newman, E.E. Reczek, R. Weissleder, and T. Jacks. 2007. Restoration of p53 function leads to tumour regression in vivo. *Nature* 445:661-665.
- Victora, G.D., D. Dominguez-Sola, A.B. Holmes, S. Deroubaix, R. Dalla-Favera, and M.C. Nussenzweig. 2012. Identification of human germinal center light and dark zone cells and their relationship to human B-cell lymphomas. *Blood* 120:2240-2248.
- Victora, G.D., T.A. Schwickert, D.R. Fooksman, A.O. Kamphorst, M. Meyer-Hermann, M.L. Dustin, and M.C. Nussenzweig. 2010. Germinal center dynamics revealed by multiphoton microscopy with a photoactivatable fluorescent reporter. *Cell* 143:592-605.

- Vikstrom, I., S. Carotta, K. Luthje, V. Peperzak, P.J. Jost, S. Glaser, M. Busslinger, P. Bouillet, A. Strasser, S.L. Nutt, and D.M. Tarlinton. 2010. Mcl-1 is essential for germinal center formation and B cell memory. *Science* 330:1095-1099.
- Vinuesa, C.G., M.C. Cook, C. Angelucci, V. Athanasopoulos, L. Rui, K.M. Hill, D. Yu, H. Domaschenz, B. Whittle, T. Lambe, I.S. Roberts, R.R. Copley, J.I. Bell, R.J. Cornall, and C.C. Goodnow. 2005. A RING-type ubiquitin ligase family member required to repress follicular helper T cells and autoimmunity. *Nature* 435:452-458.
- Vinuesa, C.G., M.A. Linterman, D. Yu, and I.C. MacLennan. 2016. Follicular Helper T Cells. *Annual review of immunology* 34:335-368.
- Vos, Q., A. Lees, Z.Q. Wu, C.M. Snapper, and J.J. Mond. 2000. B-cell activation by T-cell-independent type 2 antigens as an integral part of the humoral immune response to pathogenic microorganisms. *Immunological reviews* 176:154-170.
- Walport, L.J., R.J. Hopkinson, R. Chowdhury, R. Schiller, W. Ge, A. Kawamura, and C.J. Schofield. 2016. Arginine demethylation is catalysed by a subset of JmjC histone lysine demethylases. *Nature communications* 7:11974.
- Wang, L., S. Pal, and S. Sif. 2008. Protein arginine methyltransferase 5 suppresses the transcription of the RB family of tumor suppressors in leukemia and lymphoma cells. *Molecular and cellular biology* 28:6262-6277.
- Wang, M., J. Fuhrmann, and P.R. Thompson. 2014. Protein arginine methyltransferase 5 catalyzes substrate dimethylation in a distributive fashion. *Biochemistry* 53:7884-7892.
- Wang, W., A.K. Erbe, J.A. Hank, Z.S. Morris, and P.M. Sondel. 2015. NK Cell-Mediated Antibody-Dependent Cellular Cytotoxicity in Cancer Immunotherapy. *Frontiers in immunology* 6:368.
- Ward, E.S., and V. Ghetie. 1995. The effector functions of immunoglobulins: implications for therapy. *Ther Immunol* 2:77-94.
- Webb, L.M., S.A. Amici, K.A. Jablonski, H. Savardekar, A.R. Panfil, L. Li, W. Zhou, K. Peine, V. Karkhanis, E.M. Bachelder, K.M. Ainslie, P.L. Green, C. Li, R.A. Baiocchi, and M. Guerau-de-Arellano. 2017. PRMT5-Selective Inhibitors Suppress Inflammatory T Cell Responses and Experimental Autoimmune Encephalomyelitis. *Journal of immunology* 198:1439-1451.
- Wei, H., B. Wang, M. Miyagi, Y. She, B. Gopalan, D.B. Huang, G. Ghosh, G.R. Stark, and T. Lu. 2013. PRMT5 dimethylates R30 of the p65 subunit to activate NF-kappaB. *Proceedings of the National Academy of Sciences of the United States of America* 110:13516-13521.
- Weinstein, J.S., E.I. Herman, B. Lainez, P. Licona-Limon, E. Esplugues, R. Flavell, and J. Craft. 2016. TFH cells progressively differentiate to regulate the germinal center response. *Nature immunology* 17:1197-1205.
- Weisel, F.J., G.V. Zuccarino-Catania, M. Chikina, and M.J. Shlomchik. 2016. A Temporal Switch in the Germinal Center Determines Differential Output of Memory B and Plasma Cells. *Immunity* 44:116-130.
- Wu, J.L., M.F. Chiang, P.H. Hsu, D.Y. Tsai, K.H. Hung, Y.H. Wang, T. Angata, and K.I. Lin. 2017. O-GlcNAcylation is required for B cell homeostasis and antibody responses. *Nature communications* 8:1854.
- Yamagata, K., H. Daitoku, Y. Takahashi, K. Namiki, K. Hisatake, K. Kako, H. Mukai, Y. Kasuya, and A. Fukamizu. 2008. Arginine methylation of FOXO transcription factors inhibits their phosphorylation by Akt. *Molecular cell* 32:221-231.

- Yan, F., L. Alinari, M.E. Lustberg, L.K. Martin, H.M. Cordero-Nieves, Y. Banasavadi-Siddegowda, S. Virk, J. Barnholtz-Sloan, E.H. Bell, J. Wojton, N.K. Jacob, A. Chakravarti, M.O. Nowicki, X. Wu, R. Lapalombella, J. Datta, B. Yu, K. Gordon, A. Haseley, J.T. Patton, P.L. Smith, J. Ryu, X. Zhang, X. Mo, G. Marcucci, G. Nuovo, C.H. Kwon, J.C. Byrd, E.A. Chiocca, C. Li, S. Sif, S. Jacob, S. Lawler, B. Kaur, and R.A. Baiocchi. 2014. Genetic validation of the protein arginine methyltransferase PRMT5 as a candidate therapeutic target in glioblastoma. *Cancer research* 74:1752-1765.
- Yang, M., J. Sun, X. Sun, Q. Shen, Z. Gao, and C. Yang. 2009. Caenorhabditis elegans protein arginine methyltransferase PRMT-5 negatively regulates DNA damage-induced apoptosis. *PLoS genetics* 5:e1000514.
- Yang, Y., and M.T. Bedford. 2013. Protein arginine methyltransferases and cancer. *Nature reviews. Cancer* 13:37-50.
- Yang, Y., Y. Lu, A. Espejo, J. Wu, W. Xu, S. Liang, and M.T. Bedford. 2010. TDRD3 is an effector molecule for arginine-methylated histone marks. *Molecular cell* 40:1016-1023.
- Yang, Y., K.M. McBride, S. Hensley, Y. Lu, F. Chedin, and M.T. Bedford. 2014. Arginine methylation facilitates the recruitment of TOP3B to chromatin to prevent R loop accumulation. *Molecular cell* 53:484-497.
- Yasuda, T., K. Kometani, N. Takahashi, Y. Imai, Y. Aiba, and T. Kurosaki. 2011. ERKs induce expression of the transcriptional repressor Blimp-1 and subsequent plasma cell differentiation. *Sci Signal* 4:ra25.
- Ying, Z., M. Mei, P. Zhang, C. Liu, H. He, F. Gao, and S. Bao. 2015. Histone Arginine Methylation by PRMT7 Controls Germinal Center Formation via Regulating Bcl6 Transcription. *Journal of immunology* 195:1538-1547.
- Yu, Z., T. Chen, J. Hebert, E. Li, and S. Richard. 2009. A mouse PRMT1 null allele defines an essential role for arginine methylation in genome maintenance and cell proliferation. *Molecular and cellular biology* 29:2982-2996.
- Yu, Z., G. Vogel, Y. Coulombe, D. Dubeau, E. Spelhalski, J. Hebert, D.O. Ferguson, J.Y. Masson, and S. Richard. 2012. The MRE11 GAR motif regulates DNA double-strand break processing and ATR activation. *Cell Res* 22:305-320.
- Zahn, A., M. Daugan, S. Safavi, D. Godin, C. Cheong, A. Lamarre, and J.M. Di Noia. 2013. Separation of function between isotype switching and affinity maturation in vivo during acute immune responses and circulating autoantibodies in UNG-deficient mice. *Journal of immunology* 190:5949-5960.
- Zeller, K.I., X. Zhao, C.W. Lee, K.P. Chiu, F. Yao, J.T. Yustein, H.S. Ooi, Y.L. Orlov, A. Shahab, H.C. Yong, Y. Fu, Z. Weng, V.A. Kuznetsov, W.K. Sung, Y. Ruan, C.V. Dang, and C.L. Wei. 2006. Global mapping of c-Myc binding sites and target gene networks in human B cells. *Proceedings of the National Academy of Sciences of the United States of America* 103:17834-17839.
- Zhang, B., S. Dong, R. Zhu, C. Hu, J. Hou, Y. Li, Q. Zhao, X. Shao, Q. Bu, H. Li, Y. Wu, X. Cen, and Y. Zhao. 2015a. Targeting protein arginine methyltransferase 5 inhibits colorectal cancer growth by decreasing arginine methylation of eIF4E and FGFR3. *Oncotarget* 6:22799-22811.
- Zhang, J., D. Jima, A.B. Moffitt, Q. Liu, M. Czader, E.D. Hsi, Y. Fedoriw, C.H. Dunphy, K.L. Richards, J.I. Gill, Z. Sun, C. Love, P. Scotland, E. Lock, S. Levy, D.S. Hsu, D.

- Dunson, and S.S. Dave. 2014. The genomic landscape of mantle cell lymphoma is related to the epigenetically determined chromatin state of normal B cells. *Blood* 123:2988-2996.
- Zhang, J., I.C. MacLennan, Y.J. Liu, and P.J. Lane. 1988. Is rapid proliferation in B centroblasts linked to somatic mutation in memory B cell clones? *Immunol Lett* 18:297-299.
- Zhang, T., S. Gunther, M. Looso, C. Kunne, M. Kruger, J. Kim, Y. Zhou, and T. Braun. 2015b. Prmt5 is a regulator of muscle stem cell expansion in adult mice. *Nature communications* 6:7140.
- Zhang, Y., L. Tech, L.A. George, A. Acs, R.E. Durrett, H. Hess, L.S.K. Walker, D.M. Tarlinton, A.L. Fletcher, A.E. Hauser, and K.M. Toellner. 2018. Plasma cell output from germinal centers is regulated by signals from Tfh and stromal cells. *The Journal of experimental medicine* 215:1227-1243.
- Zhao, D.Y., G. Gish, U. Braunschweig, Y. Li, Z. Ni, F.W. Schmitges, G. Zhong, K. Liu, W. Li, J. Moffat, M. Vedadi, J. Min, T.J. Pawson, B.J. Blencowe, and J.F. Greenblatt. 2016. SMN and symmetric arginine dimethylation of RNA polymerase II C-terminal domain control termination. *Nature* 529:48-53.
- Zhao, Q., G. Rank, Y.T. Tan, H. Li, R.L. Moritz, R.J. Simpson, L. Cerruti, D.J. Curtis, D.J. Patel, C.D. Allis, J.M. Cunningham, and S.M. Jane. 2009. PRMT5-mediated methylation of histone H4R3 recruits DNMT3A, coupling histone and DNA methylation in gene silencing. *Nature structural & molecular biology* 16:304-311.
- Zhao, X., V. Jankovic, A. Gural, G. Huang, A. Pardnani, S. Menendez, J. Zhang, R. Dunne, A. Xiao, H. Erdjument-Bromage, C.D. Allis, P. Tempst, and S.D. Nimer. 2008. Methylation of RUNX1 by PRMT1 abrogates SIN3A binding and potentiates its transcriptional activity. *Genes & development* 22:640-653.
- Zheng, S., J. Moehlenbrink, Y.C. Lu, L.P. Zalmas, C.A. Sagum, S. Carr, J.F. McGouran, L. Alexander, O. Fedorov, S. Munro, B. Kessler, M.T. Bedford, Q. Yu, and N.B. La Thangue. 2013. Arginine methylation-dependent reader-writer interplay governs growth control by E2F-1. *Molecular cell* 52:37-51.
- Zhu, J., H. Yamane, and W.E. Paul. 2010. Differentiation of effector CD4 T cell populations (*). *Annual review of immunology* 28:445-489.
- Zotos, D., J.M. Coquet, Y. Zhang, A. Light, K. D'Costa, A. Kallies, L.M. Corcoran, D.I. Godfrey, K.M. Toellner, M.J. Smyth, S.L. Nutt, and D.M. Tarlinton. 2010. IL-21 regulates germinal center B cell differentiation and proliferation through a B cell-intrinsic mechanism. *The Journal of experimental medicine* 207:365-378.
- Zotos, D., and D.M. Tarlinton. 2012. Determining germinal centre B cell fate. *Trends in immunology* 33:281-288.
- Zou, L., H. Zhang, C. Du, X. Liu, S. Zhu, W. Zhang, Z. Li, C. Gao, X. Zhao, M. Mei, S. Bao, and H. Zheng. 2012. Correlation of SRSF1 and PRMT1 expression with clinical status of pediatric acute lymphoblastic leukemia. *Journal of hematology & oncology* 5:42.

